ornl

OAK
RIDGE
NATIONAL
LABORATORY

UNION CARBIDE

NUREG/CR-2525, Vol. 6
ORNL/NUREG/TM-407/V6

ORNL Rod Bundle Heat Transfer Test Data

Volume 6. Thermal-Hydraulic Test Facil[illegible] Experimental Data Report for Test 3.05.5B—Double-Ended Cold-Leg Break Simulation

C. B. Mullins
D. K. Felde
A. G. Sutton
S. S. Gould
D. G. Morris
J. J. Robinson
K. N. Schwinkendorf

Prepared for the U.S. Nuclear Regulatory Commission
Office of Nuclear Regulatory Research
Under Interagency Agreements DOE 40-551-75 and 40-552-75

OPERATED BY
UNION CARBIDE CORPORATION
FOR THE UNITED STATES

Printed in the United States of America. Available from
National Technical Information Service
U.S. Department of Commerce
5285 Port Royal Road, Springfield, Virginia 22161

Available from
GPO Sales Program
Division of Technical Information and Document Control
U.S. Nuclear Regulatory Commission
Washington, D.C. 20555

NUREG/CR-2525, Vol. 6
ORNL/NUREG/TM-407/V6
Dist. Category R2

Contract No. W-7405-eng-26

Engineering Technology Division

ORNL ROD BUNDLE HEAT TRANSFER TEST DATA

VOLUME 6. THERMAL-HYDRAULIC TEST FACILITY EXPERIMENTAL DATA REPORT FOR TEST 3.05.5B - DOUBLE-ENDED COLD-LEG BREAK SIMULATION

C. B. Mullins S. S. Gould
D. K. Felde D. G. Morris
A. G. Sutton J. J. Robinson
K. M. Schwinkendorf

Manuscript Completed - May 18, 1982
Date Published - June 1982

Prepared for the
U.S. Nuclear Regulatory Commission
Office of Nuclear Regulatory Research
Under Interagency Agreeements DOE 40-551-75 and 40-552-75

NRC FIN No. B0125

Prepared by the
OAK RIDGE NATIONAL LABORATORY
Oak Ridge, Tennessee 37830
operated by
UNION CARBIDE CORPORATION
for the
DEPARTMENT OF ENERGY

CONTENTS

LIST OF FIGURES

ACKNOWLEDGMENTS

In the conduct of a large experimental and analytical program, there are always a great many individuals whose contributions should be recognized. The dedicated efforts of the entire Blowdown Heat Transfer Program staff are reflected in this report. The authors express sincere appreciation to the following personnel:

M. C. Adair
T. M. Anklam
J. L. Bartley
D. H. Cook
W. G. Craddick
R. D. Dabbs
R. L. Durall
R. M. Flanders
D. J. Fraysier
R. H. Greene
R. C. Hagar
D. F. Hunt
C. R. Hyman
A. F. Johnson
R. W. McCulloch
D. G. Madewell
G. S. Mailen
R. W. Murphy
L. J. Ott
H. R. Payne
W. Ragan, Jr.
N. R. Raulston
R. D. Stulting
J. W. Teague, Jr.
R. E. Textor
M. S. Thompson
H. E. Trammell
B. J. Veazie
J. D. White
M. D. White
J. E. Wolfe
G. L. Yoder

ORNL ROD BUNDLE HEAT TRANSFER TEST DATA

VOLUME 6. THERMAL-HYDRAULIC TEST FACILITY EXPERIMENTAL DATA REPORT FOR TEST 3.05.5B – DOUBLE-ENDED COLD-LEG BREAK SIMULATION

C. B. Mullins   S. S. Gould
D. K. Felde   D. G. Morris
A. G. Sutton   J. J. Robinson
K. N. Schwinkendorf

ABSTRACT

Thermal-Hydraulic Test Facility (THTF) Test 3.05.5B was conducted by members of the Oak Ridge National Laboratory (ORNL) Pressurized-Water Reactor (PWR) Blowdown Heat Transfer (BDHT) Separate-Effects Program on July 3, 1980. The objective of the program is to investigate heat transfer phenomena believed to occur in PWRs during accidents, including small and large break loss-of-coolant accidents.

Test 3.05.5B was designed to provide transient thermal-hydraulics data in rod bundle geometry under reactor accident-type conditions. Reduced instrument responses are presented. Also included are uncertainties in the instrument responses, calculated mass flows, and calculated rod powers.

1. INTRODUCTION

The Oak Ridge National Laboratory (ORNL) Pressurized-Water Reactor (PWR) Blowdown Heat Transfer (BDHT) Program is studying several aspects of heat transfer thought to occur in accident situations in PWRs, including dispersed flow film boiling. The study involves experimental as well as analytical efforts. This report presents reduced instrument responses obtained during Test 3.05.5B in the Thermal-Hydraulic Test Facility (THTF).

Test 3.05.5B data are analyzed in Ref. 1.

2. THERMAL-HYDRAULIC TEST FACILITY DESCRIPTION

The THTF is a heavily instrumented, non-nuclear pressurized-water loop (Fig. 1) containing 64 full-length rods (of which 60 are electrically heated) arranged in an 8 x 8 bundle. Rod diameter and pitch are typical of a PWR with 17 x 17 fuel assemblies. Figure 2 is a schematic diagram of the THTF rod bundle cross section. Figure 3 shows a simplified cross section of a typical fuel rod simulator. Note that at each axial location where a rod has thermocouples (T/C), there are three individual thermocouples spaced azimuthally around the rod. The axial and radial power profile of the THTF bundle is flat. The axial locations of fuel rod simulator thermocouples are shown schematically in Fig. 4. The heated length of the bundle is 3.66 m (12 ft), and there are six spacer grids in the heated length.

Figure 5 is a simplified diagram of the THTF included to help aid in visualizing the facility. In the steady-state mode, fluid flows from the pump through the horizontal inlet (SHI) and vertical inlet (SVI) spool pieces respectively. From the SVI spool piece, fluid enters the external downcomer (BI1) spool piece into the test section lower plenum. Fluid flows from the lower plenum through the heated length of the bundle, into the test section upper plenum, through the outlet spool pieces (BO1, SVO, SHO) into the main heat exchangers, and back to the inlet of the pump. The test section steady-state conditions prior to transient initiation are shown in Table 1.

Figure 6 is a more detailed diagram showing the location of pressure and differential pressure instrumentation for Test 3.05.5B. Figure 7 is a detailed diagram of the entire THTF piping system and its associated instrumentation. The THTF is described more completely in Ref. 2.

The transient was initiated by breaking both inlet and outlet rupture disk assemblies. The outlet break area was 3.512×10^{-4} m² (0.00378 ft²); the inlet break area was 4.013×10^{-4} m² (0.00432 ft²). The transient phenomenology is discussed in Appendix A.

Table 1. Test section steady-state conditions

Outlet temperature	602 K (624°F)
Inlet temperature	550 K (530°F)
Average pressure	14.46 MN/m² (2097 psi)
Inlet volumetric flow	0.0317 m³/s (502 gpm)
Bundle power	7.453 MW

ORNL-DWG 81-7835R ETD

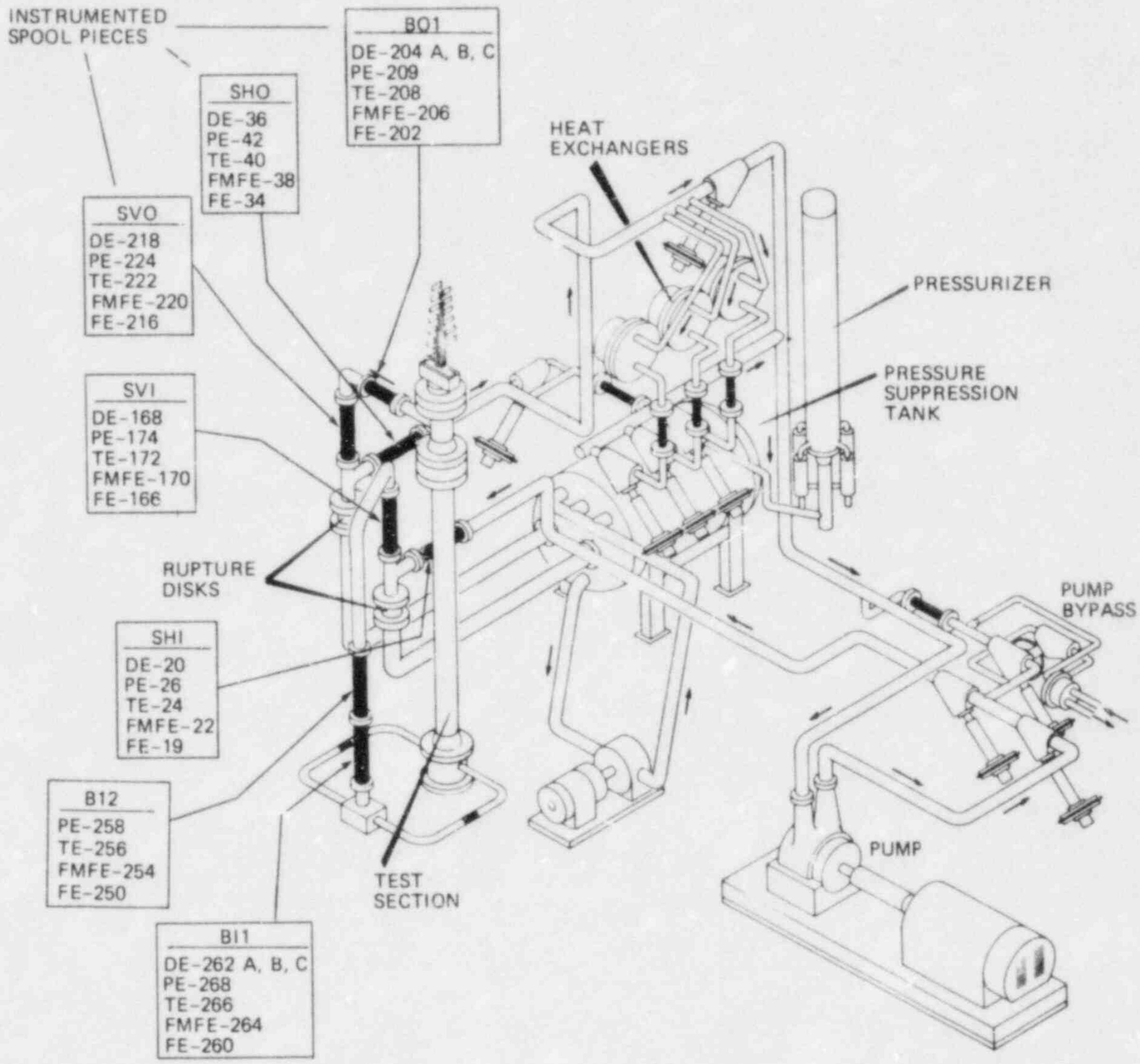

Fig. 1. THTF system with instrumented spool pieces labeled.

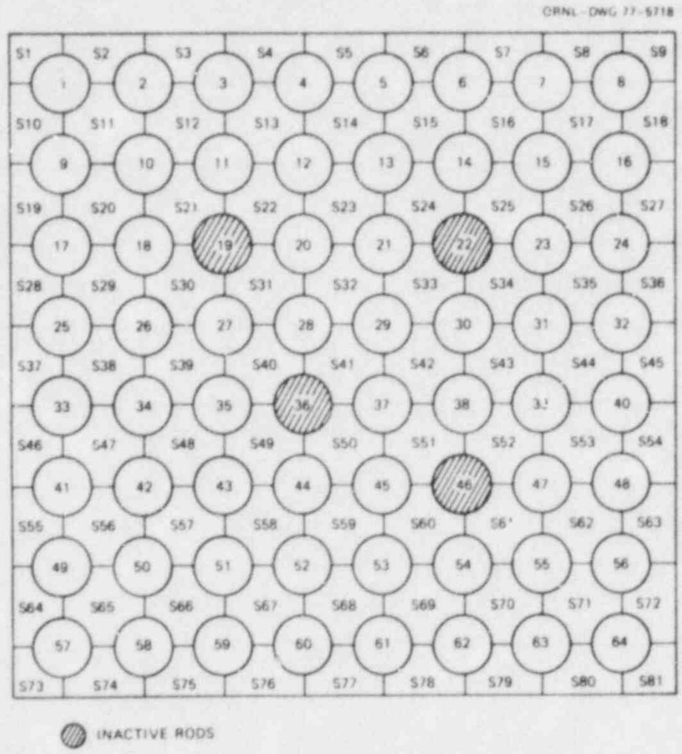

Fig. 2. Identification of THTF heater rods, subchannel location, and inactive rods in THTF heater bundle.

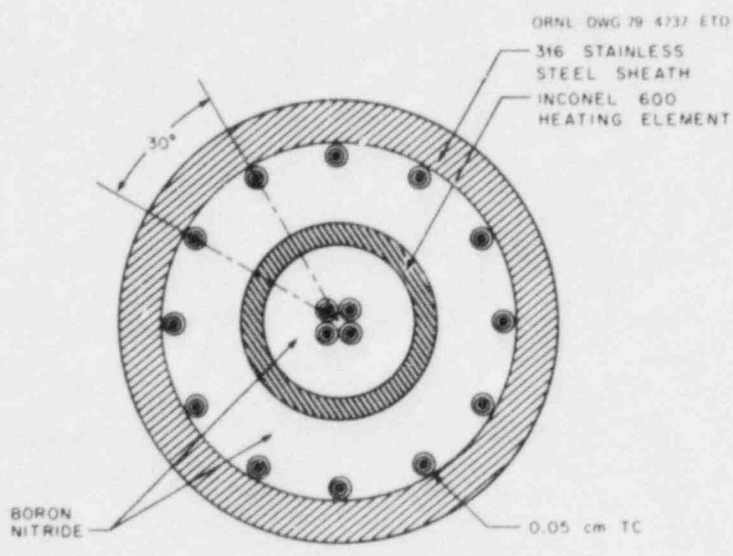

Fig. 3. Cross section of a typical fuel rod simulator.

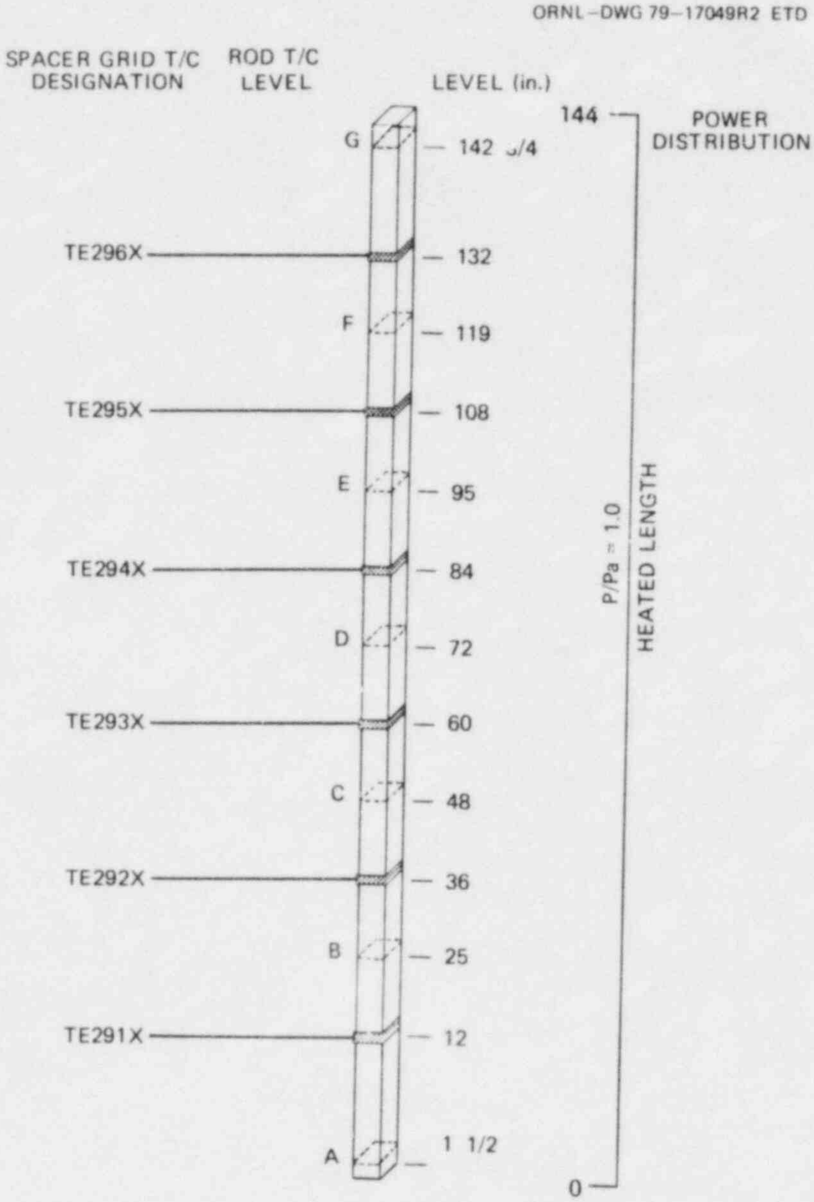

Fig. 4. Axial location of spacer grids and fuel rod simulator thermocouples.

ORNL–DWG 79–4231AR ETD

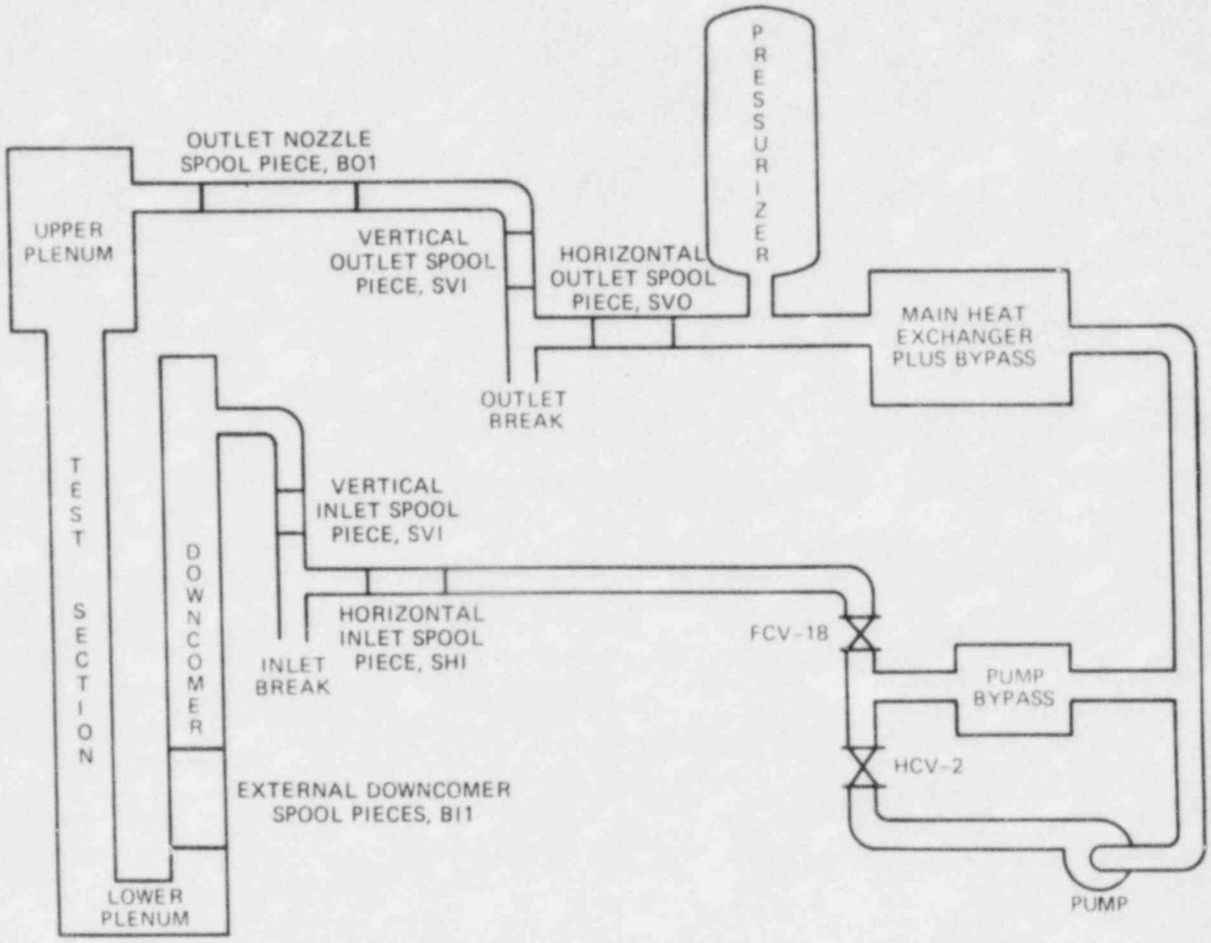

Fig. 5. Diagram of THTF.

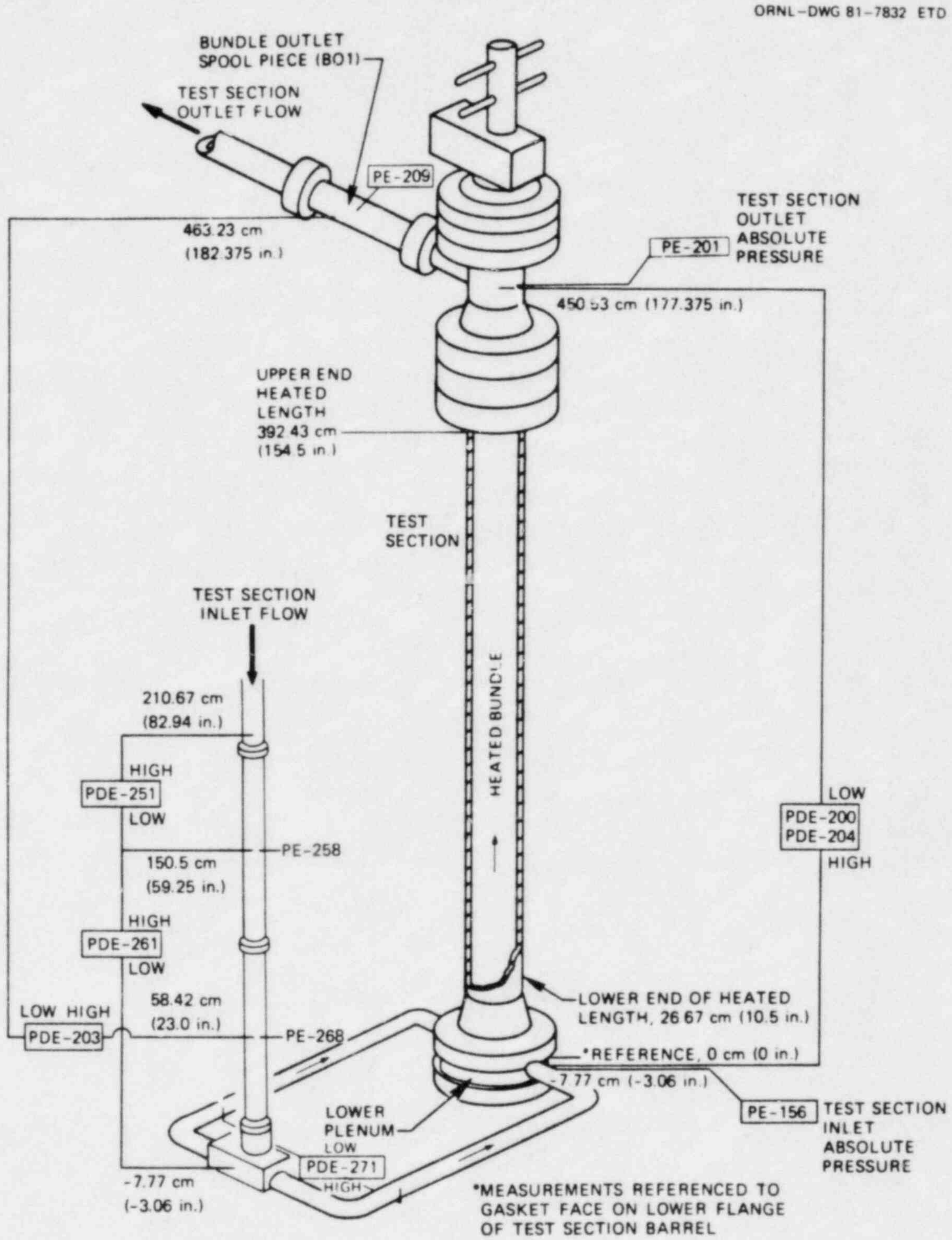

Fig. 6. Positions of differential pressure and pressure instrumentation for THTF Test 3.05.5B.

ORNL-DWG 82-5722 (PART A)

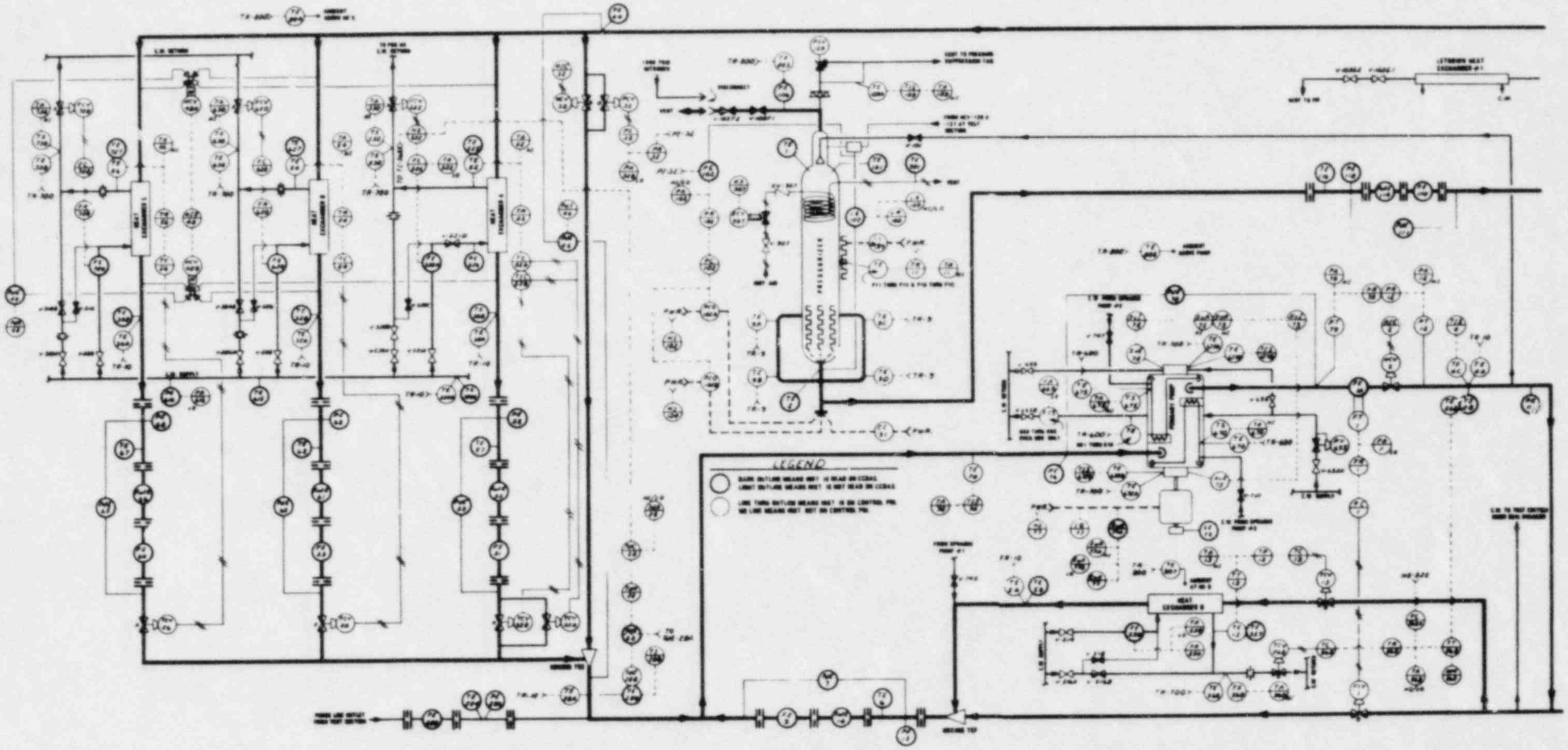

Fig. 7. THTF instrumentation diagram.

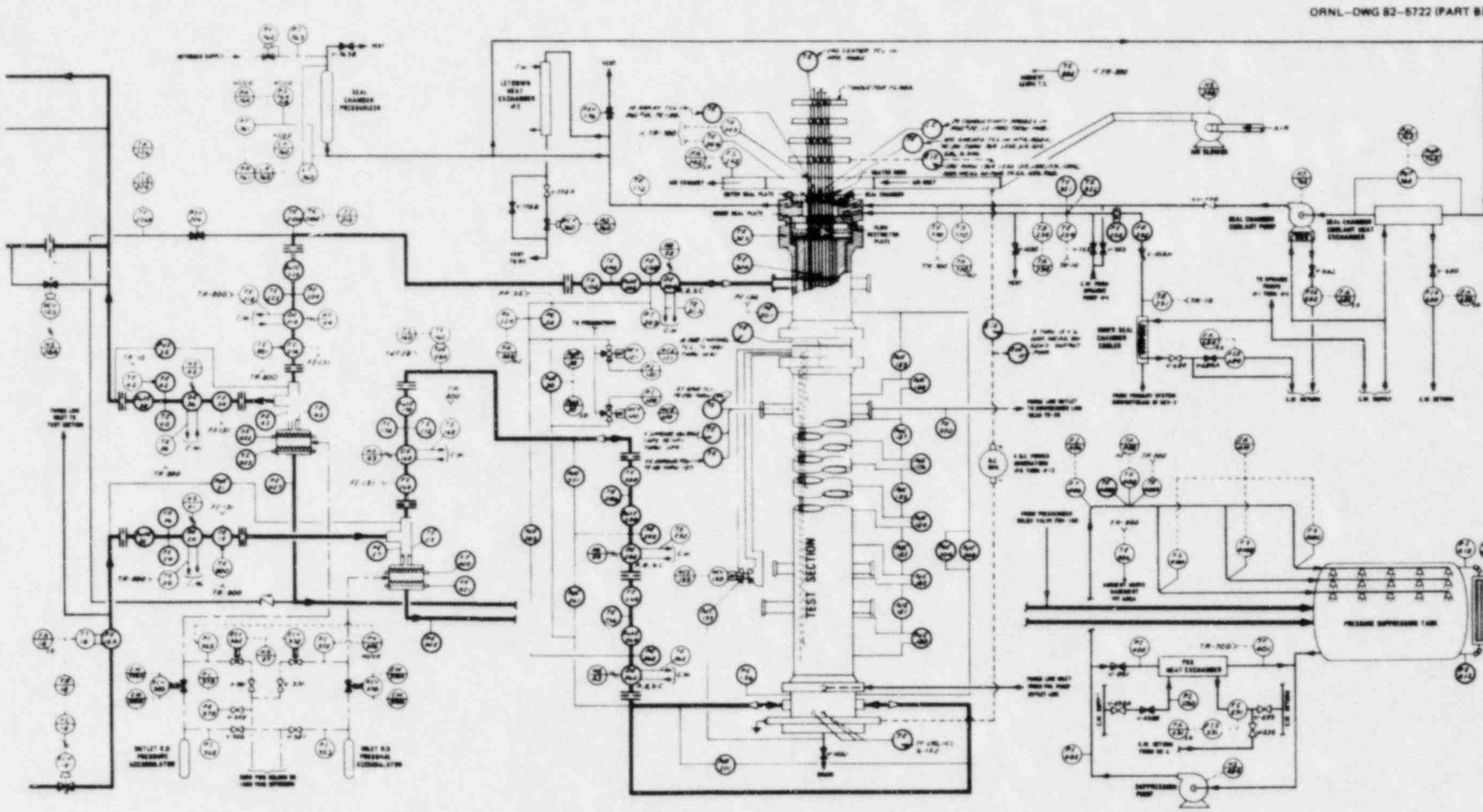

Fig. 7 (continued)

3. DATA PRESENTATION

The recorded instrument responses for THTF Test 3.05.5B are shown graphically on the microfiche in the back of this report. Three types of tables have been constructed to assist in the use of the data. Table 2 lists instrumentation in terms of instrument function, type, and location; also included are a brief description of each instrument and an instrument application number (IAN), which is a unique identifier associated with each instrument. The following example illustrates the format:

Example

BUNDLE TEMPERATURE — Heading denoting function
SHEATH THERMOCOUPLE — Heading denoting type
LEVEL A — Subheading denoting location

Instrument application number	Instrument description
TE-306AA	SHEATH THERMOCOUPLE, ROD 6, LEVEL A

Table 3 lists instruments in the order they are shown graphically on the microfiche in the back of this report. Included are figure number, IAN, instrument description, instrument range, and comments on the functionability of the instrument. There are two possible comments: "Failed instrument" means the instrument was expected to function but failed to function properly. "Questionable" implies the instrument could be functioning properly but the data from such an instrument could be faulty.

Table 4 lists instruments alphabetically in terms of the IAN. Included are IAN, corresponding figure number, and instrument type code, (see Appendix D). Table 4 coordinates the information in Tables 2 and 3. One can look up an instrument by function using Table 2; then, by the use of the IAN and Table 4, the associated figure number can be determined. Table 3 can be used to check the instrument status.

Table 5 presents the nomenclature used in designating thermocouples. This table, together with Figs. 2 and 4, allows location of thermocouples in the THTF test section.

The reduced instrument responses presented in this report were recorded by a computer-controlled digital data acquisition system. Further information on this system can be found in Ref. 2.

Graphical results and a discussion of the calculation of mass flux at various THTF spool pieces are included in Appendix B. Appendix C is a graphical presentation of rod powers for THTF Test 3.05.5B. Appendix D is devoted to discussion and calculation of uncertainties for THTF instrumentation. Appendix E presents a composite density from the three-beam densitometers.

Table 2

SENSOR	DESCRIPTION
BUNDLE TEMPERATURE	
SHEATH THERMOCOUPLES	
LEVEL A	
TE-306AA	SHEATH THERMOCOUPLE, ROD 6, LEVEL A
TE-308BA	SHEATH THERMOCOUPLE, ROD 8, LEVEL A
TE-311AA	SHEATH THERMOCOUPLE, ROD 11, LEVEL A
TE-314AA	SHEATH THERMOCOUPLE, ROD 14, LEVEL A
TE-321AA	SHEATH THERMOCOUPLE, ROD 21, LEVEL A
TE-323AA	SHEATH THERMOCOUPLE, ROD 23, LEVEL A
TE-325AA	SHEATH THERMOCOUPLE, ROD 25, LEVEL A
TE-325BA	SHEATH THERMOCOUPLE, ROD 25, LEVEL A
TE-325CA	SHEATH THERMOCOUPLE, ROD 25, LEVEL A
TE-327AA	SHEATH THERMOCOUPLE, ROD 27, LEVEL A
TE-327BA	SHEATH THERMOCOUPLE, ROD 27, LEVEL A
TE-327CA	SHEATH THERMOCOUPLE, ROD 27, LEVEL A
TE-340CA	SHEATH THERMOCOUPLE, ROD 40, LEVEL A
TE-343BA	SHEATH THERMOCOUPLE, ROD 43, LEVEL A
TE-354CA	SHEATH THERMOCOUPLE, ROD 54, LEVEL A
TE-355AA	SHEATH THERMOCOUPLE, ROD 55, LEVEL A
TE-357AA	SHEATH THERMOCOUPLE, ROD 57, LEVEL A
TE-357BA	SHEATH THERMOCOUPLE, ROD 57, LEVEL A
TE-360AA	SHEATH THERMOCOUPLE, ROD 60, LEVEL A
LEVEL B	
TE-302AB	SHEATH THERMOCOUPLE, ROD 2, LEVEL B
TE-306AB	SHEATH THERMOCOUPLE, ROD 6, LEVEL B
TE-308CB	SHEATH THERMOCOUPLE, ROD 8, LEVEL B
TE-309CB	SHEATH THERMOCOUPLE, ROD 9, LEVEL B
TE-311AB	SHEATH THERMOCOUPLE, ROD 11, LEVEL B
TE-311CB	SHEATH THERMOCOUPLE, ROD 11, LEVEL B
TE-312CB	SHEATH THERMOCOUPLE, ROD 12, LEVEL B
TE-314AB	SHEATH THERMOCOUPLE, ROD 14, LEVEL B
TE-317CB	SHEATH THERMOCOUPLE, ROD 17, LEVEL B
TE-321AB	SHEATH THERMOCOUPLE, ROD 21, LEVEL B
TE-324AB	SHEATH THERMOCOUPLE, ROD 24, LEVEL B
TE-324CB	SHEATH THERMOCOUPLE, ROD 24, LEVEL B
TE-325AB	SHEATH THERMOCOUPLE, ROD 25, LEVEL B
TE-325BB	SHEATH THERMOCOUPLE, ROD 25, LEVEL B
TE-325CB	SHEATH THERMOCOUPLE, ROD 25, LEVEL B
TE-326BB	SHEATH THERMOCOUPLE, ROD 26, LEVEL B
TE-327CB	SHEATH THERMOCOUPLE, ROD 27, LEVEL B
TE-329AB	SHEATH THERMOCOUPLE, ROD 29, LEVEL B
TE-329BB	SHEATH THERMOCOUPLE, ROD 29, LEVEL B

Table 2 (continued)

SENSOR	DESCRIPTION
BUNDLE TEMPERATURE (CONT.)	
SHEATH THERMOCOUPLES (CONT.)	
LEVEL B (CONT.)	
TE-329CB	SHEATH THERMOCOUPLE, ROD 29, LEVEL B
TE-330CB	SHEATH THERMOCOUPLE, ROD 30, LEVEL B
TE-333CB	SHEATH THERMOCOUPLE, ROD 33, LEVEL B
TE-335BB	SHEATH THERMOCOUPLE, ROD 35, LEVEL B
TE-338AB	SHEATH THERMOCOUPLE, ROD 38, LEVEL B
TE-339BB	SHEATH THERMOCOUPLE, ROD 39, LEVEL B
TE-340CB	SHEATH THERMOCOUPLE, ROD 40, LEVEL B
TE-341AB	SHEATH THERMOCOUPLE, ROD 41, LEVEL B
TE-343BB	SHEATH THERMOCOUPLE, ROD 43, LEVEL B
TE-344CB	SHEATH THERMOCOUPLE, ROD 44, LEVEL B
TE-349CB	SHEATH THERMOCOUPLE, ROD 49, LEVEL B
TE-351AB	SHEATH THERMOCOUPLE, ROD 51, LEVEL B
TE-354CB	SHEATH THERMOCOUPLE, ROD 54, LEVEL B
TE-355CB	SHEATH THERMOCOUPLE, ROD 55, LEVEL B
TE-357AB	SHEATH THERMOCOUPLE, ROD 57, LEVEL B
TE-357BB	SHEATH THERMOCOUPLE, ROD 57, LEVEL B
TE-357CB	SHEATH THERMOCOUPLE, ROD 57, LEVEL B
TE-360AB	SHEATH THERMOCOUPLE, ROD 60, LEVEL B
TE-361AB	SHEATH THERMOCOUPLE, ROD 61, LEVEL B
TE-362AB	SHEATH THERMOCOUPLE, ROD 62, LEVEL B
TE-363CB	SHEATH THERMOCOUPLE, ROD 63, LEVEL B
LEVEL C	
TE-302BC	SHEATH THERMOCOUPLE, ROD 2, LEVEL C
TE-304AC	SHEATH THERMOCOUPLE, ROD 4, LEVEL C
TE-307AC	SHEATH THERMOCOUPLE, ROD 7, LEVEL C
TE-308BC	SHEATH THERMOCOUPLE, ROD 8, LEVEL C
TE-309AC	SHEATH THERMOCOUPLE, ROD 9, LEVEL C
TE-310CC	SHEATH THERMOCOUPLE, ROD 10, LEVEL C
TE-311CC	SHEATH THERMOCOUPLE, ROD 11, LEVEL C
TE-312BC	SHEATH THERMOCOUPLE, ROD 12, LEVEL C
TE-313BC	SHEATH THERMOCOUPLE, ROD 13, LEVEL C
TE-314AC	SHEATH THERMOCOUPLE, ROD 14, LEVEL C
TE-315AC	SHEATH THERMOCOUPLE, ROD 15, LEVEL C
TE-317CC	SHEATH THERMOCOUPLE, ROD 17, LEVEL C
TE-321BC	SHEATH THERMOCOUPLE, ROD 21, LEVEL C
TE-323BC	SHEATH THERMOCOUPLE, ROD 23, LEVEL C
TE-324AC	SHEATH THERMOCOUPLE, ROD 24, LEVEL C
TE-325AC	SHEATH THERMOCOUPLE, ROD 25, LEVEL C
TE-325BC	SHEATH THERMOCOUPLE, ROD 25, LEVEL C
TE-325CC	SHEATH THERMOCOUPLE, ROD 25, LEVEL C
TE-326AC	SHEATH THERMOCOUPLE, ROD 26, LEVEL C
TE-327AC	SHEATH THERMOCOUPLE, ROD 27, LEVEL C
TE-327BC	SHEATH THERMOCOUPLE, ROD 27, LEVEL C
TE-327CC	SHEATH THERMOCOUPLE, ROD 27, LEVEL C

Table 2 (continued)

SENSOR	DESCRIPTION
BUNDLE TEMPERATURE (CONT.)	
SHEATH THERMOCOUPLES (CONT.)	
LEVEL C (CONT.)	
TE-328AC	SHEATH THERMOCOUPLE, ROD 28, LEVEL C
TE-328CC	SHEATH THERMOCOUPLE, ROD 28, LEVEL C
TE-329AC	SHEATH THERMOCOUPLE, ROD 29, LEVEL C
TE-329BC	SHEATH THERMOCOUPLE, ROD 29, LEVEL C
TE-330AC	SHEATH THERMOCOUPLE, ROD 30, LEVEL C
TE-333AC	SHEATH THERMOCOUPLE, ROD 33, LEVEL C
TE-338BC	SHEATH THERMOCOUPLE, ROD 38, LEVEL C
TE-339AC	SHEATH THERMOCOUPLE, ROD 39, LEVEL C
TE-340BC	SHEATH THERMOCOUPLE, ROD 40, LEVEL C
TE-343BC	SHEATH THERMOCOUPLE, ROD 43, LEVEL C
TE-344CC	SHEATH THERMOCOUPLE, ROD 44, LEVEL C
TE-349CC	SHEATH THERMOCOUPLE, ROD 49, LEVEL C
TE-350AC	SHEATH THERMOCOUPLE, ROD 50, LEVEL C
TE-350BC	SHEATH THERMOCOUPLE, ROD 50, LEVEL C
TE-351BC	SHEATH THERMOCOUPLE, ROD 51, LEVEL C
TE-353CC	SHEATH THERMOCOUPLE, ROD 53, LEVEL C
TE-354CC	SHEATH THERMOCOUPLE, ROD 54, LEVEL C
TE-355BC	SHEATH THERMOCOUPLE, ROD 55, LEVEL C
TE-356AC	SHEATH THERMOCOUPLE, ROD 56, LEVEL C
TE-357AC	SHEATH THERMOCOUPLE, ROD 57, LEVEL C
TE-357BC	SHEATH THERMOCOUPLE, ROD 57, LEVEL C
TE-359CC	SHEATH THERMOCOUPLE, ROD 59, LEVEL C
TE-360AC	SHEATH THERMOCOUPLE, ROD 60, LEVEL C
TE-361AC	SHEATH THERMOCOUPLE, ROD 61, LEVEL C
TE-363BC	SHEATH THERMOCOUPLE, ROD 63, LEVEL C
LEVEL U	
TE-305BU	SHEATH THERMOCOUPLE, ROD 5, LEVEL U
TE-334BU	SHEATH THERMOCOUPLE, ROD 34, LEVEL U
TE-334CU	SHEATH THERMOCOUPLE, ROD 34, LEVEL U
TE-352AU	SHEATH THERMOCOUPLE, ROD 52, LEVEL U
TE-352BU	SHEATH THERMOCOUPLE, ROD 52, LEVEL U
TE-352CU	SHEATH THERMOCOUPLE, ROD 52, LEVEL U
LEVEL H	
TE-305BH	SHEATH THERMOCOUPLE, ROD 5, LEVEL H
TE-334AH	SHEATH THERMOCOUPLE, ROD 34, LEVEL H
TE-334BH	SHEATH THERMOCOUPLE, ROD 34, LEVEL H
TE-334CH	SHEATH THERMOCOUPLE, ROD 34, LEVEL H
TE-348AH	SHEATH THERMOCOUPLE, ROD 48, LEVEL H
TE-352AH	SHEATH THERMOCOUPLE, ROD 52, LEVEL H
TE-352BH	SHEATH THERMOCOUPLE, ROD 52, LEVEL H
TE-352CH	SHEATH THERMOCOUPLE, ROD 52, LEVEL H
LEVEL S	

Table 2 (continued)

SENSOR	DESCRIPTION
BUNDLE TEMPERATURE (CONT.)	
SHEATH THERMOCOUPLES (CONT.)	
LEVEL S (CONT.)	
TE-305AS	SHEATH THERMOCOUPLE, ROD 5, LEVEL S
TE-334AS	SHEATH THERMOCOUPLE, ROD 34, LEVEL S
TE-334BS	SHEATH THERMOCOUPLE, ROD 34, LEVEL S
TE-334CS	SHEATH THERMOCOUPLE, ROD 34, LEVEL S
TE-352AS	SHEATH THERMOCOUPLE, ROD 52, LEVEL S
TE-352BS	SHEATH THERMOCOUPLE, ROD 52, LEVEL S
TE-352CS	SHEATH THERMOCOUPLE, ROD 52, LEVEL S
LEVEL Y	
TE-305CY	SHEATH THERMOCOUPLE, ROD 5, LEVEL Y
TE-334AY	SHEATH THERMOCOUPLE, ROD 34, LEVEL Y
TE-334BY	SHEATH THERMOCOUPLE, ROD 34, LEVEL Y
TE-334CY	SHEATH THERMOCOUPLE, ROD 34, LEVEL Y
TE-348AY	SHEATH THERMOCOUPLE, ROD 48, LEVEL Y
TE-352AY	SHEATH THERMOCOUPLE, ROD 52, LEVEL Y
TE-352BY	SHEATH THERMOCOUPLE, ROD 52, LEVEL Y
TE-352CY	SHEATH THERMOCOUPLE, ROD 52, LEVEL Y
LEVEL D	
TE-301AD	SHEATH THERMOCOUPLE, ROD 1, LEVEL D
TE-301CD	SHEATH THERMOCOUPLE, ROD 1, LEVEL D
TE-302AD	SHEATH THERMOCOUPLE, ROD 2, LEVEL D
TE-303CD	SHEATH THERMOCOUPLE, ROD 3, LEVEL D
TE-304AD	SHEATH THERMOCOUPLE, ROD 4, LEVEL D
TE-308AD	SHEATH THERMOCOUPLE, ROD 8, LEVEL D
TE-308BD	SHEATH THERMOCOUPLE, ROD 8, LEVEL D
TE-308CD	SHEATH THERMOCOUPLE, ROD 8, LEVEL D
TE-309CD	SHEATH THERMOCOUPLE, ROD 9, LEVEL D
TE-310BD	SHEATH THERMOCOUPLE, ROD 10, LEVEL D
TE-310CD	SHEATH THERMOCOUPLE, ROD 10, LEVEL D
TE-312CD	SHEATH THERMOCOUPLE, ROD 12, LEVEL D
TE-313CD	SHEATH THERMOCOUPLE, ROD 13, LEVEL D
TE-314BD	SHEATH THERMOCOUPLE, ROD 14, LEVEL D
TE-316AD	SHEATH THERMOCOUPLE, ROD 16, LEVEL D
TE-317CD	SHEATH THERMOCOUPLE, ROD 17, LEVEL D
TE-318AD	SHEATH THERMOCOUPLE, ROD 18, LEVEL D
TE-318BD	SHEATH THERMOCOUPLE, ROD 18, LEVEL D
TE-318CD	SHEATH THERMOCOUPLE, ROD 18, LEVEL D
TE-320AD	SHEATH THERMOCOUPLE, ROD 20, LEVEL D
TE-320BD	SHEATH THERMOCOUPLE, ROD 20, LEVEL D
TE-320CD	SHEATH THERMOCOUPLE, ROD 20, LEVEL D
TE-321AD	SHEATH THERMOCOUPLE, ROD 21, LEVEL D
TE-321BD	SHEATH THERMOCOUPLE, ROD 21, LEVEL D
TE-321CD	SHEATH THERMOCOUPLE, ROD 21, LEVEL D
TE-324BD	SHEATH THERMOCOUPLE, ROD 24, LEVEL D

Table 2 (continued)

SENSOR	DESCRIPTION
BUNDLE TEMPERATURE (CONT.)	
SHEATH THERMOCOUPLES (CONT.)	
LEVEL D (CONT.)	
TE-325BD	SHEATH THERMOCOUPLE, ROD 25, LEVEL D
TE-325CD	SHEATH THERMOCOUPLE, ROD 25, LEVEL D
TE-326AD	SHEATH THERMOCOUPLE, ROD 26, LEVEL D
TE-326BD	SHEATH THERMOCOUPLE, ROD 26, LEVEL D
TE-326CD	SHEATH THERMOCOUPLE, ROD 26, LEVEL D
TE-327AD	SHEATH THERMOCOUPLE, ROD 27, LEVEL D
TE-327BD	SHEATH THERMOCOUPLE, ROD 27, LEVEL D
TE-327CD	SHEATH THERMOCOUPLE, ROD 27, LEVEL D
TE-328AD	SHEATH THERMOCOUPLE, ROD 28, LEVEL D
TE-328BD	SHEATH THERMOCOUPLE, ROD 28, LEVEL D
TE-328CD	SHEATH THERMOCOUPLE, ROD 28, LEVEL D
TE-329AD	SHEATH THERMOCOUPLE, ROD 29, LEVEL D
TE-329BD	SHEATH THERMOCOUPLE, ROD 29, LEVEL D
TE-329CD	SHEATH THERMOCOUPLE, ROD 29, LEVEL D
TE-331CD	SHEATH THERMOCOUPLE, ROD 31, LEVEL D
TE-332CD	SHEATH THERMOCOUPLE, ROD 32, LEVEL D
TE-333AD	SHEATH THERMOCOUPLE, ROD 33, LEVEL D
TE-335AD	SHEATH THERMOCOUPLE, ROD 35, LEVEL D
TE-335BD	SHEATH THERMOCOUPLE, ROD 35, LEVEL D
TE-337BD	SHEATH THERMOCOUPLE, ROD 37, LEVEL D
TE-337CD	SHEATH THERMOCOUPLE, ROD 37, LEVEL D
TE-338BD	SHEATH THERMOCOUPLE, ROD 38, LEVEL D
TE-338CD	SHEATH THERMOCOUPLE, ROD 38, LEVEL D
TE-339BD	SHEATH THERMOCOUPLE, ROD 39, LEVEL D
TE-340BD	SHEATH THERMOCOUPLE, ROD 40, LEVEL D
TE-342BD	SHEATH THERMOCOUPLE, ROD 42, LEVEL D
TE-343AD	SHEATH THERMOCOUPLE, ROD 43, LEVEL D
TE-343BD	SHEATH THERMOCOUPLE, ROD 43, LEVEL D
TE-344AD	SHEATH THERMOCOUPLE, ROD 44, LEVEL D
TE-344CD	SHEATH THERMOCOUPLE, ROD 44, LEVEL D
TE-345AD	SHEATH THERMOCOUPLE, ROD 45, LEVEL D
TE-345BD	SHEATH THERMOCOUPLE, ROD 45, LEVEL D
TE-349CD	SHEATH THERMOCOUPLE, ROD 49, LEVEL D
TE-350AD	SHEATH THERMOCOUPLE, ROD 50, LEVEL D
TE-350BD	SHEATH THERMOCOUPLE, ROD 50, LEVEL D
TE-350CD	SHEATH THERMOCOUPLE, ROD 50, LEVEL D
TE-351BD	SHEATH THERMOCOUPLE, ROD 51, LEVEL D
TE-354AD	SHEATH THERMOCOUPLE, ROD 54, LEVEL D
TE-355CD	SHEATH THERMOCOUPLE, ROD 55, LEVEL D
TE-356CD	SHEATH THERMOCOUPLE, ROD 56, LEVEL D
TE-357BD	SHEATH THERMOCOUPLE, ROD 57, LEVEL D
TE-357CD	SHEATH THERMOCOUPLE, ROD 57, LEVEL D
TE-358AD	SHEATH THERMOCOUPLE, ROD 58, LEVEL D
TE-358CD	SHEATH THERMOCOUPLE, ROD 58, LEVEL D
TE-359AD	SHEATH THERMOCOUPLE, ROD 59, LEVEL D

Table 2 (continued)

SENSOR	DESCRIPTION
BUNDLE TEMPERATURE (CONT.)	
SHEATH THERMOCOUPLES (CONT.)	
LEVEL D (CONT.)	
TE-360AD	SHEATH THERMOCOUPLE, ROD 60, LEVEL D
TE-360BD	SHEATH THERMOCOUPLE, ROD 60, LEVEL D
TE-360CD	SHEATH THERMOCOUPLE, ROD 60, LEVEL D
TE-361AD	SHEATH THERMOCOUPLE, ROD 61, LEVEL D
TE-362CD	SHEATH THERMOCOUPLE, ROD 62, LEVEL D
TE-364AD	SHEATH THERMOCOUPLE, ROD 64, LEVEL D
TE-364BD	SHEATH THERMOCOUPLE, ROD 64, LEVEL D
TE-364CD	SHEATH THERMOCOUPLE, ROD 64, LEVEL D
LEVEL E	
TE-302AE	SHEATH THERMOCOUPLE, ROD 2, LEVEL E
TE-303BE	SHEATH THERMOCOUPLE, ROD 3, LEVEL E
TE-303CE	SHEATH THERMOCOUPLE, ROD 3, LEVEL E
TE-304AE	SHEATH THERMOCOUPLE, ROD 4, LEVEL E
TE-304BE	SHEATH THERMOCOUPLE, ROD 4, LEVEL E
TE-304CE	SHEATH THERMOCOUPLE, ROD 4, LEVEL E
TE-307BE	SHEATH THERMOCOUPLE, ROD 7, LEVEL E
TE-307CE	SHEATH THERMOCOUPLE, ROD 7, LEVEL E
TE-310AE	SHEATH THERMOCOUPLE, ROD 10, LEVEL E
TE-310BE	SHEATH THERMOCOUPLE, ROD 10, LEVEL E
TE-312AE	SHEATH THERMOCOUPLE, ROD 12, LEVEL E
TE-313AE	SHEATH THERMOCOUPLE, ROD 13, LEVEL E
TE-313CE	SHEATH THERMOCOUPLE, ROD 13, LEVEL E
TE-316BE	SHEATH THERMOCOUPLE, ROD 16, LEVEL E
TE-316CE	SHEATH THERMOCOUPLE, ROD 16, LEVEL E
TE-317AE	SHEATH THERMOCOUPLE, ROD 17, LEVEL E
TE-317BE	SHEATH THERMOCOUPLE, ROD 17, LEVEL E
TE-317CE	SHEATH THERMOCOUPLE, ROD 17, LEVEL E
TE-318AE	SHEATH THERMOCOUPLE, ROD 18, LEVEL E
TE-318BE	SHEATH THERMOCOUPLE, ROD 18, LEVEL E
TE-318CE	SHEATH THERMOCOUPLE, ROD 18, LEVEL E
TE-320AE	SHEATH THERMOCOUPLE, ROD 20, LEVEL E
TE-320BE	SHEATH THERMOCOUPLE, ROD 20, LEVEL E
TE-320CE	SHEATH THERMOCOUPLE, ROD 20, LEVEL E
TE-324AE	SHEATH THERMOCOUPLE, ROD 24, LEVEL E
TE-324CE	SHEATH THERMOCOUPLE, ROD 24, LEVEL E
TE-326AE	SHEATH THERMOCOUPLE, ROD 26, LEVEL E
TE-326BE	SHEATH THERMOCOUPLE, ROD 26, LEVEL E
TE-326CE	SHEATH THERMOCOUPLE, ROD 26, LEVEL E
TE-328AE	SHEATH THERMOCOUPLE, ROD 28, LEVEL E
TE-328CE	SHEATH THERMOCOUPLE, ROD 28, LEVEL E
TE-329AE	SHEATH THERMOCOUPLE, ROD 29, LEVEL E
TE-329BE	SHEATH THERMOCOUPLE, ROD 29, LEVEL E
TE-329CE	SHEATH THERMOCOUPLE, ROD 29, LEVEL E
TE-330AE	SHEATH THERMOCOUPLE, ROD 30, LEVEL E

Table 2 (continued)

SENSOR	DESCRIPTION
BUNDLE TEMPERATURE (CONT.)	
SHEATH THERMOCOUPLES (CONT.)	
LEVEL E (CONT.)	
TE-330BE	SHEATH THERMOCOUPLE, ROD 30, LEVEL E
TE-331CE	SHEATH THERMOCOUPLE, ROD 31, LEVEL E
TE-332AE	SHEATH THERMOCOUPLE, ROD 32, LEVEL E
TE-332CE	SHEATH THERMOCOUPLE, ROD 32, LEVEL E
TE-333AE	SHEATH THERMOCOUPLE, ROD 33, LEVEL E
TE-333BE	SHEATH THERMOCOUPLE, ROD 33, LEVEL E
TE-333CE	SHEATH THERMOCOUPLE, ROD 33, LEVEL E
TE-335AE	SHEATH THERMOCOUPLE, ROD 35, LEVEL E
TE-335BE	SHEATH THERMOCOUPLE, ROD 35, LEVEL E
TE-335CE	SHEATH THERMOCOUPLE, ROD 35, LEVEL E
TE-337AE	SHEATH THERMOCOUPLE, ROD 37, LEVEL E
TE-337BE	SHEATH THERMOCOUPLE, ROD 37, LEVEL E
TE-342BE	SHEATH THERMOCOUPLE, ROD 42, LEVEL E
TE-344AE	SHEATH THERMOCOUPLE, ROD 44, LEVEL E
TE-344CE	SHEATH THERMOCOUPLE, ROD 44, LEVEL E
TE-345AE	SHEATH THERMOCOUPLE, ROD 45, LEVEL E
TE-345BE	SHEATH THERMOCOUPLE, ROD 45, LEVEL E
TE-349AE	SHEATH THERMOCOUPLE, ROD 49, LEVEL E
TE-349BE	SHEATH THERMOCOUPLE, ROD 49, LEVEL E
TE-349CE	SHEATH THERMOCOUPLE, ROD 49, LEVEL E
TE-350BE	SHEATH THERMOCOUPLE, ROD 50, LEVEL E
TE-350CE	SHEATH THERMOCOUPLE, ROD 50, LEVEL E
TE-351AE	SHEATH THERMOCOUPLE, ROD 51, LEVEL E
TE-351BE	SHEATH THERMOCOUPLE, ROD 51, LEVEL E
TE-353AE	SHEATH THERMOCOUPLE, ROD 53, LEVEL E
TE-353BE	SHEATH THERMOCOUPLE, ROD 53, LEVEL E
TE-356AE	SHEATH THERMOCOUPLE, ROD 56, LEVEL E
TE-358AE	SHEATH THERMOCOUPLE, ROD 58, LEVEL E
TE-358BE	SHEATH THERMOCOUPLE, ROD 58, LEVEL E
TE-359AE	SHEATH THERMOCOUPLE, ROD 59, LEVEL E
TE-359BE	SHEATH THERMOCOUPLE, ROD 59, LEVEL E
TE-359CE	SHEATH THERMOCOUPLE, ROD 59, LEVEL E
TE-361AE	SHEATH THERMOCOUPLE, ROD 61, LEVEL E
TE-361BE	SHEATH THERMOCOUPLE, ROD 61, LEVEL E
TE-361CE	SHEATH THERMOCOUPLE, ROD 61, LEVEL E
TE-362AE	SHEATH THERMOCOUPLE, ROD 62, LEVEL E
TE-363AE	SHEATH THERMOCOUPLE, ROD 63, LEVEL E
TE-363BE	SHEATH THERMOCOUPLE, ROD 63, LEVEL E
TE-364AE	SHEATH THERMOCOUPLE, ROD 64, LEVEL E
TE-364BE	SHEATH THERMOCOUPLE, ROD 64, LEVEL E
LEVEL F	
TE-303BF	SHEATH THERMOCOUPLE, ROD 3, LEVEL F
TE-304AF	SHEATH THERMOCOUPLE, ROD 4, LEVEL F
TE-307AF	SHEATH THERMOCOUPLE, ROD 7, LEVEL F

Table 2 (continued)

SENSOR	DESCRIPTION
BUNDLE TEMPERATURE (CONT.)	
SHEATH THERMOCOUPLES (CONT.)	
LEVEL F (CONT.)	
TE-307BF	SHEATH THERMOCOUPLE, ROD 7, LEVEL F
TE-310AF	SHEATH THERMOCOUPLE, ROD 10, LEVEL F
TE-310BF	SHEATH THERMOCOUPLE, ROD 10, LEVEL F
TE-310CF	SHEATH THERMOCOUPLE, ROD 10, LEVEL F
TE-313BF	SHEATH THERMOCOUPLE, ROD 13, LEVEL F
TE-313CF	SHEATH THERMOCOUPLE, ROD 13, LEVEL F
TE-315AF	SHEATH THERMOCOUPLE, ROD 15, LEVEL F
TE-316BF	SHEATH THERMOCOUPLE, ROD 16, LEVEL F
TE-316CF	SHEATH THERMOCOUPLE, ROD 16, LEVEL F
TE-318AF	SHEATH THERMOCOUPLE, ROD 18, LEVEL F
TE-318BF	SHEATH THERMOCOUPLE, ROD 18, LEVEL F
TE-318CF	SHEATH THERMOCOUPLE, ROD 18, LEVEL F
TE-320AF	SHEATH THERMOCOUPLE, ROD 20, LEVEL F
TE-320BF	SHEATH THERMOCOUPLE, ROD 20, LEVEL F
TE-320CF	SHEATH THERMOCOUPLE, ROD 20, LEVEL F
TE-328AF	SHEATH THERMOCOUPLE, ROD 28, LEVEL F
TE-328BF	SHEATH THERMOCOUPLE, ROD 28, LEVEL F
TE-328CF	SHEATH THERMOCOUPLE, ROD 26, LEVEL F
TE-331BF	SHEATH THERMOCOUPLE, ROD 31, LEVEL F
TE-331CF	SHEATH THERMOCOUPLE, ROD 31, LEVEL F
TE-332CF	SHEATH THERMOCOUPLE, ROD 32, LEVEL F
TE-337BF	SHEATH THERMOCOUPLE, ROD 37, LEVEL F
TE-337CF	SHEATH THERMOCOUPLE, ROD 37, LEVEL F
TE-342BF	SHEATH THERMOCOUPLE, ROD 42, LEVEL F
TE-345AF	SHEATH THERMOCOUPLE, ROD 45, LEVEL F
TE-345BF	SHEATH THERMOCOUPLE, ROD 45, LEVEL F
TE-345CF	SHEATH THERMOCOUPLE, ROD 45, LEVEL F
TE-347CF	SHEATH THERMOCOUPLE, ROD 47, LEVEL F
TE-350AF	SHEATH THERMOCOUPLE, ROD 50, LEVEL F
TE-350BF	SHEATH THERMOCOUPLE, ROD 50, LEVEL F
TE-350CF	SHEATH THERMOCOUPLE, ROD 50, LEVEL F
TE-353BF	SHEATH THERMOCOUPLE, ROD 59, LEVEL F
TE-356AF	SHEATH THERMOCOUPLE, ROD 56, LEVEL F
TE-358BF	SHEATH THERMOCOUPLE, ROD 58, LEVEL F
TE-359AF	SHEATH THERMOCOUPLE, ROD 59, LEVEL F
TE-359BF	SHEATH THERMOCOUPLE, ROD 59, LEVEL F
TE-359CF	SHEATH THERMOCOUPLE, ROD 59, LEVEL F
TE-364AF	SHEATH THERMOCOUPLE, ROD 64, LEVEL F
TE-364BF	SHEATH THERMOCOUPLE, ROD 64, LEVEL F
TE-364CF	SHEATH THERMOCOUPLE, ROD 64, LEVEL F
LEVEL G	
TE-303CG	SHEATH THERMOCOUPLE, ROD 3, LEVEL G
TE-316BG	SHEATH THERMOCOUPLE, ROD 16, LEVEL G
TE-316CG	SHEATH THERMOCOUPLE, ROD 16, LEVEL G

Table 2 (continued)

SENSOR	DESCRIPTION
BUNDLE TEMPERATURE (CONT.)	
SHEATH THERMOCOUPLES (CONT.)	
LEVEL G (CONT.)	
TE-318AG	SHEATH THERMOCOUPLE, ROD 18, LEVEL G
TE-318BG	SHEATH THERMOCOUPLE, ROD 18, LEVEL G
TE-318CG	SHEATH THERMOCOUPLE, ROD 18, LEVEL G
TE-320AG	SHEATH THERMOCOUPLE, ROD 20, LEVEL G
TE-320BG	SHEATH THERMOCOUPLE, ROD 20, LEVEL G
TE-320CG	SHEATH THERMOCOUPLE, ROD 20, LEVEL G
TE-332CG	SHEATH THERMOCOUPLE, ROD 32, LEVEL G
TE-342AG	SHEATH THERMOCOUPLE, ROD 42, LEVEL G
TE-342BG	SHEATH THERMOCOUPLE, ROD 42, LEVEL G
TE-342CG	SHEATH THERMOCOUPLE, ROD 42, LEVEL G
TE-345AG	SHEATH THERMOCOUPLE, ROD 45, LEVEL G
TE-345BG	SHEATH THERMOCOUPLE, ROD 45, LEVEL G
TE-345CG	SHEATH THERMOCOUPLE, ROD 45, LEVEL G
TE-347CG	SHEATH THERMOCOUPLE, ROD 47, LEVEL G
TE-358CG	SHEATH THERMOCOUPLE, ROD 58, LEVEL G
TE-364AG	SHEATH THERMOCOUPLE, ROD 64, LEVEL G
TE-364CG	SHEATH THERMOCOUPLE, ROD 64, LEVEL G
LEVEL J	
TE-361CJ	SHEATH THERMOCOUPLE, ROD 61, LEVEL J
TE-361BJ	SHEATH THERMOCOUPLE, ROD 61, LEVEL J
MIDDLE THERMOCOUPLES	
LEVEL A	
TE-306MA	MIDDLE THERMOCOUPLE, ROD 6, LEVEL A
TE-311MA	MIDDLE THERMOCOUPLE, ROD 11, LEVEL A
TE-314MA	MIDDLE THERMOCOUPLE, ROD 14, LEVEL A
TE-321MA	MIDDLE THERMOCOUPLE, ROD 21, LEVEL A
TE-325MA	MIDDLE THERMOCOUPLE, ROD 25, LEVEL A
TE-338MA	MIDDLE THERMOCOUPLE, ROD 38, LEVEL A
TE-340MA	MIDDLE THERMOCOUPLE, ROD 40, LEVEL A
TE-341MA	MIDDLE THERMOCOUPLE, ROD 41, LEVEL A
TE-343MA	MIDDLE THERMOCOUPLE, ROD 43, LEVEL A
TE-354MA	MIDDLE THERMOCOUPLE, ROD 54, LEVEL A
TE-355MA	MIDDLE THERMOCOUPLE, ROD 55, LEVEL A
TE-357MA	MIDDLE THERMOCOUPLE, ROD 57, LEVEL A
TE-360MA	MIDDLE THERMOCOUPLE, ROD 60, LEVEL A
LEVEL B	
TE-302MB	MIDDLE THERMOCOUPLE, ROD 2, LEVEL B
TE-308MB	MIDDLE THERMOCOUPLE, ROD 8, LEVEL B
TE-309MB	MIDDLE THERMOCOUPLE, ROD 9, LEVEL B
TE-312MB	MIDDLE THERMOCOUPLE, ROD 12, LEVEL B
TE-314MB	MIDDLE THERMOCOUPLE, ROD 14, LEVEL B

Table 2 (continued)

BUNDLE TEMPERATURE (CONT.)

MIDDLE THERMOCOUPLES (CONT.)

SENSOR	DESCRIPTION
LEVEL B (CONT.)	
TE-321MB	MIDDLE THERMOCOUPLE, ROD 21, LEVEL B
TE-325MB	MIDDLE THERMOCOUPLE, ROD 25, LEVEL B
TE-327MB	MIDDLE THERMOCOUPLE, ROD 27, LEVEL B
TE-329MB	MIDDLE THERMOCOUPLE, ROD 29, LEVEL B
TE-330MB	MIDDLE THERMOCOUPLE, ROD 30, LEVEL B
TE-335MB	MIDDLE THERMOCOUPLE, ROD 35, LEVEL B
TE-338MB	MIDDLE THERMOCOUPLE, ROD 38, LEVEL B
TE-339MB	MIDDLE THERMOCOUPLE, ROD 39, LEVEL B
TE-340MB	MIDDLE THERMOCOUPLE, ROD 40, LEVEL B
TE-341MB	MIDDLE THERMOCOUPLE, ROD 41, LEVEL B
TE-343MB	MIDDLE THERMOCOUPLE, ROD 43, LEVEL B
TE-344MB	MIDDLE THERMOCOUPLE, ROD 44, LEVEL B
TE-349MB	MIDDLE THERMOCOUPLE, ROD 49, LEVEL B
TE-354MB	MIDDLE THERMOCOUPLE, ROD 54, LEVEL B
TE-355MB	MIDDLE THERMOCOUPLE, ROD 55, LEVEL B
TE-357MB	MIDDLE THERMOCOUPLE, ROD 57, LEVEL B
TE-360MB	MIDDLE THERMOCOUPLE, ROD 60, LEVEL B
TE-361MB	MIDDLE THERMOCOUPLE, ROD 61, LEVEL B
TE-362MB	MIDDLE THERMOCOUPLE, ROD 62, LEVEL B
TE-363MB	MIDDLE THERMOCOUPLE, ROD 63, LEVEL B
LEVEL C	
TE-302MC	MIDDLE THERMOCOUPLE, ROD 2, LEVEL C
TE-304MC	MIDDLE THERMOCOUPLE, ROD 4, LEVEL C
TE-306MC	MIDDLE THERMOCOUPLE, ROD 6, LEVEL C
TE-307MC	MIDDLE THERMOCOUPLE, ROD 7, LEVEL C
TE-308MC	MIDDLE THERMOCOUPLE, ROD 8, LEVEL C
TE-309MC	MIDDLE THERMOCOUPLE, ROD 9, LEVEL C
TE-310MC	MIDDLE THERMOCOUPLE, ROD 10, LEVEL C
TE-311MC	MIDDLE THERMOCOUPLE, ROD 11, LEVEL C
TE-312MC	MIDDLE THERMOCOUPLE, ROD 12, LEVEL C
TE-314MC	MIDDLE THERMOCOUPLE, ROD 14, LEVEL C
TE-315MC	MIDDLE THERMOCOUPLE, ROD 15, LEVEL C
TE-324MC	MIDDLE THERMOCOUPLE, ROD 24, LEVEL C
TE-325MC	MIDDLE THERMOCOUPLE, ROD 25, LEVEL C
TE-326MC	MIDDLE THERMOCOUPLE, ROD 26, LEVEL C
TE-328MC	MIDDLE THERMOCOUPLE, ROD 28, LEVEL C
TE-329MC	MIDDLE THERMOCOUPLE, ROD 29, LEVEL C
TE-330MC	MIDDLE THERMOCOUPLE, ROD 30, LEVEL C
TE-333MC	MIDDLE THERMOCOUPLE, ROD 33, LEVEL C
TE-335MC	MIDDLE THERMOCOUPLE, ROD 35, LEVEL C
TE-337MC	MIDDLE THERMOCOUPLE, ROD 37, LEVEL C
TE-338MC	MIDDLE THERMOCOUPLE, ROD 38, LEVEL C
TE-339MC	MIDDLE THERMOCOUPLE, ROD 39, LEVEL C
TE-340MC	MIDDLE THERMOCOUPLE, ROD 40, LEVEL C

Table 2 (continued)

SENSOR	DESCRIPTION
BUNDLE TEMPERATURE (CONT.)	
MIDDLE THERMOCOUPLES (CONT.)	
LEVEL C (CONT.)	
TE-341MC	MIDDLE THERMOCOUPLE, ROD 41, LEVEL C
TE-343MC	MIDDLE THERMOCOUPLE, ROD 43, LEVEL C
TE-344MC	MIDDLE THERMOCOUPLE, ROD 44, LEVEL C
TE-349MC	MIDDLE THERMOCOUPLE, ROD 49, LEVEL C
TE-350MC	MIDDLE THERMOCOUPLE, ROD 50, LEVEL C
TE-351MC	MIDDLE THERMOCOUPLE, ROD 51, LEVEL C
TE-353MC	MIDDLE THERMOCOUPLE, ROD 53, LEVEL C
TE-354MC	MIDDLE THERMOCOUPLE, ROD 54, LEVEL C
TE-355MC	MIDDLE THERMOCOUPLE, ROD 55, LEVEL C
TE-356MC	MIDDLE THERMOCOUPLE, ROD 56, LEVEL C
TE-357MC	MIDDLE THERMOCOUPLE, ROD 57, LEVEL C
TE-359MC	MIDDLE THERMOCOUPLE, ROD 59, LEVEL C
TE-360MC	MIDDLE THERMOCOUPLE, ROD 60, LEVEL C
TE-361MC	MIDDLE THERMOCOUPLE, ROD 61, LEVEL C
TE-362MC	MIDDLE THERMOCOUPLE, ROD 62, LEVEL C
TE-363MC	MIDDLE THERMOCOUPLE, ROD 63, LEVEL C
LEVEL U	
TE-305MU	MIDDLE THERMOCOUPLE, ROD 5, LEVEL U
TE-348MU	MIDDLE THERMOCOUPLE, ROD 48, LEVEL U
TE-352MU	MIDDLE THERMOCOUPLE, ROD 52, LEVEL U
LEVEL H	
TE-305MH	MIDDLE THERMOCOUPLE, ROD 5, LEVEL H
TE-334MH	MIDDLE THERMOCOUPLE, ROD 34, LEVEL H
TE-348MH	MIDDLE THERMOCOUPLE, ROD 48, LEVEL H
TE-352MH	MIDDLE THERMOCOUPLE, ROD 52, LEVEL H
LEVEL S	
TE-305MS	MIDDLE THERMOCOUPLE, ROD 5, LEVEL S
TE-334MS	MIDDLE THERMOCOUPLE, ROD 34, LEVEL S
TE-348MS	MIDDLE THERMOCOUPLE, ROD 48, LEVEL S
TE-352MS	MIDDLE THERMOCOUPLE, ROD 52, LEVEL S
LEVEL Y	
TE-305MY	MIDDLE THERMOCOUPLE, ROD 5, LEVEL Y
TE-348MY	MIDDLE THERMOCOUPLE, ROD 48, LEVEL Y
TE-352MY	MIDDLE THERMOCOUPLE, ROD 52, LEVEL Y
LEVEL D	
TE-302MD	MIDDLE THERMOCOUPLE, ROD 2, LEVEL D
TE-303MD	MIDDLE THERMOCOUPLE, ROD 3, LEVEL D
TE-304MD	MIDDLE THERMOCOUPLE, ROD 4, LEVEL D
TE-306MD	MIDDLE THERMOCOUPLE, ROD 6, LEVEL D
TE-307MD	MIDDLE THERMOCOUPLE, ROD 7, LEVEL D

Table 2 (continued)

SENSOR	DESCRIPTION
BUNDLE TEMPERATURE (CONT.)	
MIDDLE THERMOCOUPLES (CONT.)	
LEVEL D (CONT.)	
TE-308MD	MIDDLE THERMOCOUPLE, ROD 8, LEVEL D
TE-310MD	MIDDLE THERMOCOUPLE, ROD 10, LEVEL D
TE-311MD	MIDDLE THERMOCOUPLE, ROD 11, LEVEL D
TE-312MD	MIDDLE THERMOCOUPLE, ROD 12, LEVEL D
TE-315MD	MIDDLE THERMOCOUPLE, ROD 15, LEVEL D
TE-316MD	MIDDLE THERMOCOUPLE, ROD 16, LEVEL D
TE-318MD	MIDDLE THERMOCOUPLE, ROD 18, LEVEL D
TE-320MD	MIDDLE THERMOCOUPLE, ROD 20, LEVEL D
TE-321MD	MIDDLE THERMOCOUPLE, ROD 21, LEVEL D
TE-324MD	MIDDLE THERMOCOUPLE, ROD 24, LEVEL D
TE-325MD	MIDDLE THERMOCOUPLE, ROD 25, LEVEL D
TE-326MD	MIDDLE THERMOCOUPLE, ROD 26, LEVEL D
TE-328MD	MIDDLE THERMOCOUPLE, ROD 28, LEVEL D
TE-329MD	MIDDLE THERMOCOUPLE, ROD 29, LEVEL D
TE-332MD	MIDDLE THERMOCOUPLE, ROD 32, LEVEL D
TE-335MD	MIDDLE THERMOCOUPLE, ROD 35, LEVEL D
TE-337MD	MIDDLE THERMOCOUPLE, ROD 37, LEVEL D
TE-338MD	MIDDLE THERMOCOUPLE, ROD 38, LEVEL D
TE-339MD	MIDDLE THERMOCOUPLE, ROD 39, LEVEL D
TE-341MD	MIDDLE THERMOCOUPLE, ROD 41, LEVEL D
TE-343MD	MIDDLE THERMOCOUPLE, ROD 43, LEVEL D
TE-345MD	MIDDLE THERMOCOUPLE, ROD 45, LEVEL D
TE-347MD	MIDDLE THERMOCOUPLE, ROD 47, LEVEL D
TE-349MD	MIDDLE THERMOCOUPLE, ROD 49, LEVEL D
TE-350MD	MIDDLE THERMOCOUPLE, ROD 50, LEVEL D
TE-353MD	MIDDLE THERMOCOUPLE, ROD 53, LEVEL D
TE-354MD	MIDDLE THERMOCOUPLE, ROD 54, LEVEL D
TE-355MD	MIDDLE THERMOCOUPLE, ROD 55, LEVEL D
TE-356MD	MIDDLE THERMOCOUPLE, ROD 56, LEVEL D
TE-357MD	MIDDLE THERMOCOUPLE, ROD 57, LEVEL D
TE-358MD	MIDDLE THERMOCOUPLE, ROD 58, LEVEL D
TE-360MD	MIDDLE THERMOCOUPLE, ROD 60, LEVEL D
TE-361MD	MIDDLE THERMOCOUPLE, ROD 61, LEVEL D
TE-363MD	MIDDLE THERMOCOUPLE, ROD 63, LEVEL D
TE-364MD	MIDDLE THERMOCOUPLE, ROD 64, LEVEL D
LEVEL E	
TE-303ME	MIDDLE THERMOCOUPLE, ROD 3, LEVEL E
TE-304ME	MIDDLE THERMOCOUPLE, ROD 4, LEVEL E
TE-307ME	MIDDLE THERMOCOUPLE, ROD 7, LEVEL E
TE-310ME	MIDDLE THERMOCOUPLE, ROD 10, LEVEL E
TE-312ME	MIDDLE THERMOCOUPLE, ROD 12, LEVEL E
TE-316ME	MIDDLE THERMOCOUPLE, ROD 16, LEVEL E
TE-317ME	MIDDLE THERMOCOUPLE, ROD 17, LEVEL E
TE-318ME	MIDDLE THERMOCOUPLE, ROD 18, LEVEL E

Table 2 (continued)

SENSOR	DESCRIPTION
BUNDLE TEMPERATURE (CONT.)	
MIDDLE THERMOCOUPLES (CONT.)	
LEVEL E (CONT.)	
TE-324ME	MIDDLE THERMOCOUPLE, ROD 24, LEVEL E
TE-326ME	MIDDLE THERMOCOUPLE, ROD 26, LEVEL E
TE-328ME	MIDDLE THERMOCOUPLE, ROD 28, LEVEL E
TE-329ME	MIDDLE THERMOCOUPLE, ROD 29, LEVEL E
TE-330ME	MIDDLE THERMOCOUPLE, ROD 30, LEVEL E
TE-332ME	MIDDLE THERMOCOUPLE, ROD 32, LEVEL E
TE-335ME	MIDDLE THERMOCOUPLE, ROD 35, LEVEL E
TE-337ME	MIDDLE THERMOCOUPLE, ROD 37, LEVEL E
TE-339ME	MIDDLE THERMOCOUPLE, ROD 39, LEVEL E
TE-344ME	MIDDLE THERMOCOUPLE, ROD 44, LEVEL E
TE-345ME	MIDDLE THERMOCOUPLE, ROD 45, LEVEL E
TE-347ME	MIDDLE THERMOCOUPLE, ROD 47, LEVEL E
TE-349ME	MIDDLE THERMOCOUPLE, ROD 49, LEVEL E
TE-350ME	MIDDLE THERMOCOUPLE, ROD 50, LEVEL E
TE-353ME	MIDDLE THERMOCOUPLE, ROD 53, LEVEL E
TE-356ME	MIDDLE THERMOCOUPLE, ROD 56, LEVEL E
TE-358ME	MIDDLE THERMOCOUPLE, ROD 58, LEVEL E
TE-359ME	MIDDLE THERMOCOUPLE, ROD 59, LEVEL E
TE-362ME	MIDDLE THERMOCOUPLE, ROD 62, LEVEL E
TE-363ME	MIDDLE THERMOCOUPLE, ROD 63, LEVEL E
LEVEL F	
TE-303MF	MIDDLE THERMOCOUPLE, ROD 3, LEVEL F
TE-304MF	MIDDLE THERMOCOUPLE, ROD 4, LEVEL F
TE-307MF	MIDDLE THERMOCOUPLE, ROD 7, LEVEL F
TE-316MF	MIDDLE THERMOCOUPLE, ROD 16, LEVEL F
TE-318MF	MIDDLE THERMOCOUPLE, ROD 18, LEVEL F
TE-328MF	MIDDLE THERMOCOUPLE, ROD 28, LEVEL F
TE-331MF	MIDDLE THERMOCOUPLE, ROD 31, LEVEL F
TE-337MF	MIDDLE THERMOCOUPLE, ROD 37, LEVEL F
TE-347MF	MIDDLE THERMOCOUPLE, ROD 47, LEVEL F
TE-350MF	MIDDLE THERMOCOUPLE, ROD 50, LEVEL F
TE-356MF	MIDDLE THERMOCOUPLE, ROD 56, LEVEL F
TE-358MF	MIDDLE THERMOCOUPLE, ROD 58, LEVEL F
TE-359MF	MIDDLE THERMOCOUPLE, ROD 59, LEVEL F
TE-364MF	MIDDLE THERMOCOUPLE, ROD 64, LEVEL F
LEVEL G	
TE-303MG	MIDDLE THERMOCOUPLE, ROD 3, LEVEL G
TE-316MG	MIDDLE THERMOCOUPLE, ROD 16, LEVEL G
TE-320MG	MIDDLE THERMOCOUPLE, ROD 20, LEVEL G
TE-332MG	MIDDLE THERMOCOUPLE, ROD 32, LEVEL G
TE-345MG	MIDDLE THERMOCOUPLE, ROD 45, LEVEL G
TE-347MG	MIDDLE THERMOCOUPLE, ROD 47, LEVEL G
TE-358MG	MIDDLE THERMOCOUPLE, ROD 58, LEVEL G

Table 2 (continued)

SENSOR	DESCRIPTION
BUNDLE TEMPERATURE (CONT.)	
MIDDLE THERMOCOUPLES (CONT.)	
LEVEL G (CONT.)	
TE-364MG	MIDDLE THERMOCOUPLE, ROD 64, LEVEL G
SHROUD BOX THERMOCOUPLES	
LEVEL A	
TE-181W	SHROUD BOX THERMOCOUPLE, LEVEL A, WEST SIDE
LEVEL B	
TE-182E	SHROUD BOX THERMOCOUPLE, LEVEL B, EAST SIDE
TE-182S	SHROUD BOX THERMOCOUPLE, LEVEL B, SOUTH SIDE
LEVEL C	
TE-183N	SHROUD BOX THERMOCOUPLE, LEVEL C, NORTH SIDE
TE-183W	SHROUD BOX THERMOCOUPLE, LEVEL C, WEST SIDE
LEVEL D	
TE-184E	SHROUD BOX THERMOCOUPLE, LEVEL D, EAST SIDE
TE-184S	SHROUD BOX THERMOCOUPLE, LEVEL D, SOUTH SIDE
LEVEL E	
TE-185W	SHROUD BOX THERMOCOUPLE, LEVEL E, WEST SIDE
LEVEL G	
TE-186E	SHROUD BOX THERMOCOUPLE, LEVEL G, EAST SIDE
TE-186S	SHROUD BOX THERMOCOUPLE, LEVEL G, SOUTH SIDE
TE-187N	SHROUD BOX THERMOCOUPLE, LEVEL G, NORTH SIDE
TE-187W	SHROUD BOX THERMOCOUPLE, LEVEL G, WEST SIDE
THERMOCOUPLE ARRAY ROD	
LEVEL A	
TE-188AA	ARRAY ROD THERMOCOUPLE, GRID 19, SUBCHANNEL 22, LEVEL A
TE-188BA	ARRAY ROD THERMOCOUPLE, GRID 19, SUBCHANNEL 30, LEVEL A
LEVEL B	
TE-188AB	ARRAY ROD THERMOCOUPLE, GRID 19, SUBCHANNEL 22, LEVEL B
TE-188BB	ARRAY ROD THERMOCOUPLE, GRID 19, SUBCHANNEL 30, LEVEL B
LEVEL C	
TE-188AC	ARRAY ROD THERMOCOUPLE, GRID 19, SUBCHANNEL 22, LEVEL C
TE-188BC	ARRAY ROD THERMOCOUPLE, GRID 19, SUBCHANNEL 30, LEVEL C
LEVEL D	
TE-188AD	ARRAY ROD THERMOCOUPLE, GRID 19, SUBCHANNEL 22, LEVEL D
TE-188BD	ARRAY ROD THERMOCOUPLE, GRID 19, SUBCHANNEL 30, LEVEL D

Table 2 (continued)

SENSOR	DESCRIPTION
BUNDLE TEMPERATURE (CONT.)	
THERMOCOUPLE ARRAY ROD (CONT.)	
LEVEL E	
TE-188AE	ARRAY ROD THERMOCOUPLE, GRID 19, SUBCHANNEL 22, LEVEL E
TE-188BE	ARRAY ROD THERMOCOUPLE, GRID 19, SUBCHANNEL 30, LEVEL E
LEVEL F	
TE-188AF	ARRAY ROD THERMOCOUPLE, GRID 19, SUBCHANNEL 22, LEVEL F
TE-188BF	ARRAY ROD THERMOCOUPLE, GRID 19, SUBCHANNEL 30, LEVEL F
LEVEL G	
TE-188AG	ARRAY ROD THERMOCOUPLE, GRID 19, SUBCHANNEL 22, LEVEL G
SPACER GRID THERMOCOUPLES	
GRID NO. 2	
TE-291A	SPACER GRID NUMBER 2 THERMOCOUPLE, SUBCHANNEL 32
TE-291B	SPACER GRID NUMBER 2 THERMOCOUPLE, SUBCHANNEL 43
TE-291C	SPACER GRID NUMBER 2 THERMOCOUPLE, SUBCHANNEL 57
TE-291D	SPACER GRID NUMBER 2 THERMOCOUPLE, SUBCHANNEL 70
GRID NO. 3	
TE-292A	SPACER GRID NUMBER 3 THERMOCOUPLE, SUBCHANNEL 32
TE-292B	SPACER GRID NUMBER 3 THERMOCOUPLE, SUBCHANNEL 43
TE-292D	SPACER GRID NUMBER 3 THERMOCOUPLE, SUBCHANNEL 70
GRID NO. 4	
TE-293A	SPACER GRID NUMBER 4 THERMOCOUPLE, SUBCHANNEL 32
TE-293B	SPACER GRID NUMBER 4 THERMOCOUPLE, SUBCHANNEL 43
TE-293C	SPACER GRID NUMBER 4 THERMOCOUPLE, SUBCHANNEL 57
TE-293D	SPACER GRID NUMBER 4 THERMOCOUPLE, SUBCHANNEL 70
TE-293E	SPACER GRID NUMBER 4 THERMOCOUPLE, SUBCHANNEL 17
TE-293F	SPACER GRID NUMBER 4 THERMOCOUPLE, SUBCHANNEL 38
GRID NO. 5	
TE-294B	SPACER GRID NUMBER 5 THERMOCOUPLE, SUBCHANNEL 43
TE-294D	SPACER GRID NUMBER 5 THERMOCOUPLE, SUBCHANNEL 70
TE-294E	SPACER GRID NUMBER 5 THERMOCOUPLE, SUBCHANNEL 17
TE-294F	SPACER GRID NUMBER 5 THERMOCOUPLE, SUBCHANNEL 38
GRID NO. 6	
TE-295A	SPACER GRID NUMBER 6 THERMOCOUPLE, SUBCHANNEL 32
TE-295B	SPACER GRID NUMBER 6 THERMOCOUPLE, SUBCHANNEL 43
TE-295C	SPACER GRID NUMBER 6 THERMOCOUPLE, SUBCHANNEL 57
TE-295D	SPACER GRID NUMBER 6 THERMOCOUPLE, SUBCHANNEL 70
GRID NO. 7	

Table 2 (continued)

SENSOR	DESCRIPTION
BUNDLE TEMPERATURE (CONT.)	
SPACER GRID THERMOCOUPLES (CONT.)	
GRID NO. 7 (CONT.)	
TE-296B	SPACER GRID NUMBER 7 THERMOCOUPLE, SUBCHANNEL 43
TE-296D	SPACER GRID NUMBER 7 THERMOCOUPLE, SUBCHANNEL 70
SUBCHANNEL THERMOCOUPLES	
TE-1201	SUBCHANNEL NUMBER 1 THERMOCOUPLE
TE-1205	SUBCHANNEL NUMBER 5 THERMOCOUPLE
TE-1207	SUBCHANNEL NUMBER 7 THERMOCOUPLE
TE-1209	SUBCHANNEL NUMBER 9 THERMOCOUPLE
TE-1211	SUBCHANNEL NUMBER 11 THERMOCOUPLE
TE-1213	SUBCHANNEL NUMBER 13 THERMOCOUPLE
TE-1214	SUBCHANNEL NUMBER 14 THERMOCOUPLE
TE-1216	SUBCHANNEL NUMBER 16 THERMOCOUPLE
TE-1217	SUBCHANNEL NUMBER 17 THERMOCOUPLE
TE-1219	SUBCHANNEL NUMBER 19 THERMOCOUPLE
TE-1220	SUBCHANNEL NUMBER 20 THERMOCOUPLE
TE-1221	SUBCHANNEL NUMBER 21 THERMOCOUPLE
TE-1223	SUBCHANNEL NUMBER 23 THERMOCOUPLE
TE-1225	SUBCHANNEL NUMBER 25 THERMOCOUPLE
TE-1226	SUBCHANNEL NUMBER 26 THERMOCOUPLE
TE-1227	SUBCHANNEL NUMBER 27 THERMOCOUPLE
TE-1229	SUBCHANNEL NUMBER 29 THERMOCOUPLE
TE-1230	SUBCHANNEL NUMBER 30 THERMOCOUPLE
TE-1231	SUBCHANNEL NUMBER 31 THERMOCOUPLE
TE-1232	SUBCHANNEL NUMBER 32 THERMOCOUPLE
TE-1234	SUBCHANNEL NUMBER 34 THERMOCOUPLE
TE-1235	SUBCHANNEL NUMBER 35 THERMOCOUPLE
TE-1237	SUBCHANNEL NUMBER 37 THERMOCOUPLE
TE-1238	SUBCHANNEL NUMBER 38 THERMOCOUPLE
TE-1239	SUBCHANNEL NUMBER 39 THERMOCOUPLE
TE-1240	SUBCHANNEL NUMBER 40 THERMOCOUPLE
TE-1241	SUBCHANNEL NUMBER 41 THERMOCOUPLE
TE-1242	SUBCHANNEL NUMBER 42 THERMOCOUPLE
TE-1244	SUBCHANNEL NUMBER 44 THERMOCOUPLE
TE-1245	SUBCHANNEL NUMBER 45 THERMOCOUPLE
TE-1247	SUBCHANNEL NUMBER 47 THERMOCOUPLE
TE-1248	SUBCHANNEL NUMBER 48 THERMOCOUPLE
TE-1249	SUBCHANNEL NUMBER 49 THERMOCOUPLE
TE-1250	SUBCHANNEL NUMBER 50 THERMOCOUPLE
TE-1251	SUBCHANNEL NUMBER 51 THERMOCOUPLE
TE-1252	SUBCHANNEL NUMBER 52 THERMOCOUPLE
TE-1255	SUBCHANNEL NUMBER 55 THERMOCOUPLE
TE-1256	SUBCHANNEL NUMBER 56 THERMOCOUPLE
TE-1258	SUBCHANNEL NUMBER 58 THERMOCOUPLE
TE-1259	SUBCHANNEL NUMBER 59 THERMOCOUPLE
TE-1260	SUBCHANNEL NUMBER 60 THERMOCOUPLE

Table 2 (continued)

SENSOR	DESCRIPTION
BUNDLE TEMPERATURE (CONT.)	
SUBCHANNEL THERMOCOUPLES (CONT.)	
TE-1261	SUBCHANNEL NUMBER 61 THERMOCOUPLE
TE-1263	SUBCHANNEL NUMBER 63 THERMOCOUPLE
TE-1265	SUBCHANNEL NUMBER 65 THERMOCOUPLE
TE-1266	SUBCHANNEL NUMBER 66 THERMOCOUPLE
TE-1268	SUBCHANNEL NUMBER 68 THERMOCOUPLE
TE-1269	SUBCHANNEL NUMBER 69 THERMOCOUPLE
TE-1270	SUBCHANNEL NUMBER 70 THERMOCOUPLE
TE-1271	SUBCHANNEL NUMBER 71 THERMOCOUPLE
TE-1273	SUBCHANNEL NUMBER 73 THERMOCOUPLE
TE-1275	SUBCHANNEL NUMBER 75 THERMOCOUPLE
TE-1277	SUBCHANNEL NUMBER 77 THERMOCOUPLE
TE-1279	SUBCHANNEL NUMBER 79 THERMOCOUPLE
TE-1281	SUBCHANNEL NUMBER 81 THERMOCOUPLE
SPOOL PIECE INSTRUMENTS	
TEMPERATURE	
TE-24	HORIZONTAL INLET SPOOL TEMPERATURE
TE-172	VERTICAL INLET SPOOL TEMPERATURE
TE-222	VERTICAL OUTLET SPOOL TEMPERATURE
TE-40	HORIZONTAL OUTLET SPOOL TEMPERATURE
TE-208	BUNDLE OUTLET SPOOL TEMPERATURE
TE-266	BUNDLE INLET LOWER SPOOL TEMPERATURE
PRESSURE	
PE-26	HORIZONTAL INLET SPOOL TRANSIENT PRESSURE
PE-42	HORIZONTAL OUTLET SPOOL TRANSIENT PRESSURE
PE-174	VERTICAL INLET SPOOL TRANSIENT PRESSURE
PE-224	VERTICAL OUTLET SPOOL TRANSIENT PRESSURE
PE-209	BUNDLE OUTLET SPOOL TRANSIENT PRESSURE
PE-258	BUNDLE INLET LOWER SPOOL PRESSURE
PE-268	BUNDLE INLET LOWER SPOOL PRESSURE
PRESSURE DROP	
PDE-21	HORIZONTAL INLET SPOOL TRANSIENT DIFFERENTIAL PRESSURE
PDE-35	HORIZONTAL OUTLET SPOOL TRANSIENT DIFFERENTIAL PRESSURE
PDE-251	BUNDLE INLET SPOOL DIFFERENTIAL PRESSURE
VOLUMETRIC FLOW	
FE-19	HORIZONTAL INLET SPOOL VOLUMETRIC FLOW
FE-166	VERTICAL INLET SPOOL VOLUMETRIC FLOW
FE-34	HORIZONTAL OUTLET SPOOL VOLUMETRIC FLOW
FE-216	VERTICAL OUTLET SPOOL VOLUMETRIC FLOW
MOMENTUM FLUX	

Table 2 (continued)

SENSOR	DESCRIPTION
SPOOL PIECE INSTRUMENTS (CONT.)	
MOMENTUM FLUX (CONT.)	
FMFE-22	HORIZONTAL INLET SPOOL DRAG DISC
FMFE-38	HORIZONTAL OUTLET SPOOL DRAG DISC
FMFE-170	VERTICAL INLET SPOOL DRAG DISC
FMFE-220	VERTICAL OUTLET SPOOL DRAG DISC
FMFE-206	BUNDLE OUTLET SPOOL DRAG DISC
FMFE-254	BUNDLE INLET UPPER SPOOL DRAG DISC
FMFE-264	BUNDLE INLET LOWER SPOOL DRAG DISC
FLUID DENSITY	
DE-20	HORIZONTAL INLET SPOOL DENSITY
DE-36	BUNDLE INLET SPOOL 2 DENSITY
DE-168	VERTICAL INLET SPOOL DENSITY
DE-218	VERTICAL OUTLET SPOOL DENSITY
DE-204A	BUNDLE OUTLET SPOOL DENSITY
DE-204B	BUNDLE OUTLET SPOOL DENSITY
DE-204C	BUNDLE OUTLET SPOOL DENSITY
DE-262A	BUNDLE INLET SPOOL DENSITY
DE-262B	BUNDLE INLET SPOOL DENSITY
DE-262C	BUNDLE INLET SPOOL DENSITY
TEST SECTION INSTRUMENTS	
TEMPERATURE	
TE-210A	TEST SECTION OUTLET LINE STEADY-STATE TEMPERATURE
TDE-28	DIFFERENTIAL TEMPERATURE TRANSMITTER
TE-48	BASE PRIMARY STEADY-STATE TEMPERATURE
TE-150	TEST SECTION BOTTOM FLANGE TEMPERATURE SIDE
TE-151	TEST SECTION BOTTOM FLANGE TEMPERATURE SIDE
TE-152	TEST SECTION BOTTOM FLANGE TEMPERATURE SIDE
TE-29	INLET BLOWDOWN PLENUM TEMPERATURE
TE-45	OUTLET BLOWDOWN PLENUM TEMPERATURE
TE-256	TEST SECTION INLET TEMPERATURE
TE-284	OLD DOWNCOMER PURGE LINE RETURN TEMPERATURE
TE-920	PURGE LINE RETURN TEMPERATURE
TE-921	INNER SEAL COOLANT SUPPLY TEMPERATURE
TE-922	INNER SEAL COOLANT SUPPLY TEMPERATURE
PRESSURE	
PE-156	TEST SECTION INLET TRANSIENT PRESSURE
PE-201	TEST SECTION OUTLET TRANSIENT PRESSURE
PE-16	DOWNSTREAM HCV 2 TRANSIENT PRESSURE
PE-27	INLET PLENUM TRANSIENT PRESSURE
PE-43	OUTLET PLENUM TRANSIENT PRESSURE
PE-425	INLET BLOWDOWN LINE TRANSIENT PRESSURE
PE-286	SHROUD PLENUM OUTLET PRESSURE

Table 2 (continued)

SENSOR	DESCRIPTION
TEST SECTION INSTRUMENTS (CONT.)	
PRESSURE (CONT.)	
PE-32	TEST SECTION OUTLET STEADY-STATE PRESSURE
PRESSURE DROP	
PDE-180	SHROUD BOX DIFFERENTIAL PRESSURE FROM LEVEL A TO LEVEL B
PDE-181	SHROUD BOX DIFFERENTIAL PRESSURE FROM LEVEL B TO LEVEL C
PDE-182	SHROUD BOX DIFFERENTIAL PRESSURE FROM LEVEL C TO LEVEL D
PDE-183	SHROUD BOX DIFFERENTIAL PRESSURE FROM LEVEL D TO LEVEL D/E
PDE-184	SHROUD BOX DIFFERENTIAL PRESSURE FROM LEVEL D/E TO LEVEL E
PDE-185	SHROUD BOX DIFFERENTIAL PRESSURE FROM LEVEL E TO LEVEL E/F
PDE-186	SHROUD BOX DIFFERENTIAL PRESSURE FROM LEVEL E/F TO LEVEL F
PDE-187	SHROUD BOX DIFFERENTIAL PRESSURE FROM LEVEL F TO LEVEL F/G
PDE-188	SHROUD BOX DIFFERENTIAL PRESSURE FROM LEVEL F/G TO LEVEL G
PDE-189	SHROUD BOX DIFFERENTIAL PRESSURE FROM LEVEL G TO UPPER TAP
PDE-200	BUNDLE TRANSIENT DIFFERENTIAL PRESSURE
PDE-203	TEST SECTION TRANSIENT DIFFERENTIAL PRESSURE
PDE-30	TEST SECTION STEADY-STATE DIFFERENTIAL PRESSURE
PDE-261	BUNDLE TRANSIENT DIFFERENTIAL PRESSURE
PDE-271	SPLIT DOWNCOMER TRANSIENT DIFFERENTIAL PRESSURE
VOLUMETRIC FLOW	
FE-18A	TEST SECTION INLET STEADY-STATE VOLUMETRIC FLOW
FE-232	INNER SEAL COOLANT VOLUMETRIC FLOW
FE-202	BUNDLE OUTPUT LOWER VOLUMETRIC FLOW
FE-250	BUNDLE INLET UPPER VOLUMETRIC FLOW
FE-260	BUNDLE INLET LOWER VOLUMETRIC FLOW
FE-280	PURGE LINE RETURN VOLUMETRIC FLOW
LIQUID LEVEL	
LE-1400	BUNDLE LIQUID LEVEL PROBE 0
LE-1401	BUNDLE LIQUID LEVEL PROBE 1
LE-1402	BUNDLE LIQUID LEVEL PROBE 2
LE-1403	BUNDLE LIQUID LEVEL PROBE 3
LE-1404	BUNDLE LIQUID LEVEL PROBE 4
LE-1405	BUNDLE LIQUID LEVEL PROBE 5
LE-1406	BUNDLE LIQUID LEVEL PROBE 6
LE-1407	BUNDLE LIQUID LEVEL PROBE 7
LE-1408	BUNDLE LIQUID LEVEL PROBE 8
LE-1409	BUNDLE LIQUID LEVEL PROBE 9
LE-1410	BUNDLE LIQUID LEVEL PROBE 10
LE-1411	BUNDLE LIQUID LEVEL PROBE 11
LE-1412	BUNDLE LIQUID LEVEL PROBE 12
LE-1413	BUNDLE LIQUID LEVEL PROBE 13
LE-1414	BUNDLE LIQUID LEVEL PROBE 14
LE-1415	BUNDLE LIQUID LEVEL PROBE 15
LE-1416	BUNDLE LIQUID LEVEL PROBE 16

Table 2 (continued)

SENSOR	DESCRIPTION
TEST SECTION INSTRUMENTS (CONT.)	
LIQUID LEVEL (CONT.)	
LE-1417	BUNDLE LIQUID LEVEL PROBE 17
LE-1418	BUNDLE LIQUID LEVEL PROBE 18
LE-1419	BUNDLE LIQUID LEVEL CALIBRATION
PRESSURIZER INSTRUMENTS	
TEMPERATURE	
TE-101	PRESSURIZER VAPOR STEADY-STATE TEMPERATURE
TE-1	PRESSURIZER VAPOR TEMPERATURE
TE-2	PRESSURIZER WATER TEMPERATURE
TE-116	PRESSURIZER EXIT SPOOL TEMPERATURE
PRESSURE	
PE-106	PRESSURIZER VAPOR TRANSIENT PRESSURE
PE-118	PRESSURIZER LINE SPOOL PRESSURE
PE-102	PRESSURIZER STEADY-STATE PRESSURE
PRESSURE DROP	
PDE-111	PRESSURIZER LINE SPOOL DIFFERENTIAL PRESSURE
LEVEL	
LE-100	PRESSURIZER LIQUID LEVEL
MOMENTUM FLUX	
FMFE-114	PRESSURIZER LINE SPOOL DRAG DISC
VOLUMETRIC FLOW	
FE-110	PRESSURIZER LINE SPOOL VOLUMETRIC FLOW
PRIMARY PUMP INSTRUMENTS	
PDE-78	PRIMARY PUMP TRANSIENT DIFFERENTIAL PRESSURE
FE-1A	PRIMARY PUMP FLOW
PE-76	PRIMARY PUMP SUCTION TRANSIENT PRESSURE
SE-72	PRIMARY PUMP SPEED
EWE-77A	PRIMARY PUMP POWER
PUMP BYPASS INSTRUMENTS	
PE-15	PUMP BYPASS SPOOL PRESSURE
PRESSURE SUPPRESSION SYSTEM INSTRUMENTS	
PE-412	PRESSURE SUPPRESSION TRANSIENT PRESSURE
TE-408B	PRESSURE SUPPRESSION TANK SPRAY TEMPERATURE
TE-901	PRESSURE STEAM KILLER AIR VENT TEMPERATURE
DEMINERALIZED WATER SYSTEM INSTRUMENTS	

Table 2 (continued)

SENSOR	DESCRIPTION
DEMINERALIZED WATER SYSTEM INSTRUMENTS (CONT.)	
PE-616	DEMINERALIZED WATER SUPPLY HEADER PRESSURE
TE-615	DEMINERALIZED WATER 6 INCH HEADER STEADY-STATE TEMPERATURE
TE-520B	4 INCH DEMINERALIZED WATER HEADER TEMPERATURE
HEAT EXCHANGER INSTRUMENTS	
PRIMARY SIDE	
TEMPERATURE	
TE-58	HEAT EXCHANGER D OUTLET TEMPERATURE
TE-57	HEAT EXCHANGER A SPOOL TEMPERATURE
TE-62	HEAT EXCHANGER B SPOOL TEMPERATURE
TE-67	HEAT EXCHANGER C SPOOL TEMPERATURE
TE-28B	MAIN HEAT EXCHANGER MIXING TEE STEADY-STATE TEMPERATURE
VOLUMETRIC FLOW	
FE-51	HEAT EXCHANGER A SPOOL VOLUMETRIC FLOW
FE-59	HEAT EXCHANGER B SPOOL VOLUMETRIC FLOW
FE-64	HEAT EXCHANGER C SPOOL VOLUMETRIC FLOW
PRESSURE	
PE-44	UPSTREAM MAIN HEAT EXCHANGER TRANSIENT PRESSURE
PE-58	HEAT EXCHANGER A SPOOL PRESSURE
PE-63	HEAT EXCHANGER B SPOOL PRESSURE
PE-68	HEAT EXCHANGER C SPOOL PRESSURE
PRESSURE DROP	
PDE-46	MAIN HEAT EXCHANGER BYPASS TRANSIENT DIFFERENTIAL PRESSURE
PDE-48	MAIN HEAT EXCHANGER STEADY-STATE DIFFERENTIAL PRESSURE
PDE-53	HEAT EXCHANGER A SPOOL DIFFERENTIAL PRESSURE
PDE-60	HEAT EXCHANGER B SPOOL DIFFERENTIAL PRESSURE
PDE-65	HEAT EXCHANGER C SPOOL DIFFERENTIAL PRESSURE
MOMENTUM FLUX	
FMFE-55	HEAT EXCHANGER A SPOOL DRAG DISC
FMFE-61	HEAT EXCHANGER B SPOOL DRAG DISC
FMFE-66	HEAT EXCHANGER C SPOOL DRAG DISC
SECONDARY SIDE	
TEMPERATURE	
TE-525	HEAT EXCHANGER A SECONDARY OUTLET STEADY-STATE TEMPERATURE
TE-627	HEAT EXCHANGER B SECONDARY OUTLET STEADY-STATE TEMPERATURE
TE-727	HEAT EXCHANGER C SECONDARY OUTLET STEADY-STATE TEMPERATURE
TE-557	HEAT EXCHANGER D SECONDARY OUTLET STEADY-STATE TEMPERATURE

Table 2 (continued)

SENSOR	DESCRIPTION
HEAT EXCHANGER INSTRUMENTS (CONT.)	
SECONDARY SIDE (CONT.)	
VOLUMETRIC FLOW	
FE-522	HEAT EXCHANGER A SECONDARY COOLING WATER VOLUMETRIC FLOW
FE-620	HEAT EXCHANGER B SECONDARY COOLING WATER VOLUMETRIC FLOW
FE-720	HEAT EXCHANGER C SECONDARY COOLING WATER VOLUMETRIC FLOW
FE-550	HEAT EXCHANGER D SECONDARY COOLING WATER VOLUMETRIC FLOW
PRESSURE	
PE-526	HEAT EXCHANGER A SECONDARY INLET PRESSURE
GENERATOR POWER	
GENERATOR VOLTAGE	
EEE-9	GENERATOR 9 VOLTAGE
EEE-10	GENERATOR 10 VOLTAGE
EEE-11	GENERATOR 11 VOLTAGE
EEE-12	GENERATOR 12 VOLTAGE
GENERATOR CURRENT	
EIE-9	GENERATOR 9 CURRENT
EIE-10	GENERATOR 10 CURRENT
EIE-11	GENERATOR 11 CURRENT
EIE-12	GENERATOR 12 CURRENT
HEATER ROD POWER	
HEATER CURRENT	
EIE-1301	ROD 1 HEATER CURRENT
EIE-1302	ROD 2 HEATER CURRENT
EIE-1303	ROD 3 HEATER CURRENT
EIE-1304	ROD 4 HEATER CURRENT
EIE-1305	ROD 5 HEATER CURRENT
EIE-1306	ROD 6 HEATER CURRENT
EIE-1307	ROD 7 HEATER CURRENT
EIE-1308	ROD 8 HEATER CURRENT
EIE-1309	ROD 9 HEATER CURRENT
EIE-1310	ROD 10 HEATER CURRENT
EIE-1311	ROD 11 HEATER CURRENT
EIE-1312	ROD 12 HEATER CURRENT
EIE-1313	ROD 13 HEATER CURRENT
EIE-1314	ROD 14 HEATER CURRENT
EIE-1315	ROD 15 HEATER CURRENT
EIE-1316	ROD 16 HEATER CURRENT
EIE-1317	ROD 17 HEATER CURRENT
EIE-1318	ROD 18 HEATER CURRENT
EIE-1320	ROD 20 HEATER CURRENT

Table 2 (continued)

SENSOR	DESCRIPTION
HEATER ROD POWER (CONT.)	
HEATER CURRENT (CONT.)	
EIE-1321	ROD 21 HEATER CURRENT
EIE-1323	ROD 23 HEATER CURRENT
EIE-1324	ROD 24 HEATER CURRENT
EIE-1325	ROD 25 HEATER CURRENT
EIE-1326	ROD 26 HEATER CURRENT
EIE-1327	ROD 27 HEATER CURRENT
EIE-1328	ROD 28 HEATER CURRENT
EIE-1329	ROD 29 HEATER CURRENT
EIE-1330	ROD 30 HEATER CURRENT
EIE-1331	ROD 31 HEATER CURRENT
EIE-1332	ROD 32 HEATER CURRENT
EIE-1333	ROD 33 HEATER CURRENT
EIE-1334	ROD 34 HEATER CURRENT
EIE-1335	ROD 35 HEATER CURRENT
EIE-1337	ROD 37 HEATER CURRENT
EIE-1338	ROD 38 HEATER CURRENT
EIE-1339	ROD 39 HEATER CURRENT
EIE-1340	ROD 40 HEATER CURRENT
EIE-1341	ROD 41 HEATER CURRENT
EIE-1342	ROD 42 HEATER CURRENT
EIE-1343	ROD 43 HEATER CURRENT
EIE-1344	ROD 44 HEATER CURRENT
EIE-1345	ROD 45 HEATER CURRENT
EIE-1347	ROD 47 HEATER CURRENT
EIE-1348	ROD 48 HEATER CURRENT
EIE-1349	ROD 49 HEATER CURRENT
EIE-1350	ROD 50 HEATER CURRENT
EIE-1351	ROD 51 HEATER CURRENT
EIE-1352	ROD 52 HEATER CURRENT
EIE-1353	ROD 53 HEATER CURRENT
EIE-1354	ROD 54 HEATER CURRENT
EIE-1355	ROD 55 HEATER CURRENT
EIE-1356	ROD 56 HEATER CURRENT
EIE-1357	ROD 57 HEATER CURRENT
EIE-1358	ROD 58 HEATER CURRENT
EIE-1359	ROD 59 HEATER CURRENT
EIE-1360	ROD 60 HEATER CURRENT
EIE-1361	ROD 61 HEATER CURRENT
EIE-1362	ROD 62 HEATER CURRENT
EIE-1363	ROD 63 HEATER CURRENT
EIE-1364	ROD 64 HEATER CURRENT
GENERAL INSTRUMENTATION (ELECTRICAL)	
BREAKWIRE DETECTORS	

Table 2 (continued)

SENSOR	DESCRIPTION
GENERAL INSTRUMENTATION (ELECTRICAL) (CONT.)	
BREAKWIRE DETECTORS (CONT.)	
XE-430B	INLET BREAKWIRE DETECTOR
XE-430A	OUTLET BREAKWIRE DETECTOR
RTD POWER	
EIF-1001B	RTD POWER SUPPLY CURRENT
DATA ACQUISITION CALIBRATION SIGNALS	
EEE-1026AZ	ZERO INPUT CHANNELS0 TO 127
EEE-1026BZ	ZERO INPUT CHANNELS 128 TO 255
EEE-1026IZ	ZERO INPUT CHANNELS 1024 TO 1151
EEE-1026JZ	ZERO INPUT CHANNELS 1152 TO 1279
EEE-1026KZ	ZERO INPUT CHANNELS 1280 TO 1407
EEE-1026LZ	ZERO INPUT CHANNELS 1408 TO 1535
EEE-1026MZ	ZERO INPUT CHANNELS 1536 TO 1663
EEE-1026NZ	ZERO INPUT CHANNELS 1664 TO 1791
EEE-1026AC	CALIBRATION INPUT CHANNELS 0 TO 127
EEE-1026BC	CALIBRATION INPUT CHANNELS 128 TO 255
EEE-1026IC	CALIBRATION INPUT CHANNELS 1024 TO 1151
EEE-1026JC	CALIBRATION INPUT CHANNELS 1152 TO 1279
EEE-1026KC	CALIBRATION INPUT CHANNELS 1280 TO 1407
EEE-1026LC	CALIBRATION INPUT CHANNELS 1408 TO 1535
EEE-1026MC	CALIBRATION INPUT CHANNELS 1536 TO 1663
EEE-1026NC	CALIBRATION INPUT CHANNELS 1664 TO 1791
MISCELLANEOUS INSTRUMENTS	
TE-521	PURIFICATION COOLING WATER OUTLET TEMPERATURE

Table 3. Thermal-Hydraulic Test Facility Test 3.05.5B

FIGURE NUMBER	INSTRUMENT NAME	DESCRIPTION	RANGE	COMMENTS
1	EEE-1026AZ	ZERO INPUT CHANNELS0 TO 127	0 TO 40 MV	
2	EEE-1026AC	CALIBRATION INPUT CHANNELS 0 TO 127	0 TO 40 MV	
3	PDE-180	SHROUD BOX DIFFERENTIAL PRESSURE FROM LEVEL A TO LEVEL B	0 TO 151 INCHES	QUESTIONABLE
4	PDE-181	SHROUD BOX DIFFERENTIAL PRESSURE FROM LEVEL B TO LEVEL C	0 TO 151 INCHES	QUESTIONABLE
5	PDE-182	SHROUD BOX DIFFERENTIAL PRESSURE FROM LEVEL C TO LEVEL D	0 TO 151 INCHES	QUESTIONABLE
6	PDE-183	SHROUD BOX DIFFERENTIAL PRESSURE FROM LEVEL D TO LEVEL D/E	0 TO 151 INCHES	QUESTIONABLE
7	PDE-184	SHROUD BOX DIFFERENTIAL PRESSURE FROM LEVEL D/E TO LEVEL E	0 TO 151 INCHES	QUESTIONABLE
8	PDE-185	SHROUD BOX DIFFERENTIAL PRESSURE FROM LEVEL E TO LEVEL E/F	0 TO 151 INCHES	QUESTIONABLE
9	PE-26	HORIZONTAL INLET SPOOL TRANSIENT PRESSURE	0 TO 3000 PSIG	
10	PE-42	HORIZONTAL OUTLET SPOOL TRANSIENT PRESSURE	0 TO 3000 PSIG	
11	PE-44	UPSTREAM MAIN HEAT EXCHANGER TRANSIENT PRESSURE	0 TO 3000 PSIG	
12	PE-76	PRIMARY PUMP SUCTION TRANSIENT PRESSURE	0 TO 3000 PSIG	
13	PE-106	PRESSURIZER VAPOR TRANSIENT PRESSURE	0 TO 3000 PSIG	
14	PE-156	TEST SECTION INLET TRANSIENT PRESSURE	0 TO 3000 PSIG	
15	PE-201	TEST SECTION OUTLET TRANSIENT PRESSURE	0 TO 3000 PSIG	
16	PE-412	PRESSURE SUPPRESSION TRANSIENT PRESSURE	0 TO 200 PSIG	QUESTIONABLE
17	PE-526	HEAT EXCHANGER A SECONDARY INLET PRESSURE	0 TO 350 PSIG	
18	PE-616	DEMINERALIZED WATER SUPPLY HEADER PRESSURE	0 TO 350 PSIG	
19	PDE-46	MAIN HEAT EXCHANGER BYPASS TRANSIENT DIFFERENTIAL PRESSURE	-200 TO 200 PSID	
20	PDE-78	PRIMARY PUMP TRANSIENT DIFFERENTIAL PRESSURE	-1000 TO 1000 PSID	
21	PDE-200	BUNDLE TRANSIENT DIFFERENTIAL PRESSURE	-50 TO 50 PSID	

Table 3 (continued)

FIGURE NUMBER	INSTRUMENT NAME	DESCRIPTION	RANGE	COMMENTS
22	FMFE-22	HORIZONTAL INLET SPOOL DRAG DISC	-250000 TO 250000 LB/FS2	
23	FMFE-38	HORIZONTAL OUTLET SPOOL DRAG DISC	-250000 TO 250000 LB/FS2	
24	FMFE-170	VERTICAL INLET SPOOL DRAG DISC	-250000 TO 250000 LB/FS2	
25	FMFE-220	VERTICAL OUTLET SPOOL DRAG DISC	-250000 TO 250000 LB/FS2	
26	FE-18A	TEST SECTION INLET STEADY-STATE VOLUMETRIC FLOW	0 TO 700 GPM	
27	PDE-21	HORIZONTAL INLET SPOOL TRANSIENT DIFFERENTIAL PRESSURE	-200 TO 200 PSID	
28	PDE-35	HORIZONTAL OUTLET SPOOL TRANSIENT DIFFERENTIAL PRESSURE	-200 TO 200 PSID	
29	PE-174	VERTICAL INLET SPOOL TRANSIENT PRESSURE	0 TO 3000 PSIG	
30	PE-224	VERTICAL OUTLET SPOOL TRANSIENT PRESSURE	0 TO 3000 PSIG	
31	EIE-1339	ROD 39 HEATER CURRENT	0 TO 800 AMPS	
32	EIE-1331	ROD 31 HEATER CURRENT	0 TO 800 AMPS	
33	EIE-1314	ROD 14 HEATER CURRENT	0 TO 800 AMPS	
34	EIE-1313	ROD 13 HEATER CURRENT	0 TO 800 AMPS	
35	EIE-1308	ROD 8 HEATER CURRENT	0 TO 800 AMPS	
36	EIE-1306	ROD 6 HEATER CURRENT	0 TO 800 AMPS	
37	EIE-1312	ROD 12 HEATER CURRENT	0 TO 800 AMPS	
38	EIE-1307	ROD 7 HEATER CURRENT	0 TO 800 AMPS	
39	EIE-1321	ROD 21 HEATER CURRENT	0 TO 800 AMPS	
40	EIE-1316	ROD 16 HEATER CURRENT	0 TO 800 AMPS	
41	EIE-1324	ROD 24 HEATER CURRENT	0 TO 800 AMPS	
42	EIE-1362	ROD 62 HEATER CURRENT	0 TO 800 AMPS	
43	EIE-1361	ROD 61 HEATER CURRENT	0 TO 800 AMPS	
44	EIE-1364	ROD 64 HEATER CURRENT	0 TO 800 AMPS	
45	EIE-1363	ROD 63 HEATER CURRENT	0 TO 800 AMPS	

Table 3 (continued)

FIGURE NUMBER	INSTRUMENT NAME	DESCRIPTION	RANGE	COMMENTS
46	EIE-1347	ROD 47 HEATER CURRENT	0 TO 800 AMPS	
47	EIE-1338	ROD 38 HEATER CURRENT	0 TO 800 AMPS	
48	EIE-1332	ROD 32 HEATER CURRENT	0 TO 800 AMPS	
49	EIE-1340	ROD 40 HEATER CURRENT	0 TO 800 AMPS	
50	EIE-1348	ROD 48 HEATER CURRENT	0 TO 800 AMPS	
51	EIE-1355	ROD 55 HEATER CURRENT	0 TO 800 AMPS	
52	EIE-1354	ROD 54 HEATER CURRENT	0 TO 800 AMPS	
53	EIE-1345	ROD 45 HEATER CURRENT	0 TO 800 AMPS	
54	EIE-1349	ROD 49 HEATER CURRENT	0 TO 800 AMPS	
55	EIE-1325	ROD 25 HEATER CURRENT	0 TO 800 AMPS	
56	EIE-1335	ROD 35 HEATER CURRENT	0 TO 800 AMPS	
57	EIE-1309	ROD 9 HEATER CURRENT	0 TO 800 AMPS	
58	EIE-1317	ROD 17 HEATER CURRENT	0 TO 800 AMPS	
59	EIE-1328	ROD 28 HEATER CURRENT	0 TO 800 AMPS	
60	EIE-1301	ROD 1 HEATER CURRENT	0 TO 800 AMPS	
61	EIE-1318	ROD 18 HEATER CURRENT	0 TO 800 AMPS	
62	EIE-1334	ROD 34 HEATER CURRENT	0 TO 800 AMPS	
63	EIE-1326	ROD 26 HEATER CURRENT	0 TO 800 AMPS	
64	EIE-1333	ROD 33 HEATER CURRENT	0 TO 800 AMPS	
65	EIE-1350	ROD 50 HEATER CURRENT	0 TO 800 AMPS	
66	EIE-1344	ROD 44 HEATER CURRENT	0 TO 800 AMPS	
67	EIE-1343	ROD 43 HEATER CURRENT	0 TO 800 AMPS	
68	EIE-1352	ROD 52 HEATER CURRENT	0 TO 800 AMPS	
69	EIE-1351	ROD 51 HEATER CURRENT	0 TO 800 AMPS	
70	EIE-1320	ROD 20 HEATER CURRENT	0 TO 800 AMPS	

Table 3 (continued)

FIGURE NUMBER	INSTRUMENT NAME	DESCRIPTION	RANGE	COMMENTS
71	EIE-1303	ROD 3 HEATER CURRENT	0 TO 800 AMPS	
72	EIE-1305	ROD 5 HEATER CURRENT	0 TO 800 AMPS	
73	EIE-1311	ROD 11 HEATER CURRENT	0 TO 800 AMPS	
74	EIE-1357	ROD 57 HEATER CURRENT	0 TO 800 AMPS	
75	EIE-1358	ROD 58 HEATER CURRENT	0 TO 800 AMPS	
76	EIE-1359	ROD 59 HEATER CURRENT	0 TO 800 AMPS	
77	EIE-1353	ROD 53 HEATER CURRENT	0 TO 800 AMPS	
78	FMFE-206	BUNDLE OUTLET SPOOL DRAG DISC	-250000 TO 250000 LB/FS2	
79	SE-72	PRIMARY PUMP SPEED	100 TO 5400 RPM	
80	EIE-1315	ROD 15 HEATER CURRENT	0 TO 800 AMPS	
81	EIE-1330	ROD 30 HEATER CURRENT	0 TO 800 AMPS	
82	EIE-1323	ROD 23 HEATER CURRENT	0 TO 800 AMPS	
83	EIE-1329	ROD 29 HEATER CURRENT	0 TO 800 AMPS	
84	EIE-1356	ROD 56 HEATER CURRENT	0 TO 800 AMPS	
85	EIE-1337	ROD 37 HEATER CURRENT	0 TO 800 AMPS	
86	EIE-1360	ROD 60 HEATER CURRENT	0 TO 800 AMPS	
87	EIE-1327	ROD 27 HEATER CURRENT	0 TO 800 AMPS	
88	EIE-1341	ROD 41 HEATER CURRENT	0 TO 800 AMPS	
89	EIE-1342	ROD 42 HEATER CURRENT	0 TO 800 AMPS	
90	EIE-1302	ROD 2 HEATER CURRENT	0 TO 800 AMPS	
91	EIE-1310	ROD 10 HEATER CURRENT	0 TO 800 AMPS	
92	EIE-1304	ROD 4 HEATER CURRENT	0 TO 800 AMPS	
93	EIE-9	GENERATOR 9 CURRENT	0 TO 10000 AMPS	
94	EIE-10	GENERATOR 10 CURRENT	0 TO 10000 AMPS	
95	EIE-11	GENERATOR 11 CURRENT	0 TO 10000 AMPS	

Table 3 (continued)

FIGURE NUMBER	INSTRUMENT NAME	DESCRIPTION	RANGE	COMMENTS
96	EIE-12	GENERATOR 12 CURRENT	0 TO 10000 AMPS	
97	EEE-9	GENERATOR 9 VOLTAGE	0 TO 300 VOLTS	
98	EEE-10	GENERATOR 10 VOLTAGE	0 TO 300 VOLTS	
99	EEE-11	GENERATOR 11 VOLTAGE	0 TO 300 VOLTS	
100	EEE-12	GENERATOR 12 VOLTAGE	0 TO 300 VOLTS	
101	TE-210A	TEST SECTION OUTLET LINE STEADY-STATE TEMPERATURE	32 TO 800 DEGREES F	
102	EIE-1001B	RTD POWER SUPPLY CURRENT	0 TO 2 MA	
103	TE-525	HEAT EXCHANGER A SECONDARY OUTLET STEADY-STATE TEMPERATURE	32 TO 800 DEGREES F	
104	TE-627	HEAT EXCHANGER B SECONDARY OUTLET STEADY-STATE TEMPERATURE	32 TO 300 DEGREES F	
105	PE-16	DOWNSTREAM HCV 2 TRANSIENT PRESSURE	0 TO 3000 PSIG	
106	PE-27	INLET PLENUM TRANSIENT PRESSURE	0 TO 3000 PSIG	
107	PE-43	OUTLET PLENUM TRANSIENT PRESSURE	0 TO 3000 PSIG	
108	EWE-77A	PRIMARY PUMP POWER	0 TO 750 KW	
109	FE-19	HORIZONTAL INLET SPOOL VOLUMETRIC FLOW	-900 TO 900 GPM	
110	FE-166	VERTICAL INLET SPOOL VOLUMETRIC FLOW	-900 TO 900 GPM	
111	PE-425	INLET BLOWDOWN LINE TRANSIENT PRESSURE	0 TO 3000 PSIG	FAILED INSTRUMENT
112	FE-522	HEAT EXCHANGER A SECONDARY COOLING WATER VOLUMETRIC FLOW	0 TO 150 GPM	
113	FE-550	HEAT EXCHANGER D SECONDARY COOLING WATER VOLUMETRIC FLOW	0 TO 50 GPM	
114	FE-620	HEAT EXCHANGER B SECONDARY COOLING WATER VOLUMETRIC FLOW	0 TO 150 GPM	
115	FE-720	HEAT EXCHANGER C SECONDARY COOLING WATER VOLUMETRIC FLOW	0 TO 150 GPM	
116	EEE-1026BZ	ZERO INPUT CHANNELS 128 TO 255	0 TO 40 MV	
117	EEE-1026BC	CALIBRATION INPUT CHANNELS 128 TO 255	0 TO 40 MV	

Table 3 (continued)

FIGURE NUMBER	INSTRUMENT NAME	DESCRIPTION	RANGE	COMMENTS
118	PDE-186	SHROUD BOX DIFFERENTIAL PRESSURE FROM LEVEL E/F TO LEVEL F	0 TO 151 INCHES	QUESTIONABLE
119	PDE-187	SHROUD BOX DIFFERENTIAL PRESSURE FROM LEVEL F TO LEVEL F/G	0 TO 151 INCHES	QUESTIONABLE
120	PDE-188	SHROUD BOX DIFFERENTIAL PRESSURE FROM LEVEL F/G TO LEVEL G	0 TO 151 INCHES	QUESTIONABLE
121	PDE-189	SHROUD BOX DIFFERENTIAL PRESSURE FROM LEVEL G TO UPPER TAP	0 TO 151 INCHES	QUESTIONABLE
122	FMFE-55	HEAT EXCHANGER A SPOOL DRAG DISC	-20000 TO 20000 LB/FS2	
123	FMFE-61	HEAT EXCHANGER B SPOOL DRAG DISC	-20000 TO 20000 LB/FS2	
124	FMFE-66	HEAT EXCHANGER C SPOOL DRAG DISC	-20000 TO 20000 LB/FS2	
125	FMFE-114	PRESSURIZER LINE SPOOL DRAG DISC	-20000 TO 20000 LB/FS2	
126	FMFE-254	BUNDLE INLET UPPER SPOOL DRAG DISC	-20000 TO 20000 LB/FS2	
127	FMFE-264	BUNDLE INLET LOWER SPOOL DRAG DISC	-20000 TO 20000 LB/FS2	
128	PE-15	PUMP BYPASS SPOOL PRESSURE	0 TO 3000 PSIG	
129	PE-58	HEAT EXCHANGER A SPOOL PRESSURE	0 TO 3000 PSIG	
130	PE-63	HEAT EXCHANGER B SPOOL PRESSURE	0 TO 3000 PSIG	
131	PE-68	HEAT EXCHANGER C SPOOL PRESSURE	0 TO 3000 PSIG	
132	PE-118	PRESSURIZER LINE SPOOL PRESSURE	0 TO 3000 PSIG	
133	PE-209	BUNDLE OUTLET SPOOL TRANSIENT PRESSURE	0 TO 3000 PSIG	
134	PE-258	BUNDLE INLET LOWER SPOOL PRESSURE	0 TO 3000 PSIG	
135	PE-268	BUNDLE INLET LOWER SPOOL PRESSURE	0 TO 3000 PSIG	
136	PE-286	SHROUD PLENUM OUTLET PRESSURE	0 TO 3000 PSIG	
137	PDE-53	HEAT EXCHANGER A SPOOL DIFFERENTIAL PRESSURE	-50 TO 50 PSID	
138	PDE-60	HEAT EXCHANGER B SPOOL DIFFERENTIAL PRESSURE	-50 TO 50 PSID	
139	PDE-65	HEAT EXCHANGER C SPOOL DIFFERENTIAL PRESSURE	-50 TO 50 PSID	
140	PDE-111	PRESSURIZER LINE SPOOL DIFFERENTIAL PRESSURE	-50 TO 50 PSID	

Table 3 (continued)

FIGURE NUMBER	INSTRUMENT NAME	DESCRIPTION	RANGE	COMMENTS
141	PDE-203	TEST SECTION TRANSIENT DIFFERENTIAL PRESSURE	-50 TO 50 PSID	
142	PDE-251	BUNDLE INLET SPOOL DIFFERENTIAL PRESSURE	-50 TO 50 PSID	
143	FE-34	HORIZONTAL OUTLET SPOOL VOLUMETRIC FLOW	-900 TO 900 GPM	
144	FE-216	VERTICAL OUTLET SPOOL VOLUMETRIC FLOW	-819 TO 819 GPM	
145	DE-20	HORIZONTAL INLET SPOOL DENSITY	0 TO 63 LB/CF	
146	DE-36	BUNDLE INLET SPOOL 2 DENSITY	0 TO 63 LB/CF	
147	DE-168	VERTICAL INLET SPOOL DENSITY	0 TO 63 LB/CF	
148	DE-218	VERTICAL OUTLET SPOOL DENSITY	0 TO 63 LB/CF	
149	XE-430B	INLET BREAKWIRE DETECTOR	0 TO 5 VOLTS	
150	XE-430A	OUTLET BREAKWIRE DETECTOR	0 TO 5 VOLTS	
151	FE-1A	PRIMARY PUMP FLOW	0 TO 800 GPM	
152	TDE-28	DIFFERENTIAL TEMPERATURE TRANSMITTER	-50 TO 50 DEGREES F	QUESTIONABLE
153	PDE-30	TEST SECTION STEADY-STATE DIFFERENTIAL PRESSURE	0 TO 50 PSID	
154	PE-32	TEST SECTION OUTLET STEADY-STATE PRESSURE	500 TO 3951 PSIG	
155	PDE-48	MAIN HEAT EXCHANGER STEADY-STATE DIFFERENTIAL PRESSURE	0 TO 24 PSID	
156	LE-100	PRESSURIZER LIQUID LEVEL	0 TO 150 INCHES	
157	PE-102	PRESSURIZER STEADY-STATE PRESSURE	500 TO 2500 PSIG	
158	TE-727	HEAT EXCHANGER C SECONDARY OUTLET STEADY-STATE TEMPERATURE	32 TO 800 DEGREES F	
159	TE-557	HEAT EXCHANGER D SECONDARY OUTLET STEADY-STATE TEMPERATURE	32 TO 800 DEGREES F	
160	TE-28B	MAIN HEAT EXCHANGER MIXING TEE STEADY-STATE TEMPERATURE	32 TO 800 DEGREES F	
161	TE-4B	BASE PRIMARY STEADY-STATE TEMPERATURE	32 TO 800 DEGREES F	
162	TE-101	PRESSURIZER VAPOR STEADY-STATE TEMPERATURE	32 TO 800 DEGREES F	
163	TE-615	DEMINERALIZED WATER 6 INCH HEADER STEADY-STATE TEMPERATURE	32 TO 800 DEGREES F	

Table 3 (continued)

FIGURE NUMBER	INSTRUMENT NAME	DESCRIPTION	RANGE	COMMENTS
164	PDE-261	BUNDLE TRANSIENT DIFFERENTIAL PRESSURE	-500 TO 500 INCHES WATER	
165	PDE-271	SPLIT DOWNCOMER TRANSIENT DIFFERENTIAL PRESSURE	-6 TO 6 PSID	
166	DE-204A	BUNDLE OUTLET SPOOL DENSITY	0 TO 63 LB/CF	
167	DE-204B	BUNDLE OUTLET SPOOL DENSITY	0 TO 63 LB/CF	
168	DE-204C	BUNDLE OUTLET SPOOL DENSITY	0 TO 63 LB/CF	
169	DE-262A	BUNDLE INLET SPOOL DENSITY	0 TO 63 LB/CF	
170	DE-262B	BUNDLE INLET SPOOL DENSITY	0 TO 63 LB/CF	
171	LE-1400	BUNDLE LIQUID LEVEL PROBE 0	-10 TO 10 VOLTS	QUESTIONABLE
172	LE-1401	BUNDLE LIQUID LEVEL PROBE 1	-10 TO 10 VOLTS	QUESTIONABLE
173	LE-1402	BUNDLE LIQUID LEVEL PROBE 2	-10 TO 10 VOLTS	QUESTIONABLE
174	LE-1403	BUNDLE LIQUID LEVEL PROBE 3	-10 TO 10 VOLTS	QUESTIONABLE
175	LE-1404	BUNDLE LIQUID LEVEL PROBE 4	-10 TO 10 VOLTS	QUESTIONABLE
176	LE-1405	BUNDLE LIQUID LEVEL PROBE 5	-10 TO 10 VOLTS	QUESTIONABLE
177	LE-1406	BUNDLE LIQUID LEVEL PROBE 6	-10 TO 10 VOLTS	QUESTIONABLE
178	LE-1407	BUNDLE LIQUID LEVEL PROBE 7	-10 TO 10 VOLTS	QUESTIONABLE
179	LE-1408	BUNDLE LIQUID LEVEL PROBE 8	-10 TO 10 VOLTS	QUESTIONABLE
180	LE-1409	BUNDLE LIQUID LEVEL PROBE 9	-10 TO 10 VOLTS	QUESTIONABLE
181	LE-1410	BUNDLE LIQUID LEVEL PROBE 10	-10 TO 10 VOLTS	QUESTIONABLE
182	LE-1411	BUNDLE LIQUID LEVEL PROBE 11	-10 TO 10 VOLTS	QUESTIONABLE
183	LE-1412	BUNDLE LIQUID LEVEL PROBE 12	-10 TO 10 VOLTS	QUESTIONABLE
184	LE-1413	BUNDLE LIQUID LEVEL PROBE 13	-10 TO 10 VOLTS	QUESTIONABLE
185	LE-1414	BUNDLE LIQUID LEVEL PROBE 14	-10 TO 10 VOLTS	QUESTIONABLE
186	LE-1415	BUNDLE LIQUID LEVEL PROBE 15	-10 TO 10 VOLTS	QUESTIONABLE
187	LE-1416	BUNDLE LIQUID LEVEL PROBE 16	-10 TO 10 VOLTS	QUESTIONABLE
188	LE-1417	BUNDLE LIQUID LEVEL PROBE 17	-10 TO 10 VOLTS	QUESTIONABLE

Table 3 (continued)

FIGURE NUMBER	INSTRUMENT NAME	DESCRIPTION	RANGE	COMMENTS
189	LE-1418	BUNDLE LIQUID LEVEL PROBE 18	-10 TO 10 VOLTS	QUESTIONABLE
190	LE-1419	BUNDLE LIQUID LEVEL CALIBRATION	-10 TO 10 VOLTS	FAILED INSTRUMENT
191	FE-51	HEAT EXCHANGER A SPOOL VOLUMETRIC FLOW	-225 TO 225 GPM	
192	FE-59	HEAT EXCHANGER B SPOOL VOLUMETRIC FLOW	-225 TO 225 GPM	
193	FE-64	HEAT EXCHANGER C SPOOL VOLUMETRIC FLOW	-225 TO 225 GPM	
194	FE-232	INNER SEAL COOLANT VOLUMETRIC FLOW	-10 TO 10 GPM	
195	FE-110	PRESSURIZER LINE SPOOL VOLUMETRIC FLOW	-57 TO 57 GPM	
196	FE-202	BUNDLE OUTPUT LOWER VOLUMETRIC FLOW	-900 TO 900 GPM	
197	FE-250	BUNDLE INLET UPPER VOLUMETRIC FLOW	-900 TO 900 GPM	
198	FE-260	BUNDLE INLET LOWER VOLUMETRIC FLOW	-900 TO 900 GPM	
199	FE-280	PURGE LINE RETURN VOLUMETRIC FLOW	-60 TO 60 GPM	
200	DE-262C	BUNDLE INLET SPOOL DENSITY	0 TO 63 LB/CF	
201	EEE-1026IZ	ZERO INPUT CHANNELS 1024 TO 1151	0 TO 40 MV	
202	EEE-1026IC	CALIBRATION INPUT CHANNELS 1024 TO 1151	0 TO 40 MV	
203	TE-329BC	SHEATH THERMOCOUPLE, ROD 29, LEVEL C	32 TO 1897 DEGREES F	
204	TE-329BD	SHEATH THERMOCOUPLE, ROD 29, LEVEL D	32 TO 1897 DEGREES F	
205	TE-329AE	SHEATH THERMOCOUPLE, ROD 29, LEVEL E	32 TO 1897 DEGREES F	
206	TE-329BB	SHEATH THERMOCOUPLE, ROD 29, LEVEL B	32 TO 1897 DEGREES F	
207	TE-339BD	SHEATH THERMOCOUPLE, ROD 39, LEVEL D	32 TO 1897 DEGREES F	
208	TE-339BB	SHEATH THERMOCOUPLE, ROD 39, LEVEL B	32 TO 1897 DEGREES F	
209	TE-339AC	SHEATH THERMOCOUPLE, ROD 39, LEVEL C	32 TO 1897 DEGREES F	
210	TE-353BE	SHEATH THERMOCOUPLE, ROD 53, LEVEL E	32 TO 1897 DEGREES F	
211	TE-338BC	SHEATH THERMOCOUPLE, ROD 38, LEVEL C	32 TO 1897 DEGREES F	
212	TE-338BD	SHEATH THERMOCOUPLE, ROD 38, LEVEL D	32 TO 1897 DEGREES F	
213	TE-338AB	SHEATH THERMOCOUPLE, ROD 38, LEVEL B	32 TO 1897 DEGREES F	

Table 3 (continued)

FIGURE NUMBER	INSTRUMENT NAME	DESCRIPTION	RANGE	COMMENTS
214	TE-354CC	SHEATH THERMOCOUPLE, ROD 54, LEVEL C	32 TO 1897 DEGREES F	
215	TE-354AD	SHEATH THERMOCOUPLE, ROD 54, LEVEL D	32 TO 1897 DEGREES F	
216	TE-354CA	SHEATH THERMOCOUPLE, ROD 54, LEVEL A	32 TO 1897 DEGREES F	
217	TE-354CB	SHEATH THERMOCOUPLE, ROD 54, LEVEL B	32 TO 1897 DEGREES F	
218	TE-1234	SUBCHANNEL NUMBER 34 THERMOCOUPLE	32 TO 1897 DEGREES F	
219	TE-331CF	SHEATH THERMOCOUPLE, ROD 31, LEVEL F	32 TO 1897 DEGREES F	
220	TE-331CE	SHEATH THERMOCOUPLE, ROD 31, LEVEL E	32 TO 1897 DEGREES F	
221	TE-331CD	SHEATH THERMOCOUPLE, ROD 31, LEVEL D	32 TO 1897 DEGREES F	
222	TE-345AD	SHEATH THERMOCOUPLE, ROD 45, LEVEL D	32 TO 1897 DEGREES F	
223	TE-347CG	SHEATH THERMOCOUPLE, ROD 47, LEVEL G	32 TO 1897 DEGREES F	
224	TE-345CF	SHEATH THERMOCOUPLE, ROD 45, LEVEL F	32 TO 1897 DEGREES F	
225	TE-345AG	SHEATH THERMOCOUPLE, ROD 45, LEVEL G	32 TO 1897 DEGREES F	
226	TE-1252	SUBCHANNEL NUMBER 52 THERMOCOUPLE	32 TO 1897 DEGREES F	
227	TE-361BE	SHEATH THERMOCOUPLE, ROD 61, LEVEL E	32 TO 1897 DEGREES F	
228	TE-361AE	SHEATH THERMOCOUPLE, ROD 61, LEVEL E	32 TO 1897 DEGREES F	
229	TE-363AE	SHEATH THERMOCOUPLE, ROD 63, LEVEL E	32 TO 1897 DEGREES F	
230	TE-340CB	SHEATH THERMOCOUPLE, ROD 40, LEVEL B	32 TO 1897 DEGREES F	
231	TE-340CA	SHEATH THERMOCOUPLE, ROD 40, LEVEL A	32 TO 1897 DEGREES F	
232	TE-340BD	SHEATH THERMOCOUPLE, ROD 40, LEVEL D	32 TO 1897 DEGREES F	
233	TE-340BC	SHEATH THERMOCOUPLE, ROD 40, LEVEL C	32 TO 1897 DEGREES F	
234	TE-330AC	SHEATH THERMOCOUPLE, ROD 30, LEVEL C	32 TO 1897 DEGREES F	
235	TE-330AE	SHEATH THERMOCOUPLE, ROD 30, LEVEL E	32 TO 1897 DEGREES F	
236	TE-330CB	SHEATH THERMOCOUPLE, ROD 30, LEVEL B	32 TO 1897 DEGREES F	
237	TE-1242	SUBCHANNEL NUMBER 42 THERMOCOUPLE	32 TO 1897 DEGREES F	
238	TE-1245	SUBCHANNEL NUMBER 45 THERMOCOUPLE	32 TO 1897 DEGREES F	

Table 3 (continued)

FIGURE NUMBER	INSTRUMENT NAME	DESCRIPTION	RANGE	COMMENTS
239	TE-1258	SUBCHANNEL NUMBER 58 THERMOCOUPLE	32 TO 1897 DEGREES F	
240	TE-1244	SUBCHANNEL NUMBER 44 THERMOCOUPLE	32 TO 1897 DEGREES F	
241	TE-1209	SUBCHANNEL NUMBER 9 THERMOCOUPLE	32 TO 1897 DEGREES F	
242	TE-1217	SUBCHANNEL NUMBER 17 THERMOCOUPLE	32 TO 1897 DEGREES F	
243	TE-1226	SUBCHANNEL NUMBER 26 THERMOCOUPLE	32 TO 1897 DEGREES F	
244	TE-1249	SUBCHANNEL NUMBER 49 THERMOCOUPLE	32 TO 1897 DEGREES F	
245	TE-1225	SUBCHANNEL NUMBER 25 THERMOCOUPLE	32 TO 1897 DEGREES F	
246	TE-353AE	SHEATH THERMOCOUPLE, ROD 53, LEVEL E	32 TO 1897 DEGREES F	
247	TE-1227	SUBCHANNEL NUMBER 27 THERMOCOUPLE	32 TO 1897 DEGREES F	
248	TE-353CC	SHEATH THERMOCOUPLE, ROD 53, LEVEL C	32 TO 1897 DEGREES F	
249	TE-361CE	SHEATH THERMOCOUPLE, ROD 61, LEVEL E	32 TO 1897 DEGREES F	
250	TE-361AB	SHEATH THERMOCOUPLE, ROD 61, LEVEL B	32 TO 1897 DEGREES F	
251	TE-361AC	SHEATH THERMOCOUPLE, ROD 61, LEVEL C	32 TO 1897 DEGREES F	
252	TE-361AD	SHEATH THERMOCOUPLE, ROD 61, LEVEL D	32 TO 1897 DEGREES F	
253	TE-364AG	SHEATH THERMOCOUPLE, ROD 64, LEVEL G	32 TO 1897 DEGREES F	
254	TE-364BE	SHEATH THERMOCOUPLE, ROD 64, LEVEL E	32 TO 1897 DEGREES F	
255	TE-364AD	SHEATH THERMOCOUPLE, ROD 64, LEVEL D	32 TO 1897 DEGREES F	
256	TE-364BF	SHEATH THERMOCOUPLE, ROD 64, LEVEL F	32 TO 1897 DEGREES F	
257	TE-363BE	SHEATH THERMOCOUPLE, ROD 63, LEVEL E	32 TO 1897 DEGREES F	
258	TE-363BC	SHEATH THERMOCOUPLE, ROD 63, LEVEL C	32 TO 1897 DEGREES F	
259	TE-363CB	SHEATH THERMOCOUPLE, ROD 63, LEVEL B	32 TO 1897 DEGREES F	
260	TE-1263	SUBCHANNEL NUMBER 63 THERMOCOUPLE	32 TO 1897 DEGREES F	FAILED INSTRUMENT
261	TE-313CF	SHEATH THERMOCOUPLE, ROD 13, LEVEL F	32 TO 1897 DEGREES F	
262	TE-348AH	SHEATH THERMOCOUPLE, ROD 48, LEVEL H	32 TO 1897 DEGREES F	
263	TE-348AY	SHEATH THERMOCOUPLE, ROD 48, LEVEL Y	32 TO 1897 DEGREES F	

Table 3 (continued)

FIGURE NUMBER	INSTRUMENT NAME	DESCRIPTION	RANGE	COMMENTS
264	TE-331BF	SHEATH THERMOCOUPLE, ROD 31, LEVEL F	32 TO 1897 DEGREES F	
265	TE-355CB	SHEATH THERMOCOUPLE, ROD 55, LEVEL B	32 TO 1897 DEGREES F	
266	TE-355AA	SHEATH THERMOCOUPLE, ROD 55, LEVEL A	32 TO 1897 DEGREES F	
267	TE-355BC	SHEATH THERMOCOUPLE, ROD 55, LEVEL C	32 TO 1897 DEGREES F	
268	TE-337BF	SHEATH THERMOCOUPLE, ROD 37, LEVEL F	32 TO 1897 DEGREES F	
269	TE-356AC	SHEATH THERMOCOUPLE, ROD 56, LEVEL C	32 TO 1897 DEGREES F	
270	TE-356CD	SHEATH THERMOCOUPLE, ROD 56, LEVEL D	32 TO 1897 DEGREES F	
271	TE-356AF	SHEATH THERMOCOUPLE, ROD 56, LEVEL F	32 TO 1897 DEGREES F	
272	TE-356AE	SHEATH THERMOCOUPLE, ROD 56, LEVEL E	32 TO 1897 DEGREES F	
273	TE-362CD	SHEATH THERMOCOUPLE, ROD 62, LEVEL D	32 TO 1897 DEGREES F	
274	TE-362AE	SHEATH THERMOCOUPLE, ROD 62, LEVEL E	32 TO 1897 DEGREES F	
275	TE-362AB	SHEATH THERMOCOUPLE, ROD 62, LEVEL B	32 TO 1897 DEGREES F	
276	TE-337BE	SHEATH THERMOCOUPLE, ROD 37, LEVEL E	32 TO 1897 DEGREES F	
277	TE-337BD	SHEATH THERMOCOUPLE, ROD 37, LEVEL D	32 TO 1897 DEGREES F	
278	TE-337CF	SHEATH THERMOCOUPLE, ROD 37, LEVEL F	32 TO 1897 DEGREES F	
279	TE-337AE	SHEATH THERMOCOUPLE, ROD 37, LEVEL E	32 TO 1897 DEGREES F	
280	TE-334CY	SHEATH THERMOCOUPLE, ROD 34, LEVEL Y	32 TO 1897 DEGREES F	
281	TE-334AS	SHEATH THERMOCOUPLE, ROD 34, LEVEL S	32 TO 1897 DEGREES F	
282	TE-334CH	SHEATH THERMOCOUPLE, ROD 34, LEVEL H	32 TO 1897 DEGREES F	
283	TE-360AC	SHEATH THERMOCOUPLE, ROD 60, LEVEL C	32 TO 1897 DEGREES F	
284	TE-360AD	SHEATH THERMOCOUPLE, ROD 60, LEVEL D	32 TO 1897 DEGREES F	
285	TE-360CD	SHEATH THERMOCOUPLE, ROD 60, LEVEL D	32 TO 1897 DEGREES F	
286	TE-312BC	SHEATH THERMOCOUPLE, ROD 12, LEVEL C	32 TO 1897 DEGREES F	
287	TE-312AE	SHEATH THERMOCOUPLE, ROD 12, LEVEL E	32 TO 1897 DEGREES F	
288	TE-312CB	SHEATH THERMOCOUPLE, ROD 12, LEVEL B	32 TO 1897 DEGREES F	

Table 3 (continued)

FIGURE NUMBER	INSTRUMENT NAME	DESCRIPTION	RANGE	COMMENTS
289	TE-349AE	SHEATH THERMOCOUPLE, ROD 49, LEVEL E	32 TO 1897 DEGREES F	
290	TE-343BB	SHEATH THERMOCOUPLE, ROD 43, LEVEL B	32 TO 1897 DEGREES F	
291	TE-343BC	SHEATH THERMOCOUPLE, ROD 43, LEVEL C	32 TO 1897 DEGREES F	
292	TE-326AD	SHEATH THERMOCOUPLE, ROD 26, LEVEL D	32 TO 1897 DEGREES F	
293	TE-343BA	SHEATH THERMOCOUPLE, ROD 43, LEVEL A	32 TO 1897 DEGREES F	
294	TE-327AC	SHEATH THERMOCOUPLE, ROD 27, LEVEL C	32 TO 1897 DEGREES F	
295	TE-327BD	SHEATH THERMOCOUPLE, ROD 27, LEVEL D	32 TO 1897 DEGREES F	
296	TE-1235	SUBCHANNEL NUMBER 35 THERMOCOUPLE	32 TO 1897 DEGREES F	
297	TE-327CA	SHEATH THERMOCOUPLE, ROD 27, LEVEL A	32 TO 1897 DEGREES F	
298	TE-341AB	SHEATH THERMOCOUPLE, ROD 41, LEVEL B	32 TO 1897 DEGREES F	
299	TE-342AG	SHEATH THERMOCOUPLE, ROD 42, LEVEL G	32 TO 1897 DEGREES F	
300	TE-343AD	SHEATH THERMOCOUPLE, ROD 43, LEVEL D	32 TO 1897 DEGREES F	
301	TE-321AD	SHEATH THERMOCOUPLE, ROD 21, LEVEL D	32 TO 1897 DEGREES F	
302	TE-342CG	SHEATH THERMOCOUPLE, ROD 42, LEVEL G	32 TO 1897 DEGREES F	
303	TE-342BE	SHEATH THERMOCOUPLE, ROD 42, LEVEL E	32 TO 1897 DEGREES F	
304	TE-342BF	SHEATH THERMOCOUPLE, ROD 42, LEVEL F	32 TO 1897 DEGREES F	
305	TE-342BD	SHEATH THERMOCOUPLE, ROD 42, LEVEL D	32 TO 1897 DEGREES F	
306	TE-292B	SPACER GRID NUMBER 3 THERMOCOUPLE, SUBCHANNEL 43	32 TO 1897 DEGREES F	
307	TE-292D	SPACER GRID NUMBER 3 THERMOCOUPLE, SUBCHANNEL 70	32 TO 1897 DEGREES F	
308	TE-295B	SPACER GRID NUMBER 6 THERMOCOUPLE, SUBCHANNEL 43	32 TO 1897 DEGREES F	
309	TE-295D	SPACER GRID NUMBER 6 THERMOCOUPLE, SUBCHANNEL 70	32 TO 1897 DEGREES F	
310	TE-291D	SPACER GRID NUMBER 2 THERMOCOUPLE, SUBCHANNEL 70	32 TO 1897 DEGREES F	
311	TE-294F	SPACER GRID NUMBER 5 THERMOCOUPLE, SUBCHANNEL 38	32 TO 1897 DEGREES F	

Table 3 (continued)

FIGURE NUMBER	INSTRUMENT NAME	DESCRIPTION	RANGE	COMMENTS
312	TE-338CD	SHEATH THERMOCOUPLE, ROD 38, LEVEL D	32 TO 1897 DEGREES F	
313	TE-342BG	SHEATH THERMOCOUPLE, ROD 42, LEVEL G	32 TO 1897 DEGREES F	
314	TE-330BE	SHEATH THERMOCOUPLE, ROD 30, LEVEL E	32 TO 1897 DEGREES F	
315	TE-293A	SPACER GRID NUMBER 4 THERMOCOUPLE, SUBCHANNEL 32	32 TO 1897 DEGREES F	FAILED INSTRUMENT
316	TE-295C	SPACER GRID NUMBER 6 THERMOCOUPLE, SUBCHANNEL 57	32 TO 1897 DEGREES F	
317	TE-295A	SPACER GRID NUMBER 6 THERMOCOUPLE, SUBCHANNEL 32	32 TO 1897 DEGREES F	FAILED INSTRUMENT
318	EEE-1026JZ	ZERO INPUT CHANNELS 1152 TO 1279	0 TO 40 MV	
319	EEE-1026JC	CALIBRATION INPUT CHANNELS 1152 TO 1279	0 TO 40 MV	
320	TE-292A	SPACER GRID NUMBER 3 THERMOCOUPLE, SUBCHANNEL 32	32 TO 1897 DEGREES F	
321	TE-291C	SPACER GRID NUMBER 2 THERMOCOUPLE, SUBCHANNEL 57	32 TO 1897 DEGREES F	
322	TE-291B	SPACER GRID NUMBER 2 THERMOCOUPLE, SUBCHANNEL 43	32 TO 1897 DEGREES F	
323	TE-293F	SPACER GRID NUMBER 4 THERMOCOUPLE, SUBCHANNEL 38	32 TO 1897 DEGREES F	
324	TE-186S	SHROUD BOX THERMOCOUPLE, LEVEL G, SOUTH SIDE	32 TO 1897 DEGREES F	
325	TE-181W	SHROUD BOX THERMOCOUPLE, LEVEL A, WEST SIDE	32 TO 1897 DEGREES F	
326	TE-185W	SHROUD BOX THERMOCOUPLE, LEVEL E, WEST SIDE	32 TO 1897 DEGREES F	
327	TE-291A	SPACER GRID NUMBER 2 THERMOCOUPLE, SUBCHANNEL 32	32 TO 1897 DEGREES F	
328	TE-293C	SPACER GRID NUMBER 4 THERMOCOUPLE, SUBCHANNEL 57	32 TO 1897 DEGREES F	
329	TE-294B	SPACER GRID NUMBER 5 THERMOCOUPLE, SUBCHANNEL 43	32 TO 1897 DEGREES F	
330	TE-294E	SPACER GRID NUMBER 5 THERMOCOUPLE, SUBCHANNEL 17	32 TO 1897 DEGREES F	
331	TE-294D	SPACER GRID NUMBER 5 THERMOCOUPLE, SUBCHANNEL 70	32 TO 1897 DEGREES F	

Table 3 (continued)

FIGURE NUMBER	INSTRUMENT NAME	DESCRIPTION	RANGE	COMMENTS
332	TE-293E	SPACER GRID NUMBER 4 THERMOCOUPLE, SUBCHANNEL 17	32 TO 1897 DEGREES F	
333	TE-293D	SPACER GRID NUMBER 4 THERMOCOUPLE, SUBCHANNEL 70	32 TO 1897 DEGREES F	
334	TE-293B	SPACER GRID NUMBER 4 THERMOCOUPLE, SUBCHANNEL 43	32 TO 1897 DEGREES F	
335	TE-296B	SPACER GRID NUMBER 7 THERMOCOUPLE, SUBCHANNEL 43	32 TO 1897 DEGREES F	
336	TE-296D	SPACER GRID NUMBER 7 THERMOCOUPLE, SUBCHANNEL 70	32 TO 1897 DEGREES F	FAILED INSTRUMENT
337	TE-352AU	SHEATH THERMOCOUPLE, ROD 52, LEVEL U	32 TO 1897 DEGREES F	
338	TE-352BS	SHEATH THERMOCOUPLE, ROD 52, LEVEL S	32 TO 1897 DEGREES F	
339	TE-352CH	SHEATH THERMOCOUPLE, ROD 52, LEVEL H	32 TO 1897 DEGREES F	
340	TE-352CY	SHEATH THERMOCOUPLE, ROD 52, LEVEL Y	32 TO 1897 DEGREES F	
341	TE-350BE	SHEATH THERMOCOUPLE, ROD 50, LEVEL E	32 TO 1897 DEGREES F	
342	TE-349BE	SHEATH THERMOCOUPLE, ROD 49, LEVEL E	32 TO 1897 DEGREES F	
343	TE-350CD	SHEATH THERMOCOUPLE, ROD 50, LEVEL D	32 TO 1897 DEGREES F	
344	TE-350BF	SHEATH THERMOCOUPLE, ROD 50, LEVEL F	32 TO 1897 DEGREES F	
345	TE-349CB	SHEATH THERMOCOUPLE, ROD 49, LEVEL B	32 TO 1897 DEGREES F	
346	TE-349CD	SHEATH THERMOCOUPLE, ROD 49, LEVEL D	32 TO 1897 DEGREES F	
347	TE-349CC	SHEATH THERMOCOUPLE, ROD 49, LEVEL C	32 TO 1897 DEGREES F	
348	TE-349CE	SHEATH THERMOCOUPLE, ROD 49, LEVEL E	32 TO 1897 DEGREES F	
349	TE-326CE	SHEATH THERMOCOUPLE, ROD 26, LEVEL E	32 TO 1897 DEGREES F	
350	TE-326AC	SHEATH THERMOCOUPLE, ROD 26, LEVEL C	32 TO 1897 DEGREES F	
351	TE-326BD	SHEATH THERMOCOUPLE, ROD 26, LEVEL D	32 TO 1897 DEGREES F	
352	TE-326BB	SHEATH THERMOCOUPLE, ROD 26, LEVEL B	32 TO 1897 DEGREES F	
353	TE-351BC	SHEATH THERMOCOUPLE, ROD 51, LEVEL C	32 TO 1897 DEGREES F	
354	TE-351AE	SHEATH THERMOCOUPLE, ROD 51, LEVEL E	32 TO 1897 DEGREES F	

Table 3 (continued)

FIGURE NUMBER	INSTRUMENT NAME	DESCRIPTION	RANGE	COMMENTS
355	TE-351BD	SHEATH THERMOCOUPLE, ROD 51, LEVEL D	32 TO 1897 DEGREES F	
356	TE-351AB	SHEATH THERMOCOUPLE, ROD 51, LEVEL B	32 TO 1897 DEGREES F	
357	TE-1205	SUBCHANNEL NUMBER 5 THERMOCOUPLE	32 TO 1897 DEGREES F	
358	TE-1223	SUBCHANNEL NUMBER 23 THERMOCOUPLE	32 TO 1897 DEGREES F	
359	TE-1214	SUBCHANNEL NUMBER 14 THERMOCOUPLE	32 TO 1897 DEGREES F	
360	TE-1232	SUBCHANNEL NUMBER 32 THERMOCOUPLE	32 TO 1897 DEGREES F	
361	TE-1211	SUBCHANNEL NUMBER 11 THERMOCOUPLE	32 TO 1897 DEGREES F	
362	TE-1221	SUBCHANNEL NUMBER 21 THERMOCOUPLE	32 TO 1897 DEGREES F	
363	TE-1231	SUBCHANNEL NUMBER 31 THERMOCOUPLE	32 TO 1897 DEGREES F	
364	TE-1201	SUBCHANNEL NUMBER 1 THERMOCOUPLE	32 TO 1897 DEGREES F	
365	TE-1251	SUBCHANNEL NUMBER 51 THERMOCOUPLE	32 TO 1897 DEGREES F	
366	TE-1248	SUBCHANNEL NUMBER 48 THERMOCOUPLE	32 TO 1897 DEGREES F	
367	TE-1273	SUBCHANNEL NUMBER 73 THERMOCOUPLE	32 TO 1897 DEGREES F	
368	TE-1265	SUBCHANNEL NUMBER 65 THERMOCOUPLE	32 TO 1897 DEGREES F	
369	TE-1256	SUBCHANNEL NUMBER 56 THERMOCOUPLE	32 TO 1897 DEGREES F	
370	TE-1240	SUBCHANNEL NUMBER 40 THERMOCOUPLE	32 TO 1897 DEGREES F	
371	TE-1230	SUBCHANNEL NUMBER 30 THERMOCOUPLE	32 TO 1897 DEGREES F	
372	TE-1237	SUBCHANNEL NUMBER 37 THERMOCOUPLE	32 TO 1897 DEGREES F	
373	TE-1238	SUBCHANNEL NUMBER 38 THERMOCOUPLE	32 TO 1897 DEGREES F	
374	TE-1239	SUBCHANNEL NUMBER 39 THERMOCOUPLE	32 TO 1897 DEGREES F	
375	TE-1260	SUBCHANNEL NUMBER 60 THERMOCOUPLE	32 TO 1897 DEGREES F	
376	TE-1270	SUBCHANNEL NUMBER 70 THERMOCOUPLE	32 TO 1897 DEGREES F	
377	TE-1259	SUBCHANNEL NUMBER 59 THERMOCOUPLE	32 TO 1897 DEGREES F	
378	TE-1277	SUBCHANNEL NUMBER 77 THERMOCOUPLE	32 TO 1897 DEGREES F	
379	TE-1261	SUBCHANNEL NUMBER 61 THERMOCOUPLE	32 TO 1897 DEGREES F	

Table 3 (continued)

FIGURE NUMBER	INSTRUMENT NAME	DESCRIPTION	RANGE	COMMENTS
380	TE-1271	SUBCHANNEL NUMBER 71 THERMOCOUPLE	32 TO 1897 DEGREES F	
381	TE-1241	SUBCHANNEL NUMBER 41 THERMOCOUPLE	32 TO 1897 DEGREES F	
382	TE-1250	SUBCHANNEL NUMBER 50 THERMOCOUPLE	32 TO 1897 DEGREES F	
383	TE-1268	SUBCHANNEL NUMBER 68 THERMOCOUPLE	32 TO 1897 DEGREES F	
384	TE-1281	SUBCHANNEL NUMBER 81 THERMOCOUPLE	32 TO 1897 DEGREES F	
385	TE-182E	SHROUD BOX THERMOCOUPLE, LEVEL B, EAST SIDE	32 TO 1897 DEGREES F	
386	TE-187N	SHROUD BOX THERMOCOUPLE, LEVEL G, NORTH SIDE	32 TO 1897 DEGREES F	
387	TE-183N	SHROUD BOX THERMOCOUPLE, LEVEL C, NORTH SIDE	32 TO 1897 DEGREES F	
388	TE-184E	SHROUD BOX THERMOCOUPLE, LEVEL D, EAST SIDE	32 TO 1897 DEGREES F	
389	TE-150	TEST SECTION BOTTOM FLANGE TEMPERATURE SIDE	32 TO 1897 DEGREES F	
390	TE-151	TEST SECTION BOTTOM FLANGE TEMPERATURE SIDE	32 TO 1897 DEGREES F	FAILED INSTRUMENT
391	TE-152	TEST SECTION BOTTOM FLANGE TEMPERATURE SIDE	32 TO 1897 DEGREES F	
392	TE-1	PRESSURIZER VAPOR TEMPERATURE	32 TO 1897 DEGREES F	
393	TE-2	PRESSURIZER WATER TEMPERATURE	32 TO 1897 DEGREES F	
394	TE-116	PRESSURIZER EXIT SPOOL TEMPERATURE	32 TO 1897 DEGREES F	
395	TE-24	HORIZONTAL INLET SPOOL TEMPERATURE	32 TO 1897 DEGREES F	
396	TE-172	VERTICAL INLET SPOOL TEMPERATURE	32 TO 1897 DEGREES F	
397	TE-222	VERTICAL OUTLET SPOOL TEMPERATURE	32 TO 1897 DEGREES F	
398	TE-40	HORIZONTAL OUTLET SPOOL TEMPERATURE	32 TO 1897 DEGREES F	
399	TE-29	INLET BLOWDOWN PLENUM TEMPERATURE	32 TO 1897 DEGREES F	
400	TE-45	OUTLET BLOWDOWN PLENUM TEMPERATURE	32 TO 1897 DEGREES F	
401	TE-58	HEAT EXCHANGER D OUTLET TEMPERATURE	32 TO 1897 DEGREES F	
402	TE-57	HEAT EXCHANGER A SPOOL TEMPERATURE	32 TO 1897 DEGREES F	
403	TE-62	HEAT EXCHANGER B SPOOL TEMPERATURE	32 TO 1897 DEGREES F	
404	TE-67	HEAT EXCHANGER C SPOOL TEMPERATURE	32 TO 1897 DEGREES F	

Table 3 (continued)

FIGURE NUMBER	INSTRUMENT NAME	DESCRIPTION	RANGE	COMMENTS
405	TE-408B	PRESSURE SUPPRESSION TANK SPRAY TEMPERATURE	32 TO 1897 DEGREES F	
406	TE-520B	4 INCH DEMINERALIZED WATER HEADER TEMPERATURE	32 TO 1897 DEGREES F	
407	TE-521	PURIFICATION COOLING WATER OUTLET TEMPERATURE	32 TO 1897 DEGREES F	
408	TE-901	PRESSURE STEAM KILLER AIR VENT TEMPERATURE	32 TO 1897 DEGREES F	
409	TE-208	BUNDLE OUTLET SPOOL TEMPERATURE	32 TO 1897 DEGREES F	
410	TE-256	TEST SECTION INLET TEMPERATURE	32 TO 1897 DEGREES F	
411	TE-265	BUNDLE INLET LOWER SPOOL TEMPERATURE	32 TO 1897 DEGREES F	
412	TE-284	OLD DOWNCOMER PURGE LINE RETURN TEMPERATURE	32 TO 1897 DEGREES F	
413	TE-313CD	SHEATH THERMOCOUPLE, ROD 13, LEVEL D	32 TO 1897 DEGREES F	
414	TE-313BC	SHEATH THERMOCOUPLE, ROD 13, LEVEL C	32 TO 1897 DEGREES F	
415	TE-313CE	SHEATH THERMOCOUPLE, ROD 13, LEVEL E	32 TO 1897 DEGREES F	
416	TE-313BF	SHEATH THERMOCOUPLE, ROD 13, LEVEL F	32 TO 1897 DEGREES F	
417	TE-323BC	SHEATH THERMOCOUPLE, ROD 23, LEVEL C	32 TO 1897 DEGREES F	
418	TE-1220	SUBCHANNEL NUMBER 20 THERMOCOUPLE	32 TO 1897 DEGREES F	
419	TE-1219	SUBCHANNEL NUMBER 19 THERMOCOUPLE	32 TO 1897 DEGREES F	
420	TE-323AA	SHEATH THERMOCOUPLE, ROD 23, LEVEL A	32 TO 1897 DEGREES F	
421	TE-321AB	SHEATH THERMOCOUPLE, ROD 21, LEVEL B	32 TO 1897 DEGREES F	
422	TE-321AA	SHEATH THERMOCOUPLE, ROD 21, LEVEL A	32 TO 1897 DEGREES F	
423	TE-321BC	SHEATH THERMOCOUPLE, ROD 21, LEVEL C	32 TO 1897 DEGREES F	
424	TE-321CD	SHEATH THERMOCOUPLE, ROD 21, LEVEL D	32 TO 1897 DEGREES F	
425	TE-327AA	SHEATH THERMOCOUPLE, ROD 27, LEVEL A	32 TO 1897 DEGREES F	
426	TE-327CB	SHEATH THERMOCOUPLE, ROD 27, LEVEL B	32 TO 1897 DEGREES F	
427	TE-326CD	SHEATH THERMOCOUPLE, ROD 26, LEVEL D	32 TO 1897 DEGREES F	
428	TE-327AD	SHEATH THERMOCOUPLE, ROD 27, LEVEL D	32 TO 1897 DEGREES F	
429	TE-327BC	SHEATH THERMOCOUPLE, ROD 27, LEVEL C	32 TO 1897 DEGREES F	FAILED INSTRUMENT

Table 3 (continued)

FIGURE NUMBER	INSTRUMENT NAME	DESCRIPTION	RANGE	COMMENTS
430	TE-327CD	SHEATH THERMOCOUPLE, ROD 27, LEVEL D	32 TO 1897 DEGREES F	
431	TE-327CC	SHEATH THERMOCOUPLE, ROD 27, LEVEL C	32 TO 1897 DEGREES F	
432	TE-327BA	SHEATH THERMOCOUPLE, ROD 27, LEVEL A	32 TO 1897 DEGREES F	
433	EEE-1026KZ	ZERO INPUT CHANNELS 1280 TO 1407	0 TO 40 MV	
434	EEE-1026KC	CALIBRATION INPUT CHANNELS 1280 TO 1407	0 TO 40 MV	
435	TE-307AC	SHEATH THERMOCOUPLE, ROD 7, LEVEL C	32 TO 1897 DEGREES F	
436	TE-332CE	SHEATH THERMOCOUPLE, ROD 32, LEVEL E	32 TO 1897 DEGREES F	
437	TE-307AF	SHEATH THERMOCOUPLE, ROD 7, LEVEL F	32 TO 1897 DEGREES F	
438	TE-307CE	SHEATH THERMOCOUPLE, ROD 7, LEVEL E	32 TO 1897 DEGREES F	
439	TE-316BG	SHEATH THERMOCOUPLE, ROD 16, LEVEL G	32 TO 1897 DEGREES F	
440	TE-332CF	SHEATH THERMOCOUPLE, ROD 32, LEVEL F	32 TO 1897 DEGREES F	
441	TE-332CD	SHEATH THERMOCOUPLE, ROD 32, LEVEL D	32 TO 1897 DEGREES F	
442	TE-318AG	SHEATH THERMOCOUPLE, ROD 18, LEVEL G	32 TO 1897 DEGREES F	
443	TE-314AB	SHEATH THERMOCOUPLE, ROD 14, LEVEL B	32 TO 1897 DEGREES F	
444	TE-332CG	SHEATH THERMOCOUPLE, ROD 32, LEVEL G	32 TO 1897 DEGREES F	
445	TE-318AE	SHEATH THERMOCOUPLE, ROD 18, LEVEL E	32 TO 1897 DEGREES F	
446	TE-324AE	SHEATH THERMOCOUPLE, ROD 24, LEVEL E	32 TO 1897 DEGREES F	
447	TE-305BU	SHEATH THERMOCOUPLE, ROD 5, LEVEL U	32 TO 1897 DEGREES F	
448	TE-305AS	SHEATH THERMOCOUPLE, ROD 5, LEVEL S	32 TO 1897 DEGREES F	
449	TE-305BH	SHEATH THERMOCOUPLE, ROD 5, LEVEL H	32 TO 1897 DEGREES F	
450	TE-305CY	SHEATH THERMOCOUPLE, ROD 5, LEVEL Y	32 TO 1897 DEGREES F	
451	TE-188AC	ARRAY ROD THERMOCOUPLE, GRID 19, SUBCHANNEL 22, LEVEL C	32 TO 1897 DEGREES F	
452	TE-308CD	SHEATH THERMOCOUPLE, ROD 8, LEVEL [illegible]	32 TO 1897 DEGREES F	
453	TE-188BE	ARRAY ROD THERMOCOUPLE, GRID 19, SUBCHANNEL 30, LEVEL E	32 TO 1897 DEGREES F	

Table 3 (continued)

FIGURE NUMBER	INSTRUMENT NAME	DESCRIPTION	RANGE	COMMENTS
454	TE-188AF	ARRAY ROD THERMOCOUPLE, GRID 19, SUBCHANNEL 22, LEVEL F	32 TO 1897 DEGREES F	
455	TE-188BB	ARRAY ROD THERMOCOUPLE, GRID 19, SUBCHANNEL 30, LEVEL B	32 TO 1897 DEGREES F	
456	TE-188AD	ARRAY ROD THERMOCOUPLE, GRID 19, SUBCHANNEL 22, LEVEL D	32 TO 1897 DEGREES F	
457	TE-188AG	ARRAY ROD THERMOCOUPLE, GRID 19, SUBCHANNEL 22, LEVEL G	32 TO 1897 DEGREES F	
458	TE-188AB	ARRAY ROD THERMOCOUPLE, GRID 19, SUBCHANNEL 22, LEVEL B	32 TO 1897 DEGREES F	
459	TE-188BD	ARRAY ROD THERMOCOUPLE, GRID 19, SUBCHANNEL 30, LEVEL D	32 TO 1897 DEGREES F	
460	TE-188BA	ARRAY ROD THERMOCOUPLE, GRID 19, SUBCHANNEL 30, LEVEL A	32 TO 1897 DEGREES F	QUESTIONABLE
461	TE-188BF	ARRAY ROD THERMOCOUPLE, GRID 19, SUBCHANNEL 30, LEVEL F	32 TO 1897 DEGREES F	
462	TE-188BC	ARRAY ROD THERMOCOUPLE, GRID 19, SUBCHANNEL 30, LEVEL C	32 TO 1897 DEGREES F	
463	TE-188AE	ARRAY ROD THERMOCOUPLE, GRID 19, SUBCHANNEL 22, LEVEL E	32 TO 1897 DEGREES F	
464	TE-188AA	ARRAY ROD THERMOCOUPLE, GRID 19, SUBCHANNEL 22, LEVEL A	32 TO 1897 DEGREES F	
465	TE-315AF	SHEATH THERMOCOUPLE, ROD 15, LEVEL F	32 TO 1897 DEGREES F	
466	TE-307BF	SHEATH THERMOCOUPLE, ROD 7, LEVEL F	32 TO 1897 DEGREES F	
467	TE-315AC	SHEATH THERMOCOUPLE, ROD 15, LEVEL C	32 TO 1897 DEGREES F	
468	TE-307BE	SHEATH THERMOCOUPLE, ROD 7, LEVEL E	32 TO 1897 DEGREES F	
469	TE-318CG	SHEATH THERMOCOUPLE, ROD 18, LEVEL G	32 TO 1897 DEGREES F	
470	TE-306AA	SHEATH THERMOCOUPLE, ROD 6, LEVEL A	32 TO 1897 DEGREES F	
471	TE-306AB	SHEATH THERMOCOUPLE, ROD 6, LEVEL B	32 TO 1897 DEGREES F	
472	TE-308BA	SHEATH THERMOCOUPLE, ROD 8, LEVEL A	32 TO 1897 DEGREES F	
473	TE-308CB	SHEATH THERMOCOUPLE, ROD 8, LEVEL B	32 TO 1897 DEGREES F	

Table 3 (continued)

FIGURE NUMBER	INSTRUMENT NAME	DESCRIPTION	RANGE	COMMENTS
474	TE-308BD	SHEATH THERMOCOUPLE, ROD 8, LEVEL D	32 TO 1897 DEGREES F	
475	TE-308BC	SHEATH THERMOCOUPLE, ROD 8, LEVEL C	32 TO 1897 DEGREES F	
476	TE-316BF	SHEATH THERMOCOUPLE, ROD 16, LEVEL F	32 TO 1897 DEGREES F	
477	TE-316CE	SHEATH THERMOCOUPLE, ROD 16, LEVEL E	32 TO 1897 DEGREES F	
478	TE-316AD	SHEATH THERMOCOUPLE, ROD 16, LEVEL D	32 TO 1897 DEGREES F	
479	TE-316CG	SHEATH THERMOCOUPLE, ROD 16, LEVEL G	32 TO 1897 DEGREES F	
480	TE-324CE	SHEATH THERMOCOUPLE, ROD 24, LEVEL E	32 TO 1897 DEGREES F	
481	TE-324CB	SHEATH THERMOCOUPLE, ROD 24, LEVEL B	32 TO 1897 DEGREES F	
482	TE-324AC	SHEATH THERMOCOUPLE, ROD 24, LEVEL C	32 TO 1897 DEGREES F	
483	TE-324BD	SHEATH THERMOCOUPLE, ROD 24, LEVEL D	32 TO 1897 DEGREES F	
484	TE-344CD	SHEATH THERMOCOUPLE, ROD 44, LEVEL D	32 TO 1897 DEGREES F	
485	TE-344CC	SHEATH THERMOCOUPLE, ROD 44, LEVEL C	32 TO 1897 DEGREES F	
486	TE-344CB	SHEATH THERMOCOUPLE, ROD 44, LEVEL B	32 TO 1897 DEGREES F	
487	TE-344CE	SHEATH THERMOCOUPLE, ROD 44, LEVEL E	32 TO 1897 DEGREES F	
488	TE-317BE	SHEATH THERMOCOUPLE, ROD 17, LEVEL E	32 TO 1897 DEGREES F	
489	TE-335BB	SHEATH THERMOCOUPLE, ROD 35, LEVEL B	32 TO 1897 DEGREES F	
490	TE-317CE	SHEATH THERMOCOUPLE, ROD 17, LEVEL E	32 TO 1897 DEGREES F	
491	TE-335BE	SHEATH THERMOCOUPLE, ROD 35, LEVEL E	32 TO 1897 DEGREES F	
492	TE-333CB	SHEATH THERMOCOUPLE, ROD 33, LEVEL B	32 TO 1897 DEGREES F	
493	TE-333CE	SHEATH THERMOCOUPLE, ROD 33, LEVEL E	32 TO 1897 DEGREES F	
494	TE-333AC	SHEATH THERMOCOUPLE, ROD 33, LEVEL C	32 TO 1897 DEGREES F	
495	TE-333AD	SHEATH THERMOCOUPLE, ROD 33, LEVEL D	32 TO 1897 DEGREES F	
496	TE-317AE	SHEATH THERMOCOUPLE, ROD 17, LEVEL E	32 TO 1897 DEGREES F	
497	TE-317CC	SHEATH THERMOCOUPLE, ROD 17, LEVEL C	32 TO 1897 DEGREES F	
498	TE-317CD	SHEATH THERMOCOUPLE, ROD 17, LEVEL D	32 TO 1897 DEGREES F	

Table 3 (continued)

FIGURE NUMBER	INSTRUMENT NAME	DESCRIPTION	RANGE	COMMENTS
499	TE-317CB	SHEATH THERMOCOUPLE, ROD 17, LEVEL B	32 TO 1897 DEGREES F	
500	TE-1216	SUBCHANNEL NUMBER 16 THERMOCOUPLE	32 TO 1897 DEGREES F	
501	TE-359CE	SHEATH THERMOCOUPLE, ROD 59, LEVEL E	32 TO 1897 DEGREES F	
502	TE-328BD	SHEATH THERMOCOUPLE, ROD 28, LEVEL D	32 TO 1897 DEGREES F	
503	TE-328CF	SHEATH THERMOCOUPLE, ROD 28, LEVEL F	32 TO 1897 DEGREES F	
504	TE-320BG	SHEATH THERMOCOUPLE, ROD 20, LEVEL G	32 TO 1897 DEGREES F	
505	TE-320CG	SHEATH THERMOCOUPLE, ROD 20, LEVEL G	32 TO 1897 DEGREES F	
506	TE-320AD	SHEATH THERMOCOUPLE, ROD 20, LEVEL D	32 TO 1897 DEGREES F	
507	TE-320BF	SHEATH THERMOCOUPLE, ROD 20, LEVEL F	32 TO 1897 DEGREES F	
508	TE-325BB	SHEATH THERMOCOUPLE, ROD 25, LEVEL B	32 TO 1897 DEGREES F	
509	TE-325CC	SHEATH THERMOCOUPLE, ROD 25, LEVEL C	32 TO 1897 DEGREES F	
510	TE-325CD	SHEATH THERMOCOUPLE, ROD 25, LEVEL D	32 TO 1897 DEGREES F	
511	TE-325CA	SHEATH THERMOCOUPLE, ROD 25, LEVEL A	32 TO 1897 DEGREES F	
512	TE-318AD	SHEATH THERMOCOUPLE, ROD 18, LEVEL D	32 TO 1897 DEGREES F	QUESTIONABLE
513	TE-318BG	SHEATH THERMOCOUPLE, ROD 18, LEVEL G	32 TO 1897 DEGREES F	QUESTIONABLE
514	TE-318AF	SHEATH THERMOCOUPLE, ROD 18, LEVEL F	32 TO 1897 DEGREES F	QUESTIONABLE
515	TE-318BE	SHEATH THERMOCOUPLE, ROD 18, LEVEL E	32 TO 1897 DEGREES F	
516	TE-359AE	SHEATH THERMOCOUPLE, ROD 59, LEVEL E	32 TO 1897 DEGREES F	
517	TE-359AD	SHEATH THERMOCOUPLE, ROD 59, LEVEL D	32 TO 1897 DEGREES F	
518	TE-359CF	SHEATH THERMOCOUPLE, ROD 59, LEVEL F	32 TO 1897 DEGREES F	
519	TE-359CC	SHEATH THERMOCOUPLE, ROD 59, LEVEL C	32 TO 1897 DEGREES F	
520	TE-358CD	SHEATH THERMOCOUPLE, ROD 58, LEVEL D	32 TO 1897 DEGREES F	
521	TE-358BE	SHEATH THERMOCOUPLE, ROD 58, LEVEL E	32 TO 1897 DEGREES F	
522	TE-358CG	SHEATH THERMOCOUPLE, ROD 58, LEVEL G	32 TO 1897 DEGREES F	
523	TE-309CD	SHEATH THERMOCOUPLE, ROD 9, LEVEL D	32 TO 1897 DEGREES F	

Table 3 (continued)

FIGURE NUMBER	INSTRUMENT NAME	DESCRIPTION	RANGE	COMMENTS
524	TE-309AC	SHEATH THERMOCOUPLE, ROD 9, LEVEL C	32 TO 1897 DEGREES F	
525	TE-311CC	SHEATH THERMOCOUPLE, ROD 11, LEVEL C	32 TO 1897 DEGREES F	
526	TE-311CB	SHEATH THERMOCOUPLE, ROD 11, LEVEL B	32 TO 1897 DEGREES F	
527	TE-311AB	SHEATH THERMOCOUPLE, ROD 11, LEVEL B	32 TO 1897 DEGREES F	
528	TE-311AA	SHEATH THERMOCOUPLE, ROD 11, LEVEL A	32 TO 1897 DEGREES F	
529	TE-357BB	SHEATH THERMOCOUPLE, ROD 57, LEVEL B	32 TO 1897 DEGREES F	
530	TE-357BC	SHEATH THERMOCOUPLE, ROD 57, LEVEL C	32 TO 1897 DEGREES F	
531	TE-357AA	SHEATH THERMOCOUPLE, ROD 57, LEVEL A	32 TO 1897 DEGREES F	
532	TE-357BD	SHEATH THERMOCOUPLE, ROD 57, LEVEL D	32 TO 1897 DEGREES F	
533	TE-304AF	SHEATH THERMOCOUPLE, ROD 4, LEVEL F	32 TO 1897 DEGREES F	
534	TE-309CB	SHEATH THERMOCOUPLE, ROD 9, LEVEL B	32 TO 1897 DEGREES F	
535	TE-303CD	SHEATH THERMOCOUPLE, ROD 3, LEVEL D	32 TO 1897 DEGREES F	
536	TE-303BE	SHEATH THERMOCOUPLE, ROD 3, LEVEL E	32 TO 1897 DEGREES F	
537	TE-303CG	SHEATH THERMOCOUPLE, ROD 3, LEVEL G	32 TO 1897 DEGREES F	
538	TE-303BF	SHEATH THERMOCOUPLE, ROD 3, LEVEL F	32 TO 1897 DEGREES F	
539	EEE-1026LZ	ZERO INPUT CHANNELS 1408 TO 1535	0 TO 40 MV	
540	EEE-1026LC	CALIBRATION INPUT CHANNELS 1408 TO 1535	0 TO 40 MV	
541	TE-310CD	SHEATH THERMOCOUPLE, ROD 10, LEVEL D	32 TO 1897 DEGREES F	
542	TE-310[illegible]	SHEATH THERMOCOUPLE, ROD 10, LEVEL F	32 TO 1897 DEGREES F	
543	TE-310CC	SHEATH THERMOCOUPLE, ROD 10, LEVEL C	32 TO 1897 DEGREES F	
544	TE-310BE	SHEATH THERMOCOUPLE, ROD 10, LEVEL E	32 TO 1897 DEGREES F	
545	TE-304BE	SHEATH THERMOCOUPLE, ROD 4, LEVEL E	32 TO 1897 DEGREES F	
546	TE-304AC	SHEATH THERMOCOUPLE, ROD 4, LEVEL C	32 TO 1897 DEGREES F	
547	TE-303CE	SHEATH THERMOCOUPLE, ROD 3, LEVEL E	32 TO 1897 DEGREES F	
548	TE-312CD	SHEATH THERMOCOUPLE, ROD 12, LEVEL D	32 TO 1897 DEGREES F	

Table 3 (continued)

FIGURE NUMBER	INSTRUMENT NAME	DESCRIPTION	RANGE	COMMENTS
549	TE-301AD	SHEATH THERMOCOUPLE, ROD 1, LEVEL D	32 TO 1897 DEGREES F	
550	TE-343BD	SHEATH THERMOCOUPLE, ROD 43, LEVEL D	32 TO 1897 DEGREES F	
551	TE-302AD	SHEATH THERMOCOUPLE, ROD 2, LEVEL D	32 TO 1897 DEGREES F	
552	TE-302AB	SHEATH THERMOCOUPLE, ROD 2, LEVEL B	32 TO 1897 DEGREES F	
553	TE-302AE	SHEATH THERMOCOUPLE, ROD 2, LEVEL E	32 TO 1897 DEGREES F	
554	TE-302BC	SHEATH THERMOCOUPLE, ROD 2, LEVEL C	32 TO 1897 DEGREES F	
555	TE-310BF	SHEATH THERMOCOUPLE, ROD 10, LEVEL F	32 TO 1897 DEGREES F	
556	TE-310CF	SHEATH THERMOCOUPLE, ROD 10, LEVEL F	32 TO 1897 DEGREES F	
557	TE-358AE	SHEATH THERMOCOUPLE, ROD 58, LEVEL E	32 TO 1897 DEGREES F	
558	TE-357AC	SHEATH THERMOCOUPLE, ROD 57, LEVEL C	32 TO 1897 DEGREES F	
559	TE-357BA	SHEATH THERMOCOUPLE, ROD 57, LEVEL A	32 TO 1897 DEGREES F	
560	TE-357CB	SHEATH THERMOCOUPLE, ROD 57, LEVEL B	32 TO 1897 DEGREES F	
561	TE-357AB	SHEATH THERMOCOUPLE, ROD 57, LEVEL B	32 TO 1897 DEGREES F	
562	TE-359AF	SHEATH THERMOCOUPLE, ROD 59, LEVEL F	32 TO 1897 DEGREES F	
563	TE-357CD	SHEATH THERMOCOUPLE, ROD 57, LEVEL D	32 TO 1897 DEGREES F	
564	TE-359BF	SHEATH THERMOCOUPLE, ROD 59, LEVEL F	32 TO 1897 DEGREES F	
565	TE-329AB	SHEATH THERMOCOUPLE, ROD 29, LEVEL B	32 TO 1897 DEGREES F	
566	TE-329CD	SHEATH THERMOCOUPLE, ROD 29, LEVEL D	32 TO 1897 DEGREES F	
567	TE-329CB	SHEATH THERMOCOUPLE, ROD 29, LEVEL B	32 TO 1897 DEGREES F	
568	TE-329CE	SHEATH THERMOCOUPLE, ROD 29, LEVEL E	32 TO 1897 DEGREES F	
569	TE-329AC	SHEATH THERMOCOUPLE, ROD 29, LEVEL C	32 TO 1897 DEGREES F	
570	TE-329BE	SHEATH THERMOCOUPLE, ROD 29, LEVEL E	32 TO 1897 DEGREES F	
571	TE-329AD	SHEATH THERMOCOUPLE, ROD 29, LEVEL D	32 TO 1897 DEGREES F	
572	TE-347CF	SHEATH THERMOCOUPLE, ROD 47, LEVEL F	32 TO 1897 DEGREES F	
573	TE-345BD	SHEATH THERMOCOUPLE, ROD 45, LEVEL D	32 TO 1897 DEGREES F	

Table 3 (continued)

FIGURE NUMBER	INSTRUMENT NAME	DESCRIPTION	RANGE	COMMENTS
574	TE-345BF	SHEATH THERMOCOUPLE, ROD 45, LEVEL F	32 TO 1897 DEGREES F	
575	TE-345AE	SHEATH THERMOCOUPLE, ROD 45, LEVEL E	32 TO 1897 DEGREES F	
576	TE-345BE	SHEATH THERMOCOUPLE, ROD 45, LEVEL E	32 TO 1897 DEGREES F	
577	TE-345BG	SHEATH THERMOCOUPLE, ROD 45, LEVEL G	32 TO 1897 DEGREES F	
578	TE-345AF	SHEATH THERMOCOUPLE, ROD 45, LEVEL F	32 TO 1897 DEGREES F	
579	TE-345CG	SHEATH THERMOCOUPLE, ROD 45, LEVEL G	32 TO 1897 DEGREES F	
580	TE-361CJ	SHEATH THERMOCOUPLE, ROD 61, LEVEL J	32 TO 1897 DEGREES F	FAILED INSTRUMENT
581	TE-361BJ	SHEATH THERMOCOUPLE, ROD 61, LEVEL J	32 TO 1897 DEGREES F	FAILED INSTRUMENT
582	TE-364BD	SHEATH THERMOCOUPLE, ROD 64, LEVEL D	32 TO 1897 DEGREES F	
583	TE-353BF	SHEATH THERMOCOUPLE, ROD 59, LEVEL F	32 TO 1897 DEGREES F	
584	TE-364AE	SHEATH THERMOCOUPLE, ROD 64, LEVEL E	32 TO 1897 DEGREES F	
585	TE-364AF	SHEATH THERMOCOUPLE, ROD 64, LEVEL F	32 TO 1897 DEGREES F	
586	TE-313AE	SHEATH THERMOCOUPLE, ROD 13, LEVEL E	32 TO 1897 DEGREES F	
587	TE-364CF	SHEATH THERMOCOUPLE, ROD 64, LEVEL F	32 TO 1897 DEGREES F	
588	TE-364CD	SHEATH THERMOCOUPLE, ROD 64, LEVEL D	32 TO 1897 DEGREES F	
589	TE-364CG	SHEATH THERMOCOUPLE, ROD 64, LEVEL G	32 TO 1897 DEGREES F	
590	TE-334CU	SHEATH THERMOCOUPLE, ROD 34, LEVEL U	32 TO 1897 DEGREES F	
591	TE-334BS	SHEATH THERMOCOUPLE, ROD 34, LEVEL S	32 TO 1897 DEGREES F	
592	TE-334CS	SHEATH THERMOCOUPLE, ROD 34, LEVEL S	32 TO 1897 DEGREES F	
593	TE-334BU	SHEATH THERMOCOUPLE, ROD 34, LEVEL U	32 TO 1897 DEGREES F	
594	TE-360AB	SHEATH THERMOCOUPLE, ROD 60, LEVEL B	32 TO 1897 DEGREES F	
595	TE-360AA	SHEATH THERMOCOUPLE, ROD 60, LEVEL A	32 TO 1897 DEGREES F	
596	TE-360BD	SHEATH THERMOCOUPLE, ROD 60, LEVEL D	32 TO 1897 DEGREES F	
597	TE-334AH	SHEATH THERMOCOUPLE, ROD 34, LEVEL H	32 TO 1897 DEGREES F	
598	TE-334AY	SHEATH THERMOCOUPLE, ROD 34, LEVEL Y	32 TO 1897 DEGREES F	

Table 3 (continued)

FIGURE NUMBER	INSTRUMENT NAME	DESCRIPTION	RANGE	COMMENTS
599	TE-334BY	SHEATH THERMOCOUPLE, ROD 34, LEVEL Y	32 TO 1897 DEGREES F	
600	TE-334BH	SHEATH THERMOCOUPLE, ROD 34, LEVEL H	32 TO 1897 DEGREES F	
601	TE-184S	SHROUD BOX THERMOCOUPLE, LEVEL D, SOUTH SIDE	32 TO 1897 DEGREES F	
602	TE-183W	SHROUD BOX THERMOCOUPLE, LEVEL C, WEST SIDE	32 TO 1897 DEGREES F	
603	TE-187W	SHROUD BOX THERMOCOUPLE, LEVEL G, WEST SIDE	32 TO 1897 DEGREES F	
604	TE-182S	SHROUD BOX THERMOCOUPLE, LEVEL B, SOUTH SIDE	32 TO 1897 DEGREES F	
605	TE-352BU	SHEATH THERMOCOUPLE, ROD 52, LEVEL U	32 TO 1897 DEGREES F	
606	TE-352CU	SHEATH THERMOCOUPLE, ROD 52, LEVEL U	32 TO 1897 DEGREES F	
607	TE-352AS	SHEATH THERMOCOUPLE, ROD 52, LEVEL S	32 TO 1897 DEGREES F	
608	TE-352CS	SHEATH THERMOCOUPLE, ROD 52, LEVEL S	32 TO 1897 DEGREES F	
609	TE-352BH	SHEATH THERMOCOUPLE, ROD 52, LEVEL H	32 TO 1897 DEGREES F	
610	TE-352AH	SHEATH THERMOCOUPLE, ROD 52, LEVEL H	32 TO 1897 DEGREES F	
611	TE-352BY	SHEATH THERMOCOUPLE, ROD 52, LEVEL Y	32 TO 1897 DEGREES F	
612	TE-352AY	SHEATH THERMOCOUPLE, ROD 52, LEVEL Y	32 TO 1897 DEGREES F	
613	TE-350AC	SHEATH THERMOCOUPLE, ROD 50, LEVEL C	32 TO 1897 DEGREES F	
614	TE-350BD	SHEATH THERMOCOUPLE, ROD 50, LEVEL D	32 TO 1897 DEGREES F	
615	TE-326AE	SHEATH THERMOCOUPLE, ROD 26, LEVEL E	32 TO 1897 DEGREES F	
616	TE-350CE	SHEATH THERMOCOUPLE, ROD 50, LEVEL E	32 TO 1897 DEGREES F	
617	TE-350AF	SHEATH THERMOCOUPLE, ROD 50, LEVEL F	32 TO 1897 DEGREES F	
618	TE-350CF	SHEATH THERMOCOUPLE, ROD 50, LEVEL F	32 TO 1897 DEGREES F	
619	TE-350AD	SHEATH THERMOCOUPLE, ROD 50, LEVEL D	32 TO 1897 DEGREES F	FAILED INSTRUMENT
620	TE-350BC	SHEATH THERMOCOUPLE, ROD 50, LEVEL C	32 TO 1897 DEGREES F	
621	TE-321BD	SHEATH THERMOCOUPLE, ROD 21, LEVEL D	32 TO 1897 DEGREES F	
622	TE-1229	SUBCHANNEL NUMBER 29 THERMOCOUPLE	32 TO 1897 DEGREES F	
623	TE-326BE	SHEATH THERMOCOUPLE, ROD 26, LEVEL E	32 TO 1897 DEGREES F	

Table 3 (continued)

FIGURE NUMBER	INSTRUMENT NAME	DESCRIPTION	RANGE	COMMENTS
624	TE-1213	SUBCHANNEL NUMBER 13 THERMOCOUPLE	32 TO 1897 DEGREES F	
625	TE-351BE	SHEATH THERMOCOUPLE, ROD 51, LEVEL E	32 TO 1897 DEGREES F	
626	TE-186E	SHROUD BOX THERMOCOUPLE, LEVEL G, EAST SIDE	32 TO 1897 DEGREES F	
627	TE-328CD	SHEATH THERMOCOUPLE, ROD 28, LEVEL D	32 TO 1897 DEGREES F	
628	TE-320CE	SHEATH THERMOCOUPLE, ROD 20, LEVEL E	32 TO 1897 DEGREES F	QUESTIONABLE
629	TE-320BE	SHEATH THERMOCOUPLE, ROD 20, LEVEL E	32 TO 1897 DEGREES F	
630	TE-320AE	SHEATH THERMOCOUPLE, ROD 20, LEVEL E	32 TO 1897 DEGREES F	
631	TE-320CD	SHEATH THERMOCOUPLE, ROD 20, LEVEL D	32 TO 1897 DEGREES F	
632	TE-320CF	SHEATH THERMOCOUPLE, ROD 20, LEVEL F	32 TO 1897 DEGREES F	
633	TE-320AF	SHEATH THERMOCOUPLE, ROD 20, LEVEL F	32 TO 1897 DEGREES F	
634	TE-320BD	SHEATH THERMOCOUPLE, ROD 20, LEVEL D	32 TO 1897 DEGREES F	
635	TE-316BE	SHEATH THERMOCOUPLE, ROD 16, LEVEL E	32 TO 1897 DEGREES F	
636	TE-355CD	SHEATH THERMOCOUPLE, ROD 55, LEVEL D	32 TO 1897 DEGREES F	
637	TE-314AC	SHEATH THERMOCOUPLE, ROD 14, LEVEL C	32 TO 1897 DEGREES F	
638	TE-314AA	SHEATH THERMOCOUPLE, ROD 14, LEVEL A	32 TO 1897 DEGREES F	
639	TE-318BD	SHEATH THERMOCOUPLE, ROD 18, LEVEL D	32 TO 1897 DEGREES F	
640	TE-1207	SUBCHANNEL NUMBER 7 THERMOCOUPLE	32 TO 1897 DEGREES F	
641	TE-1255	SUBCHANNEL NUMBER 55 THERMOCOUPLE	32 TO 1897 DEGREES F	
642	TE-318CD	SHEATH THERMOCOUPLE, ROD 18, LEVEL D	32 TO 1897 DEGREES F	
643	TE-320AG	SHEATH THERMOCOUPLE, ROD 20, LEVEL G	32 TO 1897 DEGREES F	
644	TE-325AB	SHEATH THERMOCOUPLE, ROD 25, LEVEL B	32 TO 1897 DEGREES F	
645	TE-325AA	SHEATH THERMOCOUPLE, ROD 25, LEVEL A	32 TO 1897 DEGREES F	
646	TE-325BA	SHEATH THERMOCOUPLE, ROD 25, LEVEL A	32 TO 1897 DEGREES F	
647	TE-325BC	SHEATH THERMOCOUPLE, ROD 25, LEVEL C	32 TO 1897 DEGREES F	
648	TE-325CB	SHEATH THERMOCOUPLE, ROD 25, LEVEL B	32 TO 1897 DEGREES F	

Table 3 (continued)

FIGURE NUMBER	INSTRUMENT NAME	DESCRIPTION	RANGE	COMMENTS
649	TE-325AC	SHEATH THERMOCOUPLE, ROD 25, LEVEL C	32 TO 1897 DEGREES F	
650	TE-325AD	SHEATH THERMOCOUPLE, ROD 25, LEVEL D	32 TO 1897 DEGREES F	
651	EEE-1026MZ	ZERO INPUT CHANNELS 1536 TO 1663	0 TO 40 MV	
652	EEE-1026MC	CALIBRATION INPUT CHANNELS 1536 TO 1663	0 TO 40 MV	
653	TE-337MC	MIDDLE THERMOCOUPLE, ROD 37, LEVEL C	35 TO 1900 DEGREES F	FAILED INSTRUMENT
654	TE-337ME	MIDDLE THERMOCOUPLE, ROD 37, LEVEL E	35 TO 1900 DEGREES F	
655	TE-337MD	MIDDLE THERMOCOUPLE, ROD 37, LEVEL D	35 TO 1900 DEGREES F	
656	TE-337MF	MIDDLE THERMOCOUPLE, ROD 37, LEVEL F	35 TO 1900 DEGREES F	
657	TE-345ME	MIDDLE THERMOCOUPLE, ROD 45, LEVEL E	35 TO 1900 DEGREES F	
658	TE-345MG	MIDDLE THERMOCOUPLE, ROD 45, LEVEL G	35 TO 1900 DEGREES F	
659	TE-345MD	MIDDLE THERMOCOUPLE, ROD 45, LEVEL D	35 TO 1900 DEGREES F	
660	TE-332AE	SHEATH THERMOCOUPLE, ROD 32, LEVEL E	32 TO 1897 DEGREES F	
661	TE-328MC	MIDDLE THERMOCOUPLE, ROD 28, LEVEL C	35 TO 1900 DEGREES F	
662	TE-328ME	MIDDLE THERMOCOUPLE, ROD 28, LEVEL E	35 TO 1900 DEGREES F	
663	TE-328MF	MIDDLE THERMOCOUPLE, ROD 28, LEVEL F	35 TO 1900 DEGREES F	
664	TE-328MD	MIDDLE THERMOCOUPLE, ROD 28, LEVEL D	35 TO 1900 DEGREES F	
665	TE-329ME	MIDDLE THERMOCOUPLE, ROD 29, LEVEL E	35 TO 1900 DEGREES F	
666	TE-329MC	MIDDLE THERMOCOUPLE, ROD 29, LEVEL C	35 TO 1900 DEGREES F	
667	TE-329MD	MIDDLE THERMOCOUPLE, ROD 29, LEVEL D	35 TO 1900 DEGREES F	
668	TE-329MB	MIDDLE THERMOCOUPLE, ROD 29, LEVEL B	35 TO 1900 DEGREES F	
669	TE-338MD	MIDDLE THERMOCOUPLE, ROD 38, LEVEL D	35 TO 1900 DEGREES F	
670	TE-338MB	MIDDLE THERMOCOUPLE, ROD 38, LEVEL B	35 TO 1900 DEGREES F	
671	TE-338MA	MIDDLE THERMOCOUPLE, ROD 38, LEVEL A	35 TO 1900 DEGREES F	
672	TE-338MC	MIDDLE THERMOCOUPLE, ROD 38, LEVEL C	35 TO 1900 DEGREES F	
673	TE-355MA	MIDDLE THERMOCOUPLE, ROD 55, LEVEL A	35 TO 1900 DEGREES F	

Table 3 (continued)

FIGURE NUMBER	INSTRUMENT NAME	DESCRIPTION	RANGE	COMMENTS
674	TE-355MB	MIDDLE THERMOCOUPLE, ROD 55, LEVEL B	35 TO 1900 DEGREES F	
675	TE-355MC	MIDDLE THERMOCOUPLE, ROD 55, LEVEL C	35 TO 1900 DEGREES F	
676	TE-355MD	MIDDLE THERMOCOUPLE, ROD 55, LEVEL D	35 TO 1900 DEGREES F	
677	TE-343MA	MIDDLE THERMOCOUPLE, ROD 43, LEVEL A	35 TO 1900 DEGREES F	FAILED INSTRUMENT
678	TE-343MC	MIDDLE THERMOCOUPLE, ROD 43, LEVEL C	35 TO 1900 DEGREES F	FAILED INSTRUMENT
679	TE-343MB	MIDDLE THERMOCOUPLE, ROD 43, LEVEL B	35 TO 1900 DEGREES F	FAILED INSTRUMENT
680	TE-343MD	MIDDLE THERMOCOUPLE, ROD 43, LEVEL D	35 TO 1900 DEGREES F	FAILED INSTRUMENT
681	TE-344MC	MIDDLE THERMOCOUPLE, ROD 44, LEVEL C	35 TO 1900 DEGREES F	FAILED INSTRUMENT
682	TE-324AB	SHEATH THERMOCOUPLE, ROD 24, LEVEL B	32 TO 1897 DEGREES F	
683	TE-344MB	MIDDLE THERMOCOUPLE, ROD 44, LEVEL B	35 TO 1900 DEGREES F	QUESTIONABLE
684	TE-344ME	MIDDLE THERMOCOUPLE, ROD 44, LEVEL E	35 TO 1900 DEGREES F	QUESTIONABLE
685	TE-354MD	MIDDLE THERMOCOUPLE, ROD 54, LEVEL D	35 TO 1900 DEGREES F	
686	TE-354MC	MIDDLE THERMOCOUPLE, ROD 54, LEVEL C	35 TO 1900 DEGREES F	
687	TE-354MB	MIDDLE THERMOCOUPLE, ROD 54, LEVEL B	35 TO 1900 DEGREES F	
688	TE-354MA	MIDDLE THERMOCOUPLE, ROD 54, LEVEL A	35 TO 1900 DEGREES F	
689	TE-353MC	MIDDLE THERMOCOUPLE, ROD 53, LEVEL C	35 TO 1900 DEGREES F	
690	TE-353MD	MIDDLE THERMOCOUPLE, ROD 53, LEVEL D	35 TO 1900 DEGREES F	
691	TE-353ME	MIDDLE THERMOCOUPLE, ROD 53, LEVEL E	35 TO 1900 DEGREES F	
692	TE-360MA	MIDDLE THERMOCOUPLE, ROD 60, LEVEL A	35 TO 1900 DEGREES F	
693	TE-360MB	MIDDLE THERMOCOUPLE, ROD 60, LEVEL B	35 TO 1900 DEGREES F	
694	TE-360MD	MIDDLE THERMOCOUPLE, ROD 60, LEVEL D	35 TO 1900 DEGREES F	
695	TE-360MC	MIDDLE THERMOCOUPLE, ROD 60, LEVEL C	35 TO 1900 DEGREES F	
696	TE-361MC	MIDDLE THERMOCOUPLE, ROD 61, LEVEL C	35 TO 1900 DEGREES F	
697	TE-361MB	MIDDLE THERMOCOUPLE, ROD 61, LEVEL B	35 TO 1900 DEGREES F	
698	TE-361MD	MIDDLE THERMOCOUPLE, ROD 61, LEVEL D	35 TO 1900 DEGREES F	

Table 3 (continued)

FIGURE NUMBER	INSTRUMENT NAME	DESCRIPTION	RANGE	COMMENTS
699	TE-308AD	SHEATH THERMOCOUPLE, ROD 8, LEVEL D	35 TO 1900 DEGREES F	
700	TE-359ME	MIDDLE THERMOCOUPLE, ROD 59, LEVEL E	35 TO 1900 DEGREES F	
701	TE-359MF	MIDDLE THERMOCOUPLE, ROD 59, LEVEL F	35 TO 1900 DEGREES F	
702	TE-359MC	MIDDLE THERMOCOUPLE, ROD 59, LEVEL C	35 TO 1900 DEGREES F	
703	TE-362ME	MIDDLE THERMOCOUPLE, ROD 62, LEVEL E	35 TO 1900 DEGREES F	
704	TE-316CF	SHEATH THERMOCOUPLE, ROD 16, LEVEL F	35 TO 1900 DEGREES F	
705	TE-362MC	MIDDLE THERMOCOUPLE, ROD 62, LEVEL C	35 TO 1900 DEGREES F	
706	TE-362MB	MIDDLE THERMOCOUPLE, ROD 62, LEVEL B	35 TO 1900 DEGREES F	FAILED INSTRUMENT
707	TE-352MU	MIDDLE THERMOCOUPLE, ROD 52, LEVEL U	35 TO 1900 DEGREES F	
708	TE-352MS	MIDDLE THERMOCOUPLE, ROD 52, LEVEL S	35 TO 1900 DEGREES F	
709	TE-352MH	MIDDLE THERMOCOUPLE, ROD 52, LEVEL H	35 TO 1900 DEGREES F	
710	TE-352MY	MIDDLE THERMOCOUPLE, ROD 52, LEVEL Y	35 TO 1900 DEGREES F	
711	TE-339MD	MIDDLE THERMOCOUPLE, ROD 39, LEVEL D	35 TO 1900 DEGREES F	
712	TE-339ME	MIDDLE THERMOCOUPLE, ROD 39, LEVEL E	35 TO 1900 DEGREES F	
713	TE-339MC	MIDDLE THERMOCOUPLE, ROD 39, LEVEL C	35 TO 1900 DEGREES F	
714	TE-339MB	MIDDLE THERMOCOUPLE, ROD 39, LEVEL B	35 TO 1900 DEGREES F	
715	TE-330MC	MIDDLE THERMOCOUPLE, ROD 30, LEVEL C	35 TO 1900 DEGREES F	
716	TE-330MB	MIDDLE THERMOCOUPLE, ROD 30, LEVEL B	35 TO 1900 DEGREES F	
717	TE-335AD	SHEATH THERMOCOUPLE, ROD 35, LEVEL D	35 TO 1900 DEGREES F	
718	TE-330ME	MIDDLE THERMOCOUPLE, ROD 30, LEVEL E	35 TO 1900 DEGREES F	
719	TE-314MA	MIDDLE THERMOCOUPLE, ROD 14, LEVEL A	35 TO 1900 DEGREES F	
720	TE-314MB	MIDDLE THERMOCOUPLE, ROD 14, LEVEL B	35 TO 1900 DEGREES F	
721	TE-314MC	MIDDLE THERMOCOUPLE, ROD 14, LEVEL C	35 TO 1900 DEGREES F	
722	TE-344AE	SHEATH THERMOCOUPLE, ROD 44, LEVEL E	35 TO 1900 DEGREES F	
723	TE-314BD	SHEATH THERMOCOUPLE, ROD 14, LEVEL D	32 TO 1297 DEGREES F	

Table 3 (continued)

FIGURE NUMBER	INSTRUMENT NAME	DESCRIPTION	RANGE	COMMENTS
724	TE-306MA	MIDDLE THERMOCOUPLE, ROD 6, LEVEL A	35 TO 1900 DEGREES F	
725	TE-306MD	MIDDLE THERMOCOUPLE, ROD 6, LEVEL D	35 TO 1900 DEGREES F	
726	TE-335BD	SHEATH THERMOCOUPLE, ROD 35, LEVEL D	32 TO 1897 DEGREES F	
727	TE-306MC	MIDDLE THERMOCOUPLE, ROD 6, LEVEL C	35 TO 1900 DEGREES F	
728	TE-331MF	MIDDLE THERMOCOUPLE, ROD 31, LEVEL F	35 TO 1900 DEGREES F	
729	TE-920	PURGE LINE RETURN TEMPERATURE	35 TO 1900 DEGREES F	
730	TE-921	INNER SEAL COOLANT SUPPLY TEMPERATURE	35 TO 1900 DEGREES F	
731	TE-922	INNER SEAL COOLANT SUPPLY TEMPERATURE	35 TO 1900 DEGREES F	
732	TE-347MG	MIDDLE THERMOCOUPLE, ROD 47, LEVEL G	35 TO 1900 DEGREES F	
733	TE-347ME	MIDDLE THERMOCOUPLE, ROD 47, LEVEL E	35 TO 1900 DEGREES F	
734	TE-347MD	MIDDLE THERMOCOUPLE, ROD 47, LEVEL D	35 TO 1900 DEGREES F	
735	TE-347MF	MIDDLE THERMOCOUPLE, ROD 47, LEVEL F	35 TO 1900 DEGREES F	
736	TE-318CF	SHEATH THERMOCOUPLE, ROD 18, LEVEL F	35 TO 1900 DEGREES F	
737	TE-318BF	SHEATH THERMOCOUPLE, ROD 18, LEVEL F	35 TO 1900 DEGREES F	
738	TE-315MD	MIDDLE THERMOCOUPLE, ROD 15, LEVEL D	35 TO 1900 DEGREES F	
739	TE-315MC	MIDDLE THERMOCOUPLE, ROD 15, LEVEL C	35 TO 1900 DEGREES F	
740	TE-305MU	MIDDLE THERMOCOUPLE, ROD 5, LEVEL U	35 TO 1900 DEGREES F	
741	TE-305MS	MIDDLE THERMOCOUPLE, ROD 5, LEVEL S	35 TO 1900 DEGREES F	
742	TE-305MH	MIDDLE THERMOCOUPLE, ROD 5, LEVEL H	35 TO 1900 DEGREES F	
743	TE-305MY	MIDDLE THERMOCOUPLE, ROD 5, LEVEL Y	35 TO 1900 DEGREES F	
744	TE-307MF	MIDDLE THERMOCOUPLE, ROD 7, LEVEL F	35 TO 1900 DEGREES F	
745	TE-307ME	MIDDLE THERMOCOUPLE, ROD 7, LEVEL E	35 TO 1900 DEGREES F	
746	TE-307MC	MIDDLE THERMOCOUPLE, ROD 7, LEVEL C	35 TO 1900 DEGREES F	FAILED INSTRUMENT
747	TE-307MD	MIDDLE THERMOCOUPLE, ROD 7, LEVEL D	35 TO 1900 DEGREES F	
748	TE-344AD	SHEATH THERMOCOUPLE, ROD 44, LEVEL D	35 TO 1900 DEGREES F	

Table 3 (continued)

FIGURE NUMBER	INSTRUMENT NAME	DESCRIPTION	RANGE	COMMENTS
749	TE-340MC	MIDDLE THERMOCOUPLE, ROD 40, LEVEL C	35 TO 1900 DEGREES F	
750	TE-340MB	MIDDLE THERMOCOUPLE, ROD 40, LEVEL B	35 TO 1900 DEGREES F	
751	TE-340MA	MIDDLE THERMOCOUPLE, ROD 40, LEVEL A	35 TO 1900 DEGREES F	
752	TE-356MC	MIDDLE THERMOCOUPLE, ROD 56, LEVEL C	35 TO 1900 DEGREES F	
753	TE-356MD	MIDDLE THERMOCOUPLE, ROD 56, LEVEL D	35 TO 1900 DEGREES F	
754	TE-356ME	MIDDLE THERMOCOUPLE, ROD 56, LEVEL E	35 TO 1900 DEGREES F	
755	TE-356MF	MIDDLE THERMOCOUPLE, ROD 56, LEVEL F	35 TO 1900 DEGREES F	
756	TE-328AD	SHEATH THERMOCOUPLE, ROD 28, LEVEL D	32 TO 1897 DEGREES F	
757	TE-324ME	MIDDLE THERMOCOUPLE, ROD 24, LEVEL E	35 TO 1900 DEGREES F	
758	TE-324MC	MIDDLE THERMOCOUPLE, ROD 24, LEVEL C	35 TO 1900 DEGREES F	
759	TE-324MD	MIDDLE THERMOCOUPLE, ROD 24, LEVEL D	35 TO 1900 DEGREES F	
760	TE-363MD	MIDDLE THERMOCOUPLE, ROD 63, LEVEL D	35 TO 1900 DEGREES F	
761	TE-363ME	MIDDLE THERMOCOUPLE, ROD 63, LEVEL E	35 TO 1900 DEGREES F	
762	TE-363MB	MIDDLE THERMOCOUPLE, ROD 63, LEVEL B	35 TO 1900 DEGREES F	
763	TE-363MC	MIDDLE THERMOCOUPLE, ROD 63, LEVEL C	35 TO 1900 DEGREES F	
764	ZZZ-1026NZ	ZERO INPUT CHANNELS 1664 TO 1791	0 TO 40 MV	
765	ZZZ-1026NC	CALIBRATION INPUT CHANNELS 1664 TO 1791	0 TO 40 MV	
766	TE-316ME	MIDDLE THERMOCOUPLE, ROD 16, LEVEL E	35 TO 1900 DEGREES F	
767	TE-316MD	MIDDLE THERMOCOUPLE, ROD 16, LEVEL D	35 TO 1900 DEGREES F	
768	TE-316MF	MIDDLE THERMOCOUPLE, ROD 16, LEVEL F	35 TO 1900 DEGREES F	
769	TE-316MG	MIDDLE THERMOCOUPLE, ROD 16, LEVEL G	35 TO 1900 DEGREES F	
770	TE-364MG	MIDDLE THERMOCOUPLE, ROD 64, LEVEL G	35 TO 1900 DEGREES F	
771	TE-364MF	MIDDLE THERMOCOUPLE, ROD 64, LEVEL F	35 TO 1900 DEGREES F	
772	TE-328BF	SHEATH THERMOCOUPLE, ROD 28, LEVEL F	32 TO 1897 DEGREES F	
773	TE-364MD	MIDDLE THERMOCOUPLE, ROD 64, LEVEL D	35 TO 1900 DEGREES F	

Table 3 (continued)

FIGURE NUMBER	INSTRUMENT NAME	DESCRIPTION	RANGE	COMMENTS
774	TE-308MB	MIDDLE THERMOCOUPLE, ROD 8, LEVEL B	35 TO 1900 DEGREES F	
775	TE-328AF	SHEATH THERMOCOUPLE, ROD 28, LEVEL F	32 TO 1897 DEGREES F	
776	TE-308MD	MIDDLE THERMOCOUPLE, ROD 8, LEVEL D	35 TO 1900 DEGREES F	
777	TE-308MC	MIDDLE THERMOCOUPLE, ROD 8, LEVEL C	35 TO 1900 DEGREES F	
778	TE-328AC	SHEATH THERMOCOUPLE, ROD 28, LEVEL C	32 TO 1897 DEGREES F	
779	TE-332MD	MIDDLE THERMOCOUPLE, ROD 32, LEVEL D	35 TO 1900 DEGREES F	
780	TE-332MG	MIDDLE THERMOCOUPLE, ROD 32, LEVEL G	35 TO 1900 DEGREES F	
781	TE-332ME	MIDDLE THERMOCOUPLE, ROD 32, LEVEL E	35 TO 1900 DEGREES F	
782	TE-348MU	MIDDLE THERMOCOUPLE, ROD 48, LEVEL U	35 TO 1900 DEGREES F	
783	TE-348MH	MIDDLE THERMOCOUPLE, ROD 48, LEVEL H	35 TO 1900 DEGREES F	
784	TE-348MS	MIDDLE THERMOCOUPLE, ROD 48, LEVEL S	35 TO 1900 DEGREES F	
785	TE-348MY	MIDDLE THERMOCOUPLE, ROD 48, LEVEL Y	35 TO 1900 DEGREES F	
786	TE-357MC	MIDDLE THERMOCOUPLE, ROD 57, LEVEL C	35 TO 1900 DEGREES F	
787	TE-357MB	MIDDLE THERMOCOUPLE, ROD 57, LEVEL B	35 TO 1900 DEGREES F	
788	TE-357MD	MIDDLE THERMOCOUPLE, ROD 57, LEVEL D	35 TO 1900 DEGREES F	
789	TE-357MA	MIDDLE THERMOCOUPLE, ROD 57, LEVEL A	35 TO 1900 DEGREES F	
790	TE-349ME	MIDDLE THERMOCOUPLE, ROD 49, LEVEL E	35 TO 1900 DEGREES F	
791	TE-349MD	MIDDLE THERMOCOUPLE, ROD 49, LEVEL D	35 TO 1900 DEGREES F	
792	TE-349MC	MIDDLE THERMOCOUPLE, ROD 49, LEVEL C	35 TO 1900 DEGREES F	
793	TE-349MB	MIDDLE THERMOCOUPLE, ROD 49, LEVEL B	35 TO 1900 DEGREES F	
794	TE-318CE	SHEATH THERMOCOUPLE, ROD 18, LEVEL E	35 TO 1900 DEGREES F	
795	TE-317ME	MIDDLE THERMOCOUPLE, ROD 17, LEVEL E	35 TO 1900 DEGREES F	FAILED INSTRUMENT
796	TE-333AE	SHEATH THERMOCOUPLE, ROD 33, LEVEL E	35 TO 1900 DEGREES F	
797	TE-333BE	SHEATH THERMOCOUPLE, ROD 33, LEVEL E	35 TO 1900 DEGREES F	
798	TE-335AE	SHEATH THERMOCOUPLE, ROD 35, LEVEL E	35 TO 1900 DEGREES F	

Table 3 (continued)

FIGURE NUMBER	INSTRUMENT NAME	DESCRIPTION	RANGE	COMMENTS
799	TE-333MC	MIDDLE THERMOCOUPLE, ROD 33, LEVEL C	35 TO 1900 DEGREES F	
800	TE-1247	SUBCHANNEL NUMBER 47 THERMOCOUPLE	35 TO 1900 DEGREES F	
801	TE-335CE	SHEATH THERMOCOUPLE, ROD 35, LEVEL E	35 TO 1900 DEGREES F	
802	TE-341MA	MIDDLE THERMOCOUPLE, ROD 41, LEVEL A	35 TO 1900 DEGREES F	
803	TE-341MD	MIDDLE THERMOCOUPLE, ROD 41, LEVEL D	35 TO 1900 DEGREES F	
804	TE-341MB	MIDDLE THERMOCOUPLE, ROD 41, LEVEL B	35 TO 1900 DEGREES F	
805	TE-341MC	MIDDLE THERMOCOUPLE, ROD 41, LEVEL C	35 TO 1900 DEGREES F	
806	TE-325MC	MIDDLE THERMOCOUPLE, ROD 25, LEVEL C	35 TO 1900 DEGREES F	
807	TE-325MD	MIDDLE THERMOCOUPLE, ROD 25, LEVEL D	35 TO 1900 DEGREES F	
808	TE-325MB	MIDDLE THERMOCOUPLE, ROD 25, LEVEL B	35 TO 1900 DEGREES F	
809	TE-325MA	MIDDLE THERMOCOUPLE, ROD 25, LEVEL A	35 TO 1900 DEGREES F	
810	TE-303ME	MIDDLE THERMOCOUPLE, ROD 3, LEVEL E	35 TO 1900 DEGREES F	
811	TE-303MG	MIDDLE THERMOCOUPLE, ROD 3, LEVEL G	35 TO 1900 DEGREES F	
812	TE-303MF	MIDDLE THERMOCOUPLE, ROD 3, LEVEL F	35 TO 1900 DEGREES F	
813	TE-303MD	MIDDLE THERMOCOUPLE, ROD 3, LEVEL D	35 TO 1900 DEGREES F	
814	TE-358MF	MIDDLE THERMOCOUPLE, ROD 58, LEVEL F	35 TO 1900 DEGREES F	
815	TE-358MD	MIDDLE THERMOCOUPLE, ROD 58, LEVEL D	35 TO 1900 DEGREES F	
816	TE-358ME	MIDDLE THERMOCOUPLE, ROD 58, LEVEL E	35 TO 1900 DEGREES F	
817	TE-358MG	MIDDLE THERMOCOUPLE, ROD 58, LEVEL G	35 TO 1900 DEGREES F	
818	TE-309MC	MIDDLE THERMOCOUPLE, ROD 9, LEVEL C	35 TO 1900 DEGREES F	
819	TE-304AE	SHEATH THERMOCOUPLE, ROD 4, LEVEL E	35 TO 1900 DEGREES F	
820	TE-304CE	SHEATH THERMOCOUPLE, ROD 4, LEVEL E	35 TO 1900 DEGREES F	
821	TE-309MB	MIDDLE THERMOCOUPLE, ROD 9, LEVEL B	35 TO 1900 DEGREES F	
822	TE-328AE	SHEATH THERMOCOUPLE, ROD 28, LEVEL E	32 TO 1897 DEGREES F	
823	TE-334MS	MIDDLE THERMOCOUPLE, ROD 34, LEVEL S	35 TO 1900 DEGREES F	

Table 3 (continued)

FIGURE NUMBER	INSTRUMENT NAME	DESCRIPTION	RANGE	COMMENTS
824	TE-334MH	MIDDLE THERMOCOUPLE, ROD 34, LEVEL H	35 TO 1900 DEGREES F	
825	TE-1279	SUBCHANNEL NUMBER 79 THERMOCOUPLE	35 TO 1900 DEGREES F	
826	TE-310MC	MIDDLE THERMOCOUPLE, ROD 10, LEVEL C	35 TO 1900 DEGREES F	
827	TE-1266	SUBCHANNEL NUMBER 66 THERMOCOUPLE	35 TO 1900 DEGREES F	
828	TE-310ME	MIDDLE THERMOCOUPLE, ROD 10, LEVEL E	35 TO 1900 DEGREES F	
829	TE-310MD	MIDDLE THERMOCOUPLE, ROD 10, LEVEL D	35 TO 1900 DEGREES F	
830	TE-302MC	MIDDLE THERMOCOUPLE, ROD 2, LEVEL C	35 TO 1900 DEGREES F	QUESTIONABLE
831	TE-1269	SUBCHANNEL NUMBER 69 THERMOCOUPLE	35 TO 1900 DEGREES F	
832	TE-302MB	MIDDLE THERMOCOUPLE, ROD 2, LEVEL B	35 TO 1900 DEGREES F	QUESTIONABLE
833	TE-302MD	MIDDLE THERMOCOUPLE, ROD 2, LEVEL D	35 TO 1900 DEGREES F	QUESTIONABLE
834	TE-350MF	MIDDLE THERMOCOUPLE, ROD 50, LEVEL F	35 TO 1900 DEGREES F	
835	TE-350MC	MIDDLE THERMOCOUPLE, ROD 50, LEVEL C	35 TO 1900 DEGREES F	
836	TE-350ME	MIDDLE THERMOCOUPLE, ROD 50, LEVEL E	35 TO 1900 DEGREES F	
837	TE-350MD	MIDDLE THERMOCOUPLE, ROD 50, LEVEL D	35 TO 1900 DEGREES F	
838	TE-318ME	MIDDLE THERMOCOUPLE, ROD 18, LEVEL E	35 TO 1900 DEGREES F	QUESTIONABLE
839	TE-318MD	MIDDLE THERMOCOUPLE, ROD 18, LEVEL D	35 TO 1900 DEGREES F	
840	TE-318MF	MIDDLE THERMOCOUPLE, ROD 18, LEVEL F	35 TO 1900 DEGREES F	
841	TE-1275	SUBCHANNEL NUMBER 75 THERMOCOUPLE	35 TO 1900 DEGREES F	
842	TE-312ME	MIDDLE THERMOCOUPLE, ROD 12, LEVEL E	35 TO 1900 DEGREES F	
843	TE-312MD	MIDDLE THERMOCOUPLE, ROD 12, LEVEL D	35 TO 1900 DEGREES F	
844	TE-312MC	MIDDLE THERMOCOUPLE, ROD 12, LEVEL C	35 TO 1900 DEGREES F	
845	TE-312MB	MIDDLE THERMOCOUPLE, ROD 12, LEVEL B	35 TO 1900 DEGREES F	
846	TE-321MD	MIDDLE THERMOCOUPLE, ROD 21, LEVEL D	35 TO 1900 DEGREES F	
847	TE-328CE	SHEATH THERMOCOUPLE, ROD 28, LEVEL E	32 TO 1897 DEGREES F	
848	TE-321MB	MIDDLE THERMOCOUPLE, ROD 21, LEVEL B	35 TO 1900 DEGREES F	

Table 3 (continued)

FIGURE NUMBER	INSTRUMENT NAME	DESCRIPTION	RANGE	COMMENTS
849	TE-321MA	MIDDLE THERMOCOUPLE, ROD 21, LEVEL A	35 TO 1900 DEGREES F	FAILED INSTRUMENT
850	TE-335ME	MIDDLE THERMOCOUPLE, ROD 35, LEVEL E	35 TO 1900 DEGREES F	
851	TE-335MC	MIDDLE THERMOCOUPLE, ROD 35, LEVEL C	35 TO 1900 DEGREES F	
852	TE-335MD	MIDDLE THERMOCOUPLE, ROD 35, LEVEL D	35 TO 1900 DEGREES F	
853	TE-335MB	MIDDLE THERMOCOUPLE, ROD 35, LEVEL B	35 TO 1900 DEGREES F	
854	TE-358AD	SHEATH THERMOCOUPLE, ROD 58, LEVEL D	35 TO 1900 DEGREES F	
855	TE-327MB	MIDDLE THERMOCOUPLE, ROD 27, LEVEL B	35 TO 1900 DEGREES F	
856	TE-301CD	SHEATH THERMOCOUPLE, ROD 1, LEVEL D	35 TO 1900 DEGREES F	
857	TE-358BF	SHEATH THERMOCOUPLE, ROD 58, LEVEL F	35 TO 1900 DEGREES F	FAILED INSTRUMENT
858	TE-320MD	MIDDLE THERMOCOUPLE, ROD 20, LEVEL D	35 TO 1900 DEGREES F	
859	TE-320MG	MIDDLE THERMOCOUPLE, ROD 20, LEVEL G	35 TO 1900 DEGREES F	
860	TE-328CC	SHEATH THERMOCOUPLE, ROD 28, LEVEL C	32 TO 1897 DEGREES F	
861	TE-304AD	SHEATH THERMOCOUPLE, ROD 4, LEVEL D	35 TO 1900 DEGREES F	
862	TE-337CD	SHEATH THERMOCOUPLE, ROD 37, LEVEL D	35 TO 1900 DEGREES F	
863	TE-310BD	SHEATH THERMOCOUPLE, ROD 10, LEVEL D	35 TO 1900 DEGREES F	
864	TE-351MC	MIDDLE THERMOCOUPLE, ROD 51, LEVEL C	35 TO 1900 DEGREES F	
865	TE-311MC	MIDDLE THERMOCOUPLE, ROD 11, LEVEL C	35 TO 1900 DEGREES F	
866	TE-311MD	MIDDLE THERMOCOUPLE, ROD 11, LEVEL D	35 TO 1900 DEGREES F	
867	TE-359BE	SHEATH THERMOCOUPLE, ROD 59, LEVEL E	35 TO 1900 DEGREES F	
868	TE-311MA	MIDDLE THERMOCOUPLE, ROD 11, LEVEL A	35 TO 1900 DEGREES F	
869	TE-326MD	MIDDLE THERMOCOUPLE, ROD 26, LEVEL D	35 TO 1900 DEGREES F	
870	TE-326MC	MIDDLE THERMOCOUPLE, ROD 26, LEVEL C	35 TO 1900 DEGREES F	
871	TE-310AE	SHEATH THERMOCOUPLE, ROD 10, LEVEL E	35 TO 1900 DEGREES F	
872	TE-326ME	MIDDLE THERMOCOUPLE, ROD 26, LEVEL E	35 TO 1900 DEGREES F	
873	TE-304MD	MIDDLE THERMOCOUPLE, ROD 4, LEVEL D	35 TO 1900 DEGREES F	

Table 3 (continued)

FIGURE NUMBER	INSTRUMENT NAME	DESCRIPTION	RANGE	COMMENTS
874	TE-304MC	MIDDLE THERMOCOUPLE, ROD 4, LEVEL C	35 TO 1900 DEGREES F	
875	TE-304ME	MIDDLE THERMOCOUPLE, ROD 4, LEVEL E	35 TO 1900 DEGREES F	
876	TE-304MF	MIDDLE THERMOCOUPLE, ROD 4, LEVEL F	35 TO 1900 DEGREES F	

Table 4. Thermal-Hydraulic Test Facility Test 3.05.5B

NAME	FIGURE NUMBER	TYPE CODE
DE-168	147	106
DE-20	145	106
DE-204A	166	106
DE-204B	167	106
DE-204C	168	106
DE-218	148	106
DE-262A	169	106
DE-262B	170	106
DE-262C	200	106
DE-36	146	106
EEE-10	98	33
EEE-1026AC	2	39
EEE-1026AZ	1	38
EEE-1026BC	117	39
EEE-1026BZ	116	38
EEE-1026IC	202	39
EEE-1026IZ	201	38
EEE-1026JC	319	39
EEE-1026JZ	318	38
EEE-1026KC	434	39
EEE-1026KZ	433	38
EEE-1026LC	540	39
EEE-1026LZ	539	38

Table 4 (continued)

NAME	FIGURE NUMBER	TYPE CODE
EEE-1026MC	652	39
EEE-1026MZ	651	38
EEE-1026NC	765	39
EEE-1026NZ	764	38
EEE-11	99	33
EEE-12	100	33
EEE-9	97	33
EIE-10	94	32
EIE-1001B	102	30
EIE-11	95	32
EIE-12	96	32
EIE-1301	60	31
EIE-1302	90	31
EIE-1303	71	31
EIE-1304	92	31
EIE-1305	72	31
EIE-1306	36	31
EIE-1307	38	31
EIE-1308	35	31
EIE-1309	57	31
EIE-1310	91	31
EIE-1311	73	31
EIE-1312	37	31

Table 4 (continued)

NAME	FIGURE NUMBER	TYPE CODE
EIE-1313	34	31
EIE-1314	33	31
EIE-1315	80	31
EIE-1316	40	31
EIE-1317	58	31
EIE-1318	61	31
EIE-1320	70	31
EIE-1321	39	31
EIE-1323	82	31
EIE-1324	41	31
EIE-1325	55	31
EIE-1326	63	31
EIE-1327	87	31
EIE-1328	59	31
EIE-1329	83	31
EIE-1330	81	31
EIE-1331	32	31
EIE-1332	48	31
EIE-1333	64	31
EIE-1334	62	31
EIE-1335	56	31
EIE-1337	85	31
EIE-1338	47	31

Table 4 (continued)

NAME	FIGURE NUMBER	TYPE CODE
EIE-1339	31	31
EIE-1340	49	31
EIE-1341	88	31
EIE-1342	89	31
EIE-1343	67	31
EIE-1344	66	31
EIE-1345	53	31
EIE-1347	46	31
EIE-1348	50	31
EIE-1349	54	31
EIE-1350	65	31
EIE-1351	69	31
EIE-1352	68	31
EIE-1353	77	31
EIE-1354	52	31
EIE-1355	51	31
EIE-1356	84	31
EIE-1357	74	31
EIE-1358	75	31
EIE-1359	76	31
EIE-1360	86	31
EIE-1361	43	31
EIE-1362	42	31

Table 4 (continued)

NAME	FIGURE NUMBER	TYPE CODE
EIE-1363	45	31
EIE-1364	44	31
EIE-9	93	32
EWE-77A	108	34
FE-1A	151	107
FE-110	195	109
FE-166	110	109
FE-18A	26	108
FE-19	109	109
FE-202	196	109
FE-216	144	109
FE-232	194	109
FE-250	197	109
FE-260	198	109
FE-280	199	109
FE-34	143	109
FE-51	191	109
FE-522	112	95
FE-550	113	96
FE-59	192	109
FE-620	114	95
FE-64	193	109
FE-720	115	95

Table 4 (continued)

NAME	FIGURE NUMBER	TYPE CODE
FMFE-114	125	40
FMFE-170	24	35
FMFE-206	78	35
FMFE-22	22	35
FMFE-220	25	35
FMFE-254	126	40
FMFE-264	127	40
FMFE-38	23	35
FMFE-55	122	40
FMFE-61	123	40
FMFE-66	124	40
LE-100	156	105
LE-1400	171	50
LE-1401	172	50
LE-1402	173	50
LE-1403	174	50
LE-1404	175	50
LE-1405	176	50
LE-1406	177	50
LE-1407	178	50
LE-1408	179	50
LE-1409	180	50
LE-1410	181	50

Table 4 (continued)

NAME	FIGURE NUMBER	TYPE CODE
LE-1411	182	50
LE-1412	183	50
LE-1413	184	50
LE-1414	185	50
LE-1415	186	50
LE-1416	187	50
LE-1417	188	50
LE-1418	189	50
LE-1419	190	50
PDE-111	140	28
PDE-180	3	75
PDE-181	4	75
PDE-182	5	75
PDE-183	6	75
PDE-184	7	75
PDE-185	8	75
PDE-186	118	75
PDE-187	119	75
PDE-188	120	75
PDE-189	121	75
PDE-200	21	28
PDE-203	141	28
PDE-21	27	26

Table 4 (continued)

NAME	FIGURE NUMBER	TYPE CODE
PDE-251	142	28
PDE-261	164	42
PDE-271	165	43
PDE-30	153	98
PDE-35	28	26
PDE-46	19	26
PDE-48	155	97
PDE-53	137	28
PDE-60	138	28
PDE-65	139	26
PDE-78	20	27
PE-102	157	24
PE-106	13	23
PE-118	132	23
PE-15	128	23
PE-156	14	23
PE-16	105	23
PE-174	29	23
PE-201	15	23
PE-209	133	23
PE-224	30	23
PE-258	134	23
PE-26	9	23

Table 4 (continued)

NAME	FIGURE NUMBER	TYPE CODE
PE-268	135	23
PE-27	106	23
PE-286	136	23
PE-32	154	24
PE-412	16	25
PE-42	10	23
PE-425	111	23
PE-43	107	23
PE-44	11	23
PE-526	17	29
PE-58	129	23
PE-616	16	29
PE-63	130	23
PE-68	131	23
PE-76	12	23
SE-72	79	36
TDE-28	152	99
TE-1	392	6
TE-101	162	110
TE-116	394	6
TE-1201	364	3
TE-1205	357	3
TE-1207	640	3

Table 4 (continued)

NAME	FIGURE NUMBER	TYPE CODE
TE-1209	241	3
TE-1211	361	3
TE-1213	624	3
TE-1214	359	3
TE-1216	500	3
TE-1217	242	3
TE-1219	419	3
TE-1220	418	3
TE-1221	362	3
TE-1223	358	3
TE-1225	245	3
TE-1226	243	3
TE-1227	247	3
TE-1229	622	3
TE-1230	371	3
TE-1231	363	3
TE-1232	360	3
TE-1234	218	3
TE-1235	296	3
TE-1237	372	3
TE-1238	373	3
TE-1239	374	3
TE-1240	370	3

Table 4 (continued)

NAME	FIGURE NUMBER	TYPE CODE
TE-1241	381	3
TE-1242	237	3
TE-1244	240	3
TE-1245	238	3
TE-1247	800	3
TE-1248	366	3
TE-1249	244	3
TE-1250	382	3
TE-1251	365	3
TE-1252	226	3
TE-1255	641	3
TE-1256	369	3
TE-1258	239	3
TE-1259	377	3
TE-1260	375	3
TE-1261	379	3
TE-1263	260	3
TE-1265	368	3
TE-1266	827	3
TE-1268	383	3
TE-1269	831	3
TE-1270	376	3
TE-1271	380	3

Table 4 (continued)

NAME	FIGURE NUMBER	TYPE CODE
TE-1273	367	3
TE-1275	841	3
TE-1277	378	3
TE-1279	825	3
TE-1281	384	3
TE-150	389	6
TE-151	390	6
TE-152	391	6
TE-172	396	6
TE-181W	325	4
TE-182E	385	4
TE-182S	604	4
TE-183N	387	4
TE-183W	602	4
TE-184E	388	4
TE-184S	601	4
TE-185W	326	4
TE-186E	626	4
TE-186S	324	4
TE-187N	386	4
TE-187W	603	4
TE-188AA	464	8
TE-188AB	458	8

Table 4 (continued)

NAME	FIGURE NUMBER	TYPE CODE
TE-188AC	451	8
TE-188AD	456	8
TE-188AE	463	8
TE-188AF	454	8
TE-188AG	457	8
TE-188BA	460	8
TE-188BB	455	8
TE-188BC	462	8
TE-188BD	459	8
TE-188BE	453	8
TE-188BF	461	8
TE-2	393	6
TE-208	409	6
TE-210A	101	110
TE-222	397	6
TE-24	395	6
TE-256	410	6
TE-266	411	6
TE-28B	160	71
TE-284	412	6
TE-29	399	6
TE-291A	327	7
TE-291B	322	7

Table 4 (continued)

NAME	FIGURE NUMBER	TYPE CODE
TE-291C	321	7
TE-291D	310	7
TE-292A	320	7
TE-292B	306	7
TE-292D	307	7
TE-293A	315	7
TE-293B	334	7
TE-293C	328	7
TE-293D	333	7
TE-293E	332	7
TE-293F	[illegible]	7
TE-294B	329	7
TE-294D	331	7
TE-294E	330	7
TE-294F	311	7
TE-295A	317	7
TE-295B	309	7
TE-295C	316	7
TE-295D	303	7
TE-296B	335	7
TE-296D	336	7
TE-301AD	549	1
TE-301CD	856	1

Table 4 (continued)

NAME	FIGURE NUMBER	TYPE CODE
TE-302AB	552	1
TE-302AD	551	1
TE-302AE	553	1
TE-302BC	554	1
TE-302MB	832	2
TE-302MC	830	2
TE-302MD	833	2
TE-303BE	536	1
TE-303BF	538	[illegible]
TE-303CD	535	1
TE-303CE	547	1
TE-303CG	537	1
TE-303MD	813	2
TE-303ME	810	2
TE-303MF	812	2
TE-303MG	811	2
TE-304AC	546	1
TE-304AD	861	1
TE-304AE	819	1
TE-304AF	533	1
TE-304EE	545	1
TE-304CE	820	1
TE-304MC	874	2

Table 4 (continued)

NAME	FIGURE NUMBER	TYPE CODE
TE-304MD	873	2
TE-304ME	875	2
TE-304MF	876	2
TE-305AS	448	1
TE-305BH	449	1
TE-305BU	447	1
TE-305CY	450	1
TE-305MH	742	2
TE-305MS	741	2
TE-305MU	740	2
TE-305MY	743	2
TE-306AA	470	1
TE-306AB	471	1
TE-306MA	724	2
TE-306MC	727	2
TE-306MD	725	2
TE-307AC	435	1
TE-307AF	437	1
TE-307BE	468	1
TE-307BF	466	1
TE-307CE	438	1
TE-307MC	746	2
TE-307MD	747	2

Table 4 (continued)

NAME	FIGURE NUMBER	TYPE CODE
TE-307ME	745	2
TE-307MF	744	2
TE-308AD	699	1
TE-308BA	472	1
TE-308BC	475	1
TE-308BD	474	1
TE-308CB	473	1
TE-308CD	452	1
TE-308MB	774	2
TE-308MC	777	2
TE-308MD	776	2
TE-309AC	524	1
TE-309CB	534	1
TE-309CD	523	1
TE-309MB	821	2
TE-309MC	818	2
TE-310AE	871	1
TE-310AF	542	1
TE-310BD	863	1
TE-310BE	544	1
TE-310BF	555	1
TE-310CC	543	1
TE-310CD	541	1

Table 4 (continued)

NAME	FIGURE NUMBER	TYPE CODE
TE-310CF	556	1
TE-310MC	826	2
TE-310MD	829	2
TE-310ME	828	2
TE-311AA	528	1
TE-311AB	527	1
TE-311CB	526	1
TE-311CC	525	1
TE-311MA	868	2
TE-311MC	865	2
TE-311MD	866	2
TE-312AE	287	1
TE-312BC	286	1
TE-312CB	288	1
TE-312CD	548	1
TE-312MB	845	2
TE-312MC	844	2
TE-312MD	843	2
TE-312ME	842	2
TE-313AE	586	1
TE-313BC	414	1
TE-313BF	416	1
TE-313CD	413	1

Table 4 (continued)

NAME	FIGURE NUMBER	TYPE CODE
TE-313CE	415	1
TE-313CF	261	1
TE-314AA	638	1
TE-314AB	443	1
TE-314AC	637	1
TE-314BD	723	1
TE-314MA	719	2
TE-314MB	720	2
TE-314MC	721	2
TE-315AC	467	1
TE-315AF	465	1
TE-315MC	739	2
TE-315MD	738	2
TE-316AD	478	1
TE-316BE	635	1
TE-316BF	476	1
TE-316BG	439	1
TE-316CE	477	1
TE-316CF	704	1
TE-316CG	479	1
TE-316MD	767	2
TE-316ME	766	2
TE-316MF	768	2

Table 4 (continued)

NAME	FIGURE NUMBER	TYPE CODE
TE-316MG	769	2
TE-317AE	496	1
TE-317BE	488	1
TE-317CB	499	1
TE-317CC	497	1
TE-317CD	498	1
TE-317CE	490	1
TE-317ME	795	2
TE-318AD	512	1
TE-318AE	445	1
TE-318AF	514	1
TE-318AG	442	1
TE-318BD	639	1
TE-318BE	515	1
TE-318BF	737	1
TE-318BG	513	1
TE-318CD	642	1
TE-318CE	794	1
TE-318CF	736	1
TE-318CG	469	1
TE-318MD	839	2
TE-318ME	838	2
TE-318MF	840	2

Table 4 (continued)

NAME	FIGURE NUMBER	TYPE CODE
TE-320AD	506	1
TE-320AE	630	1
TE-320AF	633	1
TE-320AG	643	1
TE-320BD	634	1
TE-320BE	629	1
TE-320BF	507	1
TE-320BG	504	1
TE-320CD	631	1
TE-320CE	628	1
TE-320CF	632	1
TE-320CG	505	1
TE-320MD	858	2
TE-320MG	859	2
TE-321AA	422	1
TE-321AB	421	1
TE-321AD	301	1
TE-321BC	423	1
TE-321BD	621	1
TE-321CD	424	1
TE-321MA	849	2
TE-321MB	848	2
TE-321MD	846	2

Table 4 (continued)

NAME	FIGURE NUMBER	TYPE CODE
TE-323AA	420	1
TE-323BC	417	1
TE-324AB	682	1
TE-324AC	482	1
TE-324AE	446	1
TE-324BD	483	1
TE-324CB	481	1
TE-324CE	480	1
TE-324MC	758	2
TE-324MD	759	2
TE-324ME	757	2
TE-325AA	645	1
TE-325AB	644	1
TE-325AC	649	1
TE-325BA	646	1
TE-325BB	508	1
TE-325BC	647	1
TE-325BD	650	1
TE-325CA	511	1
TE-325CB	648	1
TE-325CC	509	1
TE-325CD	510	1
TE-325MA	809	2

Table 4 (continued)

NAME	FIGURE NUMBER	TYPE CODE
TE-325MB	808	2
TE-325MC	806	2
TE-325MD	807	2
TE-326AC	350	1
TE-326AD	292	1
TE-326AE	615	1
TE-326BB	352	1
TE-326BD	351	1
TE-326BE	623	1
TE-326CD	427	1
TE-326CE	349	1
TE-326MC	870	2
TE-326MD	869	2
TE-326ME	872	2
TE-327AA	425	1
TE-327AC	294	1
TE-327AD	428	1
TE-327BA	432	1
TE-327BC	429	1
TE-327BD	295	1
TE-327CA	297	1
TE-327CB	426	1
TE-327CC	431	1

Table 4 (continued)

NAME	FIGURE NUMBER	TYPE CODE
TE-327CD	430	1
TE-327MB	855	2
TE-328AC	778	1
TE-328AD	756	1
TE-328AE	822	1
TE-328AF	775	1
TE-328BD	502	1
TE-328BF	772	1
TE-328CC	860	1
TE-328CD	627	1
TE-328CE	647	1
TE-328CF	503	1
TE-328MC	661	2
TE-328MD	664	2
TE-328ME	662	2
TE-328MF	663	2
TE-329AB	565	1
TE-329AC	569	1
TE-329AD	571	1
TE-329AE	205	1
TE-329BB	206	1
TE-329BC	203	1
TE-329BD	204	1

Table 4 (continued)

NAME	FIGURE NUMBER	TYPE CODE
TE-329BE	570	1
TE-329CB	567	1
TE-329CD	566	1
TE-329CE	568	1
TE-329MB	668	2
TE-329MC	666	2
TE-329MD	667	2
TE-329ME	665	2
TE-330AC	234	1
TE-330AE	235	1
TE-330BE	314	1
TE-330CB	236	1
TE-330MB	716	2
TE-330MC	715	2
TE-330ME	718	2
TE-331BF	264	1
TE-331CD	221	1
TE-331CE	220	1
TE-331CF	219	1
TE-331MF	728	2
TE-332AE	660	1
TE-332CD	441	1
TE-332CE	436	1

Table 4 (continued)

NAME	FIGURE NUMBER	TYPE CODE
TE-332CF	440	1
TE-332CG	444	1
TE-332MD	779	2
TE-332ME	781	2
TE-332MG	780	2
TE-333AC	494	1
TE-333AD	495	1
TE-333AE	796	1
TE-333BE	797	1
TE-333CB	492	1
TE-333CE	493	1
TE-333MC	799	2
TE-334AH	597	1
TE-334AS	281	1
TE-334AY	598	1
TE-334BH	600	1
TE-334BS	591	1
TE-334BU	593	1
TE-334BY	599	1
TE-334CH	282	1
TE-334CS	592	1
TE-334CU	590	1
TE-334CY	280	1

Table 4 (continued)

NAME	FIGURE NUMBER	TYPE CODE
TE-334MH	824	2
TE-334MS	823	2
TE-335AD	717	1
TE-335AE	798	1
TE-335BB	489	1
TE-335BD	726	1
TE-335BE	491	[illegible]
TE-335CE	801	[illegible]
TE-335MB	85[illegible]	2
TE-335MC	85[illegible]	2
TE-335ML	852	2
TE-335ME	850	2
TE-337AE	279	1
TE-337BD	277	1
TE-337BE	276	1
TE-337BF	268	1
TE-337CD	862	1
TE-337CF	278	1
TE-337MC	653	2
TE-337MD	655	2
TE-337ME	654	2
TE-337MF	656	2
TE-338AB	213	1

Table 4 (continued)

NAME	FIGURE NUMBER	TYPE CODE
TE-338BC	211	1
TE-338BD	212	1
TE-338CD	312	1
TE-338MA	671	2
TE-338MB	670	2
TE-338MC	672	2
TE-338MD	669	2
TE-339AC	209	1
TE-339BD	208	1
TE-339BD	207	1
TE-339MB	714	2
TE-339MC	713	2
TE-339MD	711	2
TE-339ME	712	2
TE-340BC	233	1
TE-340BD	232	1
TE-340CA	231	1
TE-340CB	230	1
TE-340MA	751	2
TE-340MB	750	2
TE-340MC	749	2
TE-341AB	298	1
TE-341MA	802	2

Table 4 (continued)

NAME	FIGURE NUMBER	TYPE CODE
TE-341MB	804	2
TE-341MC	805	2
TE-341MD	803	2
TE-342AG	299	1
TE-342BD	305	1
TE-342BE	303	1
TE-342BF	304	1
TE-342BG	313	1
TE-342CG	302	1
TE-343AD	300	1
TE-343BA	293	1
TE-343BB	290	1
TE-343BC	291	1
TE-343BD	550	1
TE-343MA	677	2
TE-343MB	679	2
TE-343MC	678	2
TE-343MD	680	2
TE-344AD	748	1
TE-344AE	722	1
TE-344CB	486	1
TE-344CC	485	1
TE-344CD	484	1

Table 4 (continued)

NAME	FIGURE NUMBER	TYPE CODE
TE-344CE	487	1
TE-344MB	683	2
TE-344MC	681	2
TE-344ME	684	2
TE-345AD	222	1
TE-345AE	575	1
TE-345AF	578	1
TE-345AG	225	1
TE-345BD	573	1
TE-345BE	576	1
TE-345BF	574	1
TE-345BG	577	1
TE-345CF	224	1
TE-345CG	579	1
TE-345MD	659	2
TE-345ME	657	2
TE-345MG	658	2
TE-347CF	572	1
TE-347CG	223	1
TE-347MD	734	2
TE-347ME	733	2
TE-347MF	735	2
TE-347MG	732	2

Table 4 (continued)

NAME	FIGURE NUMBER	TYPE CODE
TE-348AH	262	1
TE-348AY	263	1
TE-348MH	783	2
TE-348MS	784	2
TE-348MU	782	2
TE-348MY	785	2
TE-349AE	289	1
TE-349BE	342	1
TE-349CB	345	1
TE-349CC	347	1
TE-349CD	346	1
TE-349CE	348	1
TE-349MB	793	2
TE-349MC	792	2
TE-349MD	791	2
TE-349ME	790	2
TE-350AC	613	1
TE-350AD	619	1
TE-350AF	617	1
TE-350BC	620	1
TE-350BD	614	1
TE-350BE	341	1
TE-350BF	344	1

Table 4 (continued)

NAME	FIGURE NUMBER	TYPE CODE
TE-350CD	343	1
TE-350CE	616	1
TE-350CF	618	1
TE-350MC	835	2
TE-350MD	837	2
TE-350ME	836	2
TE-350MF	834	2
TE-351AB	356	1
TE-351AE	354	1
TE-351BC	353	1
TE-351BD	355	1
TE-351BE	625	1
TE-351MC	864	2
TE-352AH	610	1
TE-352AS	607	1
TE-352AU	337	1
TE-352AY	612	1
TE-352BH	609	1
TE-352BS	338	1
TE-352BU	605	1
TE-352BY	611	1
TE-352CH	339	1
TE-352CS	608	1

Table 4 (continued)

NAME	FIGURE NUMBER	TYPE CODE
TE-352CU	606	1
TE-352CY	340	1
TE-352MH	709	2
TE-352MS	708	2
TE-352MU	707	2
TE-352MY	710	2
TE-353AE	246	1
TE-353BE	210	1
TE-353BF	583	1
TE-353CC	248	1
TE-353MC	689	2
TE-353MD	690	2
TE-353ME	691	2
TE-354AD	215	1
TE-354CA	216	1
TE-354CB	217	1
TE-354CC	214	1
TE-354MA	688	2
TE-354MB	687	2
TE-354MC	686	2
TE-354MD	685	2
TE-355AA	266	1
TE-355BC	267	1

Table 4 (continued)

NAME	FIGURE NUMBER	TYPE CODE
TE-355CB	265	1
TE-355CD	636	1
TE-355MA	673	2
TE-355MB	674	2
TE-355MC	675	2
TE-355MD	676	2
TE-356AC	269	1
TE-356AE	272	1
TE-356AF	271	1
TE-356CD	270	1
TE-356MC	752	2
TE-356MD	753	2
TE-356ME	754	2
TE-356MF	755	2
TE-357AA	531	1
TE-357AB	561	1
TE-357AC	558	1
TE-357BA	559	1
TE-357BB	529	1
TE-357BC	530	1
TE-357BD	532	1
TE-357CB	560	1
TE-357CD	563	1

Table 4 (continued)

NAME	FIGURE NUMBER	TYPE CODE
TE-357MA	789	2
TE-357MB	787	2
TE-357MC	786	2
TE-357MD	788	2
TE-358AD	854	1
TE-358AE	557	1
TE-358BE	521	1
TE-358BF	857	1
TE-358CD	520	1
TE-358CG	522	1
TE-358MD	815	2
TE-358ME	816	2
TE-358MF	814	2
TE-358MG	817	2
TE-359AD	517	1
TE-359AE	516	1
TE-359AF	562	1
TE-359BE	867	1
TE-359BF	564	1
TE-359CC	519	1
TE-359CE	501	1
TE-359CF	518	1
TE-359MC	702	2

Table 4 (continued)

NAME	FIGURE NUMBER	TYPE CODE
TE-359ME	700	2
TE-359MF	701	2
TE-360AA	595	1
TE-360AB	594	1
TE-360AC	283	1
TE-360AD	284	1
TE-360BD	596	1
TE-360CD	285	1
TE-360MA	692	2
TE-360MB	693	2
TE-360MC	695	2
TE-360MD	694	2
TE-361AB	250	1
TE-361AC	251	1
TE-361AD	252	1
TE-361AE	228	1
TE-361BE	227	1
TE-361BJ	581	9
TE-361CE	249	1
TE-361CJ	580	9
TE-361MB	697	2
TE-361MC	696	2
TE-361MD	698	2

Table 4 (continued)

NAME	FIGURE NUMBER	TYPE CODE
TE-362AB	275	1
TE-362AE	274	1
TE-362CD	273	1
TE-362MB	706	2
TE-362MC	705	2
TE-362ME	703	2
TE-363AE	229	1
TE-363BC	258	1
TE-363BE	257	1
TE-363CE	259	1
TE-363MB	762	2
TE-363MC	763	2
TE-363MD	760	2
TE-363ME	761	2
TE-364AD	255	1
TE-364AE	584	1
TE-364AF	585	1
TE-364AG	253	1
TE-364BD	582	1
TE-364BE	254	1
TE-364BF	256	1
TE-364CD	588	1
TE-364CF	587	1

Table 4 (continued)

NAME	FIGURE NUMBER	TYPE CODE
TE-364CG	589	1
TE-364MD	773	2
TE-364MF	771	2
TE-364MG	770	2
TE-4B	161	110
TE-40	398	6
TE-408B	405	5
TE-45	400	6
TE-5B	401	5
TE-520B	406	5
TE-521	407	5
TE-525	103	110
TE-557	159	110
TE-57	402	6
TE-615	163	110
TE-62	403	6
TE-627	104	110
TE-67	404	6
TE-727	158	110
TE-901	408	5
TE-920	729	5
TE-921	730	5
TE-922	731	5
XE-430A	150	37
XE-430B	149	37

Table 5. Thermocouple nomenclature

Fuel rod simulator thermocouples: TE-3nnal

nn – a number 01–64 equal to the rod number.

a – one of three letters, A, B, or C, designating the position of the thermocouple relative to the other two thermocouples in that rod at the designated level (or the letter M denoting middle thermocouple). The three sheath thermocouples at a level are labeled A, B, and C in a clockwise direction as viewed from the top of the rod.

l – the level of the thermocouple. A letter A–G (heated zone); J (above the heated zone); or Y, H, S, or U (the four levels grouped around the D level in the "special" fuel rod simulators).

Spacer grid thermocouples: TE-29na

n – a number 1–6 designating the spacer grid level as follows:

Number	Between T/C levels
1	A&B
2	B&C
3	C&D
4	D&E
5	E&F
6	F&G

a – a letter A–F designating the subchannel into which the thermocouple is projecting as follows:

Letter	Subchannel
A	32
B	43
C	57
D	70
E	17
F	38

The spacer grids numbered 1, 2, 5, and 6 have four thermocouples in subchannels designated A–D. The spacer grids numbered 3 and 4 have six thermocouples in subchannels designated A–F.

Table 5 (continued)

Shroud box thermocouples: TE-18na

n – a number 1–7 designating the level of the thermocouple in the shroud box as follows:

Number	T/C level
1	A
2	B
3	C
4	D
5	E
6	F
7	G

a – a letter designating the side of the box through which the thermocouple protrudes, N, E, S, and W (being the compass direction most closely matching the direction the side faces).

Subchannel thermocouples: TE-12nn

nn – a number 01–81 equal to the number of the subchannel in which the thermocouple is located.

Thermocouple array rod thermocouples: TE-18nal

n – the number 8 or 9 designating the bundle site in which the thermocouple array rod is located.

8 – grid position No. 19
9 – grid position No. 36

a – a letter A or B designating which of two subchannels associated with that rod the thermocouple protrudes into.

Position	A subchannel No.	B subchannel No.
19	22	30
36	41	49

l – the thermocouple level A–G (same as fuel rod simulator thermocouple level designations).

REFERENCES

1. Test 3.05.5B Final Analysis Report.

2. D. K. Felde et al., *Thermal-Hydraulic Test Facility (THTF) MOD 3, ORNL Blowdown Heat Transfer Program*, ORNL/TM-7842 (to be published).

Appendix A

TEST PHENOMENOLOGY

The transient experiment was initiated by breaking both inlet and outlet rupture disk assemblies to simulate a double-ended cold-leg break loss-of-coolant accident. Following blowdown initiation, there was an almost instantaneous subcooled decompression from the steady-state operating pressure to the saturation pressure corresponding to the outlet fluid temperature. The measured outlet pressure is shown on microfiche Fig. 15. Coolant within the test section, which had been subcooled before transient initiation, began to increase in temperature until the saturation temperature was reached (microfiche Fig. 436). The upper portion of the rod bundle underwent immediate increases in surface heat flux and decreases in surface temperature subsequent to transient initiation, indicating improved heat transfer due either to nucleate boiling at those thermocouple levels initially in a forced-convection mode or to the enhancement of nucleate boiling that accompanied the drop in coolant saturation temperature during initial depressurization. The lower part of the bundle continued in a forced-convective mode for a short period before shifting to a nucleate boiling heat transfer mode. As the coolant temperature reached the saturation temperature, departure from nucleate boiling (DNB) occurred (microfiche Figs. 554, 819, and 535).

Flow began to decrease after a very short-lived positive surge (microfiche Fig. 196), and a flow stagnation point soon developed. Between 0.2 and 5.0 s, flow was positive through the outlet spool piece and negative through the inlet spool piece, indicating flow out of the test section through both inlet and outlet. After 5.0 s and until about 10.0 s, flow through the test section was positive. Flow then reversed to negative again and remained negative throughout the remainder of the transient (microfiche Figs. 196 and 197).

After DNB, the bundle did not undergo any significant cooling. Only thermocouple level G, the uppermost level in the test section, experienced any rewet, and that occurred after the flow reversal (to downflow) at 10.0 s.

Appendix B

MASS FLUX CALCULATIONS

This appendix describes the method by which mass flux is calculated at the THTF test section boundaries and the estimated uncertainties in those calculations. Included are the mass flux calculations for the transient periods of interest.

B.1 Mass Flux Calculations for THTF Instrumented Spool Pieces

At the THTF, instrumented "spool pieces" are used to provide measurements of volumetric flow rate, momentum flux, density, pressure, and temperature at the boundaries of the test section. A spool piece consists of a fluid thermocouple, an absolute pressure tap, a turbine meter for measuring volumetric flow or velocity (V), a drag disk for measuring momentum flux (ρV^2), and a gamma densitometer for measuring an average chordal density (ρ) of the fluid. Since the mass flux is not directly measured, it is necessary to use combinations of these instruments to determine mass flux. Homogeneous models may be used combining the turbine meter and gamma densitometer (ρV), the drag disk and the gamma densitometer ($\sqrt{\rho \cdot \rho V^2}$), and the turbine meter and drag disk ($\rho V^2/V$) to obtain mass flux. These mass flux models are incorporated into the mass flux code AMICON [1] which operates on the transient instrument data. Where conditions permit, in subcooled or superheated flow, the density for the models is deduced from water properties based on temperature and pressure measurements and replaces the densitometer-measured density. The uncertainty in density determined in this manner is significantly less than the uncertainty inherent in the densitometer's measured density. Logic in the AMICON and water properties codes determines whether a temperature- and pressure-deduced density or a densitometer-measured density is appropriate (based on a comparison of measurements by these same instruments). For saturated flow conditions, the logic also prevents the use of a densitometer-measured density that is less than the saturated vapor density (within uncertainty bands) for the measured temperature and pressures in the spool piece. For high-quality mass flows, this effectively reduces uncertainties on the low side of the density measurements.

The mass flux results generated by AMICON are shown in Figs. B.1–B.23 for the different models and spool pieces. The locations of the spool pieces are indicated in Fig. 1 of the main text. The Bundle Outlet spool piece BO1 contains a three-beam gamma densitometer. Results are shown using both a single-beam and a three-beam annular densitometer model for this spool piece. The single-beam model at the BO1 site uses the center beam measurement from the three-beam densitometer. The various models

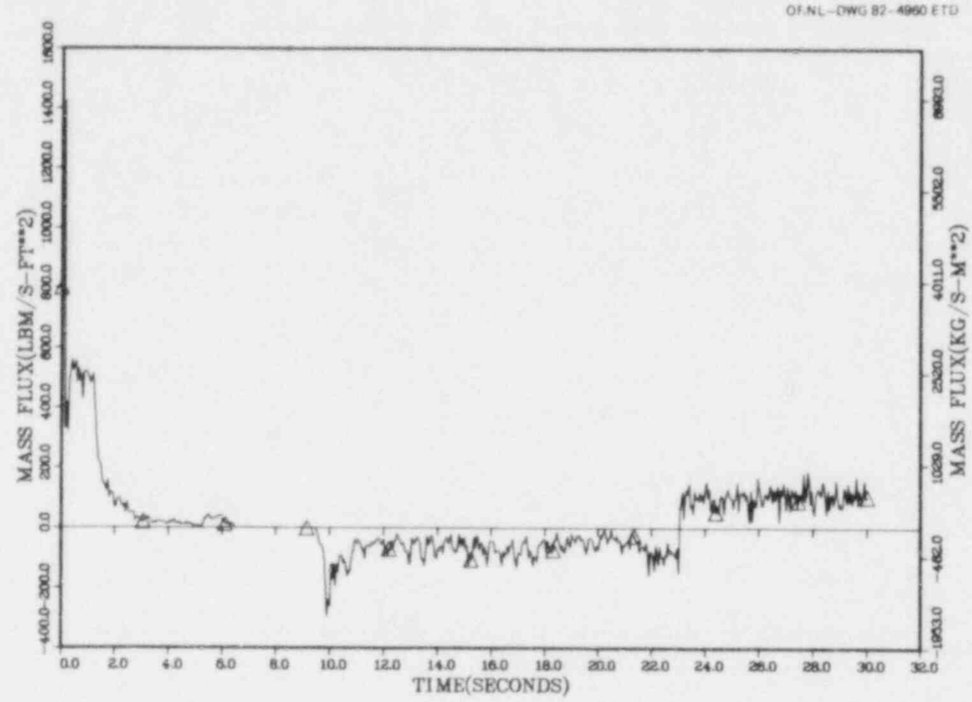

Fig. B.1. Mass flux vs time at BI1 site using TBM-GAM 3 model.

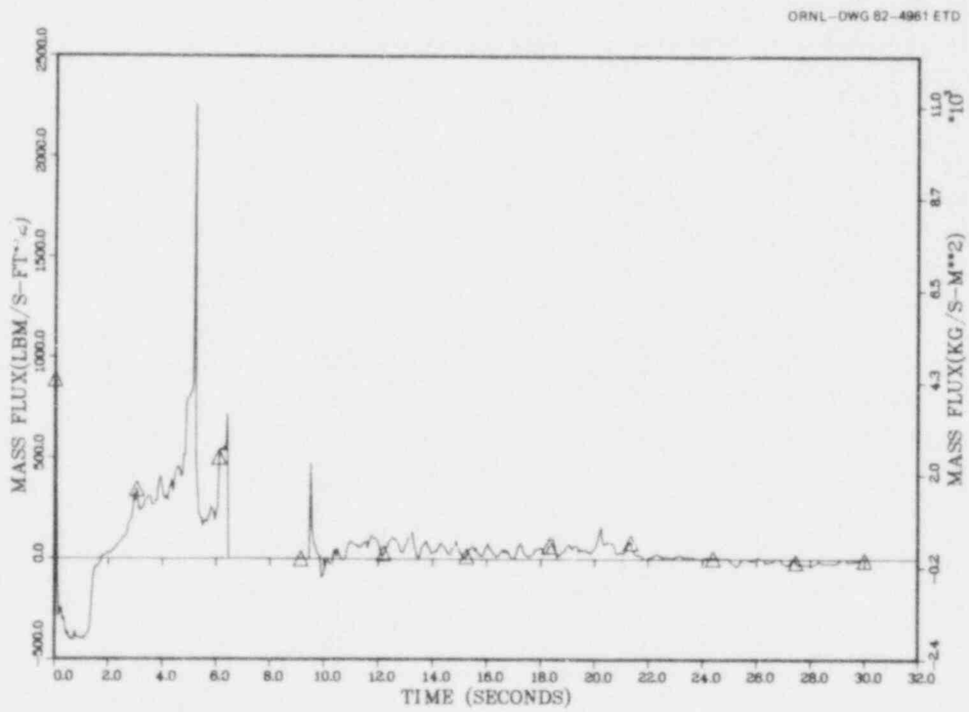

Fig. B.2. Mass flux vs time at BI1 site using TBM-DD model.

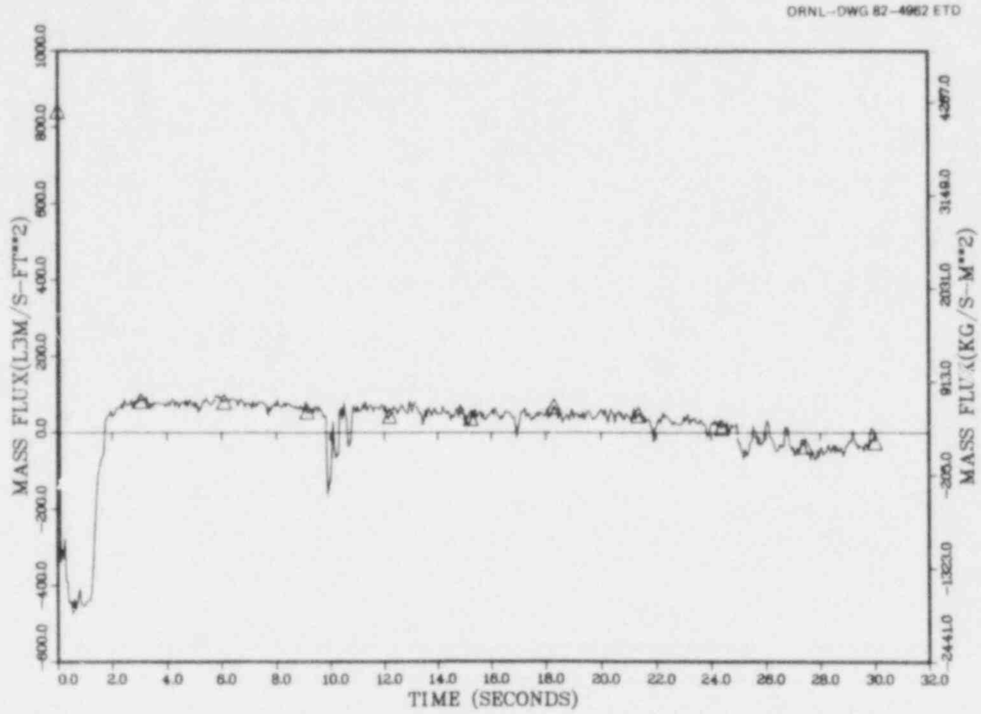

Fig. B.3. Mass flux vs time at BI1 site using DD-GAM 3 model.

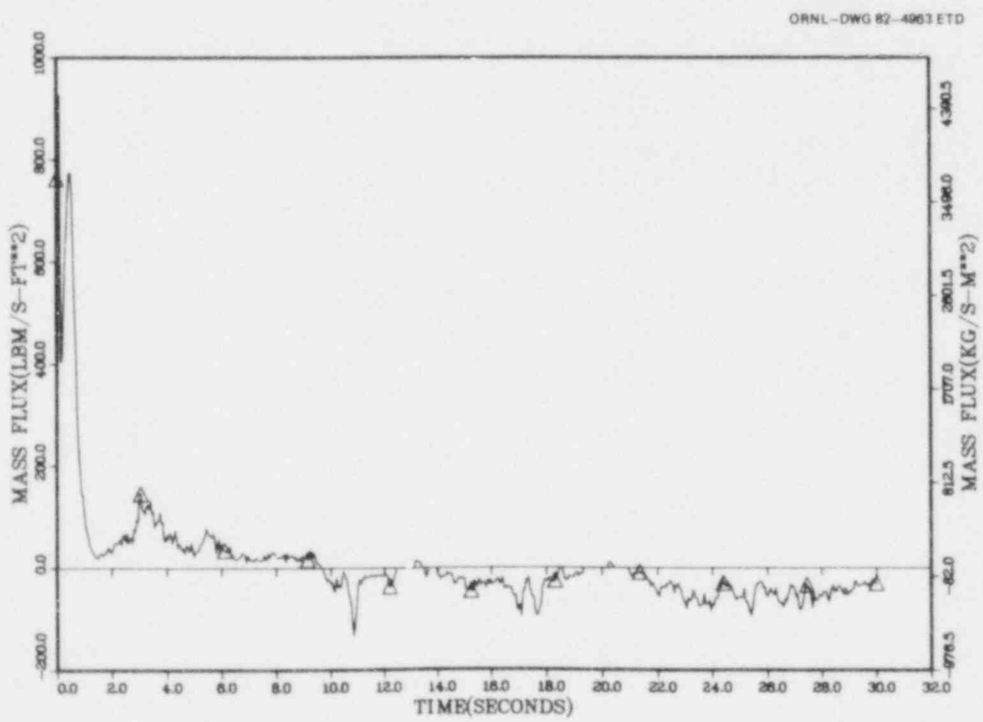

Fig. B.4. Mass flux vs time at BO1 site using TBM-GAM 3 model.

ORNL-DWG 82-4964 ETD

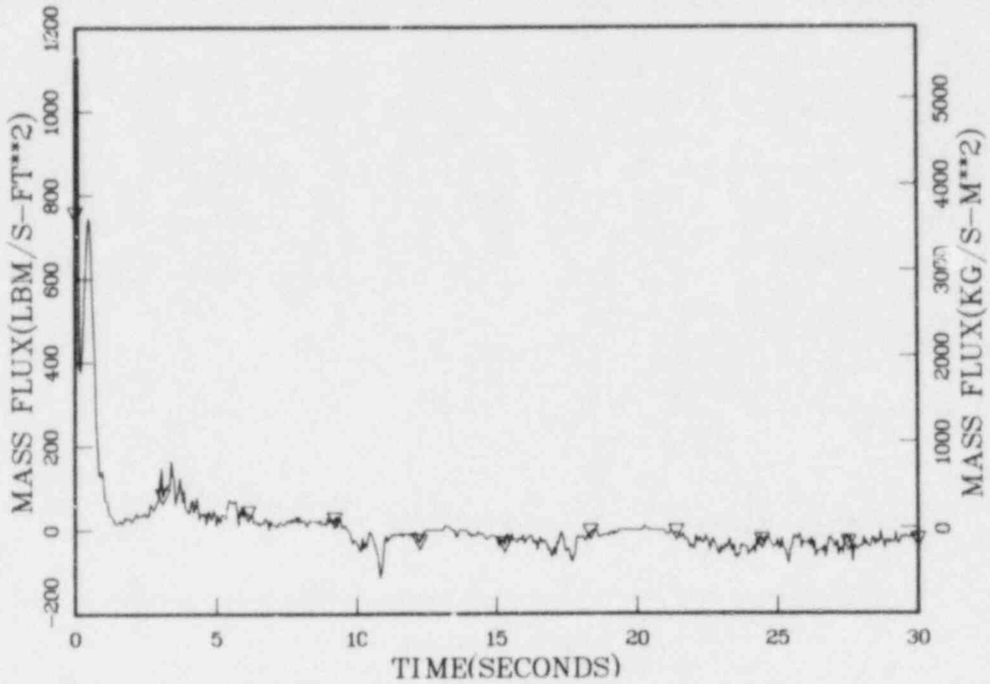

Fig. B.5. Mass flux vs time at B01 site using TBM-GAM model.

ORNL-DWG 82-4965 ETD

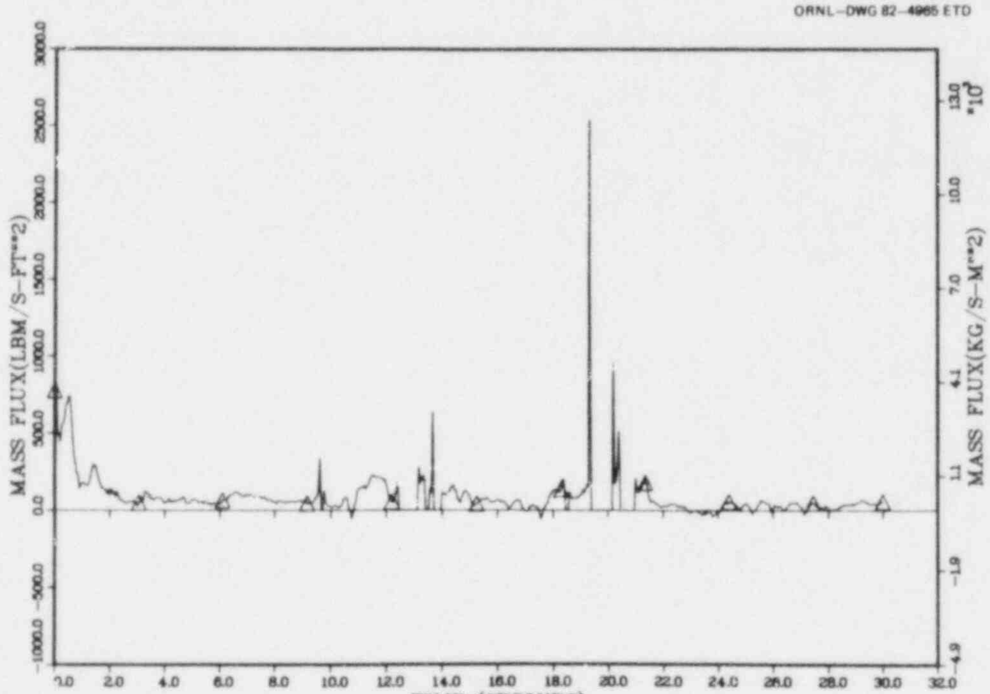

Fig. B.6. Mass flux vs time at B01 site using TBM-DD model.

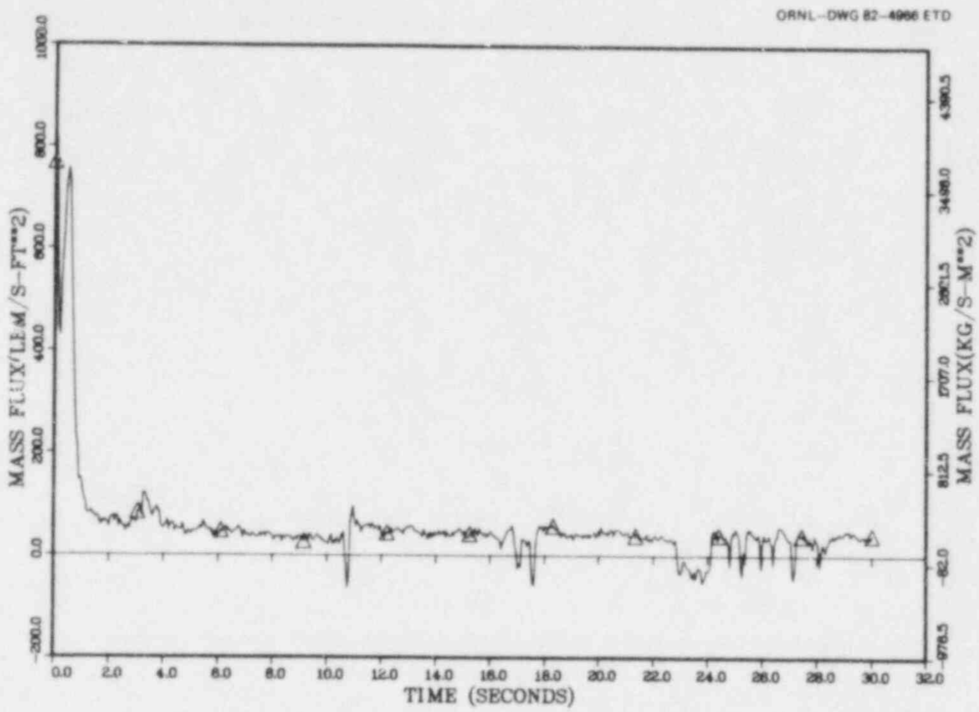

Fig. B.7. Mass flux vs time at BO1 site using DD-GAM 3 model.

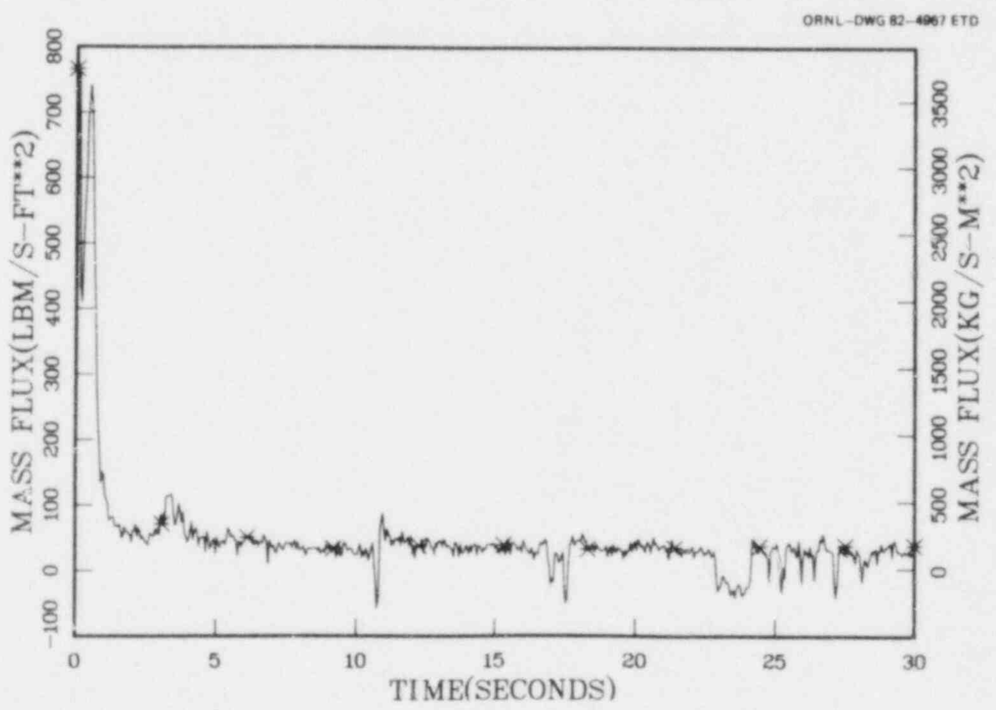

Fig. B.8. Mass flux vs time at BO1 site using DD-GAM model.

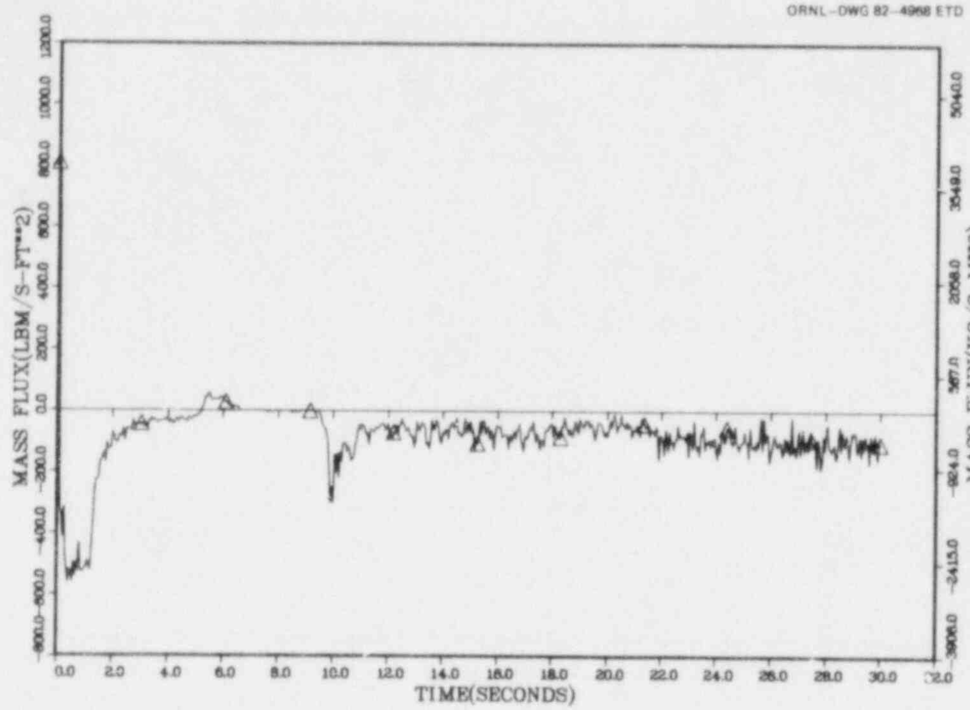

Fig. B.9. Mass flux vs time at BI2 site using DD-GAM 3 model.

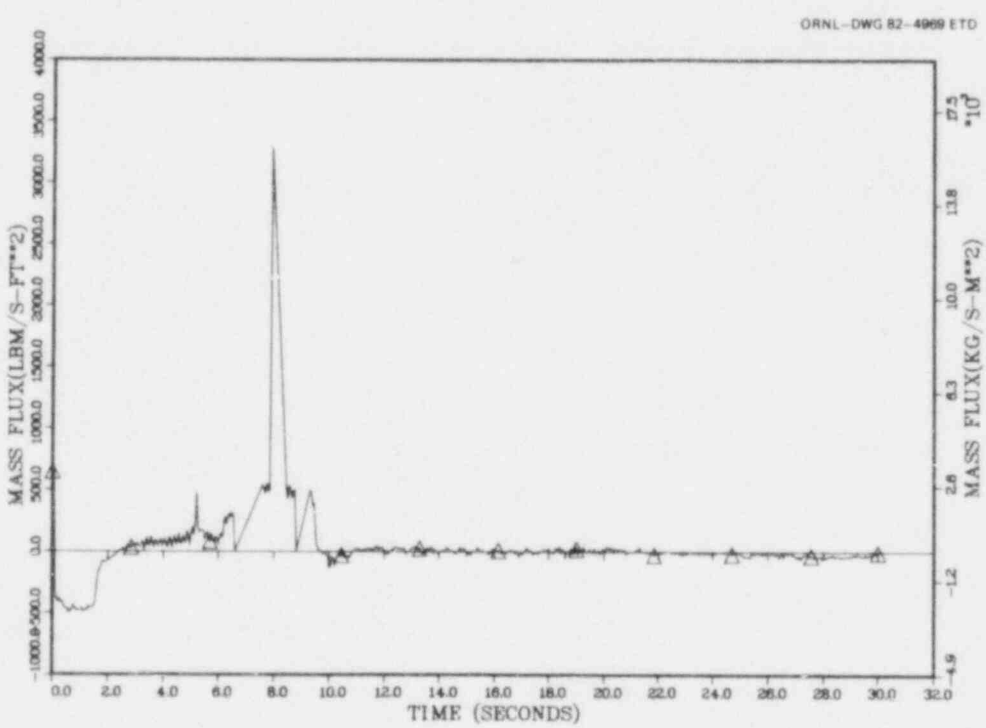

Fig. B.10. Mass flux vs time at BI2 site using TBM-DD model.

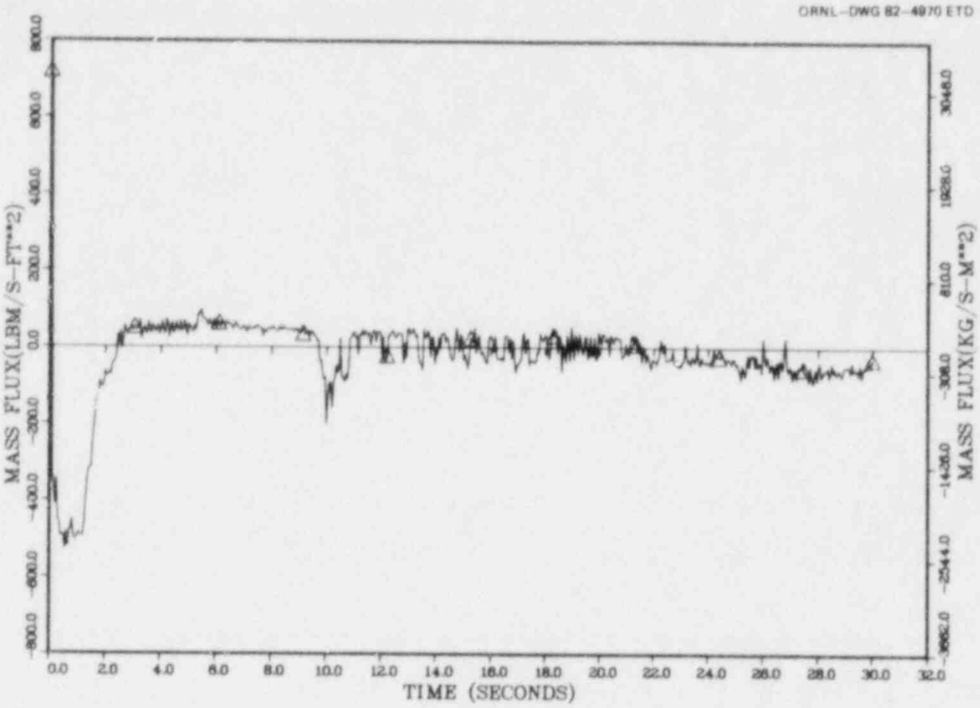

Fig. B.11. Mass flux vs time at BI2 site using DD-GAM 3 model.

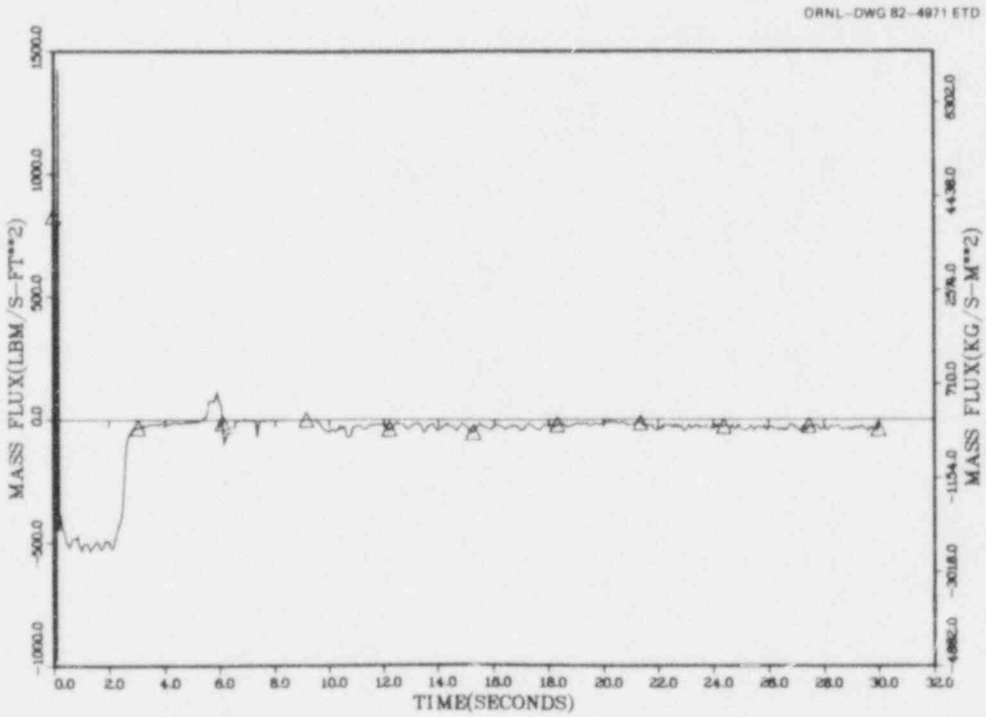

Fig. B.12. Mass flux vs time at SVI site using TEM-GAM model.

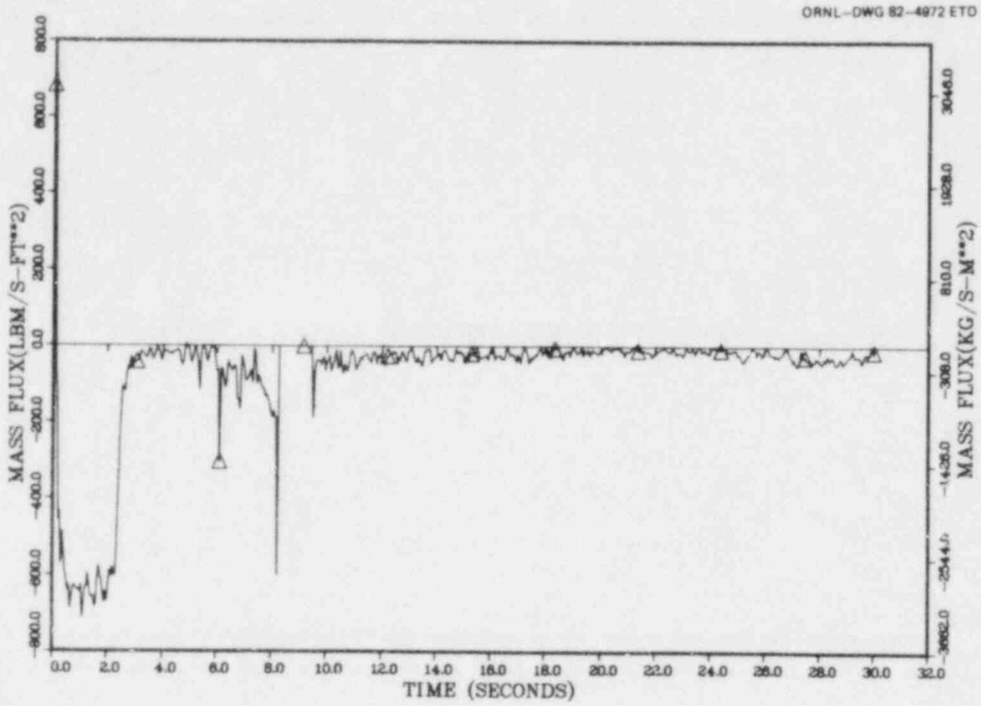

Fig. B.13. Mass flux vs time at SVI site using TBM-DD model.

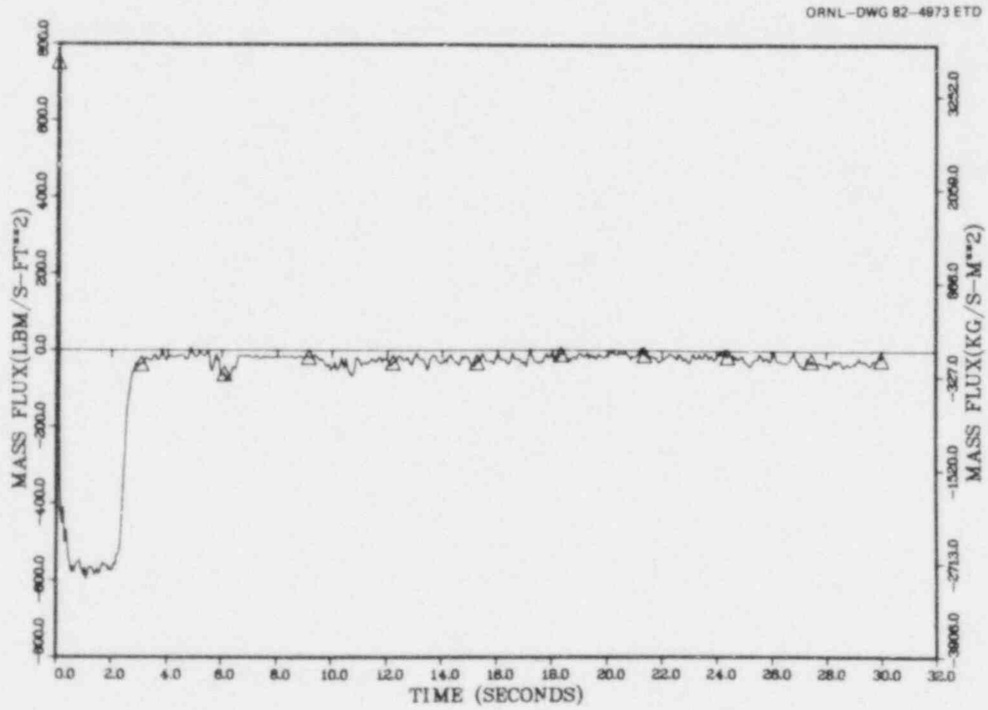

Fig. B.14. Mass flux vs time at SVI site using DD-GAM model.

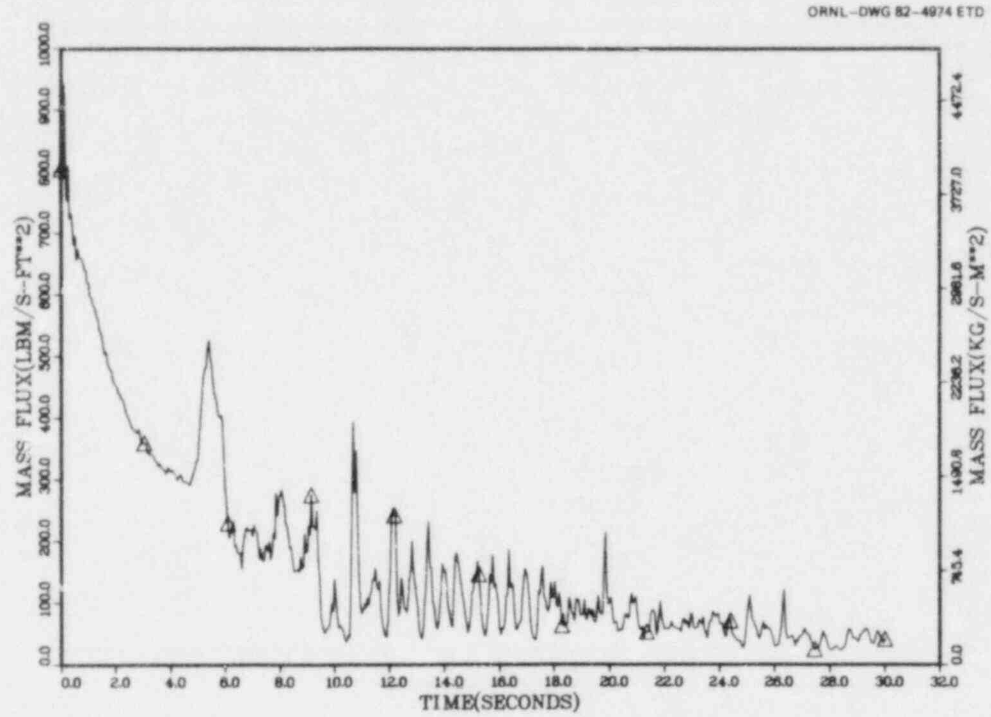

Fig. B.15. Mass flux vs time at SHI site using TBM-GAM model.

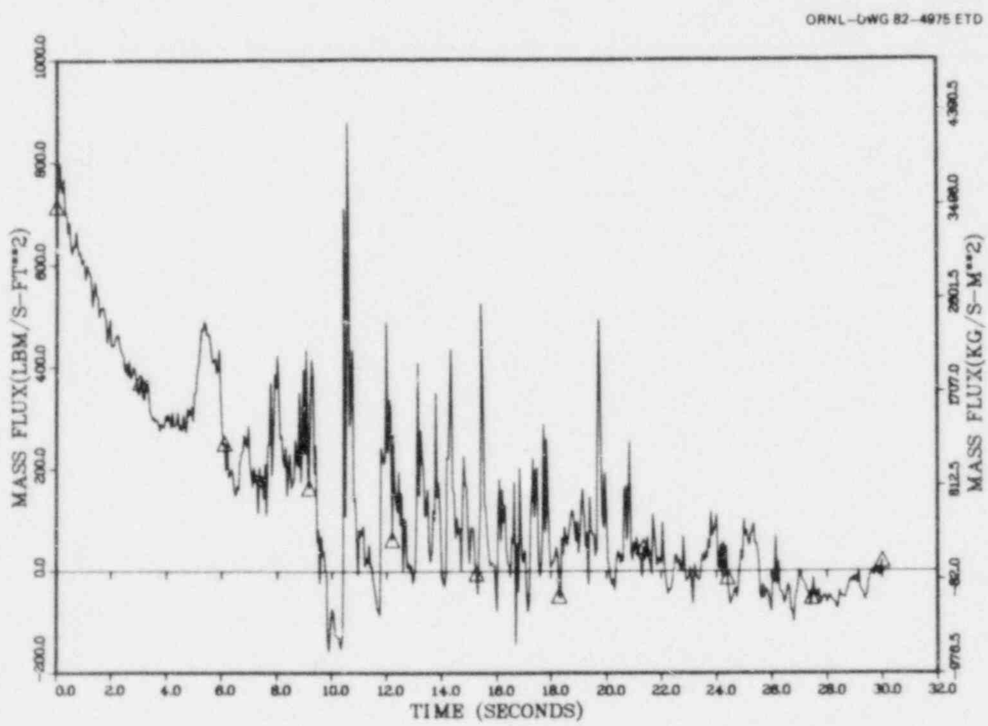

Fig. B.16. Mass flux vs time at SHI site using TBM-DD model.

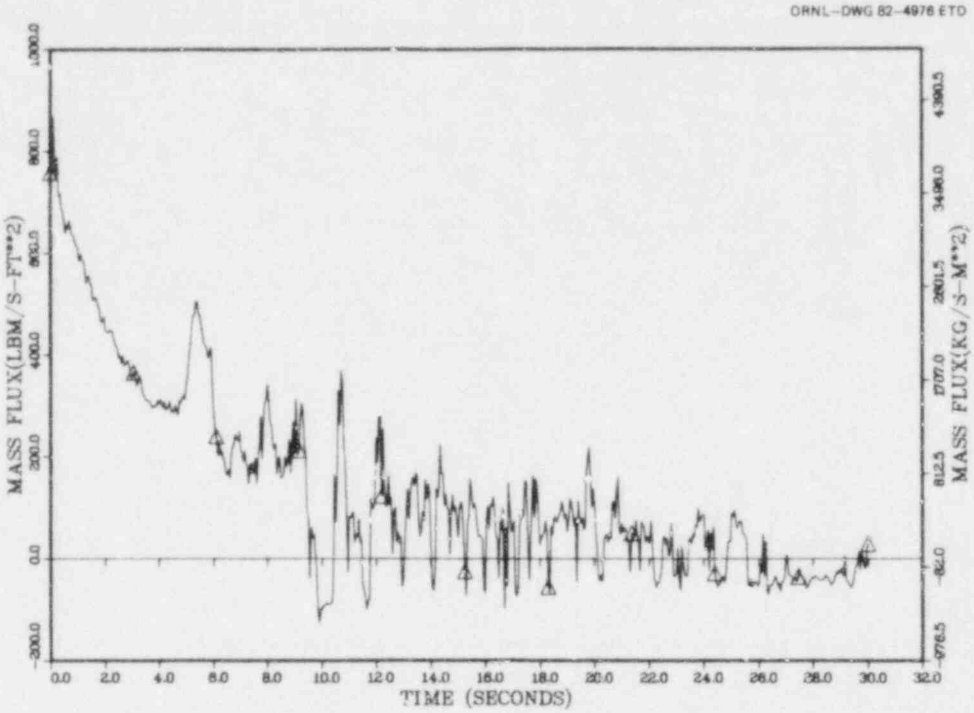

Fig. B.17. Mass flux vs time at SHI site using DD-GAM model.

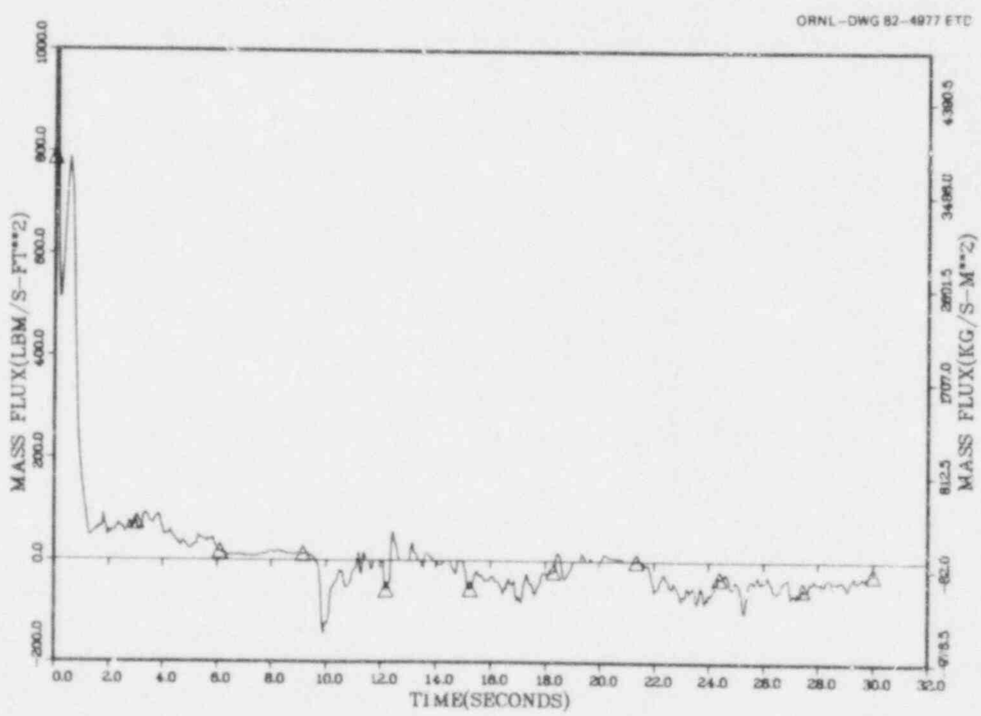

Fig. B.18. Mass flux vs time at SVO site using TBM-GAM model.

ORNL-DWG 82-4978 ETD

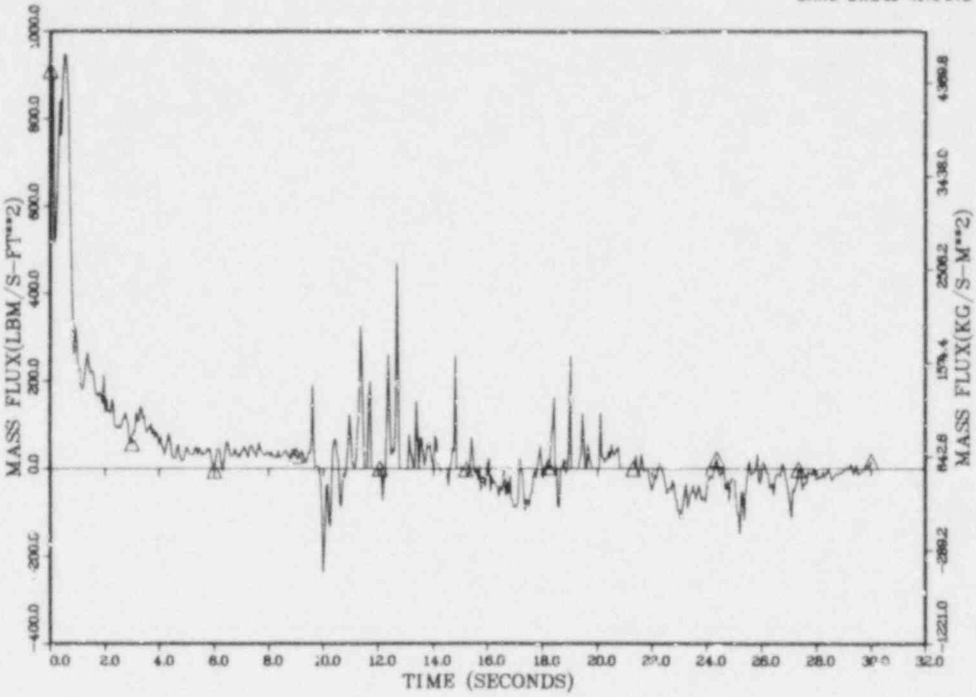

Fig. B.19. Mass flux vs time at SVO site using TBM-DD model.

ORNL-DWG 82-4979 ETD

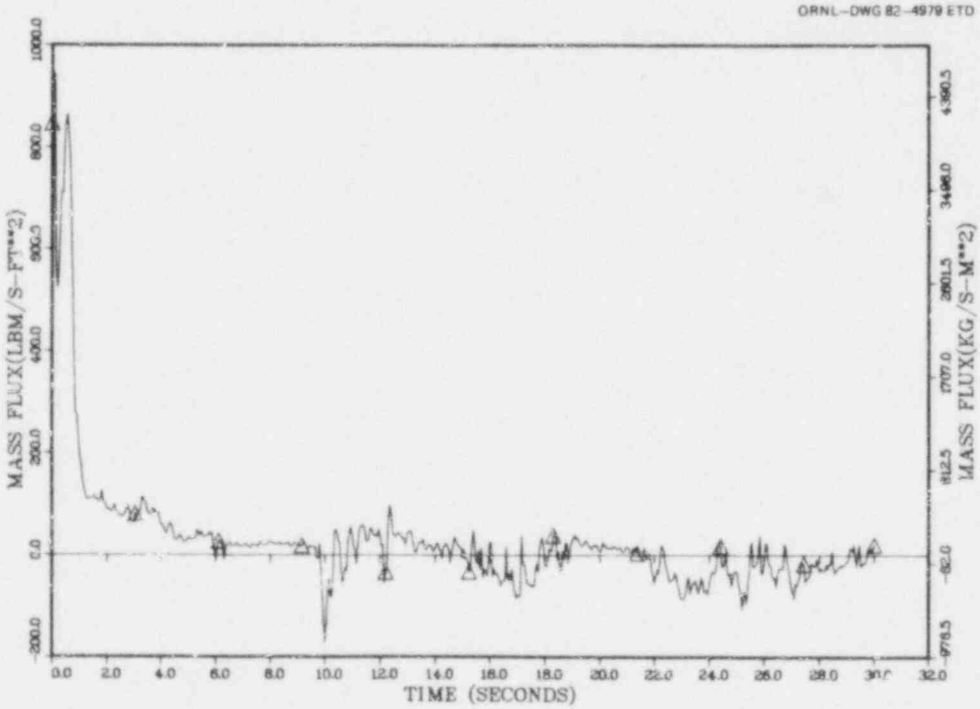

Fig. B.20. Mass flux vs time at SVO site using DD-GAM model.

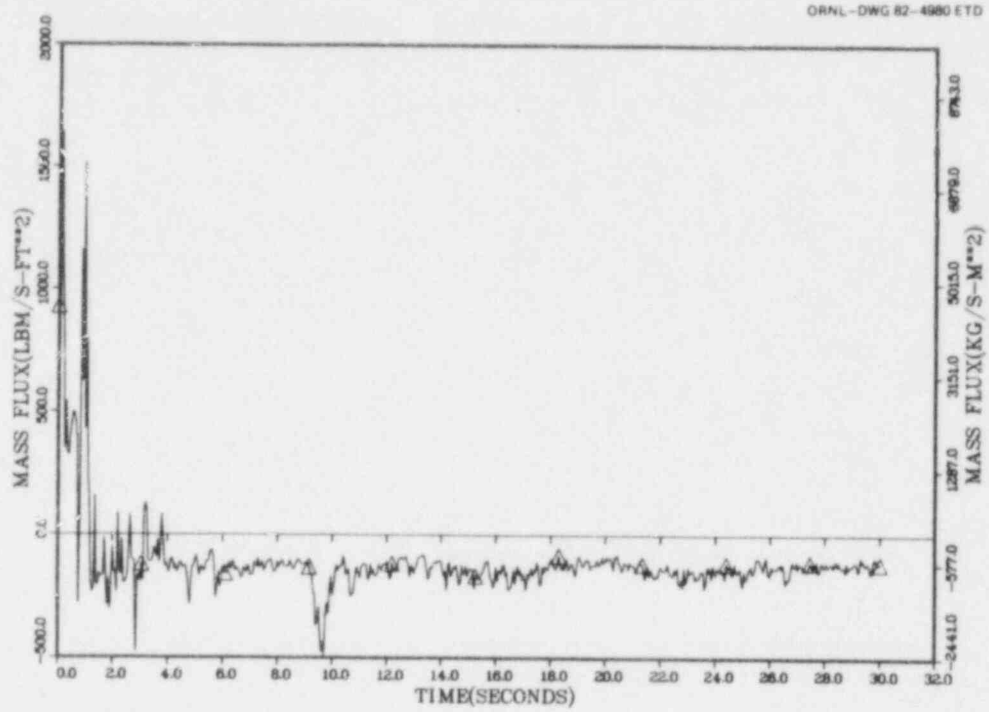

Fig. B.21. Mass flux vs time at SHO site using TBM-GAM model.

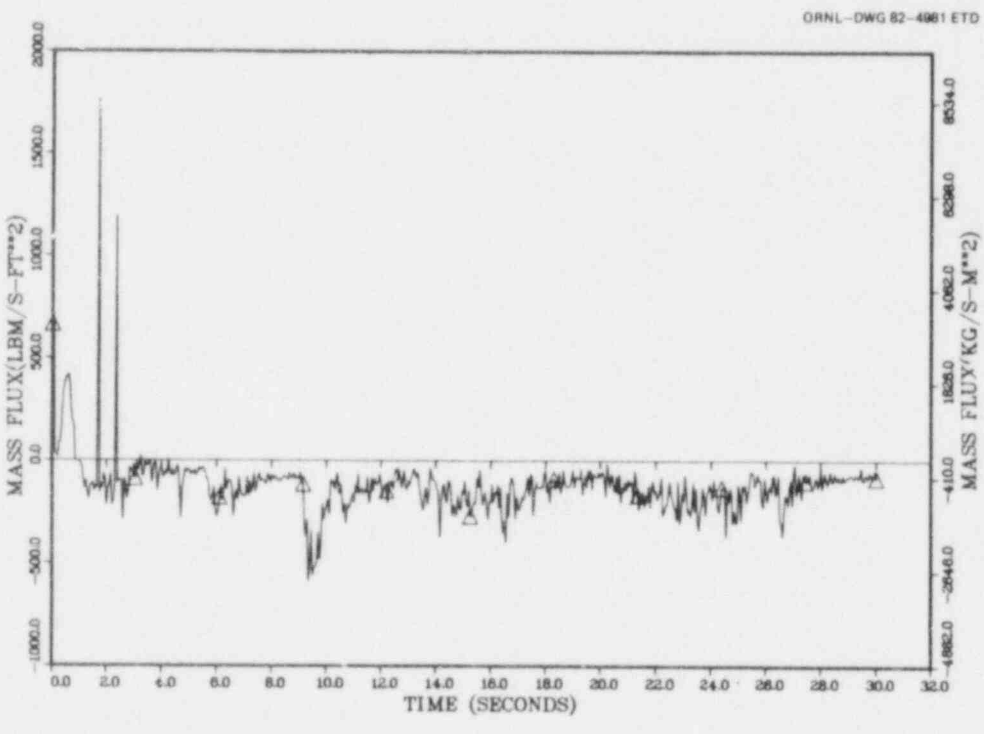

Fig. B.22. Mass flux vs time at SHO site using TBM-DD model.

ORNL-DWG 82-4982 ETD

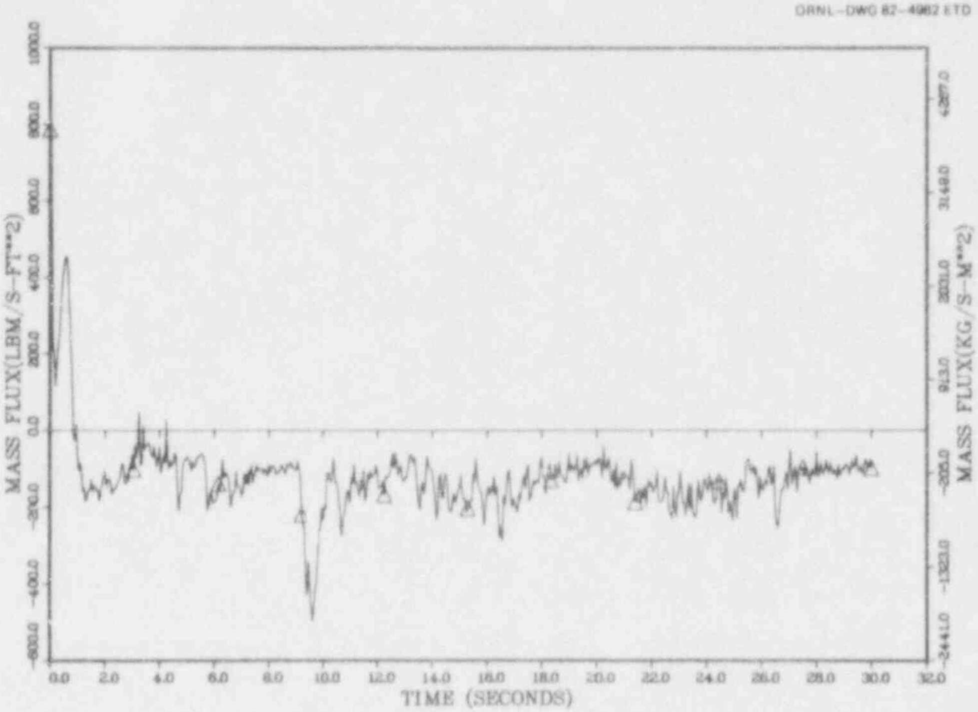

Fig. B.23. Mass flux vs time at SHO site using DD-GAM model.

are designated as:

turbine meter — single-beam densitometer = TBM-GAM
turbine meter — three-beam densitometer = TBM-GAM 3
drag disk — single-beam densitometer = DD-GAM
drag disk — three-beam densitometer = DD-GAM 3
turbine meter — drag disk = TBM-DD

A three-region annular model[2] was used to reduce the three-beam densitometer results to a composite density suitable for use in the mass flux models. The model solves for a uniform density for each region in Fig. B.24 using the density indicated by each of the three beams and the length of each beam within each region. The composite pipe density is then calculated as an area-weighted average of the three region densities. The resulting equation for the composite density is

$$\overline{\rho}_{Annular} = 0.3784\rho_A + 0.5117\rho_B + 0.1099\rho_C , \qquad (B.1)$$

where ρ_A, ρ_B, and ρ_C are indicated in Fig. B.24 and are the densities measured by the three beams.

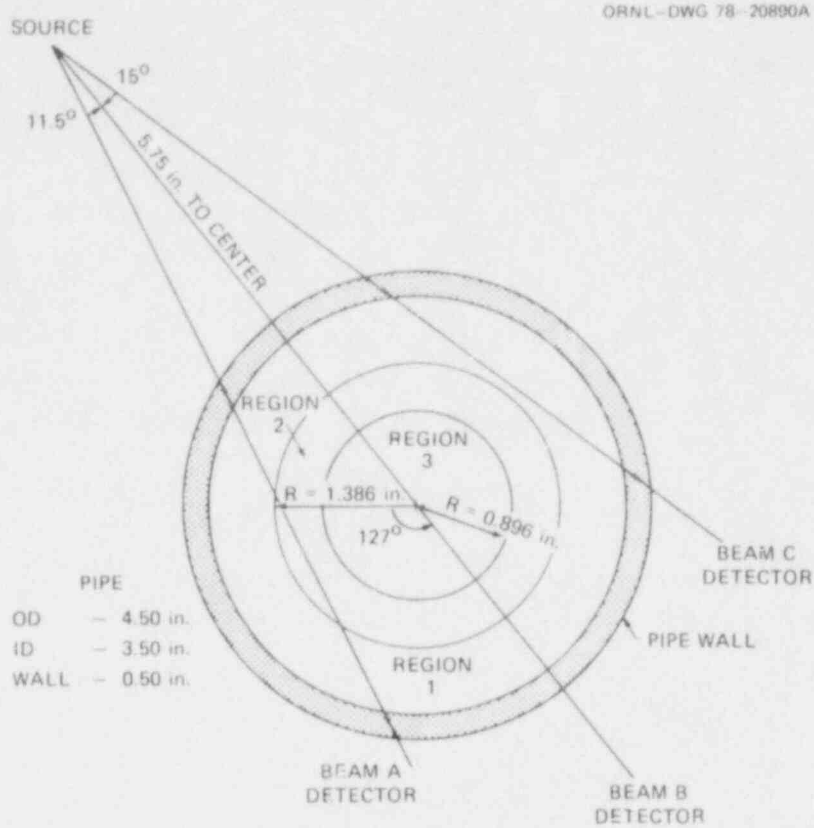

Fig. B.24. Diagram showing uniform density regions used in annular model for reduction of three-beam densitometer data.

B.2 Uncertainties in Mass Flux Calculations

Although the uncertainties obtained using the homogeneous models should be fairly small in single-phase flow, significant uncertainties may exist in two-phase flow where effects such as slip, void fraction, flow regime, and transient response affect the physical interpretation of the instrument output. This section will look first at estimated uncertainties in subcooled flow. This will be followed by discussion of uncertainties in steady-state and transient two-phase flow.

B.2.1 Subcooled flow uncertainty analysis

The Transient Upflow Film Boiling Test series (3.03.6AR, 3.06.6B, and 3.08.6C) was designed specifically to maintain subcooled inlet flow over most of the primary transient periods of interest in the heated bundle. The subcooled inlet flow conditions provide significantly lower and quantifiable uncertainties in the calculation of bounding conditions for the test section than are possible with two-phase flow conditions.

The mass flux (G) for subcooled flow conditions is calculated from a turbine meter measured velocity (V) and a fluid temperature- and pressure-deduced density (ρ);

$$G = \rho V \; . \tag{B.2}$$

It should be noted that the primary inlet flow measurement instruments in the Upflow Film Boiling Test configuration are the 2-in. turbine meters, FE-250 and FE-260. The larger 4-in. inlet turbine meters, FE-19 and FE-166, approach or fall below the lower limits of their calibrated range over most of the transient.

The mass flux uncertainty may be estimated by the standard propagation of errors method [Eq. (D.4) in Appendix D] using individual instrument uncertainties as stated in Tables D.5–D.6, Appendix D. The variance of the mass flux is given in an analogous form to Eq. (D.4) in Appendix D:

$$\text{Variance } (G) = \sigma_G{}^2 = \left(\frac{\partial G}{\partial \rho}\right)^2 \sigma_\rho{}^2 + \left(\frac{\partial G}{\partial V}\right)^2 \sigma_V{}^2 \; . \tag{B.3}$$

Expressed in terms of the standard deviation, σ, this equation becomes:

$$\sigma_G = \sqrt{(V\sigma_\rho)^2 + (\rho\sigma_V)^2} \; , \tag{B.4}$$

where

σ_ρ = density measurement uncertainty,
σ_V = velocity measurement uncertainty.

Since the uncertainties for the turbine meter are stated in terms of percent of reading, it is convenient to express the mass flux uncertainty in a similar manner. Equation (B.4) may be restated as

$$\sigma_G(\%) = \sqrt{\sigma_\rho(\%)^2 + \sigma_V(\%)^2} \; . \tag{B.5}$$

For the subcooled portion of the transients, the 2σ error bands (95% confidence bands) for the turbine meter ($2\sigma_V$) are stated as 4.1% of reading (Tables D.5–D.6 of Appendix D). Transient effects are assumed negligible after the initial subcooled decompression at blowdown. A 2σ estimate for the density is based on uncertainties generated from water properties assuming 2σ deviations of temperature ($2\sigma_T$) and pressure ($2\sigma_p$) from measured values. The 2σ uncertainties from Tables D.5–D.6 of Appendix D are

$$2\sigma_T = 3.7 \text{ K } (6.7°F)$$

and

$$2\sigma_p = 200 \text{ kPa } (29 \text{ psi}) \; ,$$

where again transient uncertainty effects are assumed negligible after the initial subcooled decompression at blowdown. For the pressures and temperatures of interest, the 2σ variation in temperature is the dominant effect and results in an estimated $2\sigma_p$ of 1.0% of reading. Substituting the 2σ measurement uncertainties into Eq. (B.5) results in a 2σ mass flux uncertainty for subcooled flow of 4.22% of reading.

B.2.2 Two-phase flow uncertainty analysis

The two-phase mass flux uncertainty estimates will be made based on results from the Steady-State Upflow Film Boiling Test series (3.07.9) and the application of a transient turbine meter model developed by Kamath and Lahey (Ref. 3) to the Transient Upflow Film Boiling Test (3.06.6B) and the Double-Ended Cold Leg Break Test (3.05.5B). Test series 3.07.9 were tests run with upflow in steady state; these tests provide a good benchmark for steady-state two-phase uncertainties. The Kamath and Lahey model provides an assessment of the effects of slip, flow regime, and transient response on the physical interpretation of the instrument output. Test 3.05.5B was a violent transient test that will provide a worst-case transient assessment.

B.2.2.1 Steady-state two-phase flow uncertainty analysis. A limited amount of steady-state two-phase mass flux uncertainty data over an equilibrium quality range of approximately 0.8–1.4 is available from the Steady-State Upflow Film Boiling Test series. Dispersed flow is expected at the test section outlet for the high-quality flow conditions. Steady-state, subcooled flow at the test section inlet provides a reference standard for estimating the two-phase mass flux uncertainty at the test section outlet spool pieces. The various homogeneous mass flux models discussed earlier are compared with each other as functions of pressure, equilibrium quality, and inlet mass flux. Results from a steady-state version of the Kamath and Lahey model (K&L) are also provided for comparison. The comparison is useful in providing confidence limits on the transient model as applied to the THTF instruments. The Kamath and Lahey model is discussed in more detail later. The steady-state model results are plotted as the ratio of the model mass flux to the reference inlet mass flux, G(MODEL)/G(REFERENCE), where perfect agreement is at 1.0. It should be noted that the reference subcooled inlet mass flux has 95% confidence bands of ±4.22% as discussed earlier.

Comparisons of the mass flux models DD-GAM 3, TBM-DD, TBM-GAM 3, and Kamath and Lahey are shown in Figs. B.25–B.27 as functions of pressure, equilibrium quality, and inlet mass flux, respectively. The results are from the horizontal Bundle Outlet spool piece (BO1). All of the models generally fall within 95% confidence bands of ±50%. Data scatter increases somewhat for lower pressures and mass flux. The DD-GAM 3 and TBM-DD models show somewhat smaller uncertainty bands (approximately ±30%) than the TBM-GAM and K&L models. The TBM-GAM 3 and the K&L models agree quite closely with each other over the range of test parameters.

The three-beam densitometer was used in the previous comparisons. The use of a single-beam densitometer in the models results in significantly higher uncertainties, as indicated in Figs. B.28 and B.29. Comparisons are made between the TBM-GAM and TBM-GAM 3 models in Fig. B.28

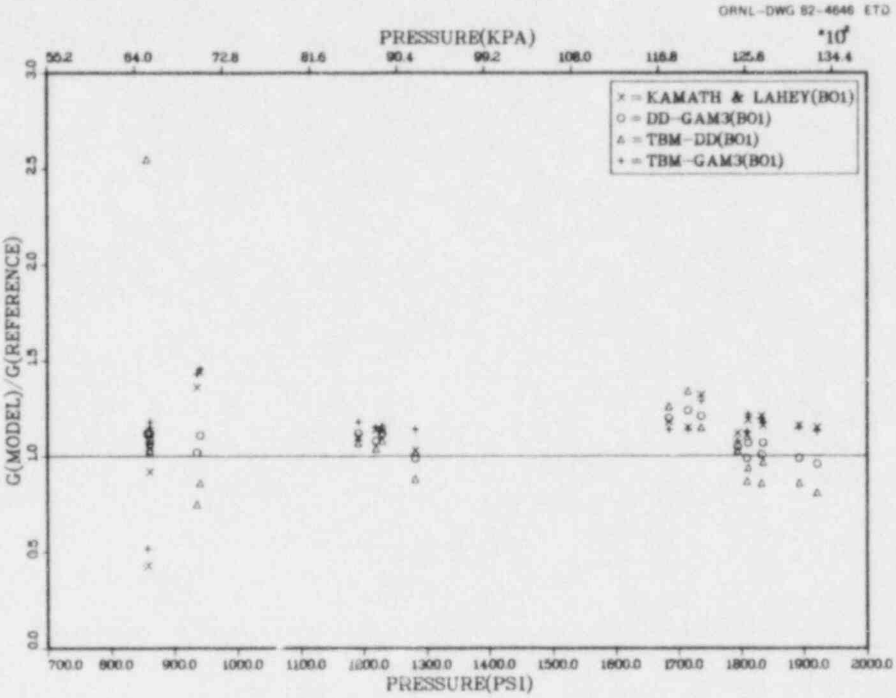

Fig. B.25. Comparison of mass flux models vs pressure at the B01 spool piece.

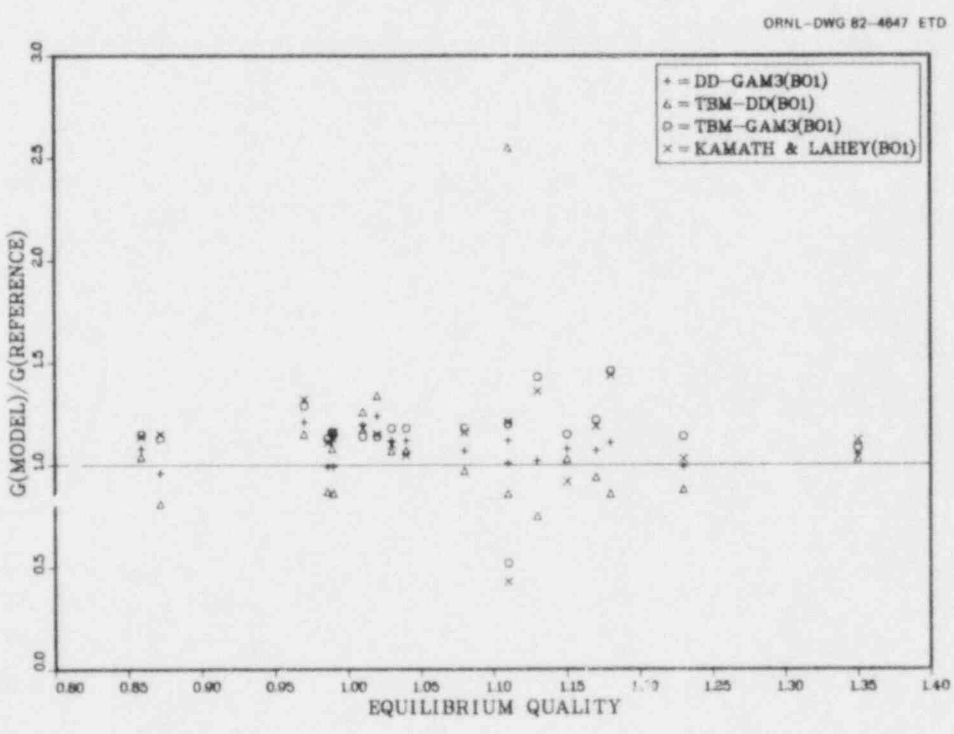

Fig. B.26. Comparison of mass flux models vs equilibrium quality at the B01 spool piece.

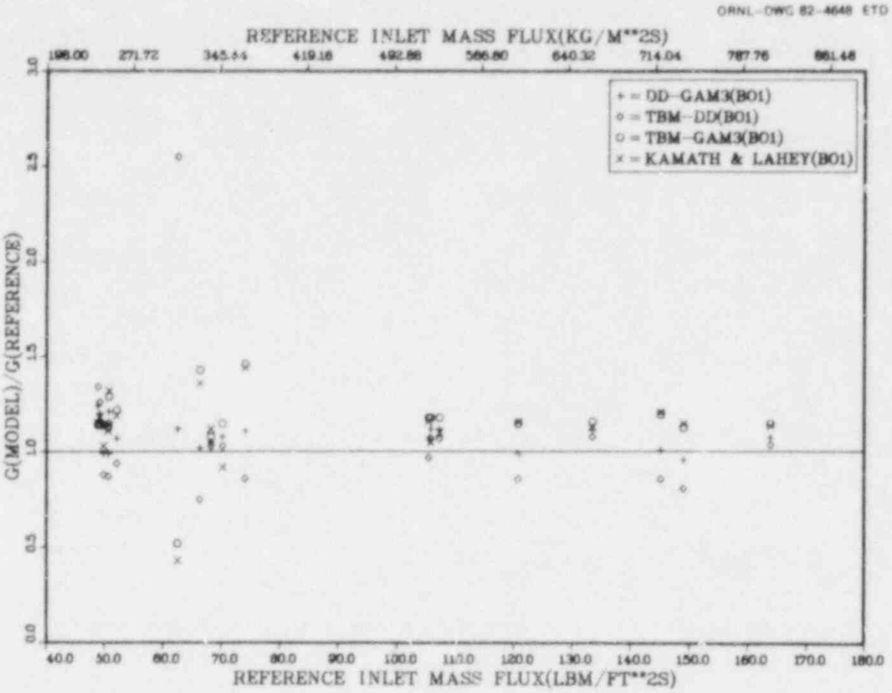

Fig. B.27. Comparison of mass flux models vs inlet mass flux at the B01 spool piece.

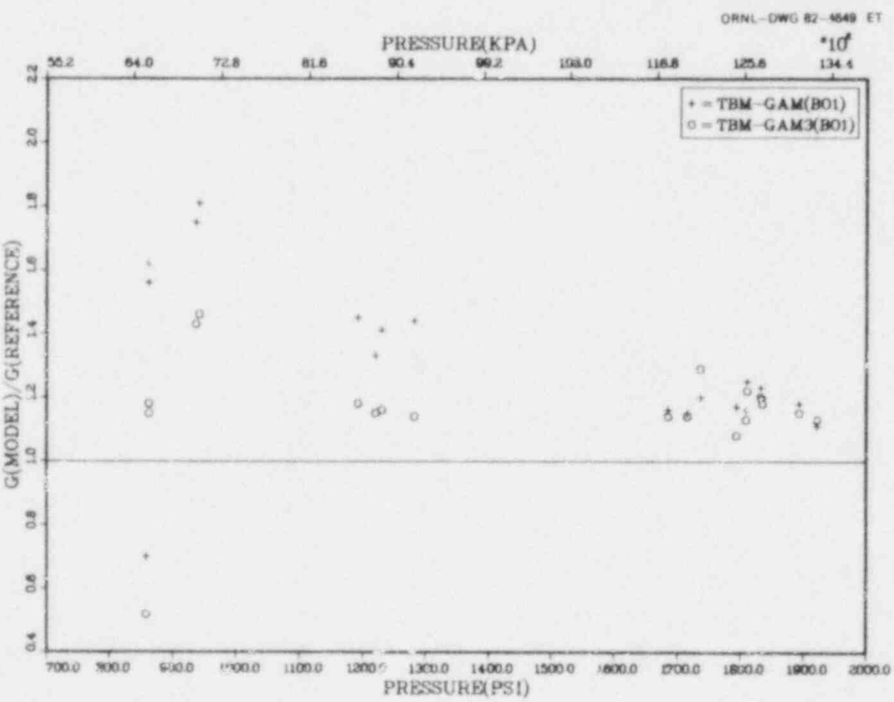

Fig. B.28. Comparison of turbine meter — densitometer model using single-beam and three-beam densitometers at the B01 spool piece.

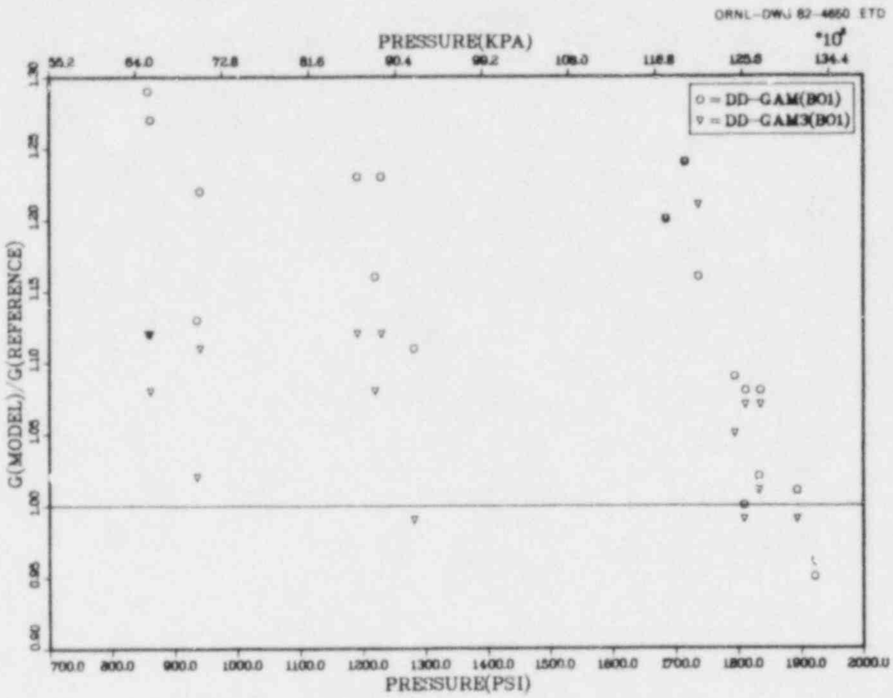

Fig. B.29. Comparison of the drag disk — densitometer model using single-beam and three-beam densitometers at the B01 spool piece.

and between the DD-GAM and DD-GAM 3 models in Fig. B.29 at the B01 spool piece. Uncertainty bands increase from approximately ±50% for the TBM-GAM 3 model to ±80% for the TBM-GAM model. Uncertainty bands for the DD-GAM model are ~10% higher than for the DD-GAM 3 model.

Mass flux model comparisons were also made at the other two outlet spool pieces, SVO and SHO. Spool piece SVO is a vertical spool piece with downflow and follows the B01 spool piece in the normal flow direction. Spool piece SHO is a horizontal spool piece that follows SVO. As mentioned earlier, flow conditions at the upper end and outlet of the test section were primarily dispersed flow with considerable nonequilibrium for many of the data points. As the flow moves downstream from the test section outlet, equilibrium is eventually reached as the liquid droplets evaporate. For equilibrium qualities greater than 1.0, single-phase superheated steam conditions should eventually exist. The three homogeneous models are compared with equilibrium quality for the SVO spool piece in Fig. B.30. Uncertainty bands for the DD-GAM model (~70%) and for the TBM-DD model (~140%) are significantly higher than those observed at the B01 spool piece. A trend is observed with decreasing uncertainty at higher equilibrium qualities. This may indicate that the flow is approaching equilibrium conditions and that the flow is essentially single-phase superheated steam. Figure B.31 shows the same comparisons for the SHO spool piece. It appears that the flow has reached equilibrium at this spool piece. The uncertainties for all of the models at the SHO spool piece are approaching the uncertainty bands expected for single-phase

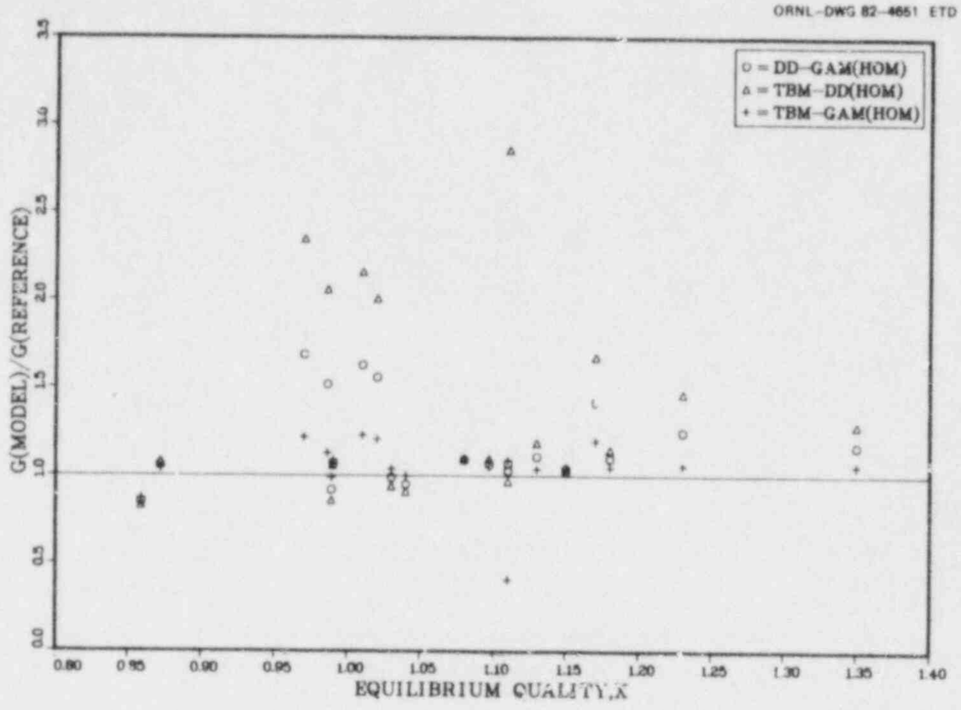

Fig. B.30. Comparison of mass flux models vs equilibrium quality at the SVO spool piece.

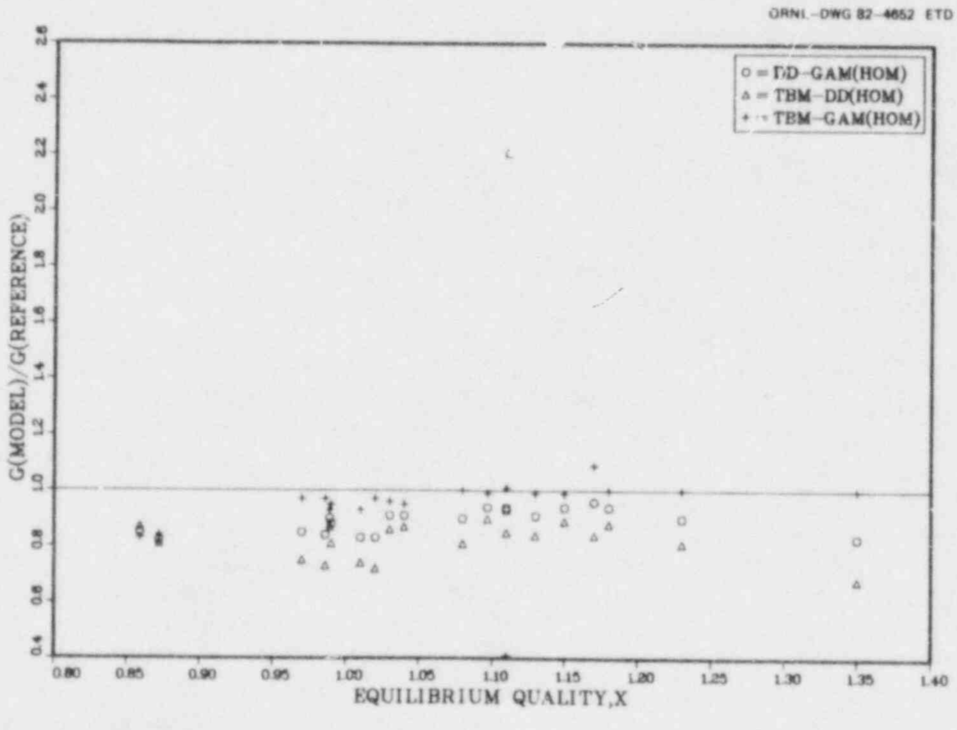

Fig. B.31. Comparison of mass flux models vs equilibrium quality at the SHO spool piece.

flow. (That is, the 2σ uncertainty bands for the drag disk instruments in subcooled flow are ±19% of reading over 10–100% of range; as a result, models using this instrument would have 2σ uncertainty bands greater than 19%.)

B.2.2.2 Transient two-phase flow uncertainty analysis. The application of the Kamath and Lahey transient two-phase turbine meter model to THTF test data is made in an attempt to assess the effects of slip, void fraction, flow regime, and transient response on the physical interpretation of the instrument output. Verification of the model in transient two-phase flow is not possible for the THTF due to the nature of the tests and system. The intent rather is to look at effects that are not accounted for in the simpler homogeneous flow models as they apply to THTF test conditions.

The turbine flowmeter model developed by Kamath and Lahey will be briefly described along with its assumptions and limitations. The computer solution technique and input parameters are also discussed.

The turbine flowmeter dynamic equation was derived from the principle of angular momentum conservation. The equation accounts for effects of nonuniformity of velocity and void profiles in conduit, imperfect guidance of the fluid by the rotor blades, rotor inertia, slip ratio, bearing friction, and windage losses. A detailed derivation of the equation of motion is presented in Ref. 3. The resulting equation of motion is shown below:

$$\frac{d\langle V_{Z\ell}\rangle}{dt} = \langle |V_{Z\ell}|\rangle \frac{V_t}{(\Delta x)} - \langle V_{Z\ell}\rangle \frac{R_1}{(S + R_1)\rho_\ell} \frac{d\rho_\ell}{dt} + \frac{S}{(S + R_1)\rho_v} \frac{d\rho_v}{dt}$$

$$\frac{S - R_2}{S + R_1} \frac{1}{\langle\alpha\rangle} \frac{d\langle\alpha\rangle}{dt} + \frac{1}{(S + R_1)} \frac{dS}{dt} - \frac{C_\ell R_1 + C_v S^2}{(S + R_1)(\Delta x)} \langle V_{Z\ell} \times |V_{Z\ell}|\rangle$$

$$+ V_t \frac{R_1}{(S + R_1)} \frac{1}{\rho_\ell} \frac{d\rho_\ell}{dt} + \frac{S}{(S + R_1)} \frac{1}{\rho_v} \frac{d\rho_v}{dt} + \frac{1 - R_2}{S + R_1} \frac{1}{\langle\alpha\rangle} \frac{d\langle\alpha\rangle}{dt}$$

$$+ \frac{dV_t}{dt} \frac{1 + R_1}{S + R_1} + \frac{I_{rotor}(1 + \eta_v)}{(S + R_1)R^2 A_{xs}(\Delta x)\rho_v\langle\alpha\rangle}$$

$$+ \frac{\mu^{0.43}\rho_\ell^{0.57}|\omega|^{0.57}\omega(1 + \eta_v)}{(S + R_1)RA_{xs}(\Delta x)\tan\beta\rho_v\langle\alpha\rangle} [0.039(Ct_b N)R_T^{2.57}(R_b - R_T)^{-0.43}$$

$$+ 0.078(L_{jb}R_S^{3.57}) \times (R_{h_1} - R_S)^{-0.43}] . \quad (B.6)$$

The angular brackets in the equation are cross-sectional average operators. The variables R_1, R_2, and V_t are defined by

$$R_1 = R_2 \frac{(1 - \alpha)}{\alpha} , \tag{B.7}$$

$$R_2 = \frac{\rho_\ell}{\rho_v} \frac{1 + \eta_v}{1 + \eta_\ell} , \tag{B.8}$$

and

$$V_t = \frac{\omega R}{\tan \beta} . \tag{B.9}$$

The variable definitions are listed in the nomenclature. Equation (B.6), a classical separated flow equation, is derived for arbitrary void fraction and velocity profiles by assuming that cross-sectional average products may be separated into products of averages using correlation coefficients. In this case the correlation coefficients C_ℓ and C_v relate commonly measured values such as average cross-sectional void fraction (average density) and average cross-sectional velocity to void fraction and velocity profile weighted averages of the separate phase momentum flux. The correlation coefficients appearing in Eq. (B.6) are defined as

$$C_\ell = \frac{\langle (1 - \alpha) V_\ell^2 \rangle}{\langle 1 - \alpha \rangle \langle V_\ell \rangle^2} \tag{B.10}$$

and

$$C_v = \frac{\langle \alpha V_v^2 \rangle}{\langle \alpha \rangle \langle V_v \rangle^2} \tag{B.11}$$

for the liquid and vapor phases, respectively. These coefficients relate the net momentum flux to the mean velocities of the components and may assume different values for various flow regimes. The parameters are, in effect, adjustments to homogeneous model inputs for nonhomogeneous flow effects. The magnitude of the effect of these coefficients on the mass flux as applied to THTF test conditions will be discussed later.

The dynamic equation is solved using an IBM subroutine, CSMP III (Continuous System Modeling Program III), designed to solve a system of first-order differential equations with initial values.[4] The subroutine is limited, however, to input parameters with analytical forms.

The main input to the program includes the turbine meter geometry, transient pressure, two-phase cross-sectional average density, and the turbine meter counting rate, which is proportional to the blade angular velocity. The turbine meter is a 5-bladed, 3.5-in. Flow Technology turbine meter. The gamma densitometer is a Measurements, Inc., three-beam densitometer. Discrete data are recorded during the transients by a DAS at 10-ms intervals. Analytical forms of the data were produced from the discrete data for input to the CSMP III program.

The equation for steady-state flow in a conduit may be obtained by setting all time derivatives to zero in Eq. (B.6). For steady-state model comparison, it is of interest to note that the steady-state model reduces to the Rouhani model[5] under certain simplifying assumptions. If the correlation coefficient between void fraction and velocity profiles is unity (i.e., $C_\ell = C_v = 1$), the guidance of the fluid by the rotor blade is perfect ($\eta_\ell = \eta_v = 0$), and the drag torque is assumed negligible, then Eq. (B.6) may be further reduced to the Rouhani model equation,

$$\langle\alpha\rangle\rho_v\langle|V_v|\rangle(\langle V_v\rangle - V_t) = \langle 1 - \alpha\rangle\rho_\ell\langle|V_\ell|\rangle(V_t - \langle V_\ell\rangle) \ , \qquad \text{(B.12)}$$

which assumes a momentum balance between two phases on the turbine blades. Values of η_ℓ and η_v for the transient results that follow are assumed to be 0.2, a typical value for single-phase flow reported in Ref. 2. Parametric studies by Kamath and Lahey indicate very little difference between the 0.0 and 0.2 assumed values for η_ℓ and η_v. For the purposes of this analysis, a steady-state and transient model reference case is defined that assumes typical parameter values of $S = 1$, $C_\ell = 0.99$, $C_v = 1.06$, $\eta_\ell = 0.2$, and $\eta_v = 0.2$. Values of C_ℓ and C_v are from Ref. 3 where power law velocity and void profiles were assumed:

$$V_k = V_{cl_k}(1 - r/R_o)^{1/n} \qquad \text{for } n = 2\text{–}7 \ ,$$

and

$$\alpha = \alpha_{cl}(1 - r/R_o)^{1/m} \qquad \text{for } m = 2\text{–}7 \ .$$

B.2.2.3 Transient two-phase solution. As stated earlier, the model incorporates the effects of rotor inertia, velocity and void profiles in the conduit, slip ratio, imperfect guidance of the fluid by the rotor blades, bearing friction, and windage losses. Of these parameters, the effects of the velocity and void profiles of the liquid phase, rotor inertia, and slip ratio were found to be the most significant for the transients of interest.

Transient model solutions were obtained from data from portions of two transient tests run at the THTF. Since reference mass flux information is not available under the transient conditions, the model results are compared with a homogeneous mass flux model. The homogeneous mass flux is obtained from the product of the average mixture density as measured by the three-beam gamma densitometer and the average velocity as deduced from the volumetric flow measurement of the turbine meter (based on subcooled water calibration factors). Comparing the homogeneous, no slip model to the transient model will provide insight into the effects of nonhomogeneous flow for the THTF transient test conditions.

Figure B.32 shows the transient model reference case compared to the homogeneous model for the initial transient portion of Test 3.06.6B. Test 3.06.6B involved a relatively slow depressurization rate, and the observed transient peaks in mass flux for the two models appear to be in phase. The smoothed input for the transient model did not include the fine structure observed for the homogeneous model and as a result it not seen in the transient model results. Differences of ~30–40% are observed from 0.5 to 2.0 s into the transient and near the mass flux peak seen at ~3 s. From 5 s to the end of the transient period shown, the fine structure of the homogeneous model varies around that of the transient model. Figure B.33 shows the effect of varying the liquid-phase distribution coefficient for the same test. The effects are considerable for higher mass flux but negligible for mass flux below ~610 kg/m²·s (125 $lb_m/ft^2 \cdot s$), with the magnitude of the mass flux increasing with decreasing C_ℓ. It is difficult to

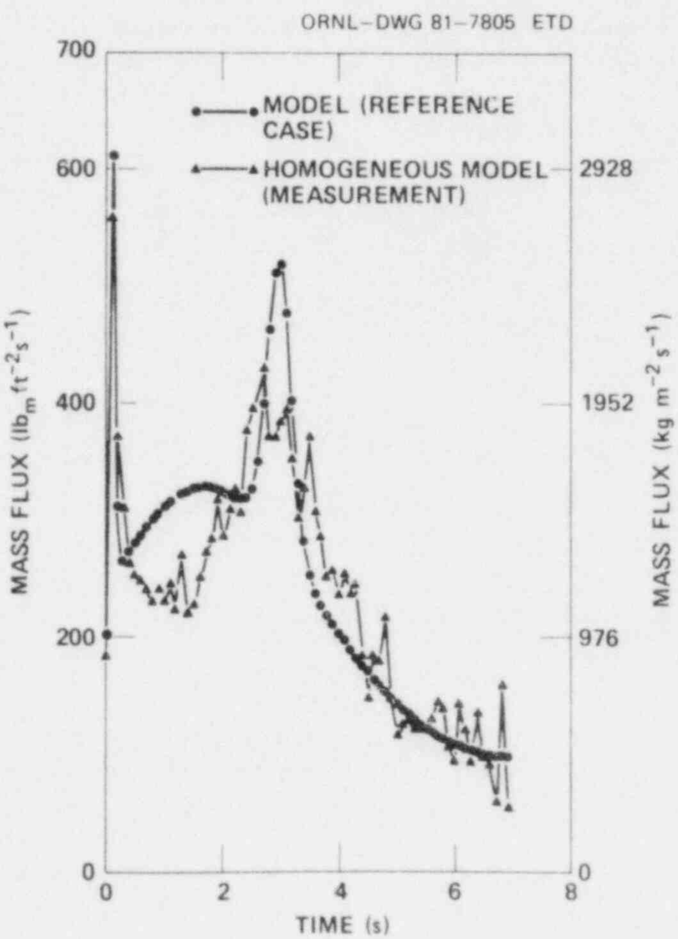

Fig. B.32. Mass flux comparison of the transient and homogeneous models for Test 3.06.6B.

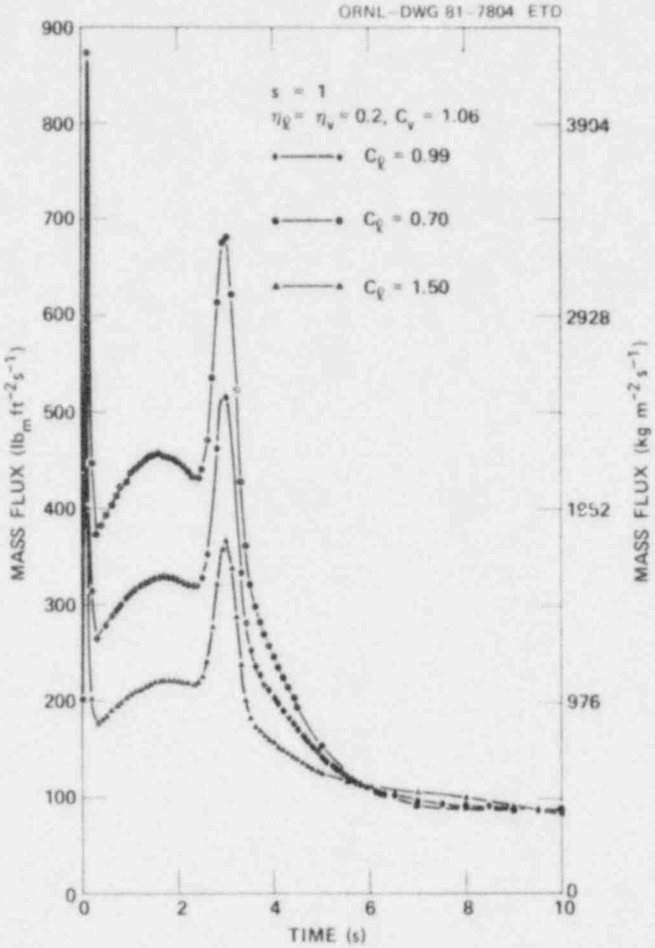

Fig. B.33. Effect of the correlation coefficient, C_ℓ, on mass flux for Test 3.06.6B.

characterize the appropriate value of C_ℓ, especially during the initial voiding of the test section, since flow regimes may be varying considerably. Simple approximations for velocity and void profiles may yield values over the ranges indicated in Fig. B.33. A simple model for an annular flow regime results in a value of 1.35 when substituted into Eq. (B.10). A stratified flow in horizontal spool pieces may produce a value of 0.7. Flow with flat profiles both in void fraction and velocity generates a C_ℓ of 1. Without experimental validation, however, values of C_ℓ obtained from simple models and applied to two-phase flow regimes, where velocity and void profiles are varying in time as well as space, may be misleading. It is of interest to note that for Test 3.06.6B, the important heat transfer data of interest is obtained from ~6 s to the end of the transient period shown. During this time, the effects of varying C_ℓ are negligible. Also, during this period, the conditions in the upper test section bundle and outlet spool pieces were similar to those of the steady-state data discussed earlier.

The reference model case is compared with the homogeneous model for the faster transient of Test 3.05.5B in Fig. B.34. The reference model leads the homogeneous model by ~50 ms, presumably due to rotor inertia effects. The second peak agrees well temporally although the peak magnitude differs by ~25%. The two models do not agree very well for times shown after 1.25 s. Figure B.35 shows the effect of varying the slip ratio for the transient model for Test 3.05.5B. A change in slip ratio leads to a change in amplitude as well as temporal phase (the larger the slip ratio, the smaller the magnitude and the earlier the peak). The slip ratio of 5 is probably higher than would be expected under THTF test conditions, but the comparison shows the trends clearly.

An example of the relationship between the input data and the reference case transient model output is shown in Fig. B.36 for Test 3.05.5B. The curves for pressure (P), average mixture density (D), and counting rate (CR) are smoothed analytical forms of discrete data measured during the test. The void fraction (α) and mass flux (G) are generated by the

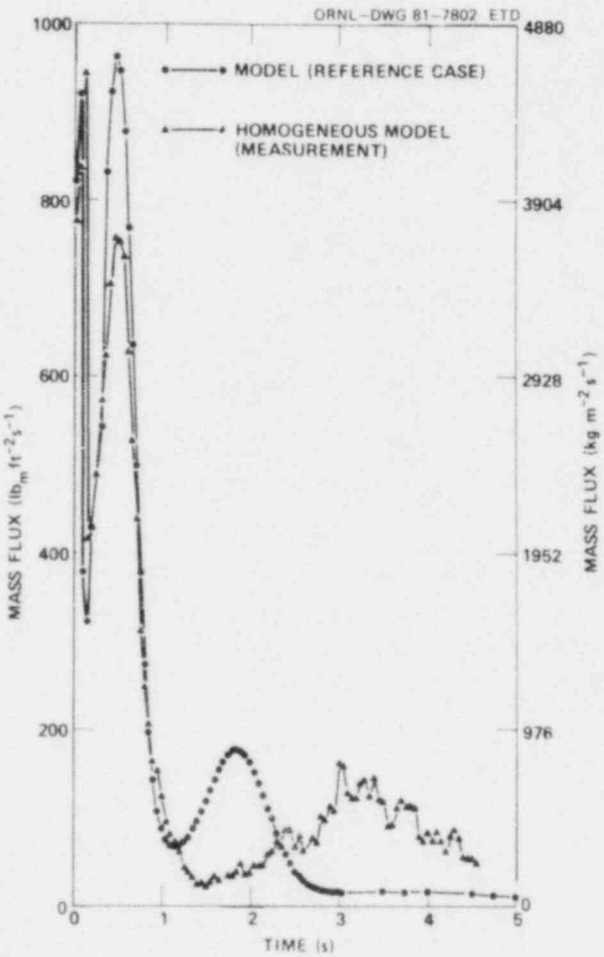

Fig. B.34. Mass flux comparison of the transient and homogeneous models for Test 3.05.5B.

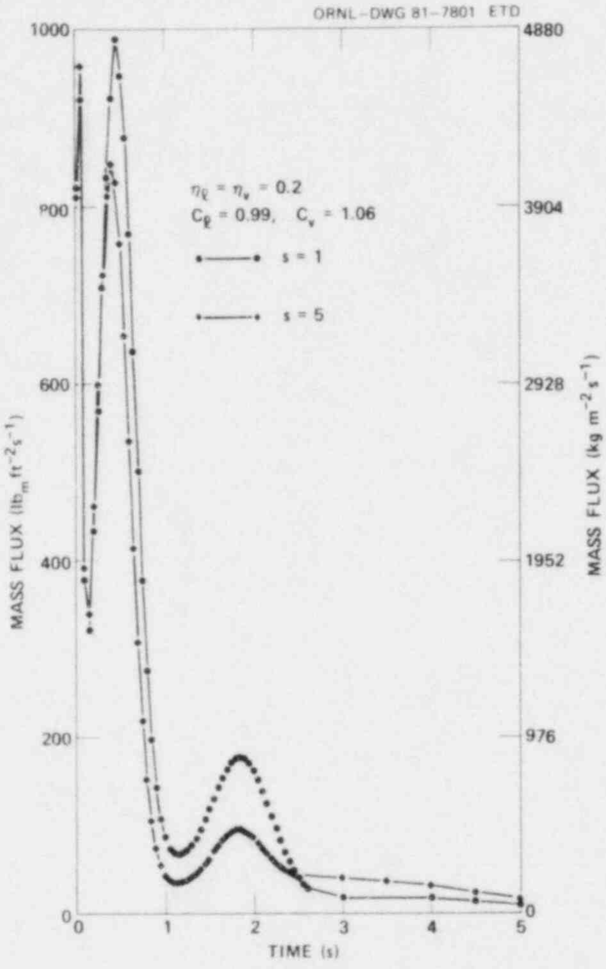

Fig. B.35. Effect of slip ratio on mass flux for Test 3.05.5B.

model. The mass flux and turbine meter counting rate are seen to be intimately related as the impulse and response. The effect of rotor inertia is observed in the second peak where the counting rate of the turbine meter lags the model-predicted mass flux.

B.3 Summary

Mass flux uncertainties for subcooled flow using a turbine meter for volumetric flow measurements and a pressure- and temperature-deduced density are estimated at ±4.22% of reading (95% confidence bands).

Steady-state tests indicate two-phase flow uncertainty bands of less than ±50% of reading (95% confidence bands) for all models at the B01 spool piece where a three-beam densitometer is used in applicable models. The DD-GAM 3 and TBM-DD models actually show somewhat smaller uncertainty bands (±30%) than the TBM-GAM 3 model at the Bundle Outlet spool piece (B01). However, at the Vertical Outlet spool piece (SVO), uncertainty

ORNL-DWG 82-5594 ETD

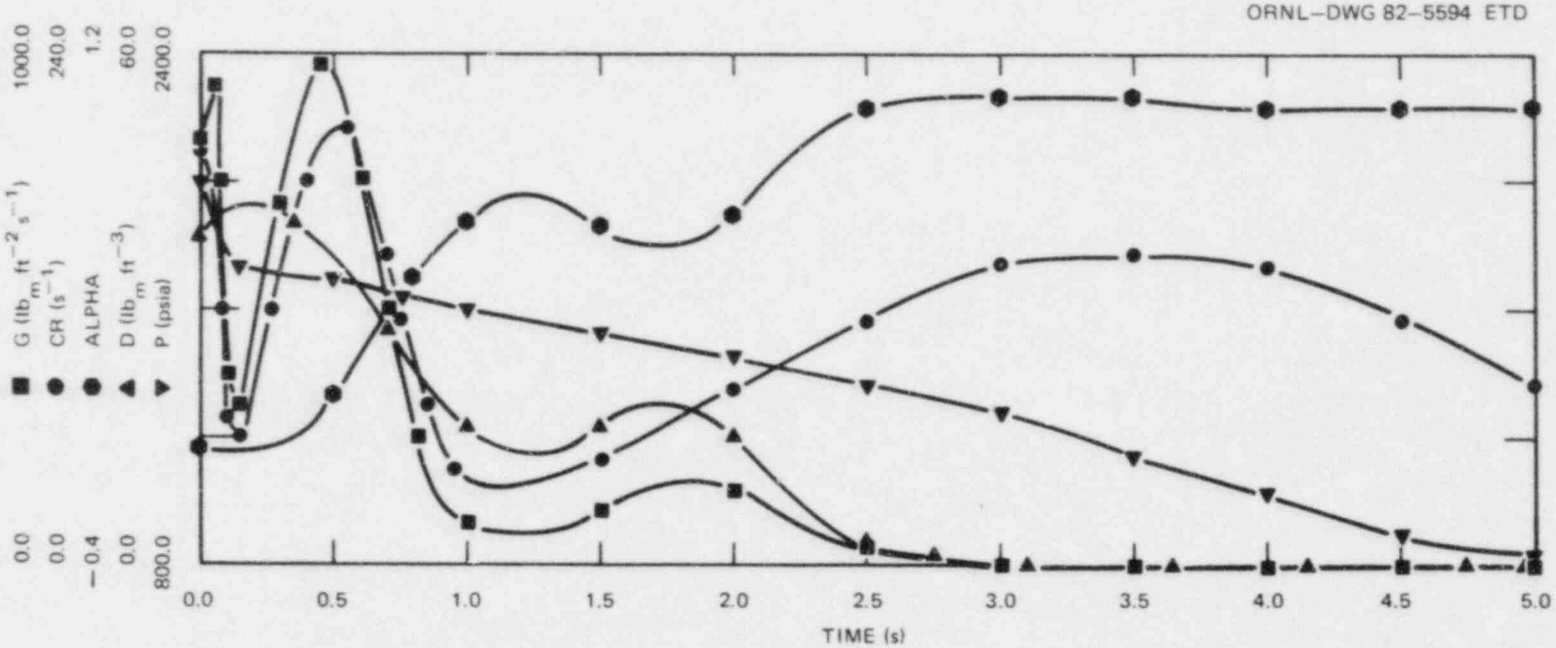

Fig. B.36. Relationship between the input and output parameters of the transient model for Test 3.05.5B.

bands for the DD-GAM model (70%) and the TBM-DD model (140%) are significantly higher. The large uncertainties in models that use measurements from the drag disks are not particularly suprising from the standpoint of previous operating experience. The drag disks are the least reliable of the spool piece instruments in terms of repeatability and consistency of instrument response.

Significant uncertainty band increases result from using a single-beam densitometer as compared to using a three-beam densitometer. At the B01 spool piece for the turbine meter-densitometer model, the use of a single-beam densitometer results in an increase of uncertainty bands from ±50% (three-beam) to ±80% of reading. Similar results are observed for the drag disk-densitometer model, where the use of a single-beam densitometer adds an additional 10% of reading to the uncertainty bands.

The application of a transient turbine meter model to transient THTF test data provides insight into possible transient uncertainties included in turbine meter-densitometer models. Comparison of the Kamath and Lahey transient model with the homogeneous model TBM-GAM 3 indicates that the effects of the velocity and void profiles of the liquid phase, rotor inertia, and slip are the most significant for the THTF transients of interest.

During the initial transient portion of the Upflow Film Boiling Test (3.06.6B) and for mass flux greater than ~610 kg/m²s (125 lb_m/ft^2s), variations in the transient model mass flux of 30–50% are observed as the void and velocity profile correlation coefficient C_ℓ is varied from 1.0 over a range of 0.7–1.5. For the same test, when mass flux is less than 610 kg/m²s (the time period in which film boiling heat transfer data of interest are available), the effect of varying C_ℓ is negligible.

Increases in slip from 1.0 reduce the magnitude of the model mass flux and slow time response of the turbine meter.

Rotor inertia effects are significant for fast transients such as the early portions of the Double-Ended Cold Leg Break Test (3.05.5B). The reference case transient model leads the homogeneous model by ~50 ms during portions of the transient, resulting in significant mass flux differences. Response time effects were not as significant for the slower transients of the Upflow Film Boiling Test (3.06.6B) although mass flux differences of 30–40% between the transient model reference case and the homogeneous model are observed.

Since the actual mass flux is not known for the transient cases, neither model may be verified. The model comparisons are able to provide test-specific information on mass flux sensitivity to uncertainties in two-phase flow parameters.

The Kamath and Lahey model results agreed well with the TBM-GAM 3 model for the Steady-State Upflow Film Boiling Test data. For this reason and because there is no additional information, in order to estimate uncertainties during the faster transient portions of the THTF tests the addition of the steady-state uncertainty estimates and the transient uncertainty estimates based on transient model comparisons to obtain a total transient uncertainty estimate would appear to be warranted. It should be noted that during the important periods of interest for the Transient Upflow Film Boiling Tests in terms of heat transfer data, the mass flux is changing fairly slowly. In addition, the outlet flow conditions of the Steady-State Upflow Film Boiling Tests were similar to the higher quality portions of the transient tests. Application of the steady-state uncertainty bands over these conditions can be made with a good degree of confidence.

Although the steady-state uncertainty data provide a good estimate of uncertainty bands over the flow conditions and parameter ranges observed for those steady-state tests, uncertainties for different quality ranges and flow regimes may be considerably different. Without data over other ranges, however, it is felt that these are the best available uncertainty estimates for use in two-phase flow conditions at the THTF. Table B.1 contains the mass flux uncertainties discussed in this appendix.

Table B.1. Mass flow errors[a]

Steady state single phase	
2σ = 4.22% of reading	
Horizontally mounted spool piece steady state two phase	
DD-GAM 3, TBM-DD	2σ = 30% of reading
TBM-GAM 3	2σ = 50% of reading
Vertically mounted spool piece steady state two phase	
DD-GAM	2σ = 70% of reading
TBM-DD	2σ = 140% of reading
TBM-GAM	2σ = 60% of reading
Transient effects on two-phase flow	
$G > 610\ kg/m^2 \cdot s$ ($4.5 \times 10^5\ lb_m/h \cdot ft^2$)	add extra 30–50% of reading
$G < 610\ kg/m^2 \cdot s$ ($4.5 \times 10^5\ lb_m/h \cdot ft^2$)	negligible effect

[a] G — Mass flux
TBM — Turbine meter
GAM 3 — Three-beam densitometer
DD — Drag disk
GAM — Single-beam densitometer

References

1. J. Teague, II, *AMICON — A Multi-Model Interpretive Code for 2ϕ Flow Instrumentation with Uncertainty Analysis*, K/CSD/TM-38 (August 1981).

2. K. G. Turnage et al., *Advanced Two-Phase Flow Instrumentation Program Quarterly Progress Report for April–June 1978*, ORNL/NUREG/TM-279 (January 1979).

3. P. S. Kamath and R. T. Lahey, *A Turbine Meter Evaluation Model for Two-Phase Transients*, NES-459, Rensselaer Polytechnic Institute (October 1977).

4. *Continuous System Modeling Program III (CSMP III) Program Ref- ce Manual*, SH19-7001-3, IBM (December 1975).

5. S. Rouhani, Application of the Turbine Type Flow Meters in the Measurement of Steam Quality and Void, presented at the Symposium on In-Core Instrumentation, Oslo, June 15, 1964.

Nomenclature

A_{xs}	effective annular flow area through the blading
C	chord length of the blade
C_ℓ, C_v	correlation coefficients for the liquid (ℓ) and vapor (v) phases, respectively
G	mass flux
L_{jb}	length of the journal bearing
r	radius measured from conduit axis
R	effective radius of the rotor
R_b	radius of the meter shroud
R_o	conduit radius
R_{R_1}	bearing radius
R_s	journal radius
R_T	blade tip radius
S	slip ratio
t	time
t_b	blade thickness
V_{cl_k}	centerline velocity of phase k
V_k	velocity of phase k
V_t	turbine axial velocity
$V_{z\ell}$	velocity of the liquid in the axial direction
α	void fraction
α_{cl}	void fraction at centerline
β	blade angle
η_ℓ, η_v	flow deviation factor for the liquid (ℓ) and vapor (v) phases, respectively

μ	dynamic viscosity of saturated liquid
ρ_ℓ, ρ_v	density of saturated liquid (ℓ) and vapor (v), respectively
ω	angular velocity of the rotor

Appendix C

ROD POWERS

Calculated rod power versus time is shown in Figs. C.1–C.60 for each of the electrically heated rods. Rods 19, 22, 36, and 46 were unheated. Section D.6 of Appendix D is a discussion of rod power uncertainty. As shown there, one standard deviation in power is 0.55% of reading.

ORNL-DWG 92-4983 ETD

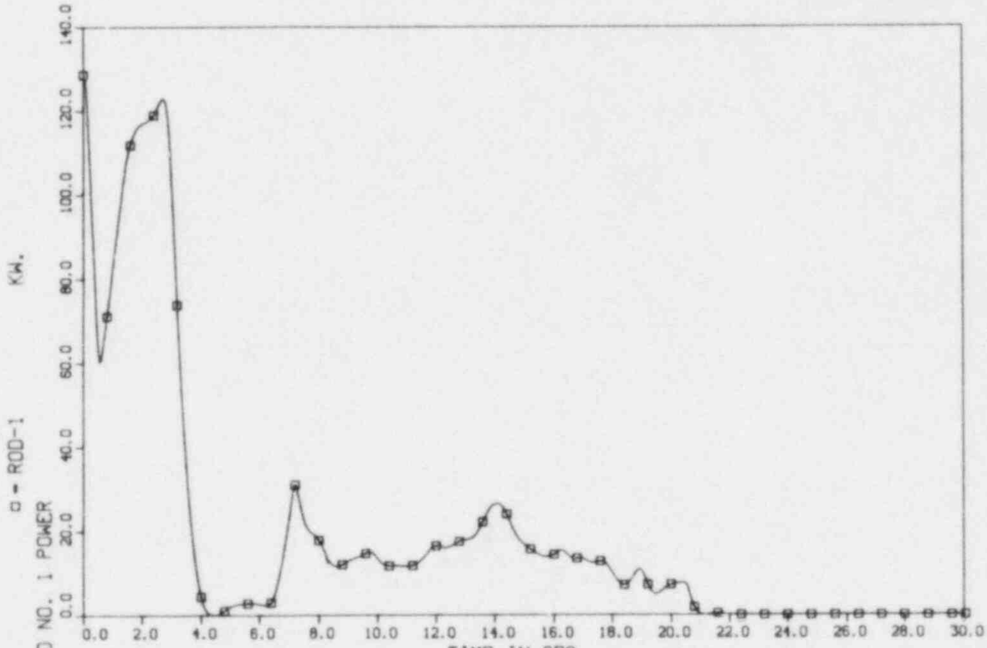

Fig. C.1. Rod power vs time for rod 1.

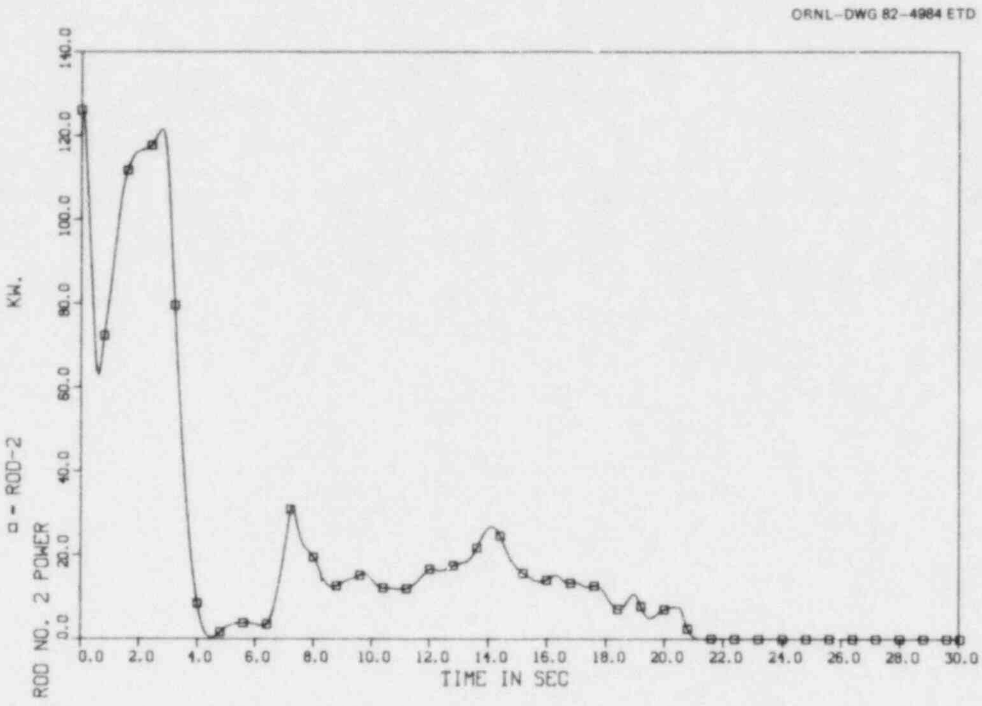

Fig. C.2. Rod power vs time for rod 2.

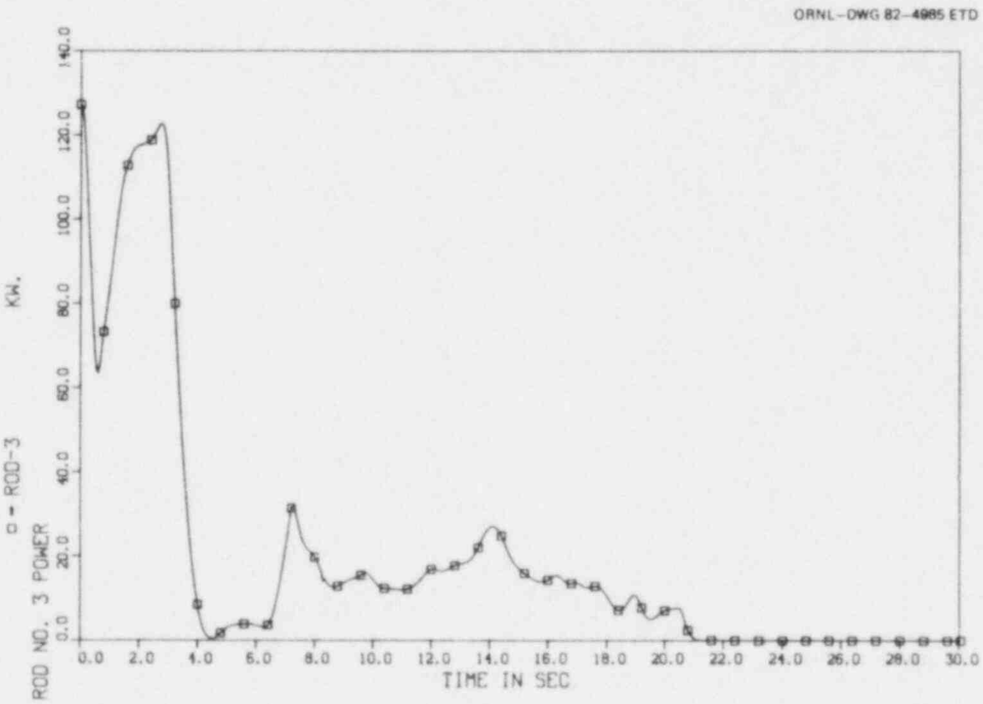

Fig. C.3. Rod power vs time for rod 3.

ORNL–DWG 82–4986 ETD

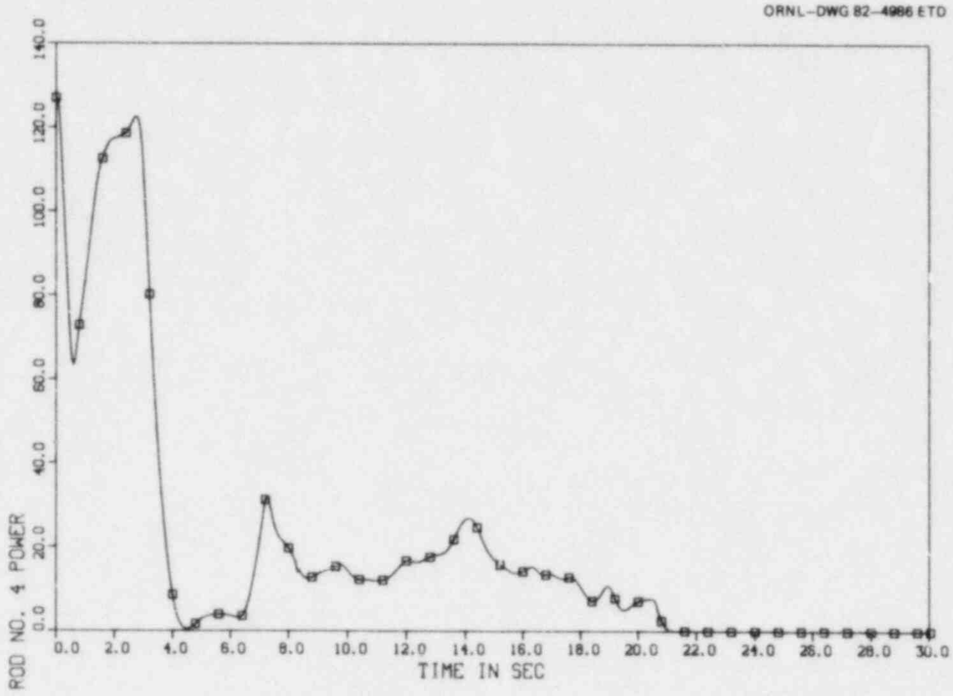

Fig. C.4. Rod power vs time for rod 4.

ORNL–DWG 82–4987 ETD

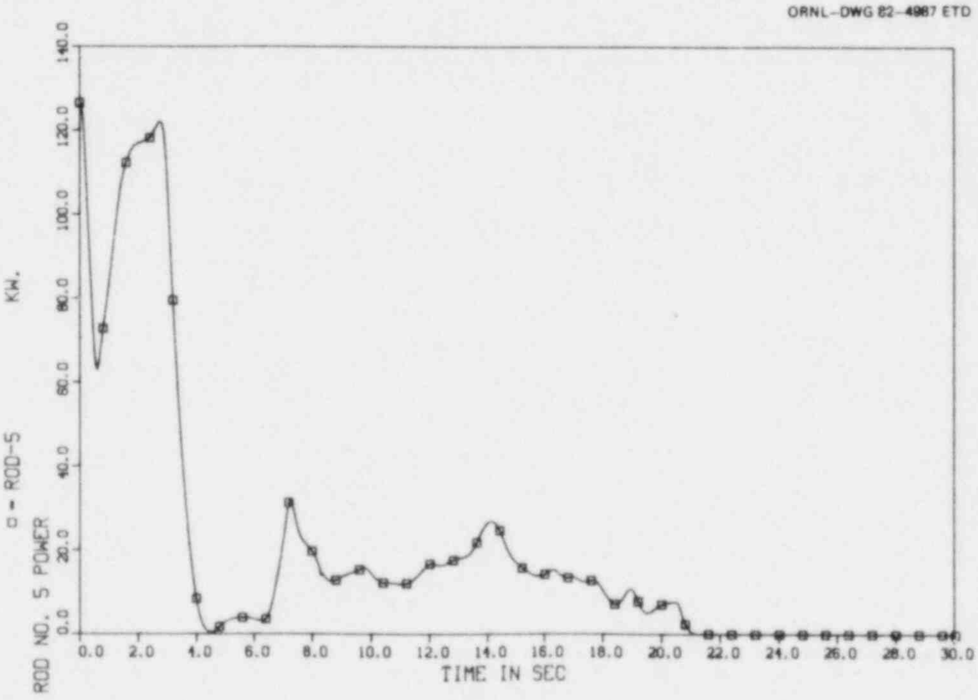

Fig. C.5. Rod power vs time for rod 5.

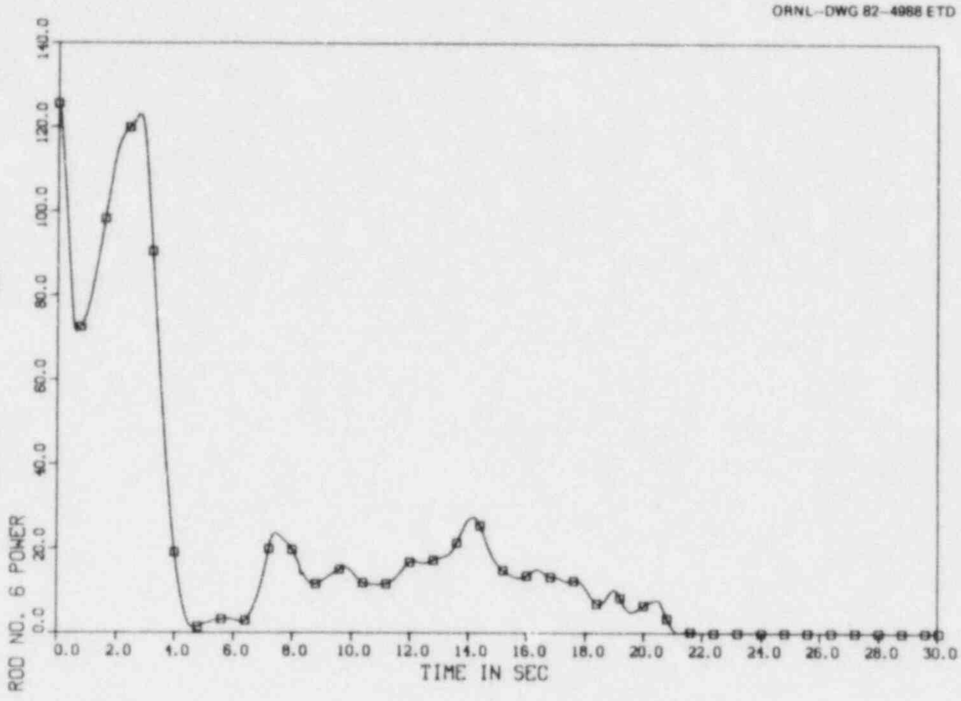

Fig. C.6. Rod power vs time for rod 6.

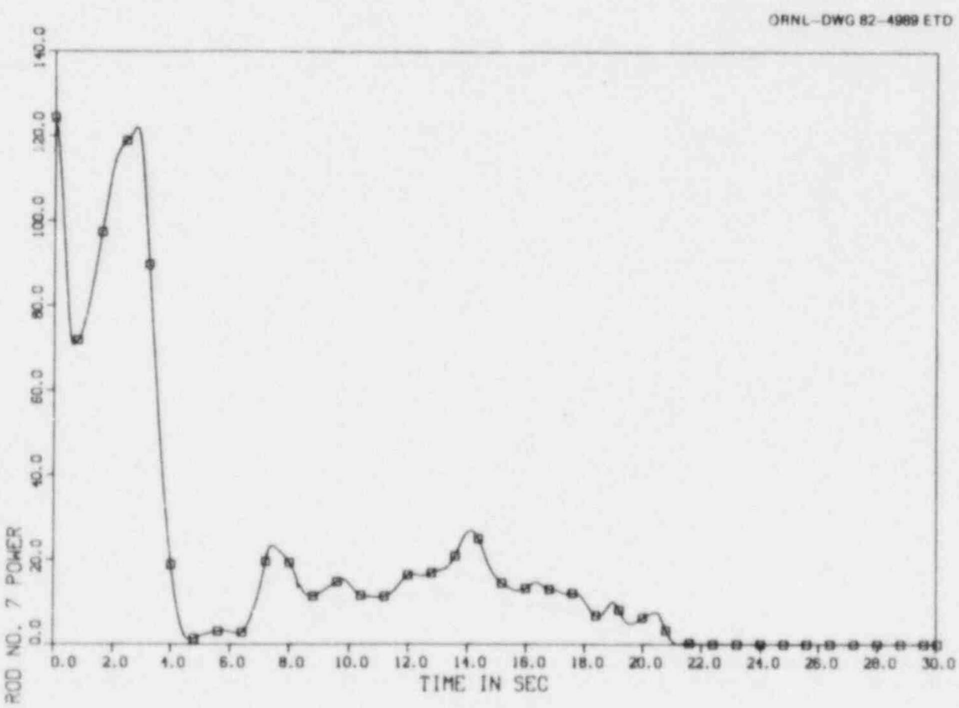

Fig. C.7. Rod power vs time for rod 7.

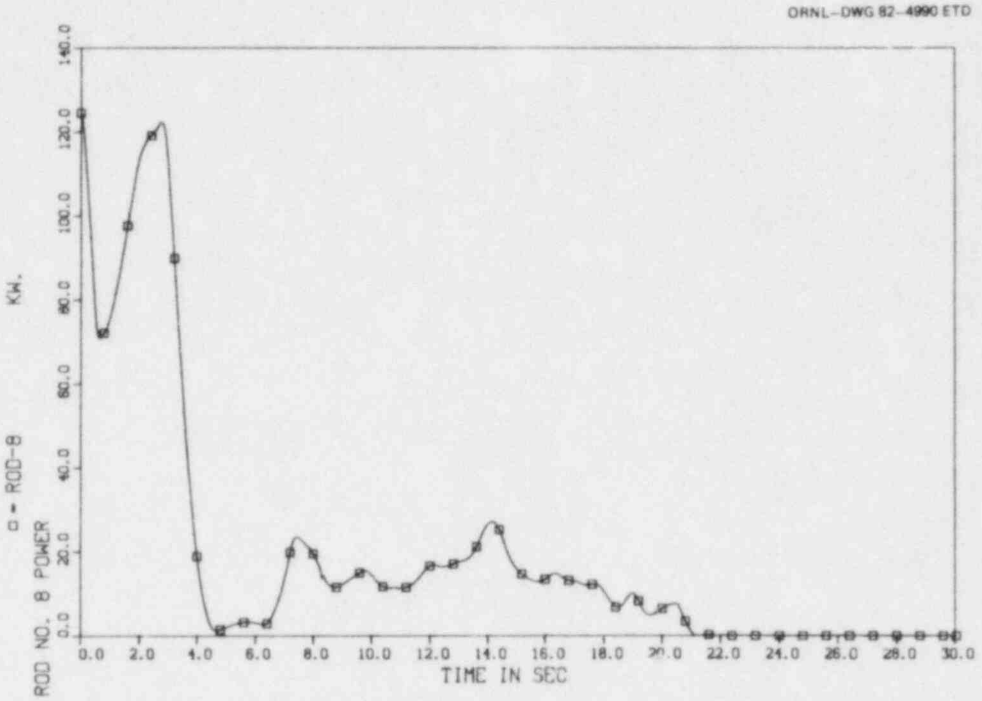

Fig. C.8. Rod power vs time for rod 8.

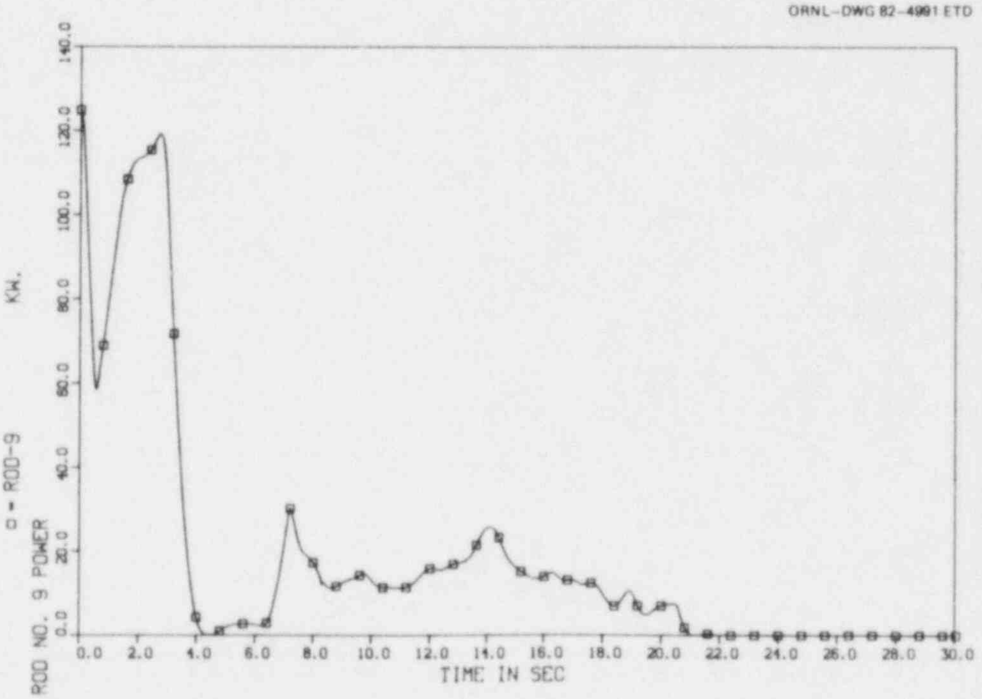

Fig. C.9. Rod power vs time for rod 9.

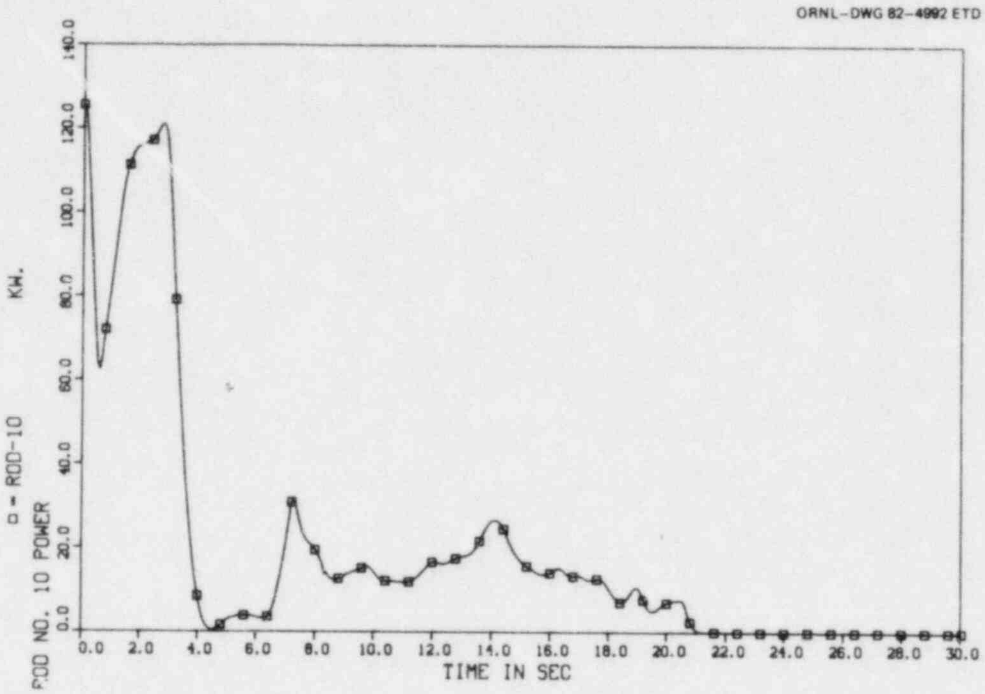

Fig. C.10. Rod power vs time for rod 10.

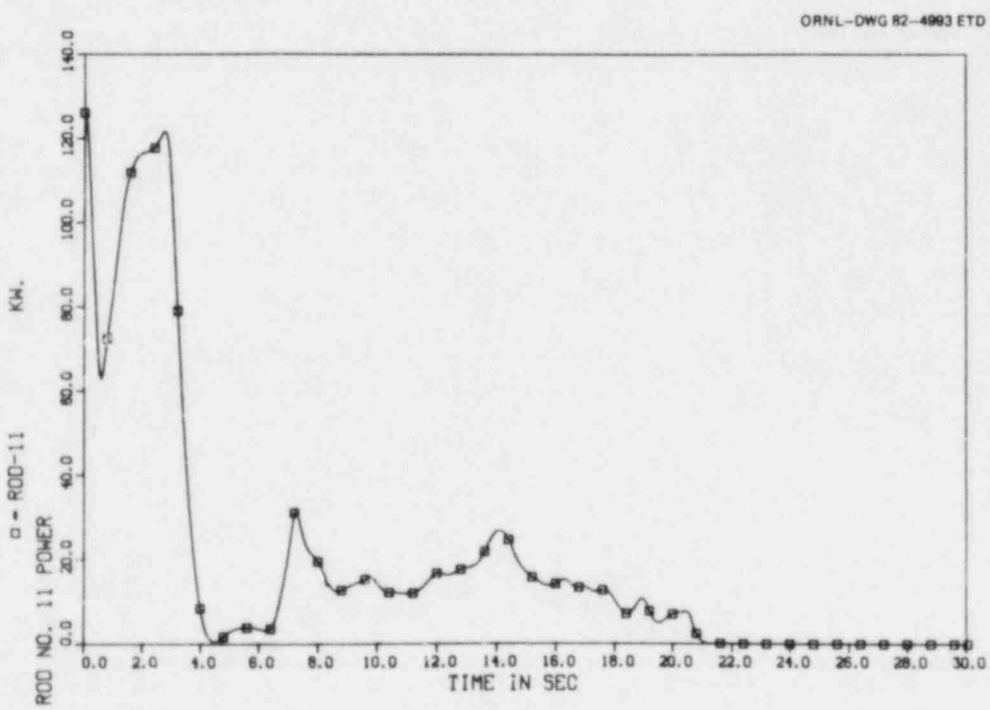

Fig. C.11. Rod power vs time for rod 11.

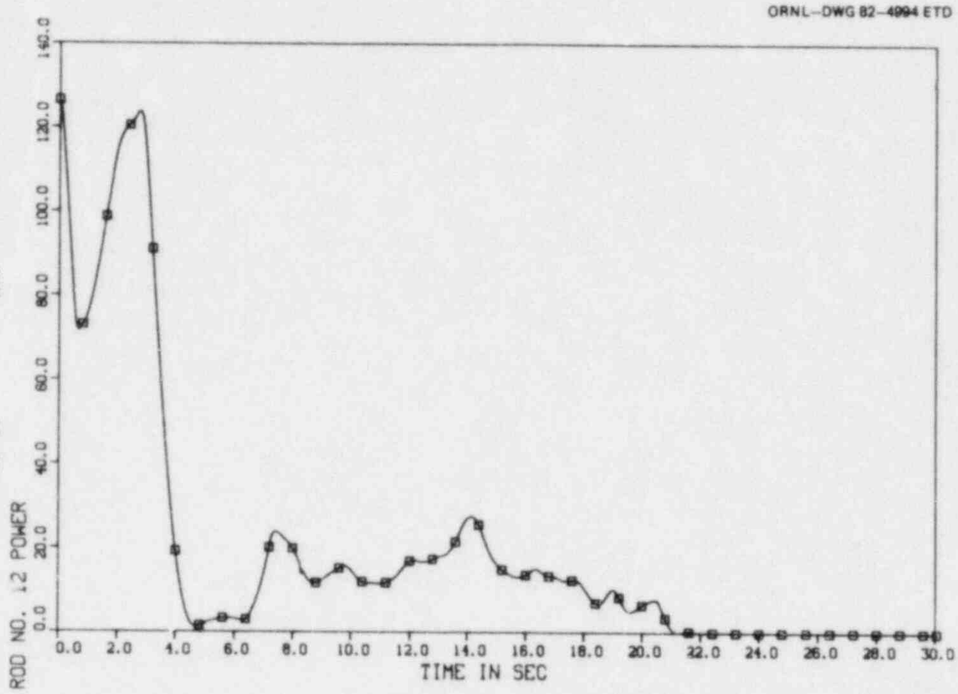

Fig. C.12. Rod power vs time for rod 12.

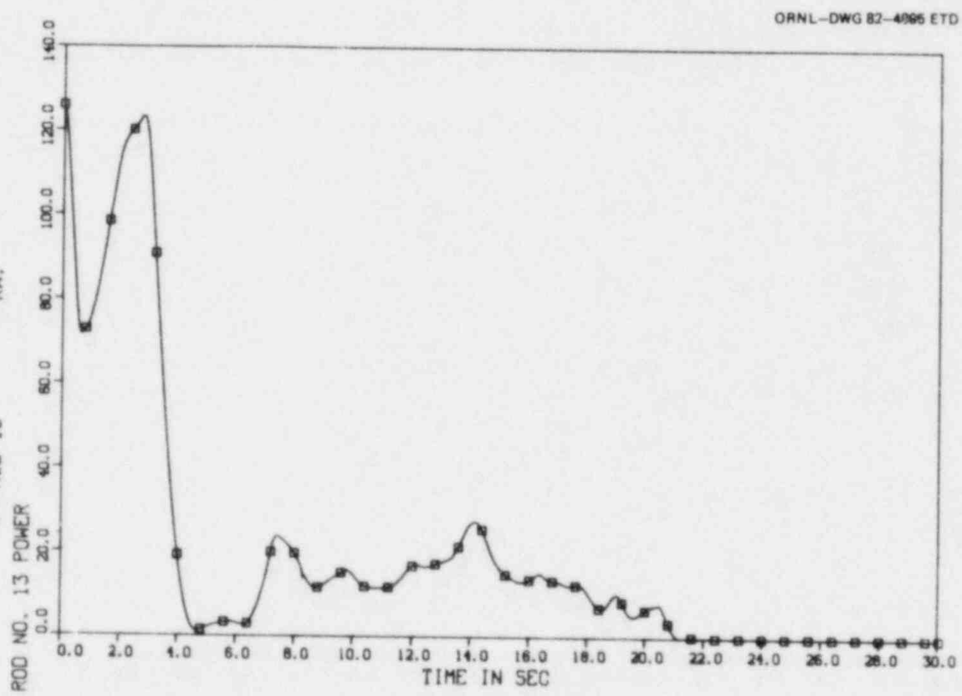

Fig. C.13. Rod power vs time for rod 13.

ORNL-DWG 82-4996 ETD

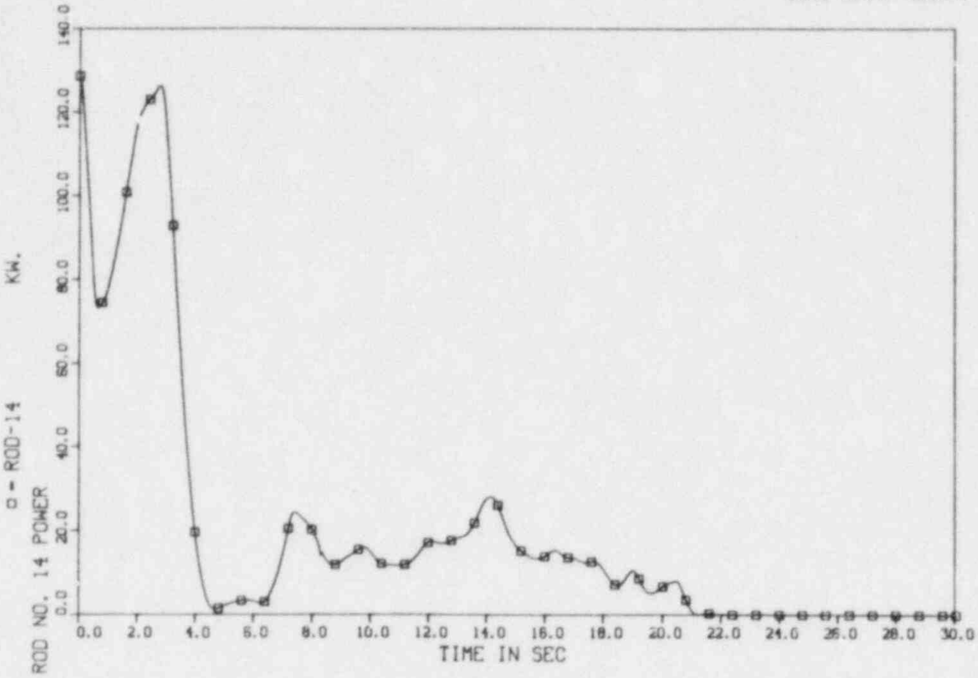

Fig. C.14. Rod power vs time for rod 14.

ORNL-DWG 82-4997 ETD

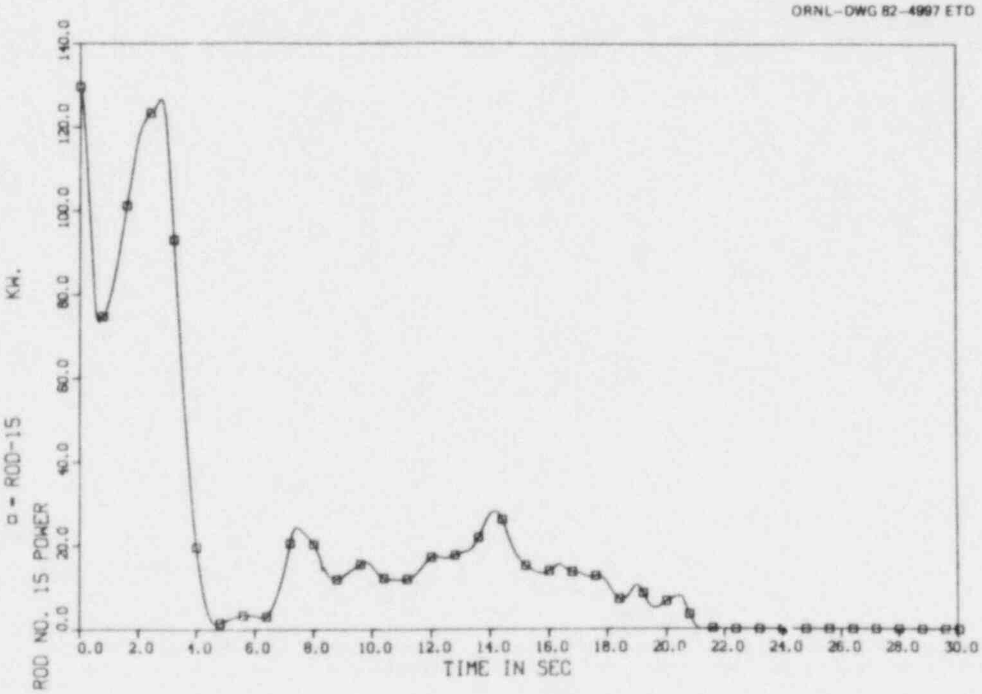

Fig. C.15. Rod power vs time for rod 15.

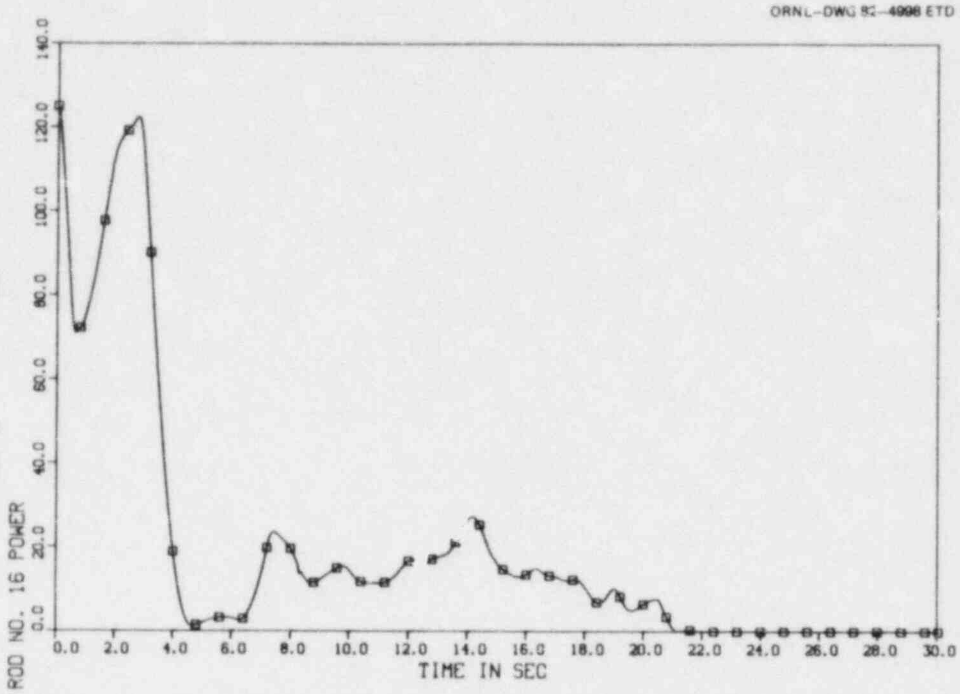

Fig. C.16. Rod power vs time for rod 16.

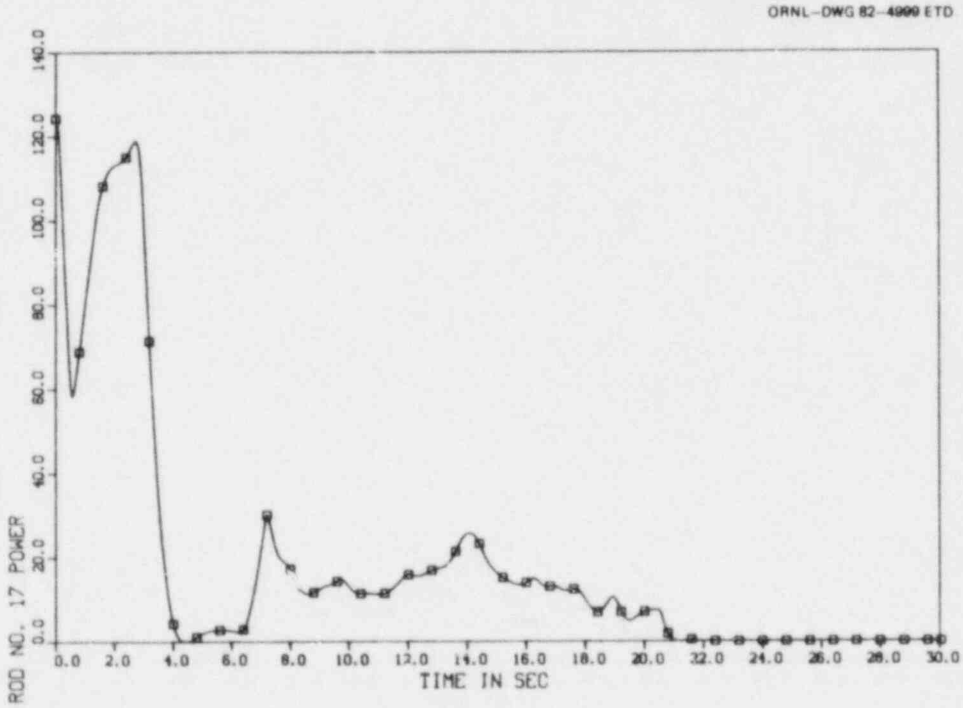

Fig. C.17. Rod power vs time for rod 17.

ORNL-DWG 82-5000 ETD

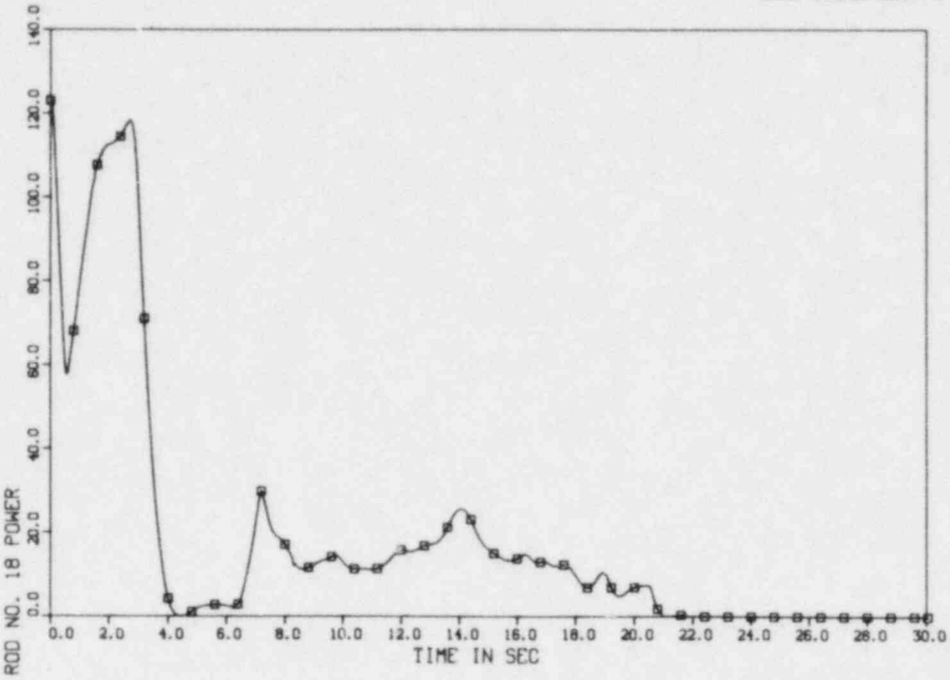

Fig. C.18. Rod power vs time for rod 18.

ORNL-DWG 82-5001 ETD

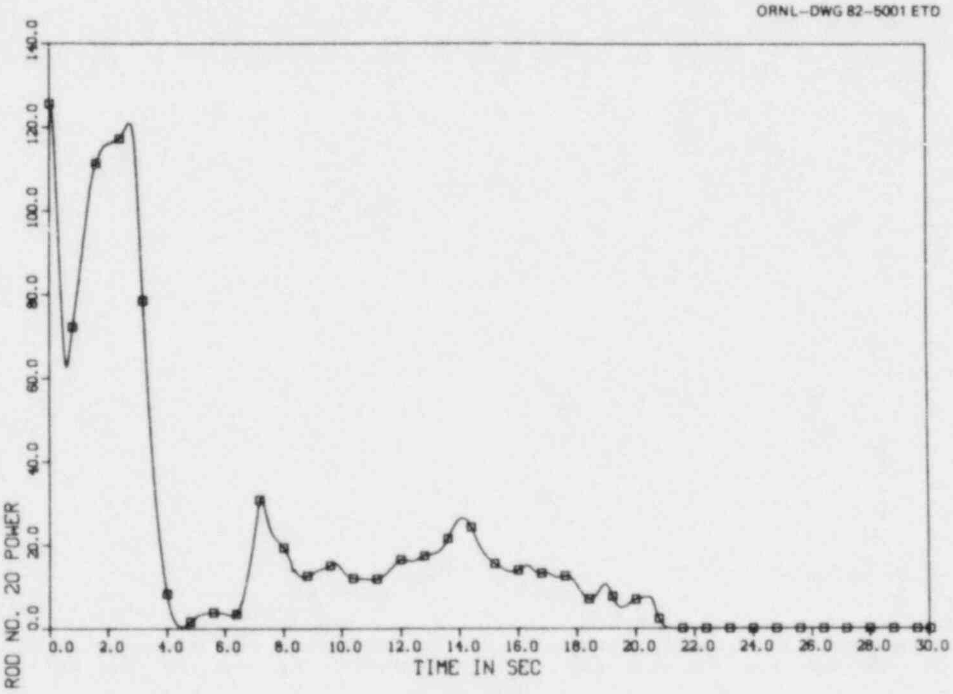

Fig. C.19. Rod power vs time for rod 20.

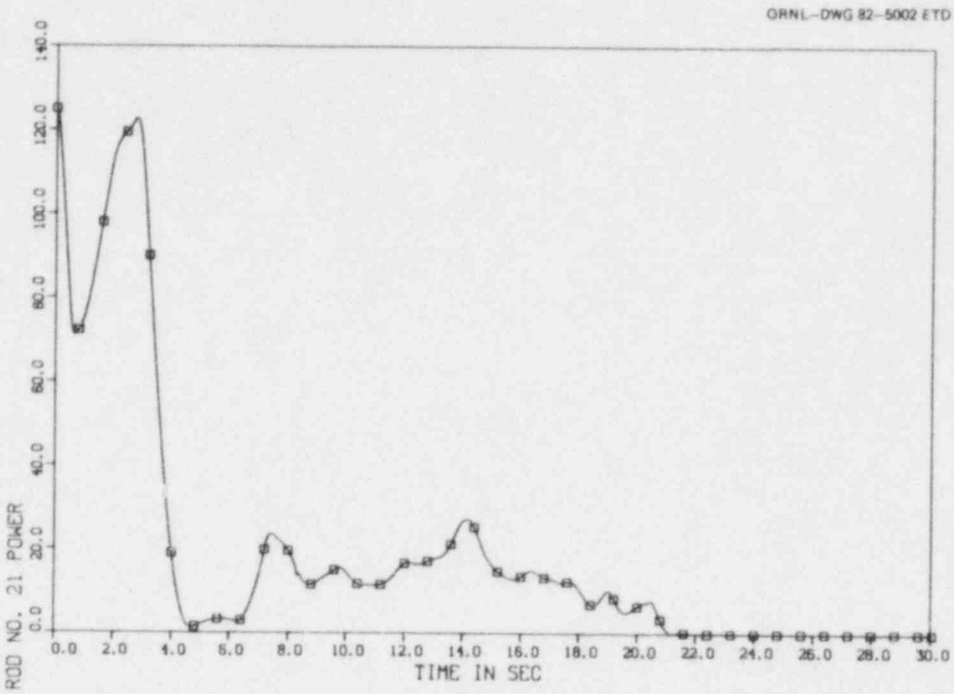

Fig. C.20. Rod power vs time for rod 21.

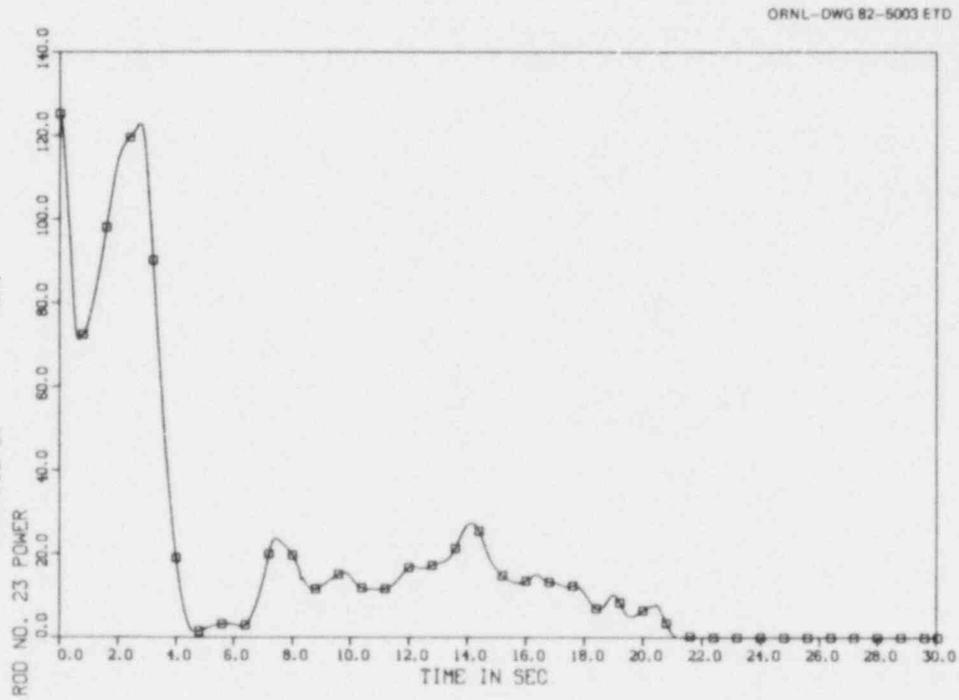

Fig. C.21. Rod power vs time for rod 23.

ORNL-DWG 82-5004 ETD

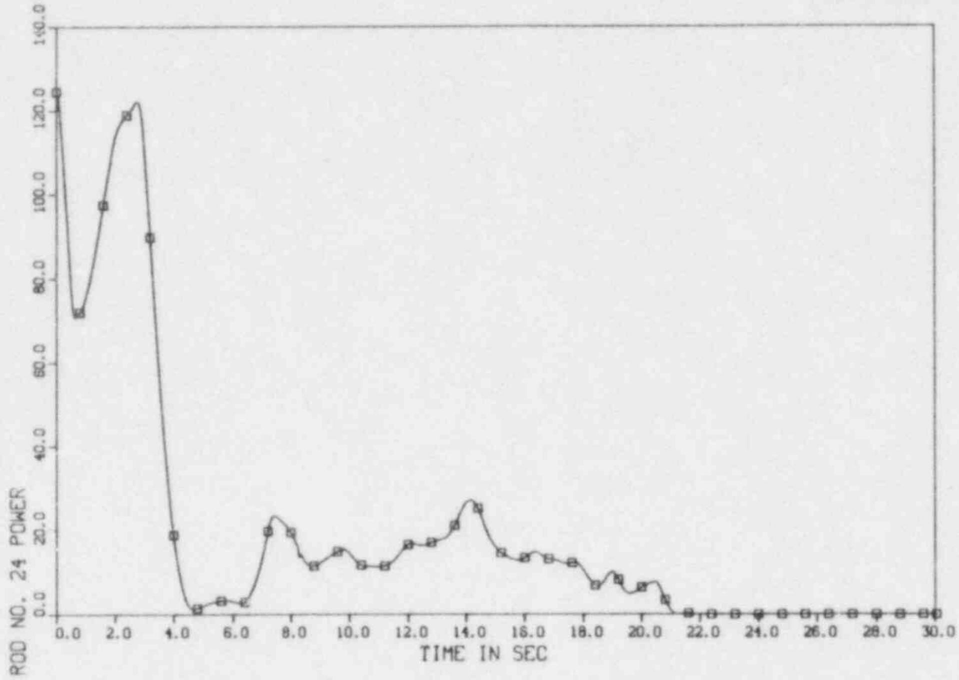

Fig. C.22. Rod power vs time for rod 24.

ORNL-DWG 82-5006 ETD

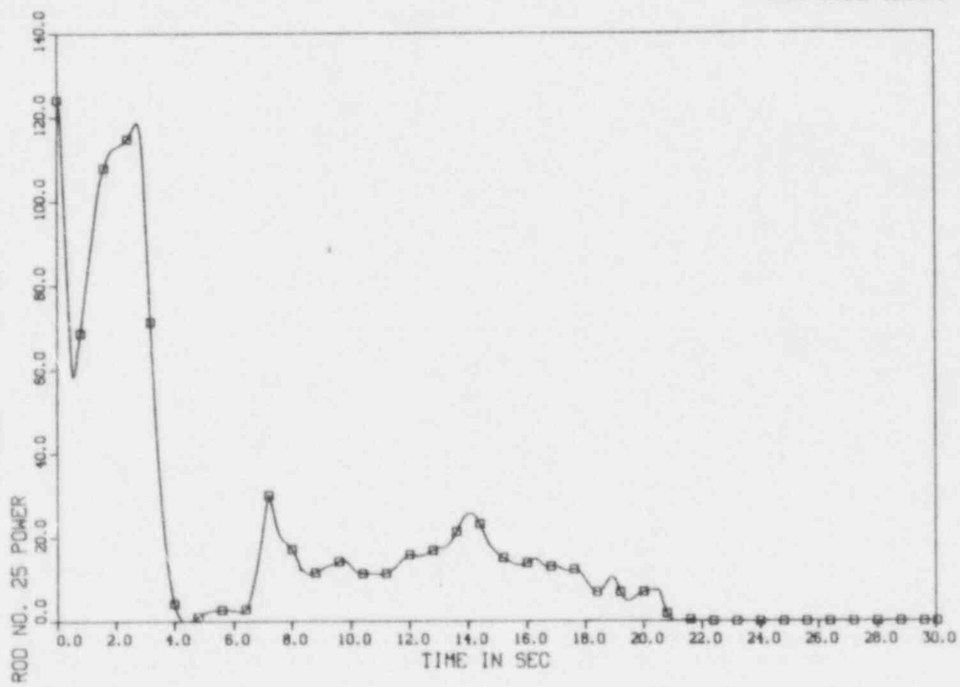

Fig. C.23. Rod power vs time for rod 25.

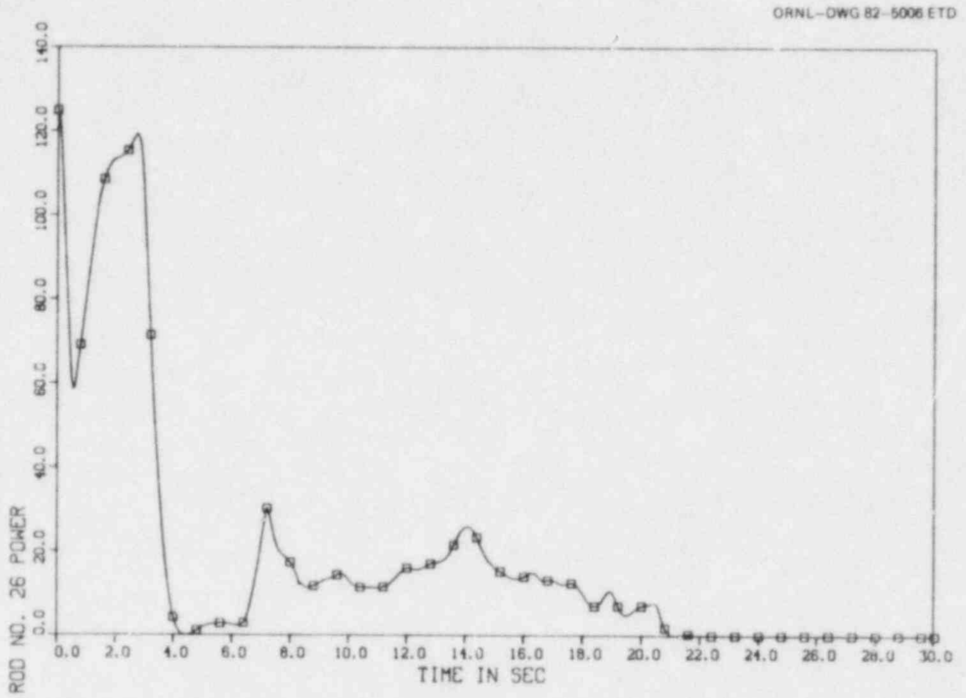

Fig. C.24. Rod power vs time for rod 26.

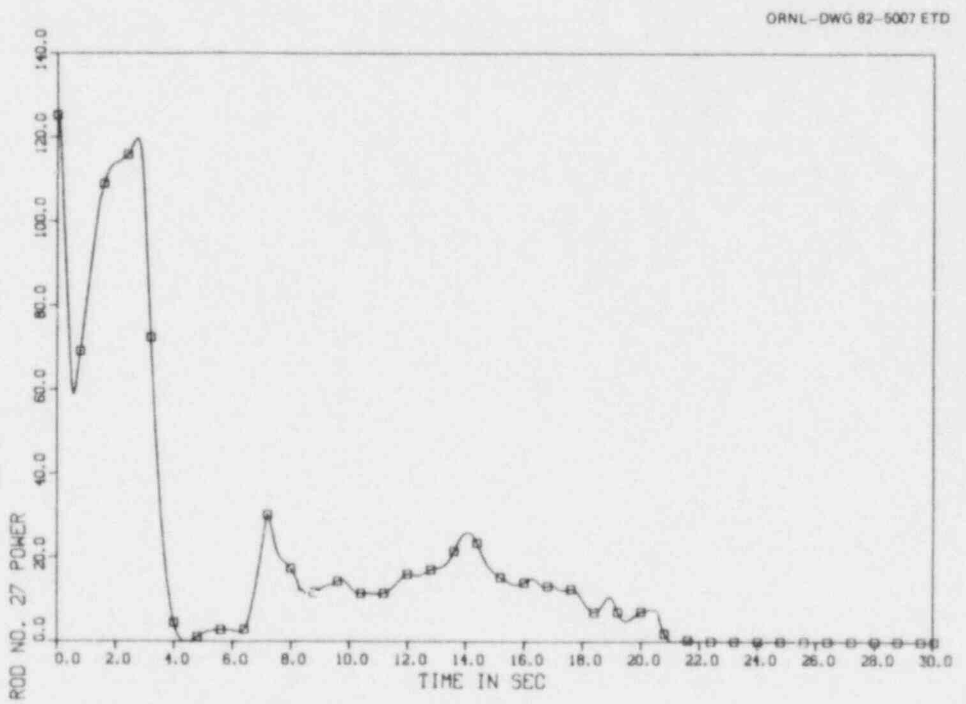

Fig. C.25. Rod power vs time for rod 27.

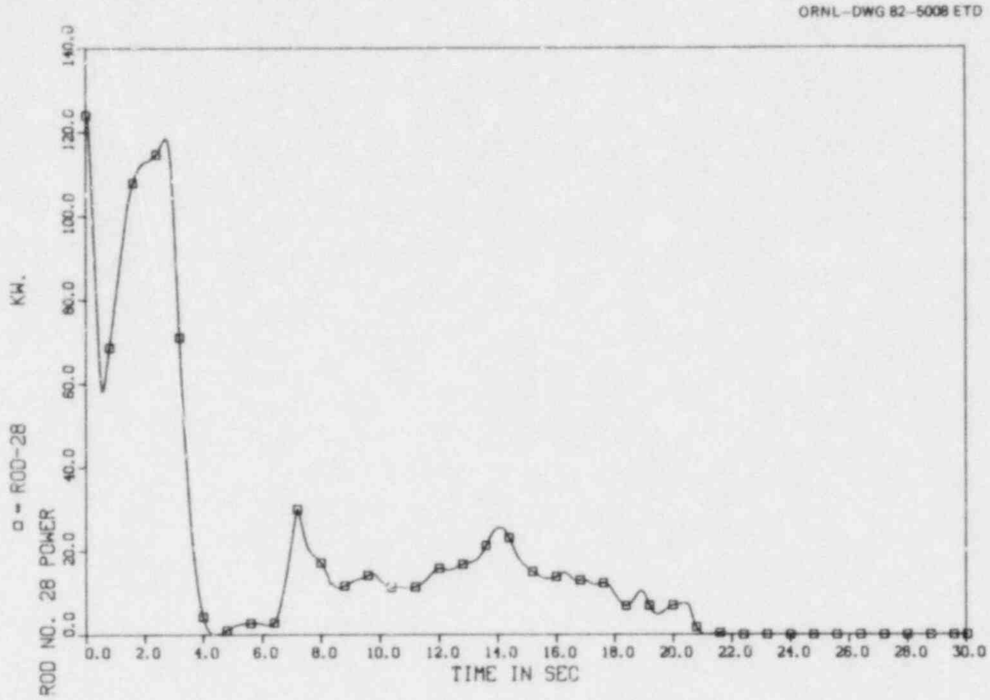

Fig. C.26. Rod power vs time for rod 28.

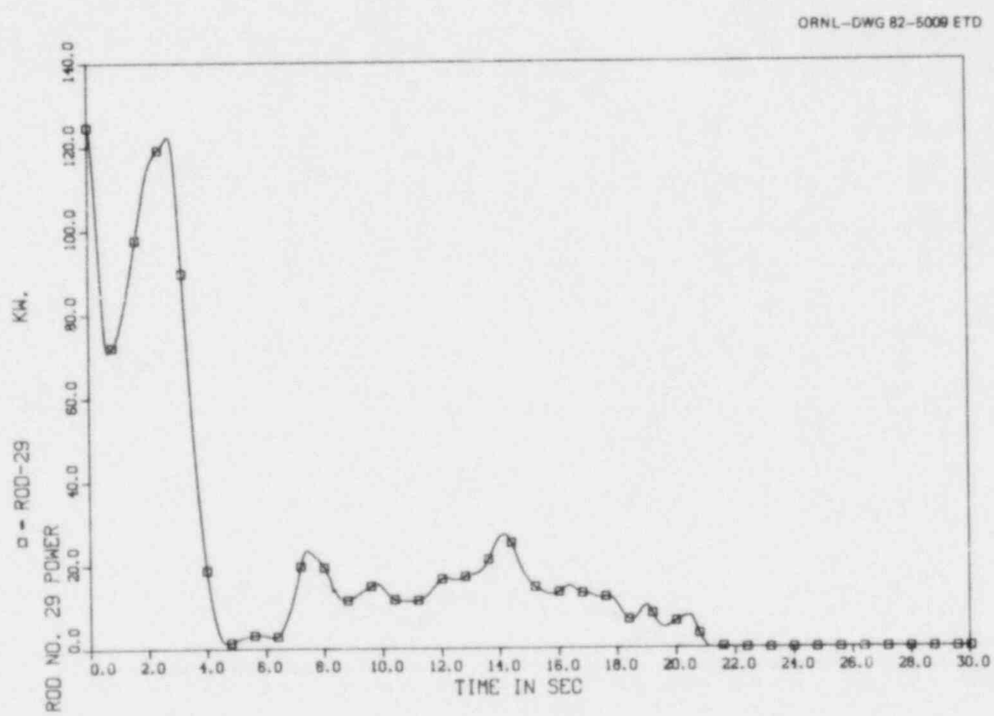

Fig. C.27. Rod power vs time for rod 29.

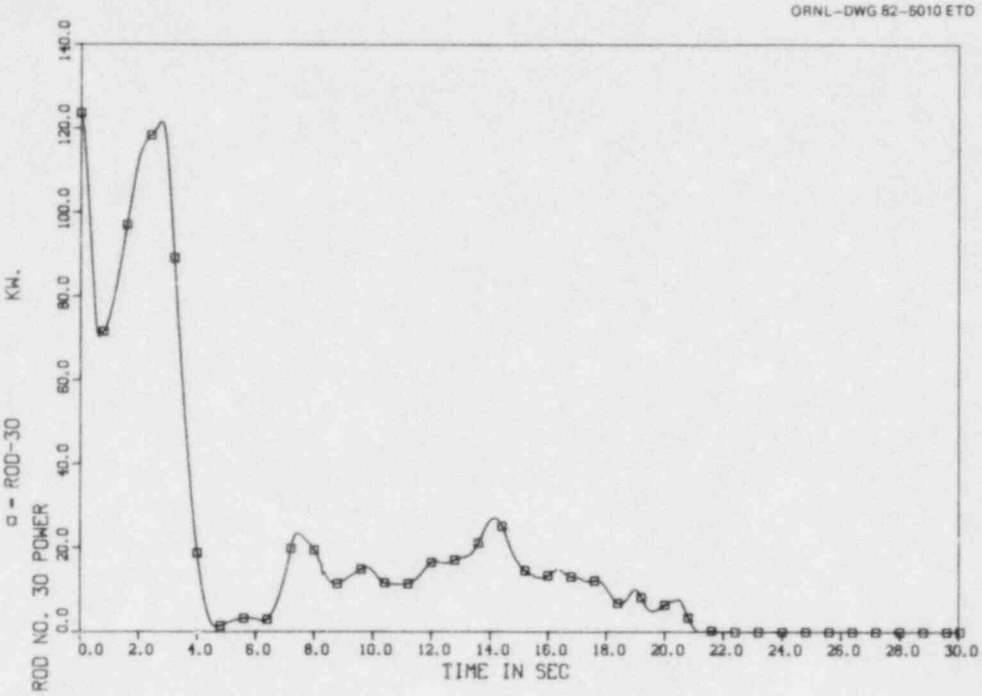

Fig. C.28. Rod power vs time for rod 30.

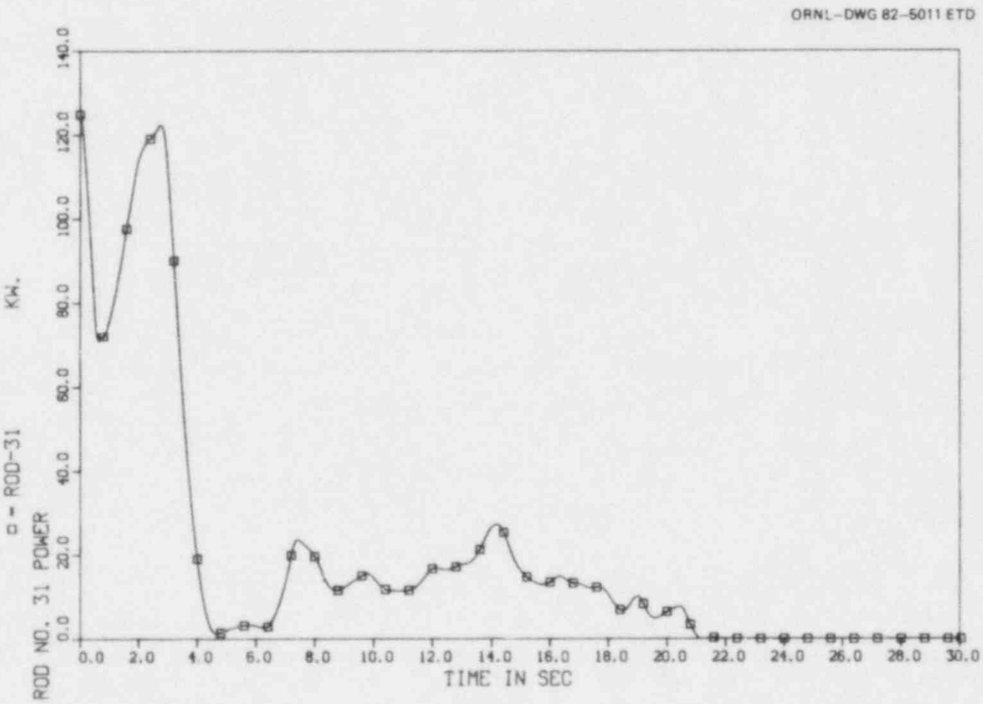

Fig. C.29. Rod power vs time for rod 31.

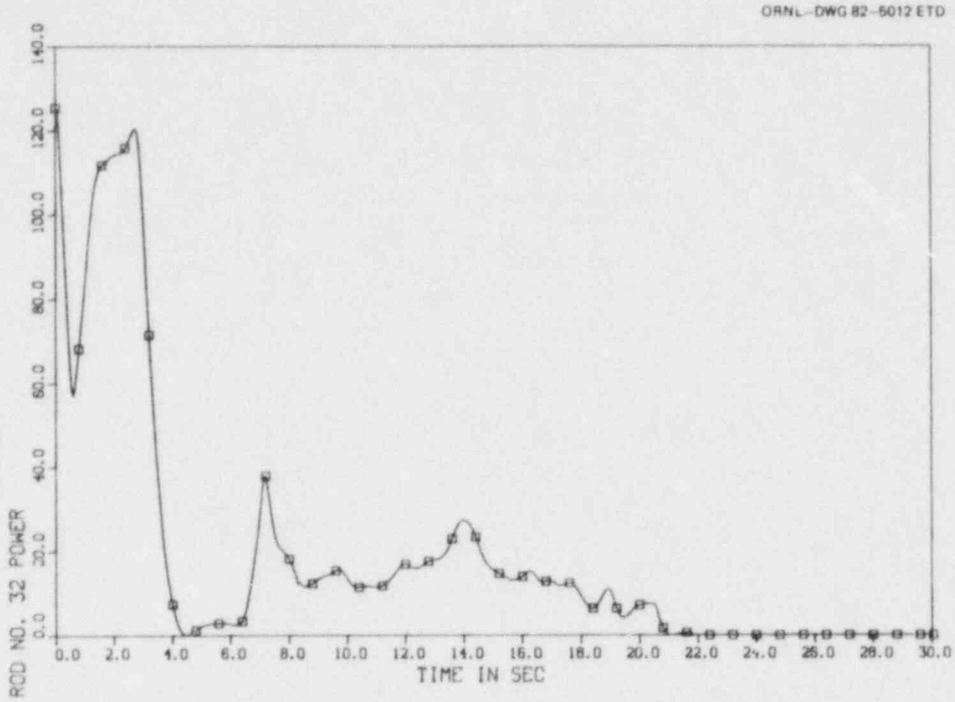

Fig. C.30. Rod power vs time for rod 32.

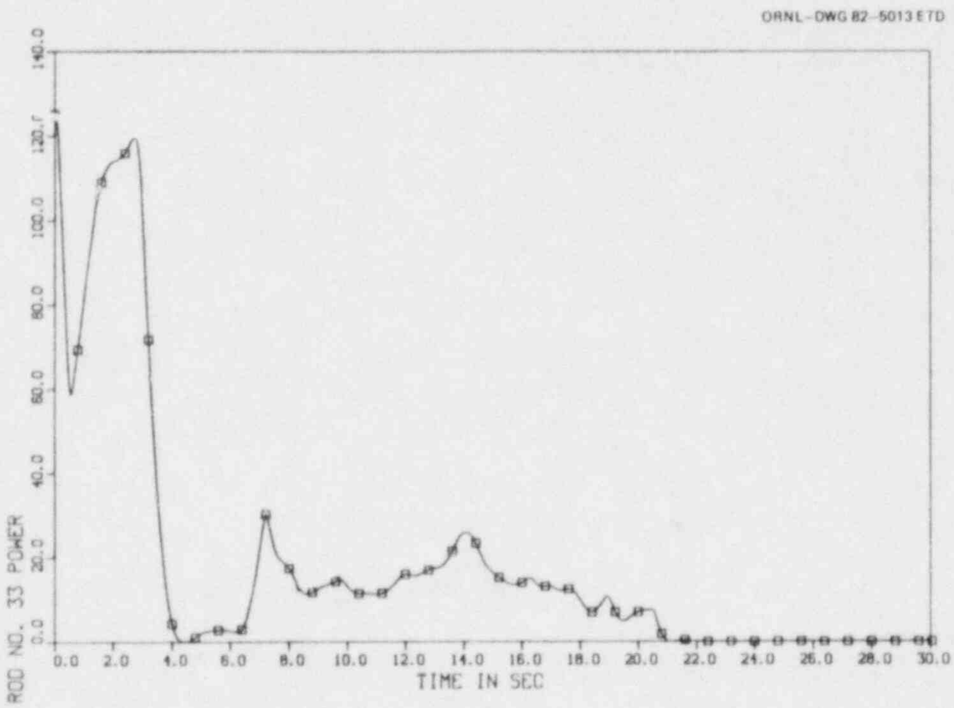

Fig. C.31. Rod power vs time for rod 33.

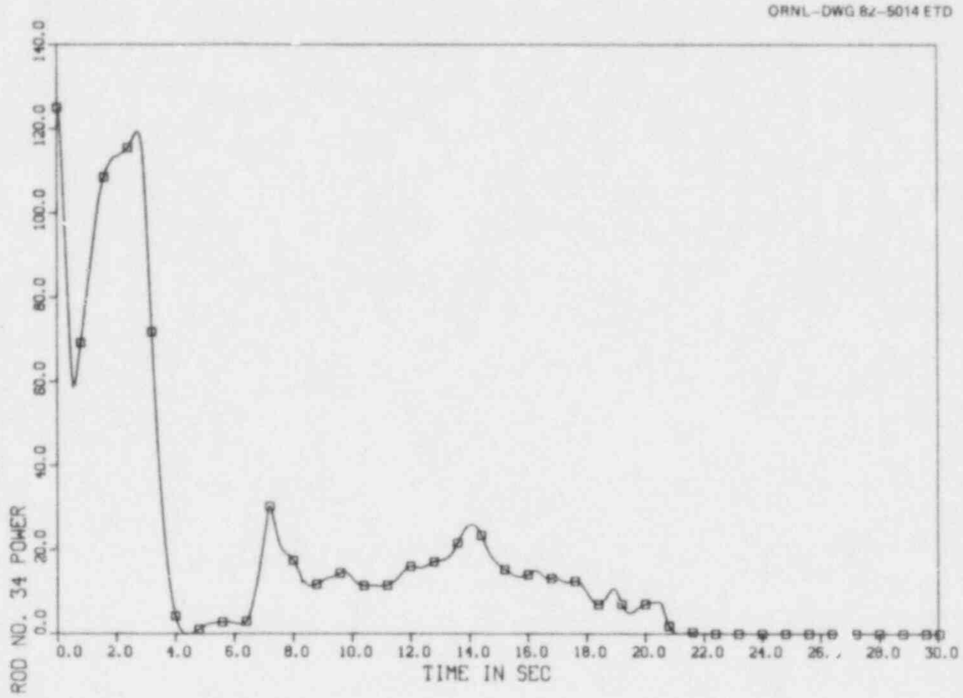

Fig. C.32. Rod power vs time for rod 34.

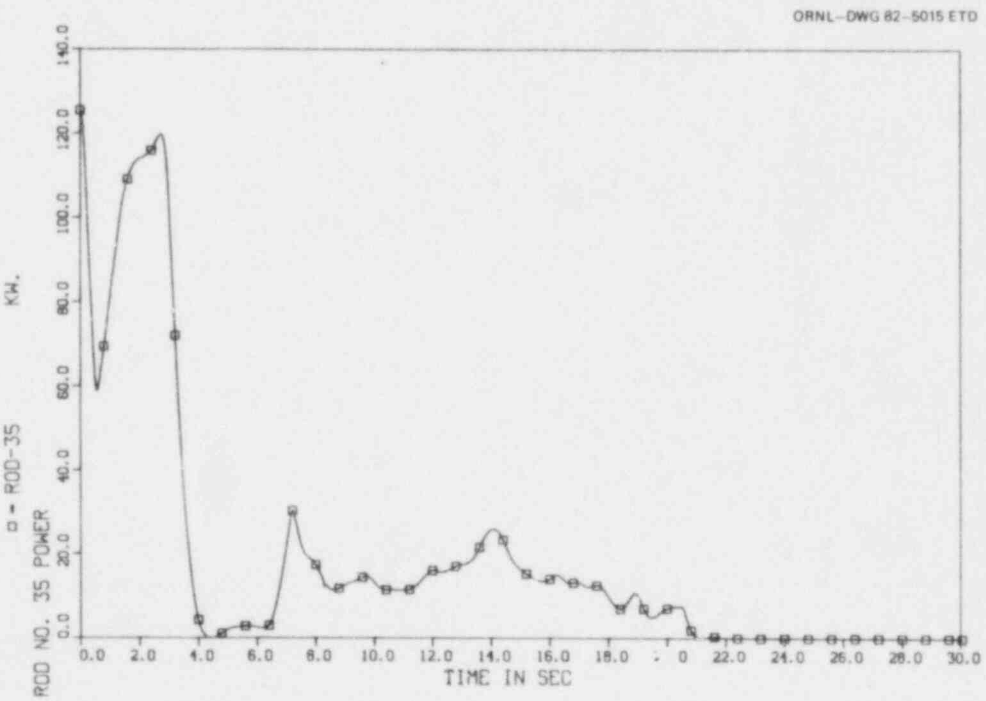

Fig. C.33. Rod power vs time for rod 35.

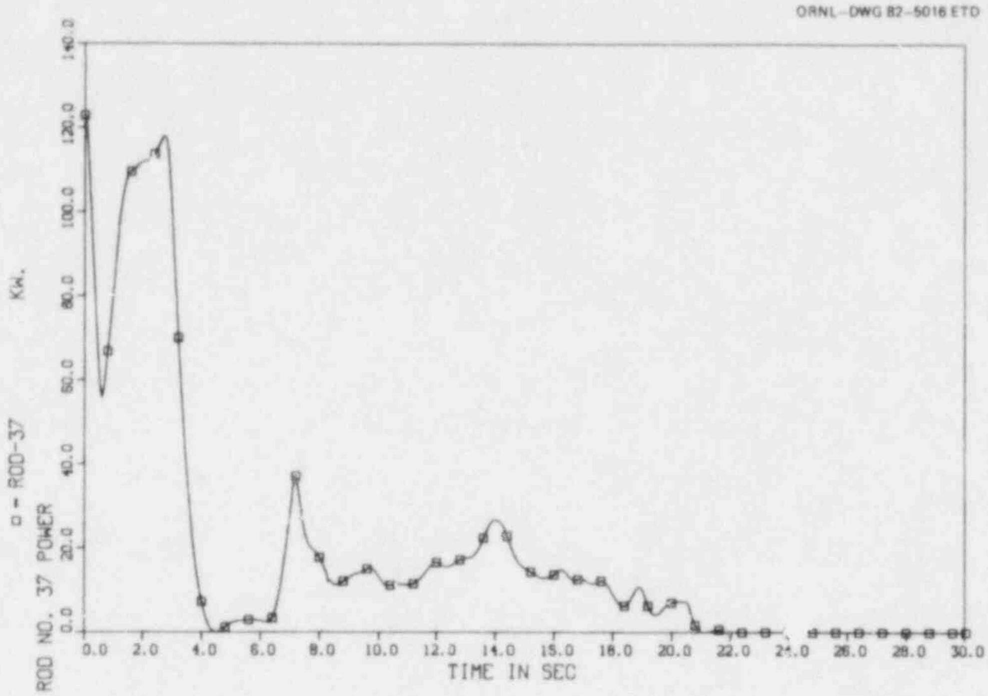

Fig. C.34. Rod power vs time for rod 37.

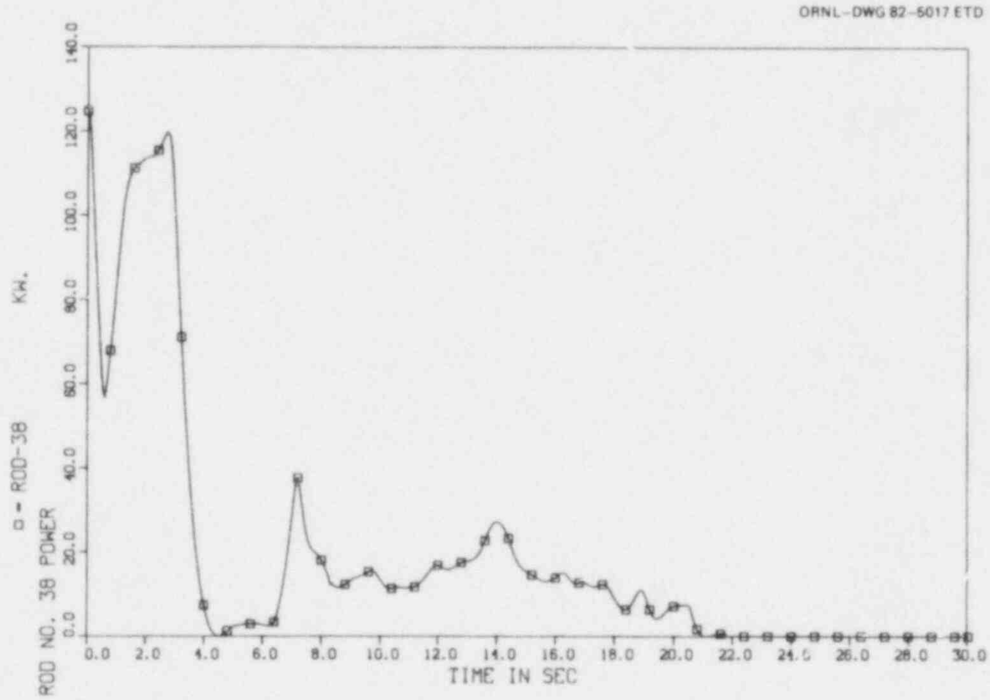

Fig. C.35. Rod power vs time for rod 38.

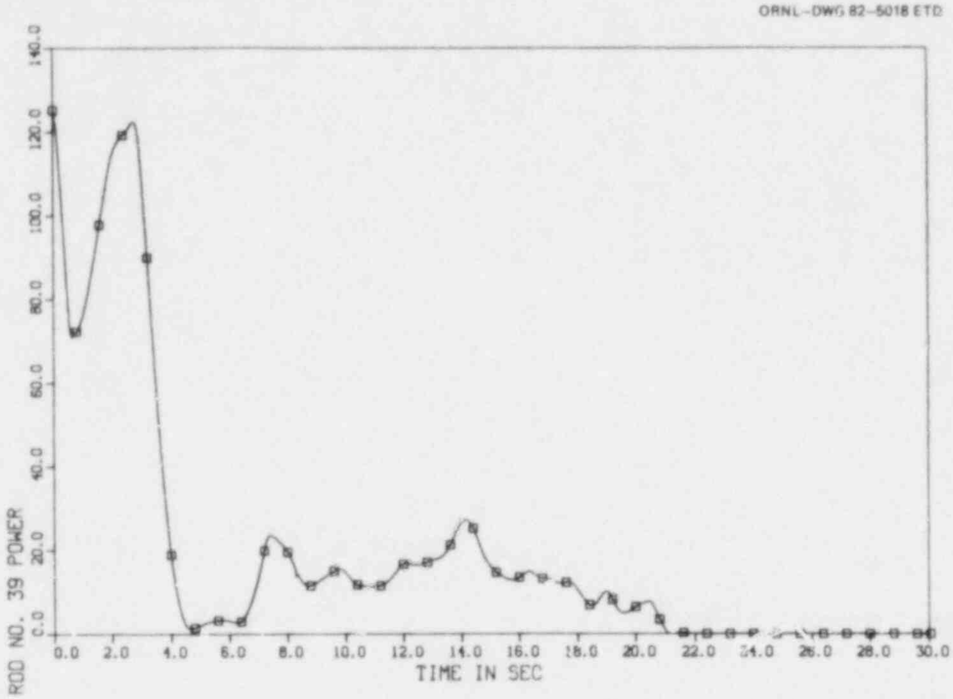

Fig. C.36. Rod power vs time for rod 39.

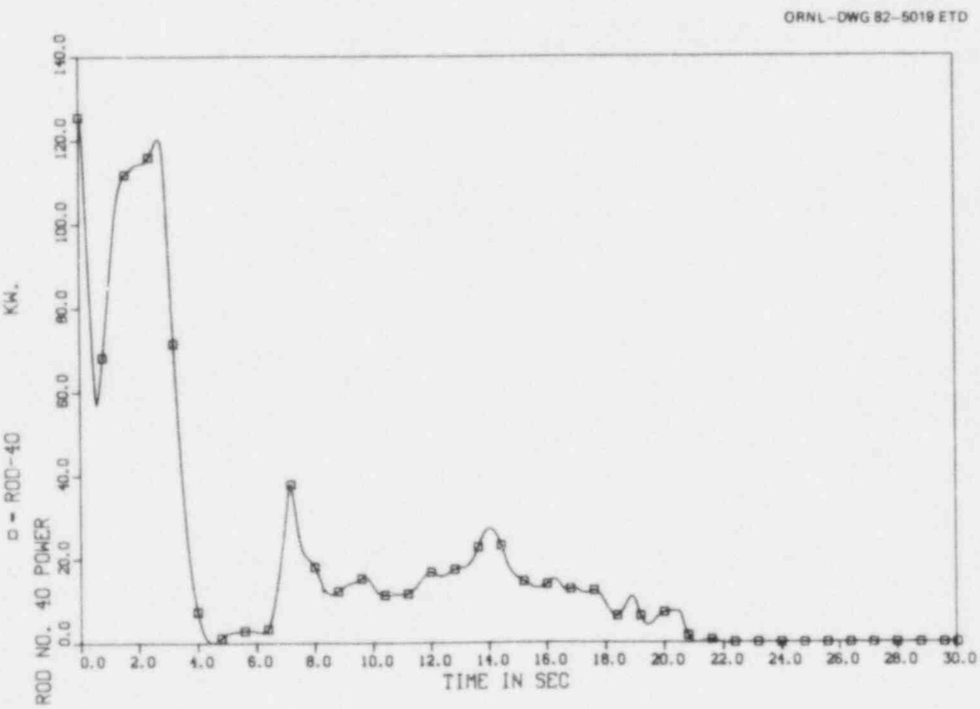

Fig. C.37. Rod power vs time for rod 40.

ORNL-DWG 82-5020 ETD

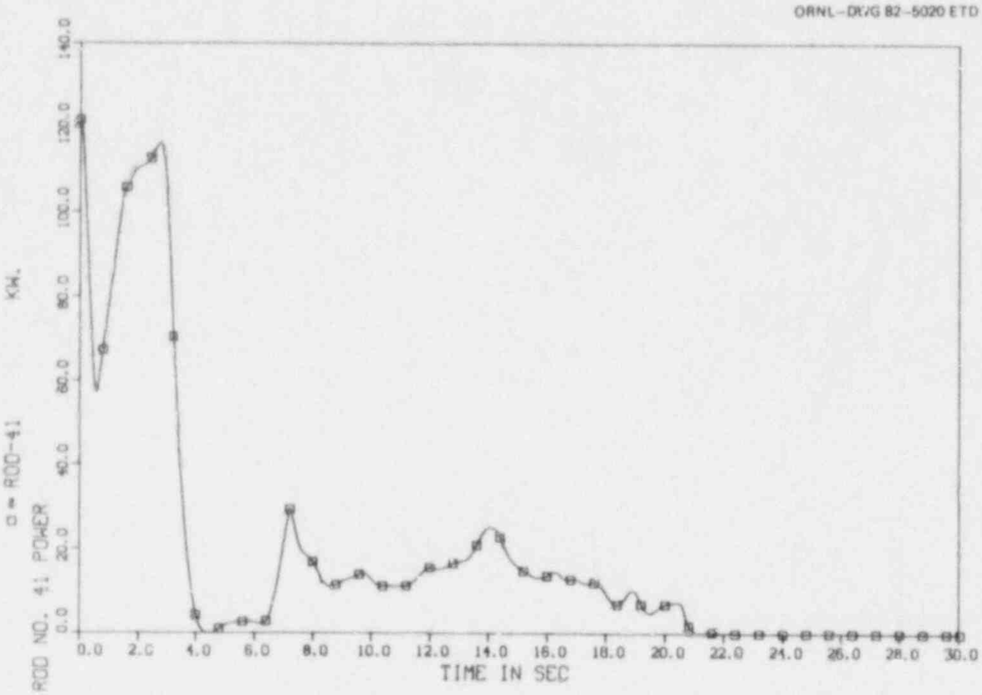

Fig. C.38. Rod power vs time for rod 41.

ORNL-DWG 82-5021 ETD

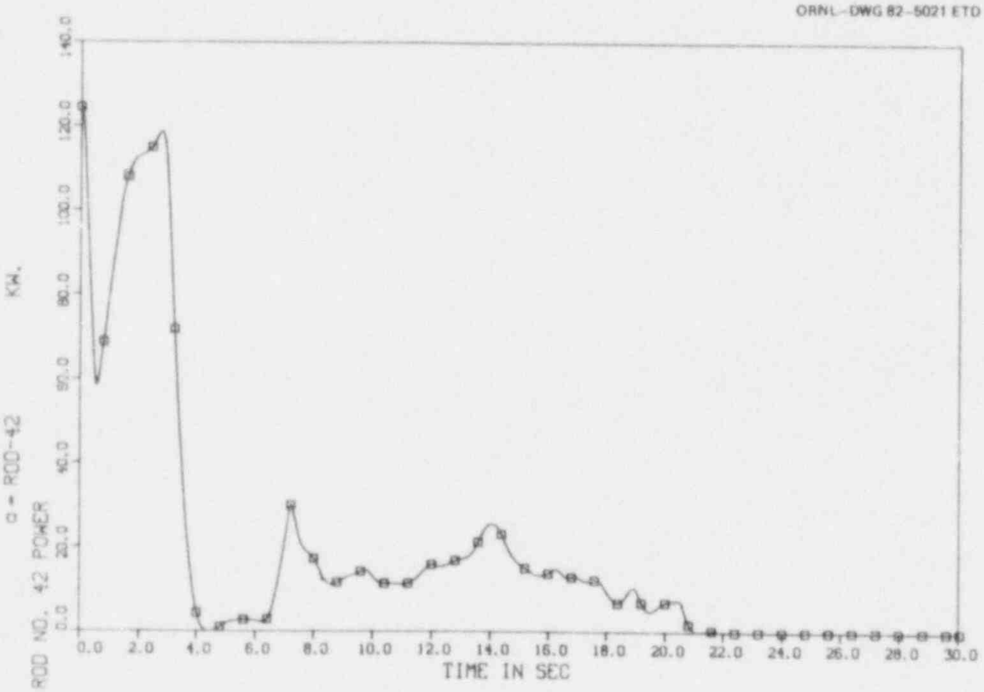

Fig. C.39. Rod power vs time for rod 42.

ORNL-DWG 82-5022 ETD

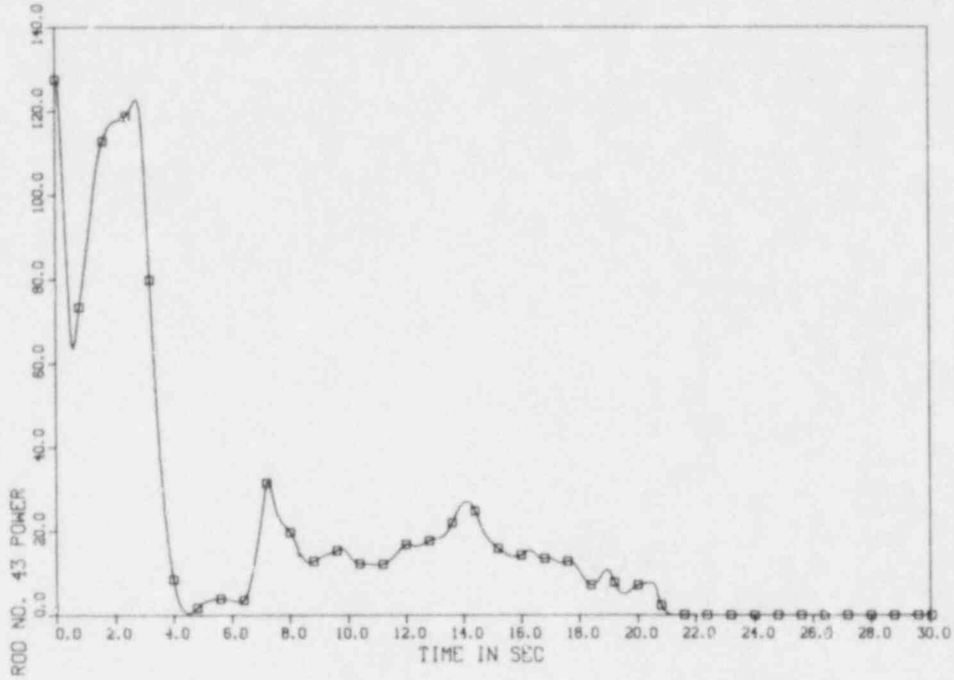

Fig. C.40. Rod power vs time for rod 43.

ORNL-DWG 82-5023 ETD

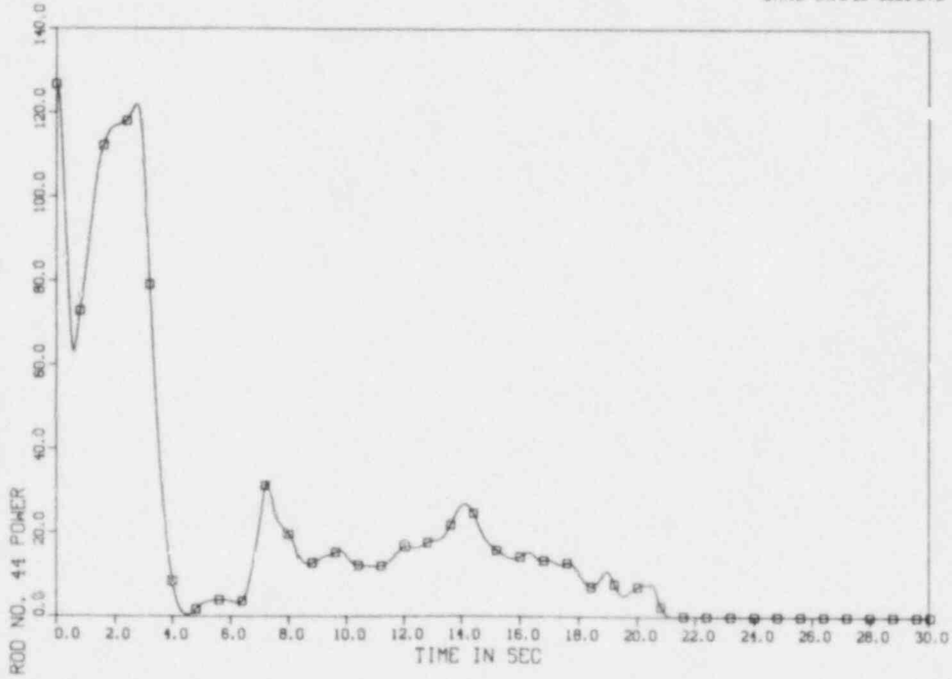

Fig. C.41. Rod power vs time for rod 44.

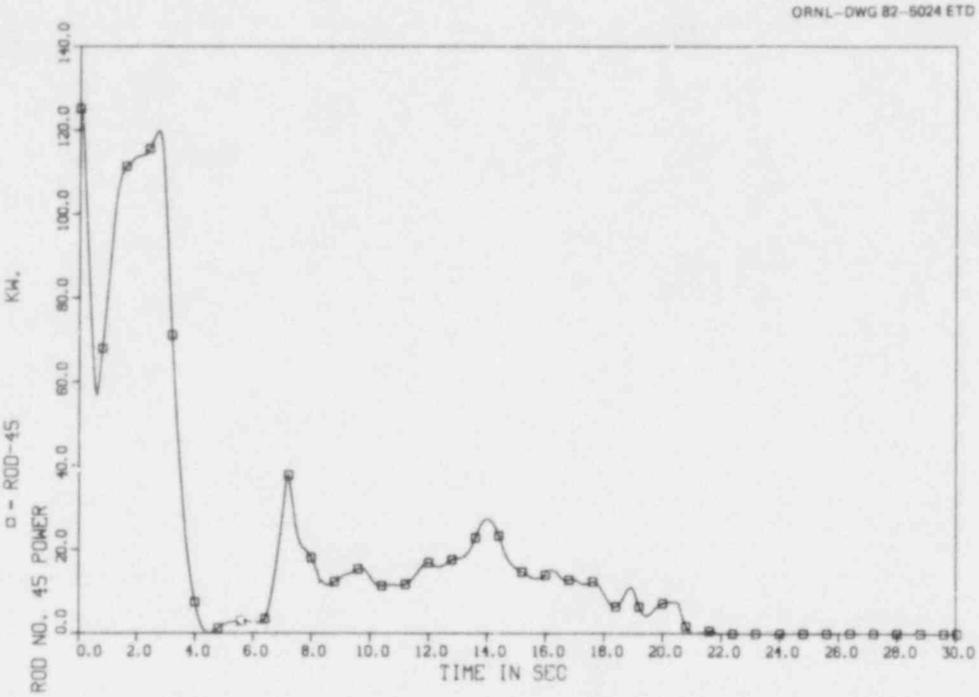

Fig. C.42. Rod power vs time for rod 45.

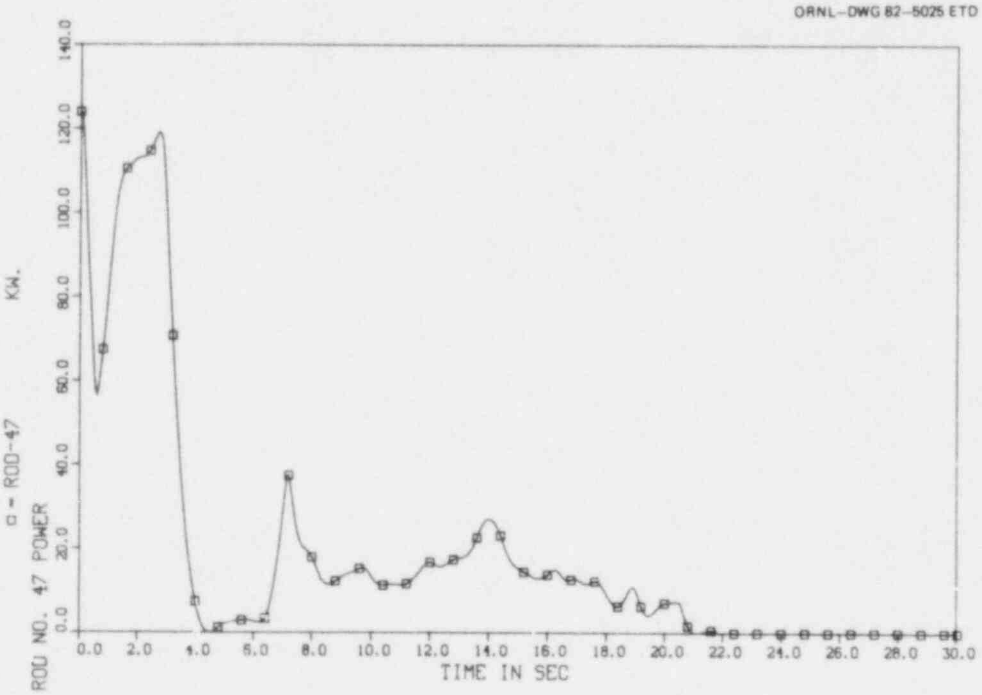

Fig. C.43. Rod power vs time for rod 47.

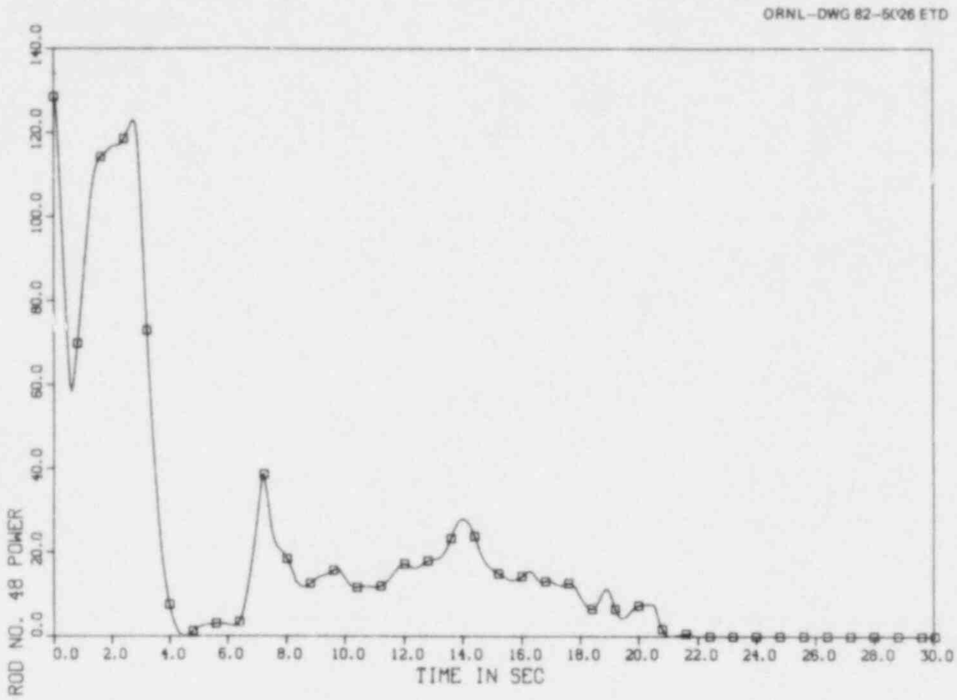

Fig. C.44. Rod power vs time for rod 48.

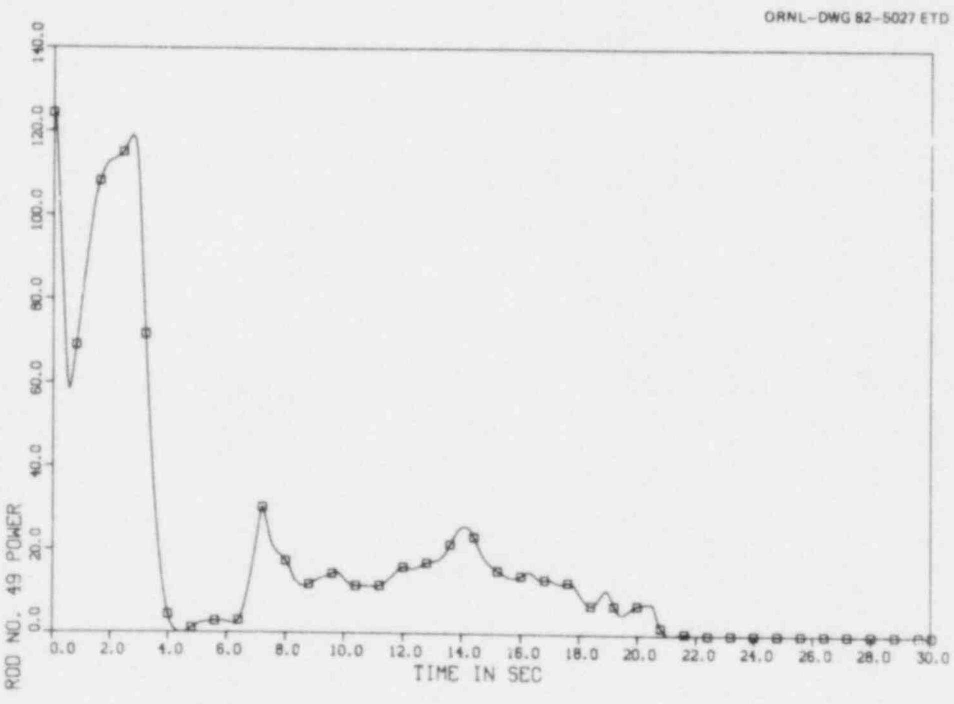

Fig. C.45. Rod power vs time for rod 49.

ORNL-DWG 82-5028 ETD

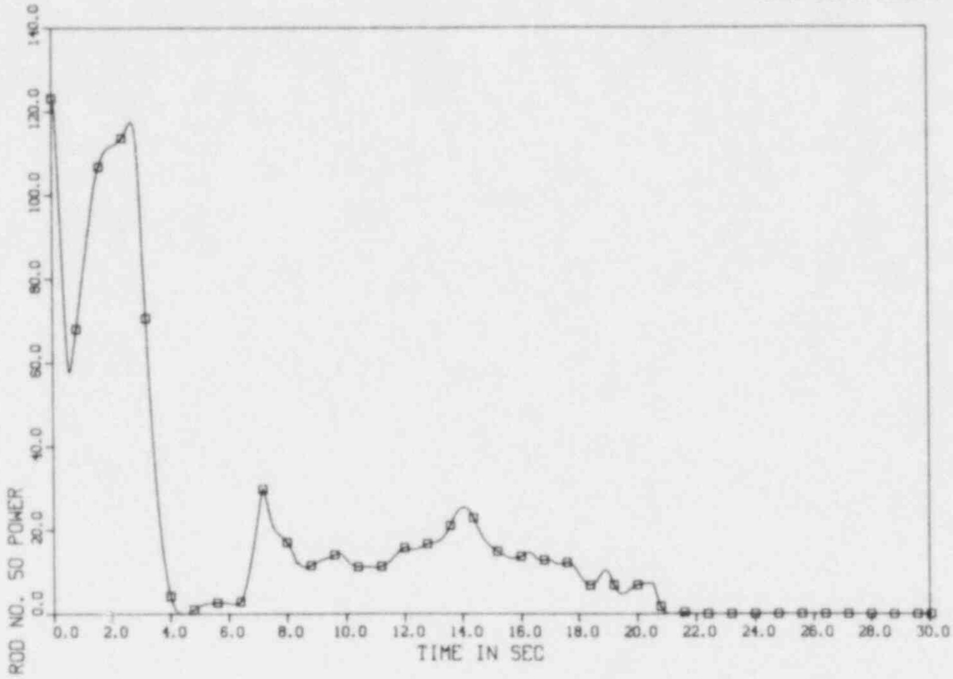

Fig. C.46. Rod power vs time for rod 50.

ORNL-DWG 82-5029 ETD

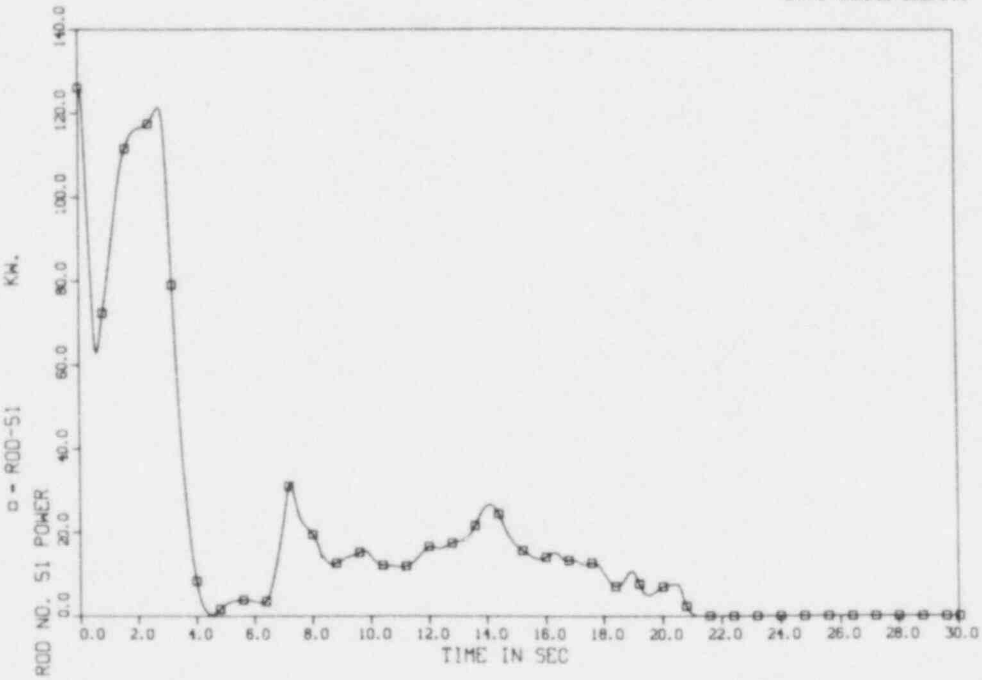

Fig. C.47. Rod power vs time for rod 51.

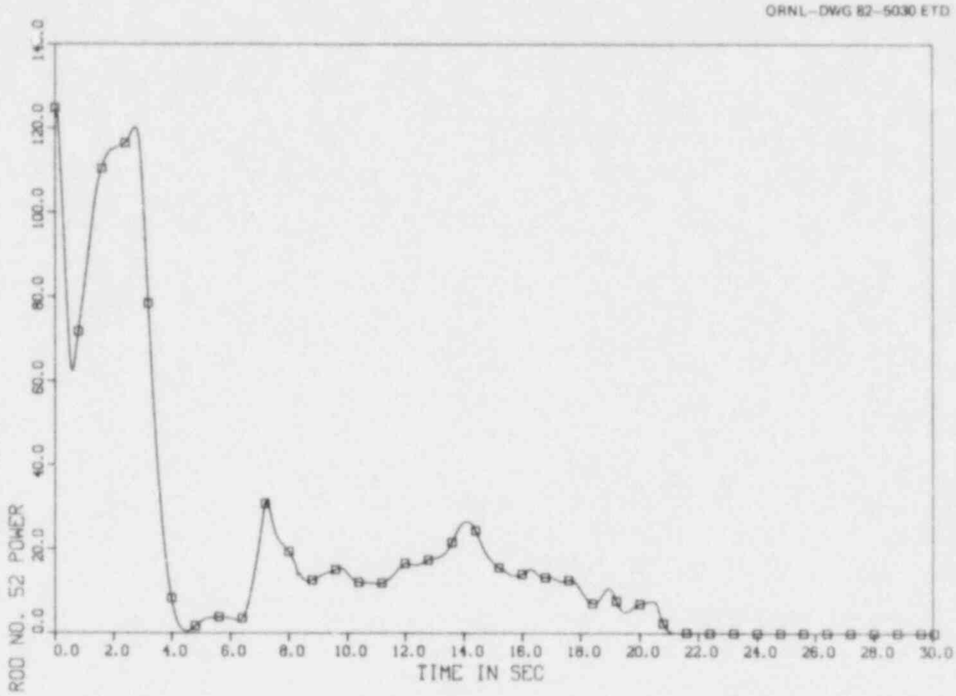

Fig. C.48. Rod power vs time for rod 52.

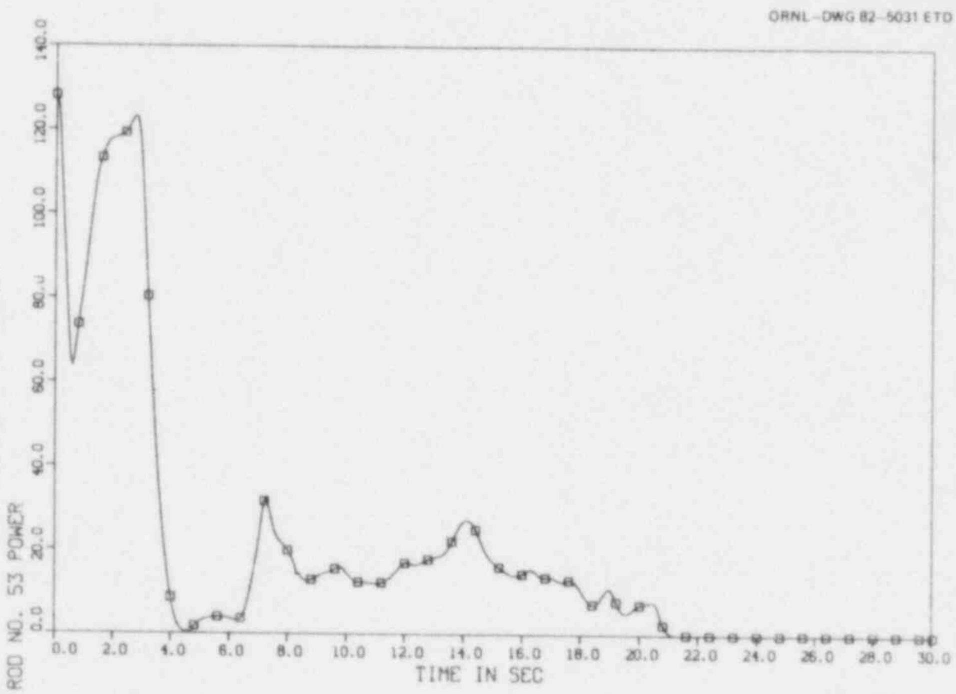

Fig. C.49. Rod power vs time for rod 53.

ORNL-DWG 82-5032 ETD

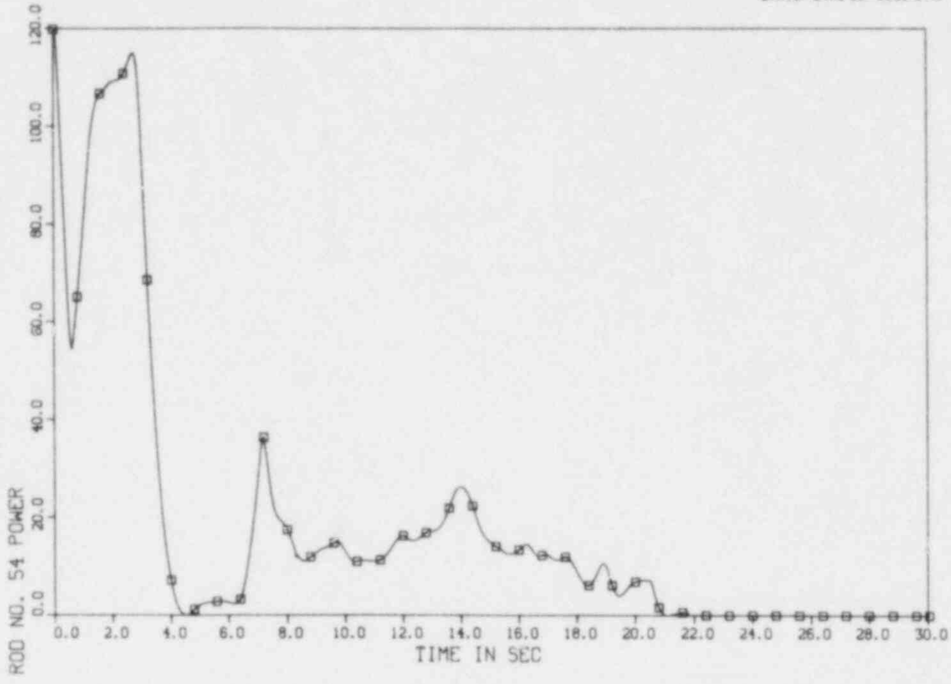

Fig. C.50. Rod power vs time for rod 54.

ORNL-DWG 82-5033 ETD

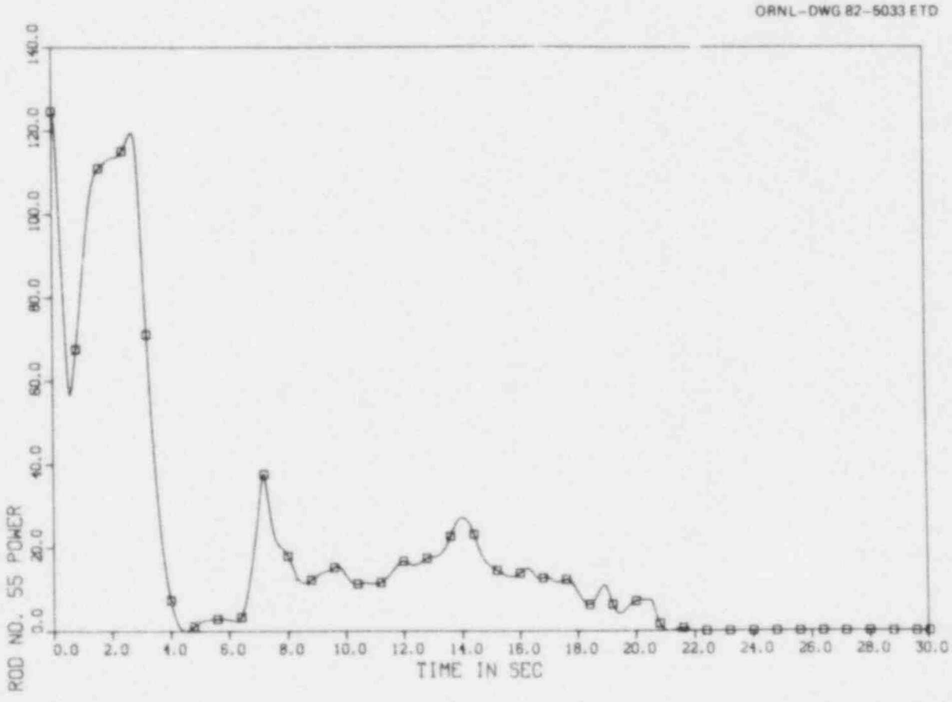

Fig. C.51. Rod power vs time for rod 55.

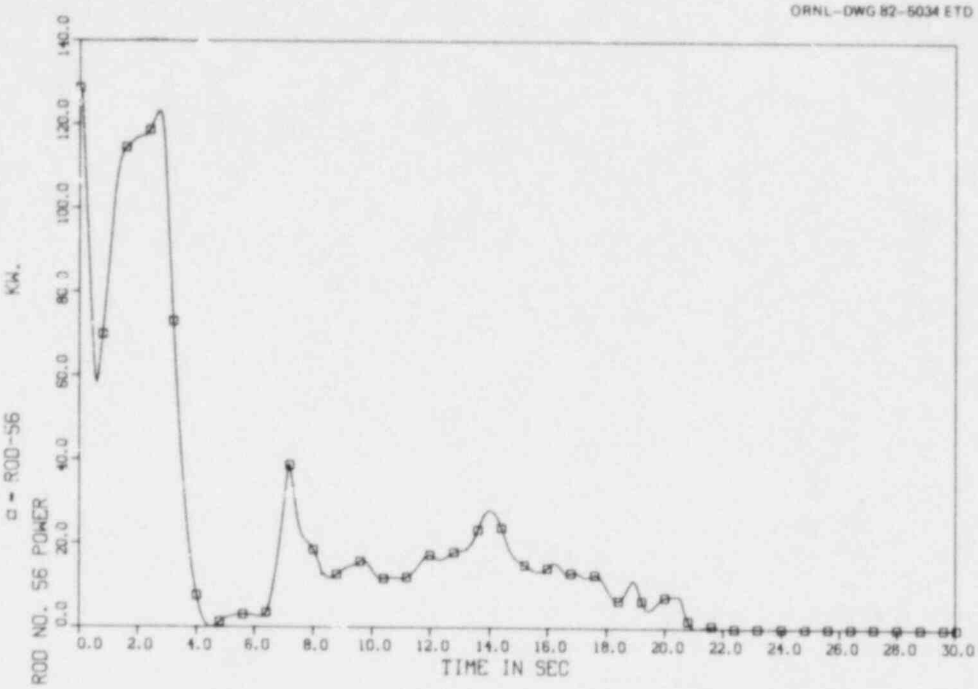

Fig. C.52. Rod power vs time for rod 56.

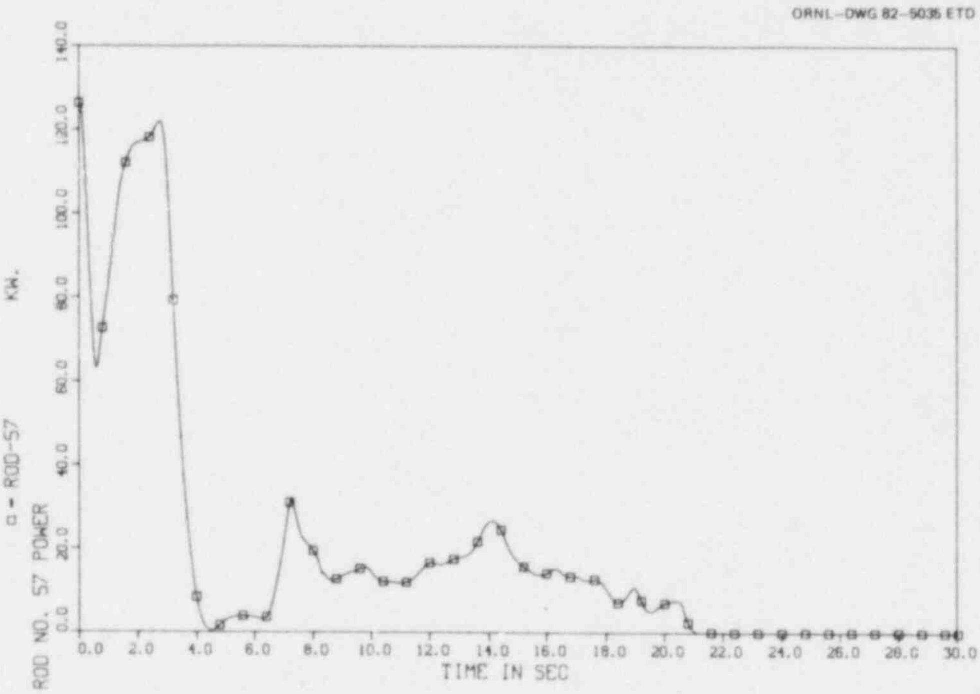

Fig. C.53. Rod power vs time for rod 57.

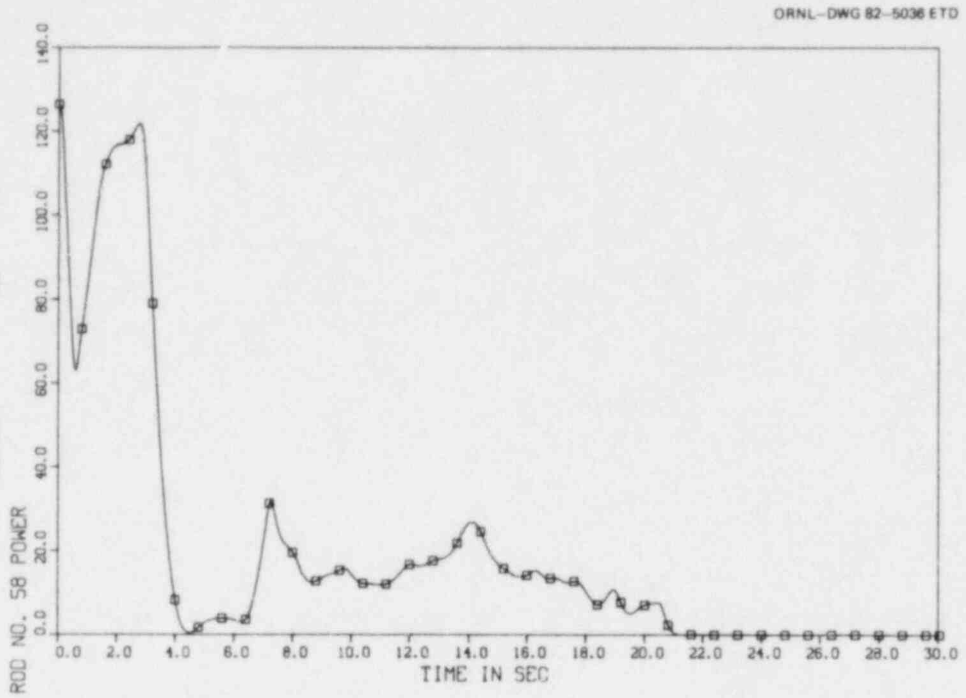

Fig. C.54. Rod power vs time for rod 58.

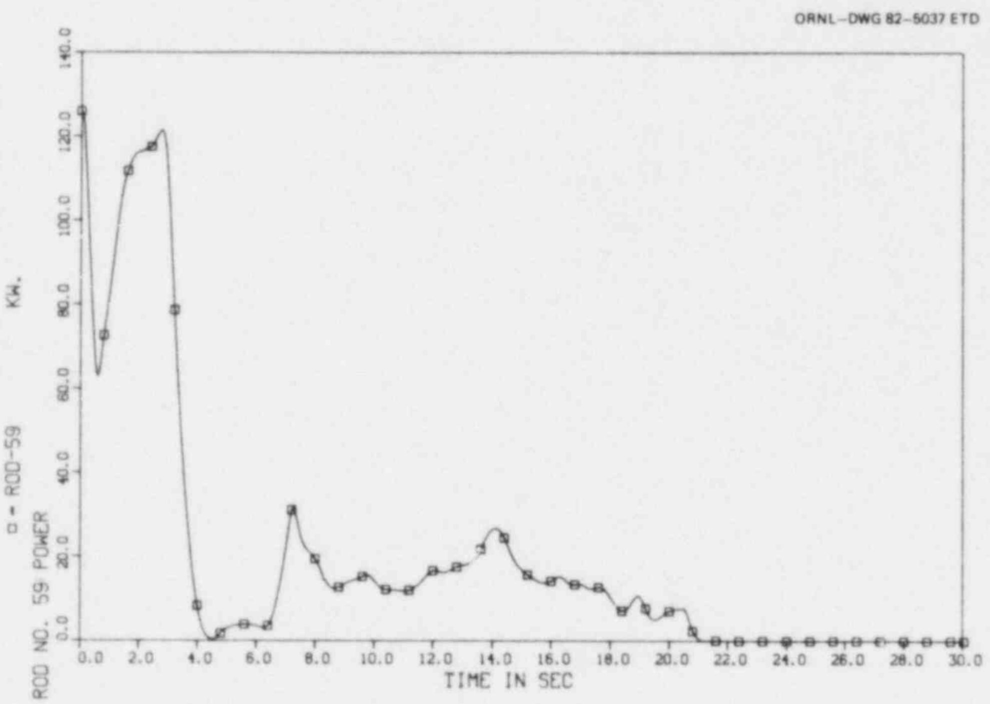

Fig. C.55. Rod power vs time for rod 59.

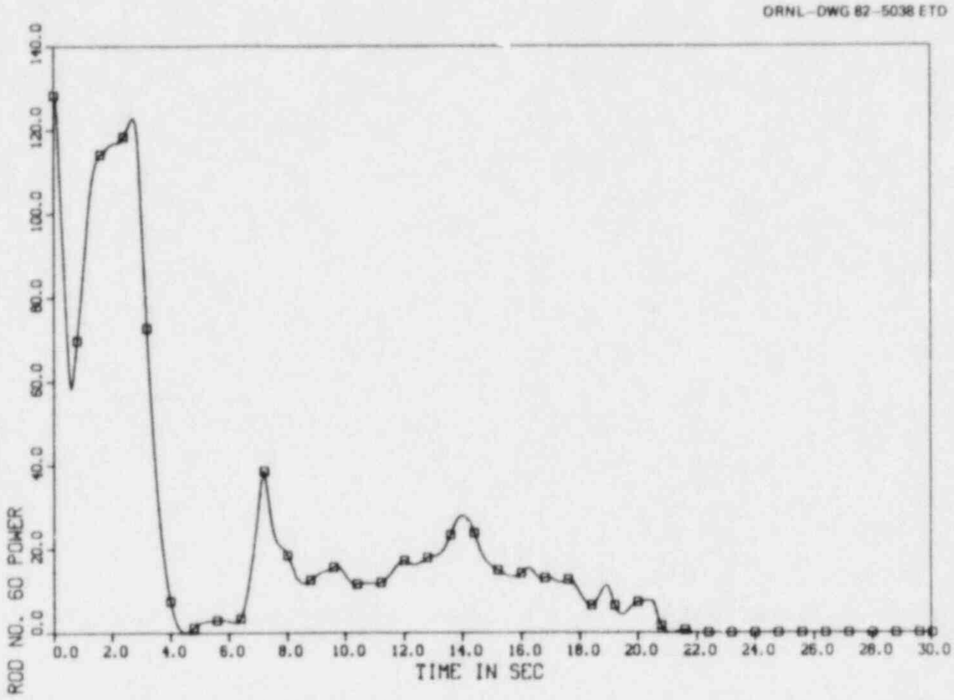

Fig. C.56. Rod power vs time for rod 60.

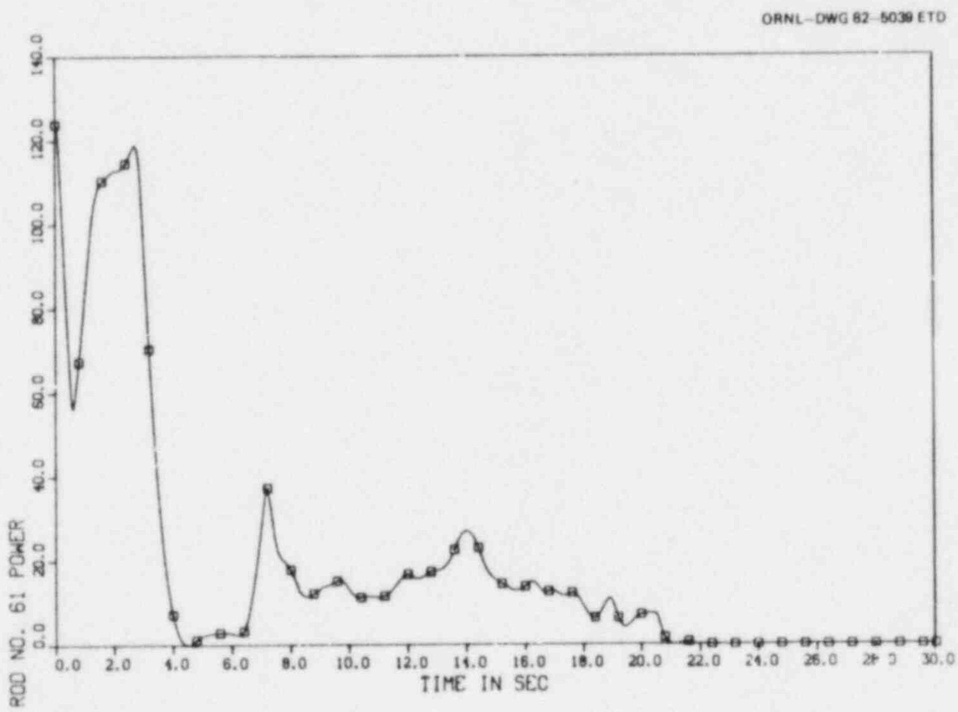

Fig. C.57. Rod power vs time for rod 61.

ORNL-DWG 82-5040 ETD

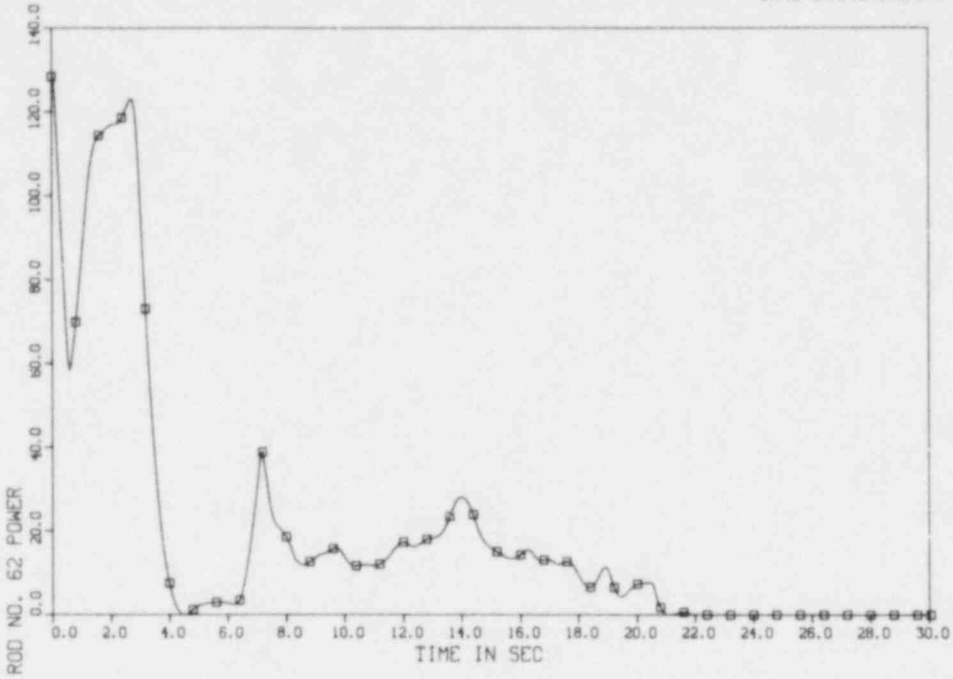

Fig. C.58. Rod power vs time for rod 62.

ORNL-DWG 82-5041 ETD

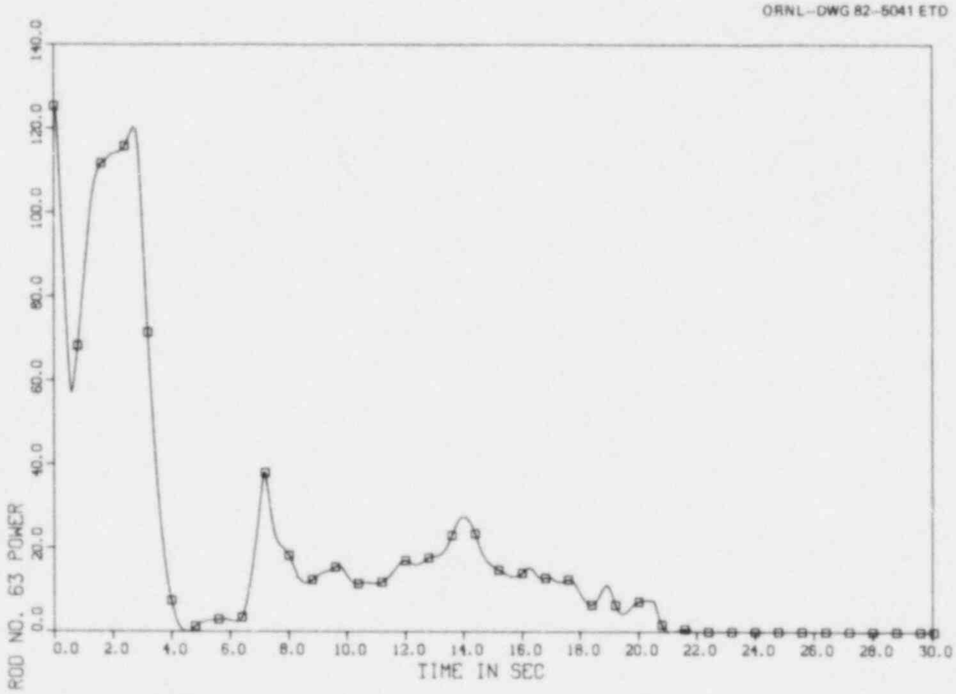

Fig. C.59. Rod power vs time for rod 63.

ORNL-DWG 82-5042 ETD

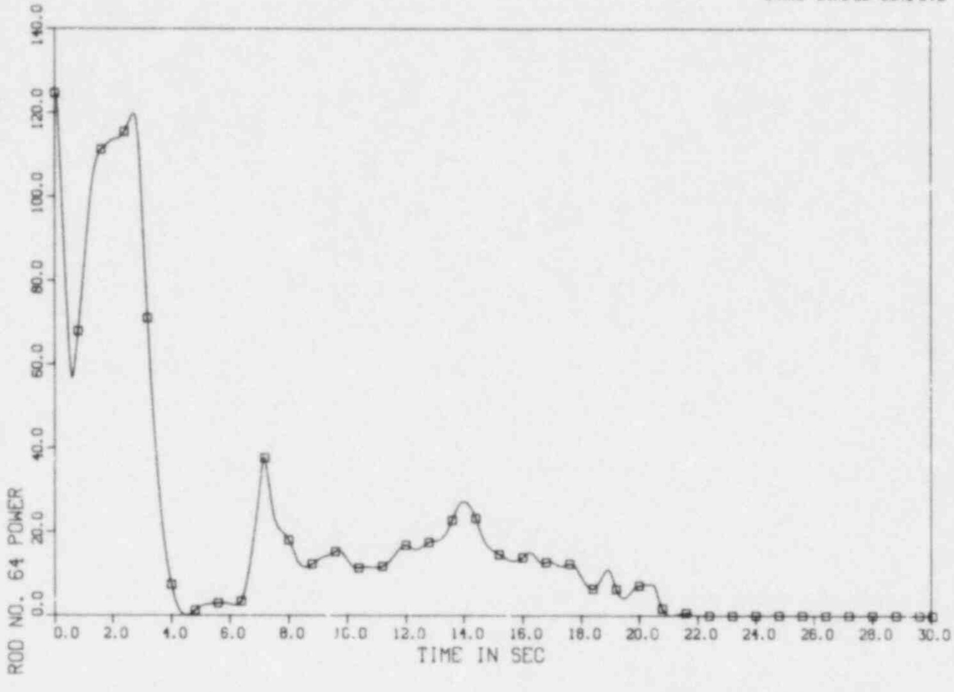

Fig. C.60. Rod power vs time for rod 64.

Appendix D

INSTRUMENT UNCERTAINTY ANALYSIS FOR THE THTF LOOP

Summary of Results

Two standard deviation uncertainty bands are described for critical instrumentation in the Thermal Hydraulic Test Facility (THTF). The analyzed instruments and their minimum, steady-state, 2σ error bands [root sum square (RSS), 95% confidence interval] include:

1. Turbine flowmeter .... 4.1% reading
2. Gamma densitometer .... 10.4% FS*
3. Strain gage pressure cell .... 1.0% FS*
4. Differential pressure cell .... 2.0% FS* min to 9.9% FS* max
5. Thermocouples .... 3.7°C min to 10.3°C max
6. Rod power instrumentation .... 1.1% reading
7. Strain gage drag disk .... 56% reading below 10% FS*; 19% reading above 10% FS*

Summary of Theory

The measure of the value of a group of n data points (x_i) with satistical significance is the mean ($\bar{x}$) or expected value given by

$$\bar{x} = \sum \frac{xi}{n} , \tag{D.1}$$

where Σ is the usual sum from data point 1 to data point n. The standard measure of the dispersion of the data is the variance [σ^2 or V(x)] defined by

$$\sigma^2 = \sum \frac{(x_i - \bar{x})^2}{n} . \tag{D.2}$$

However, V(x) has dimensions of engineering units squared, which may be inconvenient. The square root of V(x), the standard deviation (σ), is usually reported. Furthermore, in normally distributed data with mean $\bar{x}$

---

*Full-scale values are found in Tables D.5–D.8 under instrument range.

and variance σ^2 (a good approximation for much variation in physical data), statistical inferences may be drawn in terms of probabilities based on the measured values of $\bar{x}$ and σ as follows:

68% probability that $\bar{x} - \sigma < x_t < \bar{x} + \sigma$,

95% probability that $\bar{x} - 2\sigma < x_t < \bar{x} + 2\sigma$,

and

99.7% probability that $\bar{x} - 3\sigma < x_t < \bar{x} + 3\sigma$,

where x_t is the true value of the variable.

Brownlee has shown[1] that the variance of a linear function

$$Z = A_0 + A_1X_1 + A_2X_2 = \ldots A_nX_n$$

is a linear function of the variance of the variables as long as the correlation coefficients are zero, i.e., as long as they are physically unrelated. (Linearly independent variables have zero correlation coefficients, but linear independence is not a requirement.) That is,

$$V(Z) = A_1V(X_1) + A_2V(X_2) + \ldots A_nV(X_n) , \qquad \text{(D.3)}$$

where the A_1's are constants and the X_1's are independent variables.

Similarly, Scarborough has shown[2] that an analogous relation holds for a system where the independent variables are not linear:

$$Z = F(Y_1, Y_2 \ldots, Y_n) .$$

The variance of Z is given by

$$V(Z) = \left(\frac{\partial Z}{\partial Y_1}\right)^2 V(Y_1) + \left(\frac{\partial Z}{\partial Y_2}\right)^2 V(Y_2) + \ldots + \left(\frac{\partial Z}{\partial Y_n}\right)^2 V(Y_n) , \qquad \text{(D.4)}$$

where the correlation coefficients of the Y_i's are zero and the value of V(Y) is small compared to $(\partial Z/\partial Y_i)^2$. Notice that in situations where the standard deviation can be expressed legitimately as a percentage of the value of $\partial Z/\partial Y_i$, Eq. (D.4) can be rewritten as

$$\sigma\%(Z) = \sqrt{(\sigma\%Y_1)^2 + (\sigma\%Y_2)^2 + \ldots + (\sigma\%Y_n)^2} . \qquad \text{(D.5)}$$

The above equations can best be understood through the use of an illustrative example. Consider the amplifier of Fig. D.1. The uncertainty in the input voltage can be derived from the function $V_{in} = F(V_{out}, V_{offset}, GAIN)$, given the measured values for V_{out}, $V(V_{out})$, V_{offset}, $V(V_{offset})$, and GAIN, V(GAIN), when V_{in} is the input voltage, GAIN is the amplifier gain, and V_{offset} is the offset voltage.

Assuming the following data, the value of V_{in} is given by

$$V_{in} = \frac{V_{out} - V_{offset}}{GAIN} ,$$

and the variance in the input voltage can be found by applying Eq. (D.4) or (D.5):

$$V(V_{in}) = \frac{V(V_{out})}{GAIN^2} + \frac{V(V_{offset})}{GAIN^2} + \frac{V(GAIN)\ (V_{offset} - V_{out})^2}{GAIN^4} , \qquad (D.6)$$

where

$$V_{out}\ max = 20.0\ volts,$$

$$V_{out} = 10.0\ volts,$$

$$V(V_{out}) = (0.2\ volts)^2 = (2\%)^2\ reading,$$

$$V_{offset} = 0.5\ volts,$$

$$V(V_{offset}) = (0.05\ volts)^2 = (0.5\%)^2\ reading,$$

$$GAIN = 200\ volts/volt,$$

$$V(GAIN) = (1\ volt/volt)^2 = (0.5\%)^2\ reading,$$

$$V_{in} = \frac{(10.0\ volts - 0.5\ volts)}{200} = 0.0475\ volts,$$

ORNL-DWG 81-22671 ETD

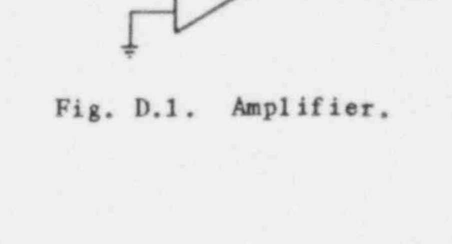

Fig. D.1. Amplifier.

$$V(V_{in}) = \frac{(0.2)^2}{(200)^2} + \frac{(0.05)^2}{(200)^2} + 1^2 \frac{(-9.5)^2}{(200)^4} ,$$

and

$$\sigma(V_{in}) = 10^{-3} \text{ volts or } 2.1\% \text{ reading} .$$

Because V_{in} is a function of V_{out}, V_{offset}, and GAIN in the form given above, it is reasonable to assume that stating the variances as percentages of the readings is equivalent to stating the variances as percentages of the respective partial differentials. In fact, this will always be reasonable as long as the variables are of the first order. The arithmetic for computing $\sigma(V_{in})$ becomes simply

$$\sigma(V_{in}) = (2\%)^2 + (0.5\%)^2 + (0.5\%)^2 = 2.1\% \text{ reading} .$$

Equation (D.4) or (D.5) applied to each major component of a complex information loop is often the only method available to arrive at an uncertainty value. However, in the case of the gamma densitometer and the strain gage pressure cell, in situ standards are available that allow direct measurement of the uncertainty. Heise gages are used as in situ standards for strain gage pressure cells. Pressure and temperature measurements in subcooled water can be used to determine density with steam tables for comparison with the gamma densitometers. Such a comparison is made using a linear regression analysis based on the method of Gauss.

The equation of a line in slope-intercept form is given by

$$y = Ax + B ,$$

where A is the slope ($\Delta y/\Delta x$) and B is the value of the y intercept.

The best-fit values of A and B can be found by minimizing the sum of the distances between the experimentally determined points and the best-fit line.

The pertinent equations are

$$A = \frac{\Sigma x_i \Sigma y_i - n \Sigma (x_i y_i)}{(\Sigma x_i)^2 - n \Sigma (x_i)^2} \tag{D.7}$$

and

$$B = \frac{\Sigma (x_i y_i) \Sigma x_i - \Sigma y_i \Sigma (x_i)^2}{(\Sigma x_i)^2 - n \Sigma (x_i)^2} , \tag{D.8}$$

where the x_i's are the values determined by the instrument under discussion and the y_i's are the corresponding values determined by the in situ standard. The uncertainty of the instrument values can then be defined analogously to Eq. (D.2):

$$\sigma = \sqrt{\sum \frac{(Y_i - y_i)}{n}} \, , \tag{D.9}$$

where the Y_i's are computed from the best-fit equation and the instrument values are y_i. A perfectly calibrated and properly operating instrument will have A = 1.0, B = 0, and $\sigma \ll$ reading.

Although the slope-intercept form of an equation is one of the easiest to interpret, it does have a disadvantage: A and B are not linearly independent variables, so drawing statistical inferences about A and B in terms of their variances is hindered. A solution to this problem is to solve for the best-fit line equation in the form

$$Y = \alpha(x - \bar{x}) + \beta \, . \tag{D.10}$$

The variances of α and β are then known to be

$$V(\alpha) = \frac{\sigma^2}{n} \tag{D.11}$$

and

$$V(\beta) = \frac{\sigma^2}{\Sigma(x_i - \bar{x})^2} \, , \tag{D.12}$$

as shown by Brownlee,[3] where σ is defined as in Eq. (D.9). We can still arrive at an estimate of V(A) and V(B) by modifying Eq. (D.10) to show

$$Y = \alpha x - \alpha\bar{x} + \beta \, ,$$

which implies α = A and B = $(-\alpha\bar{x} + \beta)$. Applying Eq. (D.4) yields

$$V(A) = \frac{\sigma^2}{n} \tag{D.13}$$

and

$$V(B) = \frac{\sigma^2}{n}\,\bar{x}^2 + \frac{\sigma^2}{\Sigma(x_i - \bar{x})^2} = \sigma^2 \quad \frac{x^2}{n} + \frac{1}{\Sigma(x_i - x)^2} \quad . \qquad (D.14)$$

Equations (D.2)–(D.5) and (D.9) should be applied with caution for several reasons.

Definitions for variance assume perfect knowledge. However, actual sampling procedures are limited to finite sample sizes, and formulas impose limits on the degrees of freedom by imposing constraints. To adjust for the limits to the number of degrees of freedom, Eq. (D.2) is modified to provide an estimator for the standard deviation denoted S such that

$$S = \quad \frac{\Sigma(x_i - \bar{x})^2}{(n - 1)} \quad . \qquad (D.15)$$

Equation (D.9) becomes

$$S = \quad \frac{\Sigma(Y_i - y_i)^2}{(n - 2)} \quad . \qquad (D.16)$$

Equations (D.15) and (D.16) are the proper equations to use in all sampling situations where the standard deviation is to be used as the measure of the uncertainty. Furthermore, the value for S should be substituted for the value of σ and S^2 for V(X) or V(Y) in each of the other equations where σ appears. Because of the common association between the standard deviation defined by Eqs. (D.15) and (D.16) with the symbol σ, the symbol σ will be used for S in the balance of this report. In a practical sense, where the standard deviation is reported as two significant figures, there is essentially no difference between σ and S [Eqs. (D.4) and (D.9) versus Eqs. (D.15) and (D.16)] as long as the number of data points is large.

A class of practical problems that arises in the actual error analysis is centered around the interpretation placed on uncertainties supplied by manufacturers. These uncertainties are often supplied as percentages in such a manner that it is difficult to determine whether it is reasonable to apply Eq. (D.5). Either it is difficult to determine how the stated error relates to the standard deviation, or it is difficult to determine whether the error can be applied as a percentage of the partial differentials required by Eq. (D.5). Furthermore, it is seldom stated whether the given uncertainties meet the required criterion of zero correlation coefficient. It is common for manufacturers to quote error bands as 2σ (95% confidence) or 3σ (99% confidence) though sometimes without assigning confidence limits. In this report it is conservatively assumed that the error reported by instrument manufacturers is 2σ. Unless otherwise stated, it is also assumed that a statement of error as a percent with respect to the partial differentials of Eq. (D.5) is reasonable and that the correlation coefficient is zero for all variables.

The second class of problems relating to the uncertainty analysis dealt with multiple estimates of σ for a class of instruments where σ varied widely from instrument-to-instrument and from trial-to-trial. The method of choice was to use a value of σ large enough to include about 95% of the measured values. This was accomplished by using

$$\sigma = \overline{\sigma} + \sigma(\sigma) \ .$$

That is, the value of the standard deviation used was the average value for all instruments and files read plus one standard deviation of σ. This is different from the probability statements above because σ is a span that includes zero to σ. Such a distribution cannot be normal in the sense that the probability statements require.

A generalized procedure for data analysis follows:

A common form for a large system is generalized in Fig. D.2. This system consists of a number of transducers (T_i), their associated signal conditioning equipment (S_i), and the data acquisition system (DAS). The DAS is understood to include both the hardware and the software. The standard deviations of the output signals are measured by reading the information from the magnetic tape written by the DAS and applying Eq. (D.2) or D.14) over an arbitrary length of time where the process is defined as being in a steady state. The measured value of the DAS output can then be incorporated with other measures of uncertainty using Eq. (D.5). If an in situ standard is going to be used to develop the total uncertainty directly, the data for the secondary standard need to be accessed and correlated in time and space with the instruments under consideration.

The development of software to perform the above estimates may be the most time-consuming part of the analysis. The software has to be able to perform the following functions for a magnetic-tape-based system:

1. Confirm that the tape is at the beginning.
2. Confirm that the tape density and number of tracks are system compatible.
3. Locate the instrument data base (IDB) and transfer the IDB to disk or core in a rapid access format.
4. Extract certain system constants from the IDB (record length, etc.).
5. Locate the scan table.
6. Use the scan table and instrument identifier code to determine the location of the desired instrument data in data records.
7. Locate the first data file of the type desired.

ORNL-DWG 81-22672 ETD

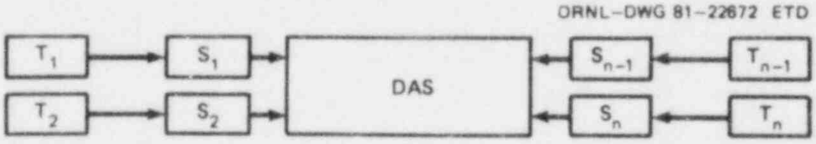

Fig. D.2. Generalized form for a large system.

8. Read a fixed number of records from the data file.
9. Store data in arrays or keep running totals for averaging.
10. Compute averages and standard deviations for steady-state data in the file.
11. Write the desired combinations of data, averages, and standard deviations to arrays.
12. Locate the next data file of the type desired and repeat steps 8–12 until end-of-tape is detected.
13. At end-of-tape, write the arrays to disk for later analysis.
14. At each tape operation, check for proper positioning.
15. Analyze data written to disk as required.

The following sections provide a detailed analysis of the critical instrumentation in the THTF loop. As stated above, the exact nature of the uncertainties is not always known. The RSS value of the uncertainty is the statistically defined one if variables are unrelated (correlation coefficient = 0) and the percentage uncertainty is given as a percent of partials required for Eq. (D.5). However, to the extent that the uncertainties stated do not comply with the assumptions, the more conservative strict sum of errors may need to be applied. Both the RSS value and the strict sum value are given in the text. The RSS values are reported in tabular form at the end of this Appendix. The superscript (*) is used to denote manufacturer derived data.

D.1 Turbine Flowmeter

The turbine flowmeter channel consists of a turbine flowmeter with integral magnetic pickup, an electronics package that conditions the signal to provide an output voltage proportional to flow rate, and the DAS, which converts the analog signal in volts to digital information and writes it onto magnetic tape. In operation, the turbine blade generates an electrical pulse as it passes the magnetic pickup. The ORNL electronics package senses this pulse and with 250 μs resets the count registers and begins accumulating the count until the next pulse disables the count. During the disabled period the count is passed to the digital-to-analog converter where it is converted to millivolt reading. The voltage divider then inverts the millivolt signal and outputs a voltage proportional to the angular velocity of the turbine blade, with 10-V full scale (FS) corresponding to 1200-Hz input signal from the flowmeter pickup. The DAS then converts the output of the ORNL electronics to a digital value and writes it onto magnetic tape. The identified sources of error in the turbine flowmeter are:

Channel noise (blade angle tolerance)	3.2%
Calibration uncertainty	2.4%
Inherent turbine linearity*	0.5%
ORNL electronics package	0.4%
A/D conversion at DAS*	0.3%
Effect of bearing change each run*	0.3%
Strict sum, 2σ error band	7.1%
RSS, 2σ error band	4.1%

The following items need to be considered when applying the above error bands to THTF data:

1. The above uncertainties are all reasonably expressed as a percent of reading. However, the value of turbine linearity quoted applies only over the range 10% rated FS through 100% rated FS. Below 10% rated FS, error bands increase rapidly (see Fig. D.3) as frictional drag becomes more significant, with a cutoff of useful information occurring near 6% of rated FS flow due to signal-to-noise problems in the electronics.

2. Random noise was measured for 30 records of data taken during Reactor Simulation Test 3.05.5B. When the standard deviation was computed for each of the 10 flowmeters without excessive channel noise, the average value (1.53% of reading) was found to agree very well with the predicted channel noise because of blade manufacturing tolerances (72° ± 1.56%). It would be optimistic, however, to conclude that this is the only source of random error. Data taken over a much wider range of flows would be needed to confirm this conclusion.

3. The calibration uncertainty was estimated from two different calibration laboratories (Flow Technology, Inc., and Measurements, Inc.) independently calibrating the same turbine flowmeters. The results of those calibrations indicated approximately 1.2% (as 1σ) differences from laboratory-to-laboratory. The supposed calibration uncertainty according to the laboratories was an order of magnitude smaller based on their NBS traceability standards. The reasons for the large difference were never satisfactorily determined. This comment applies solely to turbine meters located at the SVO, SVI, SHI, and SHO spool pieces.

4. The most troublesome problems of interpreting flowmeter er[illegible] are those that occur during two-phase flow. In a 1977 report[4] MPA Associates, Inc., investigated the possible errors due to slug flow, annular flow regimes, steam-water ratios, and differential two-phase velocities. This

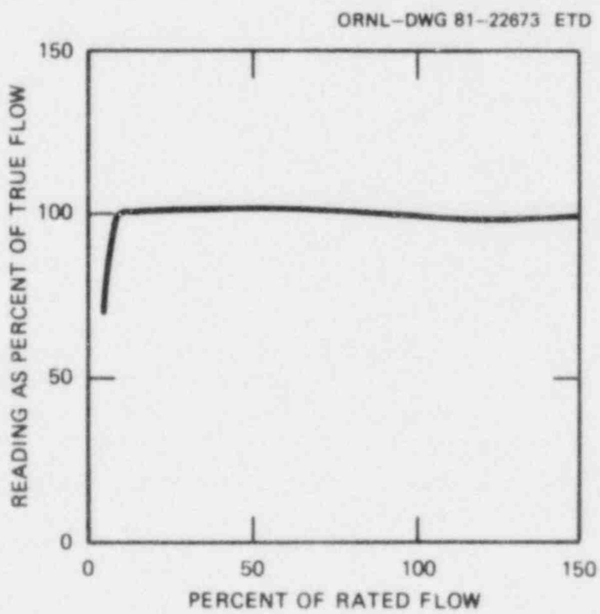

Fig. D.3. Error due to turbine linearity: characteristic curve.

investigation was strictly theoretical, based on momentum exchange between the blade and the fluid. These analyses were based on steady-state flow, balancing the transverse momentum of one phase against that of the second. Assuming no net momentum exchange with the rotor, the turbine response was interpreted in light of the point effective radius (established as the calbration constant) in the presence of two phases with different flow regimes and different velocity profiles. The conclusion reached was that errors up to ±25% might be expected.

By assuming equal probabilities for the parameters investigated, it was determined that a 1σ error band of 10% might reasonably be expected. However, until experimental verification of both model and results can be obtained, it would only be prudent to use the above figures in a qualitative manner.

D.2 Gamma Densitometer

The gamma densitometers consist of a nearly monoenergetic ^{137}Cs gamma source, an ionization chamber to detect the gamma rays, an instrument amplifier, and the DAS. In use, the gamma rays pass through the steel pipe, through the water (in whatever phase) in the pipe, and into the ionization chamber. In the ionization chamber the gamma rays are converted into an electric current such that the current is proportional to the intensity of the impinging gamma rays. The instrument amplifier takes this current and converts it into a voltage that is proportional to the input current. At the DAS the voltage is converted to a digital value and stored on magnetic tape.

Given that the source approximates a point source, the density of the water (ρ_w) in the pipe should be given by

$$\rho_w = \text{KFACTR} \ln\left(\frac{V_p - V_o}{V - V_o}\right) ,$$

where KFACTR is an experimentally determined constant that includes the effect of pipe diameter and the mass absorption coefficient of the water (including any dissolved salts), V_p is the output voltage when the pipe is empty, V_o is the output voltage with the source shielded (dark voltage or zero offset), and V is the output voltage when there is water in the pipe.

Due to the strong theoretical dependence of density error as a function of density, the 1σ error band was investigated as a statistical function of the density reading compared to an in situ standard based on the physical properties of the water in the pipe under known conditions of temperature and pressure and a steady-state, one-phase flow. Ten gamma densitometers in service during Test 3.05.5B were used as a basis of the study. The output voltage of each instrument was sampled 150 times in each of ten 3-s files. The output voltage was then used to compute the water density using values of KFACTR, V_p, and V_o measured in a recent calibration run. Those densities were then compared to the expected densities based on water properties derived from the temperature and pressure instruments located adjacent to each gamma densitometer.

The measured uncertainty expressed as 1σ in kg/m^3 (and lb/ft^3) is shown in Table D.1. It was discovered, however, that at least part of the large variation in the uncertainties resulted from a systematic error that varied from instrument to instrument (see Fig. D.4, where the densitometer density is plotted against the water property density for DE-204B). Furthermore, the expected strong dependence of error on total density is not obvious over the range of data compared. Not all densitometers showed positive deviations from the standard as did DE-204B.

Table D.1. Absolute error analysis

Densitometer	σ (kg/m^3)	σ (lb/ft^3)
DE-20	18.9	1.18
DE-36	199.0	12.42
DE-168	3.6	0.22
DE-218	87.5	5.46
DE-204A	4.4	0.27
DE-204B	57.7	3.60
DE-204C	33.6	2.10
DE-262A[a]		
DE-262B	22.9	1.43
DE-262C	37.5	2.34
Average	52.0	3.20

[a]Probable equipment failure during test.

The data for each densitometer were fit to a straight line, densitometer calculated density to water property density, using linear regression analysis. The random error, expressed as 1σ, was then calculated for each gamma densitometer using Eq. (D.16), but Y_i is the best average value from the linear regression equation. The value of uncertainty was much more uniform from densitometer to densitometer (see Table D.2). A preliminary analysis of the calibration procedure indicates that it may be possible to recalibrate the densitometers analytically to remove the systematic error. Since the analysis performed on the experimental data does not use the densitometer responses, it was not deemed worthwhile to expend the effort required to perform this recalibration.

Since the density of water at room temperature is approximately 1×10^{-3} kg/m^3 (62.4 lb/ft^3), the above results can be summarized as follows:

2σ error band under current operating procedures .... 10.4% FS

ORNL-DWG 81-22674 ETD

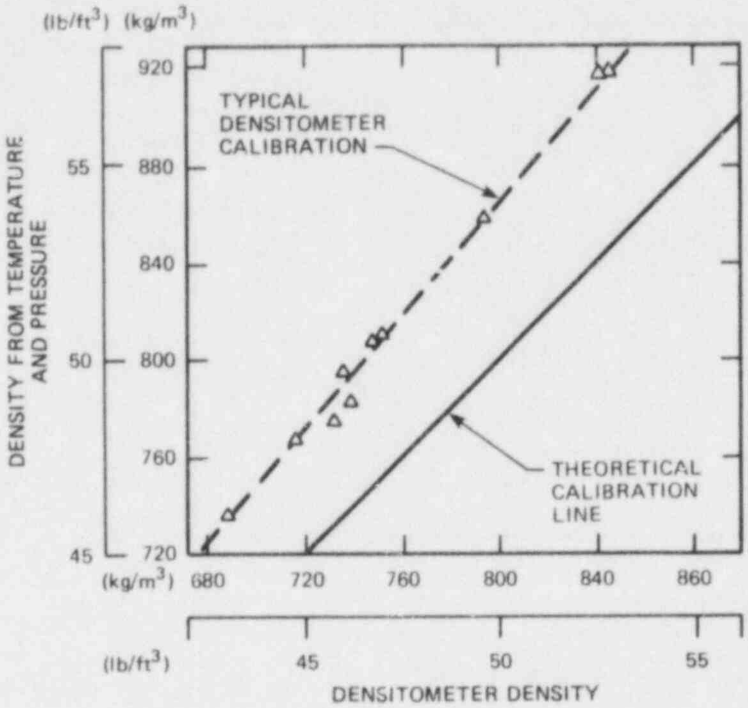

Fig. D.4. Typical densitomete. calibration.

Table D.2. Least-squares best-fit line (RHO = A x DERHO + B)

Densitometer	A	B	σ (kg/m³)	σ (lb/ft³)
DE-20	0.945	64.9	8.6	0.54
DE-36	0.131	745.0	9.7	0.61
DE-168	1.000	−0.4	0.9	0.06
DE-218	0.711	176.0	2.5	0.16
DE-204A	0.981	14.0	4.4	0.27
DE-204B	1.190	−85.9	6.0	0.37
DE-204C	1.010	24.8	12.4	0.77
DE-262A[a]				
DE-262B	0.740	246.0	5.3	0.33
DE-262C	1.160	−100.0	4.5	0.28
Average			5.8	0.36

[a]Probable equipment failure during test.

The following items need to be considered when applying the above error bands to THTF data analysis:

1. An analysis of data scatter indicates an average σ of 31 kg/m³ or 3.1% FS over 150 point data files. Therefore, individual points within a file have much higher uncertainties than those stated for files as a whole.

2. No other factor has been identified which would degrade the error bands beyond the steady-state, one-phase flow values listed above. However, it should be understood that the densities computed from densitometer voltages during transients and two-phase flow are time-and-path averaged values. Furthermore, a direct application of the above data to transient, two-phase flow is done at the risk of the data user until experimental verification can be obtained.

D.3 Strain Gage Pressure Cells

The pressure channel invertigated consists of a strain gage pressure cell, an instrument amplifier, and the DAS. In operation, pressure on the diaphragm of the pressure cell causes a change of resistance in the foil strain gages attached to the diaphragm. The change in resistance in the gages causes a voltage output from the cell that is proportional to the applied pressure. This output is amplified by the instrument amplifier. The DAS converts the amplifier output to digital format and writes it onto magnetic tape.

The following errors were identified as contributing to the pressure cell uncertainty:

Nonlinearity (P-sensor)*	0.3% FS
Repeatability (P-sensor)*	0.1% FS
Hysteresis (P-sensor)*	0.1% FS
Tempco, gage factor (P-sensor)*	0.5% Reading
Tempco, zero offset (P-sensor)*	0.5% FS
Gain instability (instrument amplifier)* ...	0.1% Reading
Output offset (instrument amplifier)*	0.1% FS
DAS calibration*	0.3% Reading
Location of calibration standards	0.4% FS
Strict sum 2σ error band	2.5% FS
RSS 2σ error band	1.0% FS

The following items need to be considered when applying the above error bands to THTF data:

It is fairly obvious that the results of the in situ calibration run (see item 2 below) agree respectably with the 2σ error band determined above. The probable reason that in situ calibration errors are smaller than the theoretically determined value can be attributed primarily to smaller than estimated temperature changes in actual operation for both gages and amplifiers. In the absence of contradictory experimental evidence, the 2σ error band for the strain gage pressure cells should be set at 1.0% FS or 200 kPa (29 psi).

1. The temperature effects were assumed to be operable over a range of only 56°C (100°F) in actual use. This seems like a reasonable assumption since the sensors themselves are installed at the end of a connecting tube ensuring cooling by ambient air flow and the instrument amplifier is mounted where ambient air flow should keep the temperature change within the 56°C (100°F) range. Channel noise was measured during Test 3.05.5B using Y_i [see Eq. (D.16)] as the average within a data file. Five instruments were sampled with 30 points per data file, 10 data files each. The 1σ value measured in this manner was quite variable, so that it was deemed expedient to select a value of σ large enough to include about 95% of the data.

2. The strain gage pressure cell does have a usable in situ standard for comparison. With data from a recent pressure cell calibration run, the standard deviation for system pressure was determined for six strain gage pressure instruments by comparing P-cell output converted to pressure using the measured calibration constants with the average reading of two Heise bourdon tube gages accurate to 20 kPa (3 psi). The results of that comparison are:

Instrument	σ (kPa)	σ (psi)	σ (% FS)
PE-26	37.2	5.4	0.18
PE-42	66.2	9.6	0.32
PE-44	18.6	2.7	0.09
PE-76	43.4	6.3	0.21
PE-106	47.6	6.9	0.23
PE-156	91.0	13.2	0.44
Average	51.0	7.4	0.24
Plus location of calibration standard	40.0	5.8	0.18
Total 2σ value	130.0	18.9	0.6

3. The in situ calibration uses the average reading of two Heise gages as system pressure. These gages may be separated by 8.53 m (26 ft) vertically. The result of the difference in static water pressure can produce an offset of ~40 kPa (5.8 psi) (1σ) depending on the location of the specific instrument.

4. The DAS seems to be the limiting factor in instrument response time, including the response time of the transducer itself since pressure waves should reach the diaphragm much faster than the normal sample rate. No other source of error has been identified to degrade the error band established for steady-state, one-phase flow. However, the application of the above error band to transient or two-phase flow without corroborating data might be overly optimistic, and any such use is the responsibility of the data user.

D.4 Differential Pressure (dp) Cells

The strain gage dp cell (A, B, C) instruments are very similar to the strain gage pressure cells above, except that they have lower full-scale capability.

A. The identified sources of error in the BLH strain gage (1380 and 6870 kPa or 200 and 1000 psi, respectively) dp cell are

Bench calibration (note 1)	2.4% FS
Tempco, gage factor (P-sensor)*	0.1% FS
Tempco, zero offset (P-sensor)*	0.1% FS
Gain instability (instrument amplifier)* ...	0.1% FS
Output offset (instrument amplifier)*	0.1% FS
A/D inaccuracy (DAS)*	0.3% FS
Random noise (note 2)	2.0% FS
Strict sum 2σ error band	5.1% FS
RMS 2σ error band	3.1% FS

B. The identified sources of error in the BLH strain gage (1380 kPa or 200 psi) (pit) dp cell are

Bench calibration (note 1)	2.4% FS
Tempco, gage factor (P-sensor)*	0.5% Reading
Tempco, zero offset (P-sensor)*	0.5% FS
Gain instability (instrument amplifier)* ...	0.1% Reading
Output offset (instrument amplifier)*	0.1% FS
A/D inaccuracy (DAS)*	0.3% Reading
Random noise (note 2)	9.6% FS
Strict sum 2σ error band	13.5% FS
RMS 2σ error band	9.9% FS

C. The identified sources of error in the GENISCO (41 kPa or 6 psi) strain gage dp cell

Static pressure offset	2.6% FS
Zero balance*	2.0% FS
Linearity, hysteresis*	0.4% FS
Tempco, sensitivity*	0.3% FS
Tempco, zero offset*	0.3% FS
Noise (note 1)	2.0% FS
A/D conversion DAS*	0.3% FS
Strict sum 2σ error band	7.9% FS
RSS 2σ error band	3.9% FS

D. The identified sources of error in the ITT Barton (25 kPa or 100 in.) dp cell are

Transduction accuracy*	0.25% FS
Static pressure effect*	0.4% FS
Tempco, zero offset*	0.2% FS

Tempco, sensitivity*	0.2% FS
Noise	2.0% FS
DAS*	0.3% FS
Strict sum 2σ error band	3.4% FS
RSS 2σ error band	2.1% FS

E. The identified sources of error in the Rosemount Capacitance dp cell are (see note 4)

	6.2 and 7.4 kPa (25 and 30 in.)	37 and 50 kPa (150 and 200 in.)
Transduction accuracy	0.25% FS	0.25% FS
Tempco, combined*	0.95% FS	0.14% FS
Static pressure offset	1.0% FS	1.0% FS
Stability*	0.25% FS	0.25% FS
Noise	0.2% FS	0.2% FS
DAS*	0.3% FS	0.3% FS
Strict sum 2σ error band	3.0% FS	2.1% FS
RSS 2σ error band	1.5% FS	1.1% FS

F. The identified sources of error in the FOXBORO force balance dp cell are

Transduction accuracy*	0.25% FS
Noise	2.0% FS
DAS	0.3% FS
Strict sum 2σ error band	2.6% FS
RSS 2σ error band	2.0% FS

The following items need to be considered in evaluating the above 2σ error bands:

1. Bench calibration data were substituted for the values of nonlinearity, repeatability, and hysteresis since bench data were available and indicated significantly larger error bands for strain gage. The dp sensors in use show a dependence on system pressure for both gain and offset (see Figs. D.5 and D.6). The approach has been to use a calibration equation based on a linear regression calibration of both gain and zero offset in the form

$$P_{dp} = (PAg + Bg)[V - (PAz + Bz)] \ ,$$

where P_{dp} is the differential pressure measured by the dp cell; Ag, Bg, Az, and Bz are the calibration coefficients; V is the sensor output voltage; and P is the system pressure. However, the linear correlation of system pressure and constants Ag, Bg, Az, and Bz is not high enough to make the correlation better than 1.2% (as 1σ) overall.

2. When the error band was checked using digital data from Reactor Simulation Test 3.05.5B, an average value of σ equivalent to 1.0% FS was measured using 13 PDE's in service prior to blowdown. The average output was used as the standard.

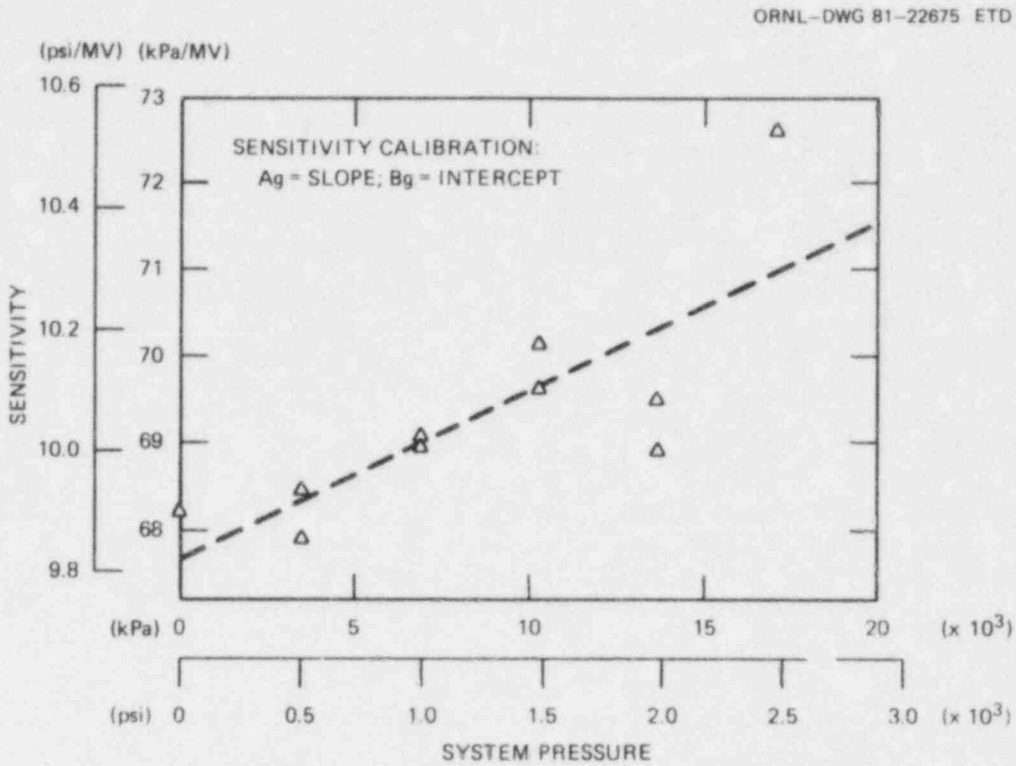

Fig. D.5. Sensitivity calibration.

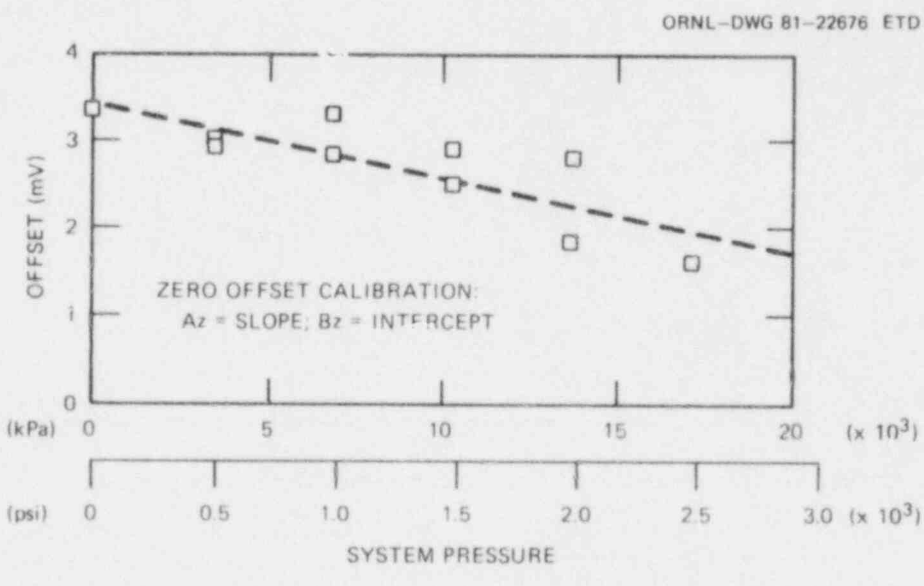

Fig. D.6. Zero offset calibration.

3. When the strain gage dp cells are used as pit dp cells, they are connected to different parts of the system by long lines of small diameter tubing. Analysis of Test 101 showed that resonant ringing could account for an increase in the noise level (as 1σ) to 4.8% FS just prior to blowdown and up to 65% FS after blowdown when the 28-Hz (the measured resonant frequency) notch filter is used as a standard (see Fig. D.7).

4. An in situ calibration was made during steady-state scans for the Small Break LOCA II tests of October and November 1980. The uncertainty estimate used water properties as a basis of known differential pressure. The results indicated an average 1σ uncertainty of ±0.05 kPa (0.2 in.) (0.8% FS).

5. Temperature coefficients were applied over a range of 15°C (27°F).

6. No parameter was identified that would degrade error bands beyond those listed above during two-phase flow. However, extension of the stated error bands to two-phase flow or transient conditions without supporting experimental evidence is done at the data user's risk.

ORNL-DWG 81-22677 ETD

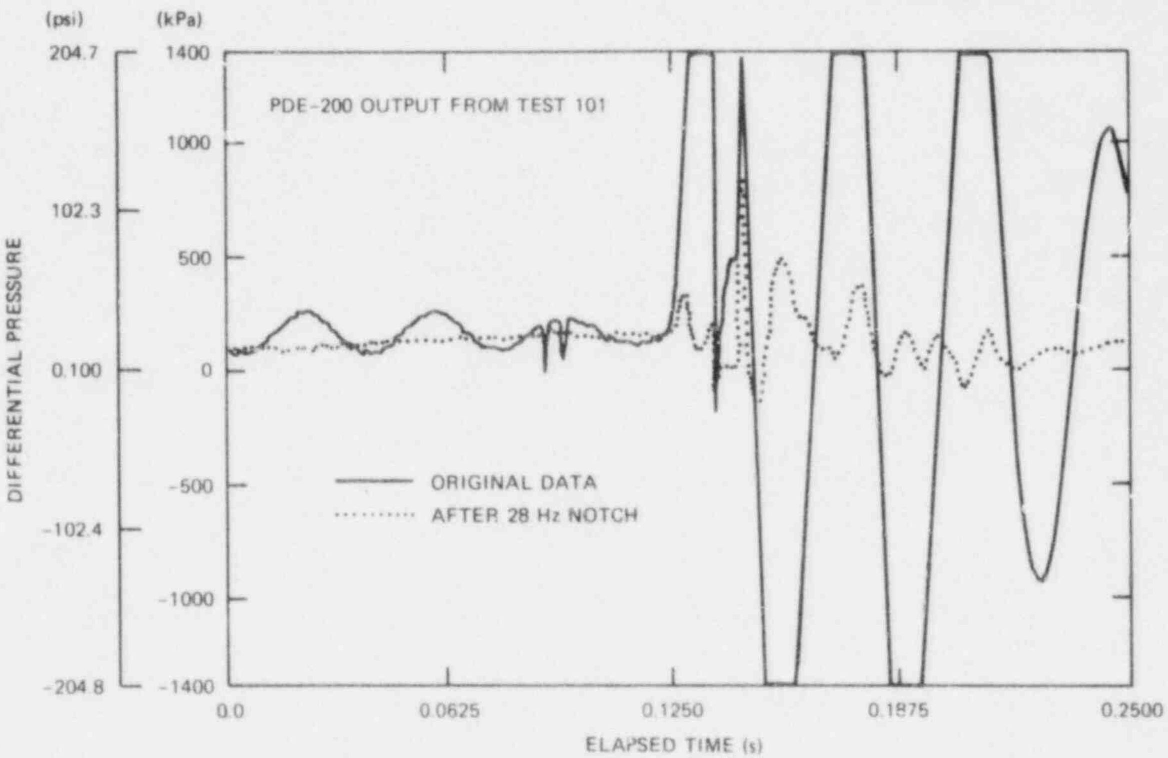

Fig. D.7. PDE-200 output from Test 101.

D.5 Thermocouple Temperature Instruments

The thermocouple instruments consist of Chromel-Alumel thermocouples, a "cold-junction" reference box, and the DAS.

The following error sources were identified for thermocouple instruments:

	Minimum value (°C)	Minimum value (°F)	Above 350°C (660°F)
Thermocouple material*	2.2	4.0	0.76%
Random noise	0.5	1.0	
DAS calibration	1.8	3.2	0.46%
Reference junction calibration	2.2	4.0	2.2°C (4.0°F)
Reference junction controller	0.16	0.3	0.16°F (0.3°F)
Strict sum 2σ error band	6.9	12.4	(See below)
RSS 2σ error band	3.7	6.7	(See below)

Conversion of the above percentage values to degrees centigrade above 350°C (660°F) results in the following:

Temperature (°C)	Temperature (°F)	2σ Error band (°C)	2σ Error band (°F)	2σ Error band strict sum (°C)	2σ Error band strict sum (°F)
350	662	3.7	6.7	7.4	13.3
400	752	4.2	7.6	8.3	14.9
450	842	4.7	8.5	9.1	16.4
500	932	5.1	9.2	10.0	18.0
550	1022	5.6	10.1	10.8	19.4
600	1112	6.1	11.0	11.7	21.1
650	1202	6.6	11.9	12.5	22.5
700	1292	7.1	12.8	13.4	24.1
750	1382	7.6	13.7	14.2	25.6
800	1472	8.0	14.4	15.1	27.8
850	1562	8.5	15.3	15.9	28.6
900	1652	9.0	16.2	16.8	30.2

The following items need to be considered when applying the above error band estimates to THTF data:

1. The reference junction box calibration error was determined by analyzing long-term calibration data from February 4, 1976, to February 10, 1981, and includes any offset from the mean set-point value of 2.666 mV. Reference junction box anomalies were discovered during a 7-day steady-state period. Controller errors up to 0.08°C (0.14°F) were observed for periods of approximately 1-h duration. Operating four units continuously over 7 days, the average error was determined to be less than 0.006°C (0.01°F).

2. Random noise was determined by analyzing the data from Reactor Simulation Test 3.05.5B for five Type Code = 6 and nine Type Code = 1 thermocouples in operation during that test for steady-state, one-phase flow conditions. Because of considerable scatter from instrument-to-instrument and file-to-file, a value of σ large enough to include approximately 95% of all data was chosen. In an effort to provide a conservative estimate, it was assumed that the noise at higher temperatures would be proportional to the millivolt signal above 350°C (660°F).

3. Data Acquisition System calibration was checked after a test calibration with the voltage output compared with a 32.0-mV input signal.

4. A thermocouple that had been in service at the THTF facility was analyzed by R. L. Anderson[5] of the I&C standards lab to determine the effect of nickel crystal reordering. The results indicate that errors from 1.2°C (2.2°F) [near 150°C (1300°F)] to 16.3°C (29.3°F) [near 900°C (1650°F)] may be expected in addition to the above values. However, the recent history of a specific thermocouple coupled with its end-to-end temperature gradient makes it difficult to extrapolate to all THTF thermocouples. The effect of crystal reordering would be to produce readings higher than actually experienced at the junction.

5. An isothermal scan taken during Test 3.06.6B was used to compare the output of 615 thermocouples believed to be operational. The measured standard (2σ) deviation of 4.0°C (7.2°F) agrees closely with the RSS estimated value of 3.7°C (6.7°F) (2σ).

D.6 Rod Power Instrumentation

The rod power instrumentation consists of two operational amplifiers, a calibrated low resistance shunt, and the DAS (see Fig. D.8). Amplifier 1 reads the voltage across the rod itself. V_1 is the output from the voltage divider. Amplifier 2 reads the voltage across the shunt. The current in the rod is then inferred using Ohm's law such that

$$I = V_2/R_s ,$$

where I is the current in amps, V_2 is the potential across the shunt in volts, and R_s is the resistance of the shunt in ohms.

The following items were identified as probable sources of error when determining rod power:

R_s	Calibration inaccuracy*	0.26% Reading
R_s	Temperature coefficiency*	0.2% Reading
V_2	Nonlinearity*	0.01% Reading
V_2	Channel noise	0.72% Reading
V_2	Tempco, gain*	0.02% Reading
V_2	Tempco, offset*	0.03% FS

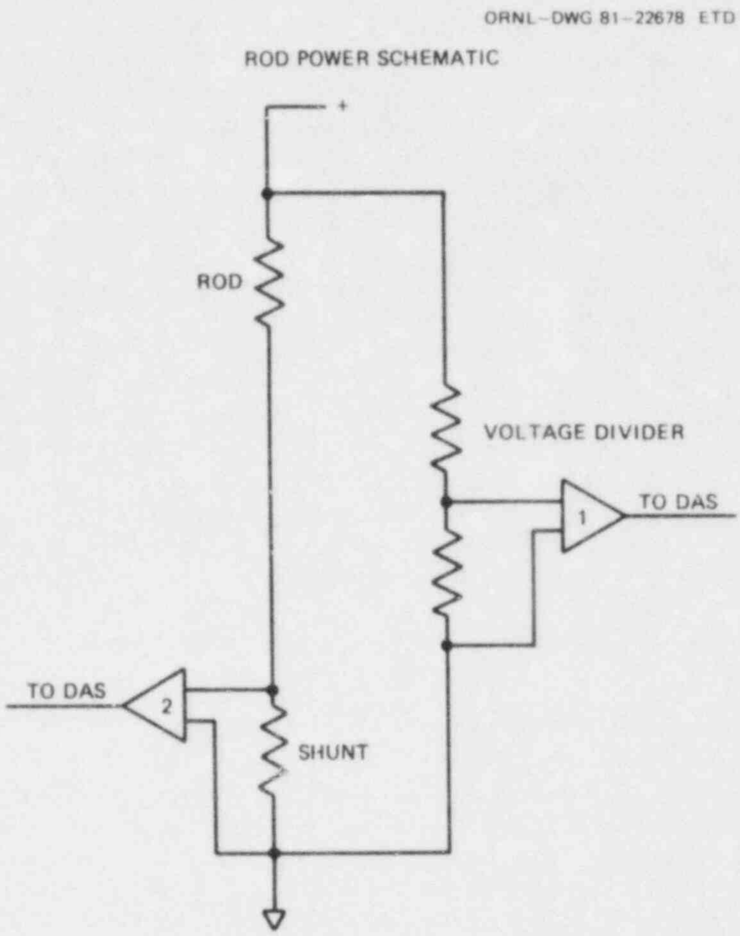

Fig. D.8. Rod power schematic.

V_2	DAS calibration inaccuracy*	0.30% Reading
V_1	Nonlinearity*	0.01% Reading
V_1	Channel noise	0.7% Reading
V_1	Tempco, gain*	0.02% Reading
V_1	Tempco, offset*	0.03% Reading
V_1	DAS calibration inaccuracy*	0.30% Reading
	Strict sum 2σ error band	2.6% Reading
	RSS sum 2σ error band	1.1% Reading

The following items need to be considered when applying the above error bands to THTF rod power data:

1. Temperature changes at the amplifiers were assumed to be less than or equal to 20°C (36°F). The temperature changes at the shunt were

assumed to be less than or equal to 40°C (72°F). The temperature changes chosen may be excessively large resulting in larger than necessary error bands.

2. Power determined using IV (amps times volts) above does not always agree well with an I^2R (amps squared times rod resistance) power calculation. No adequate explanation for the difference is known. Since both methods should yield the same value of power to the rods, actual error bands may be larger than stated.

3. No error source was identified that would degrade the steady-state, 2σ error band beyond those listed above.

4. Because of matched voltage divider temperature coefficients and the current calibration procedures, the error contributed by the voltage dividers is considered negligible. However, channel noise was measured at low power, so that the values used might be unnecessarily conservative. Furthermore, the resistance of the shunt is very much less than the rod, so that the voltage drop across the rod is essentially unaffected by the shunt.

D.7 Strain Gage Drag Disks

An analysis of steady-state, single-phase drag disk uncertainties based on subcooled flow calibrations from four THTF tests is presented. The data are from pretest drag disk calibrations performed on the same day of the test during heatup to blowdown conditions for Tests 3.04.7, 3.05.5B, 3.06.6B, and 3.08.6C.

The drag disks are calibrated using the turbine flowmeters (velocity, V) and pressure- and temperature-deduced density (ρ) to obtain an in situ standard momentum flux [$(\rho V^2)_{std}$]. A calibration equation is generated from a least-squares fit to the drag disk signal corresponding to the momentum flux over a range of momentum fluxes. The measured momentum flux [$(\rho V^2)_{meas}$] is obtained by applying the calibration equation to the instrument signal. The calibration equation takes the form:

$$(\rho V^2)_{meas} = A(IS - Z)^E ,$$

where IS is the instrument signal in millivolts and A, Z, and E are calibration parameters determined by the least-squares fit. The value of E is generally near 1.0.

An estimate of the uncertainty in the drag disk instrument is made by comparing the in situ standard to the instrument-measured momentum flux. The errors are formulated in terms of percent of actual momentum flux, which is approximately equivalent to percent of reading. For each data point, the percent error is calculated from

$$\% \text{ error} = \frac{(\rho V^2)_{std} - (\rho V^2)_{meas}}{(\rho V^2)_{std}} .$$

Two different drag disk instrument ranges and two different geometries (2-in. and 4-in. spool piece configurations) resulted in three different instrument measurement ranges. It was observed that values of σ for the three different types of drag disks (target and geometry) agree well with each other. It would appear reasonable to combine the data for all three types and to report average uncertainties. However, separate uncertainty estimates are made for instrument signals below 10% of maximum range due to a pronounced temperature effect that is especially noticeable at the lower readings. This effect is caused by the strain gage elements being in intimate contact with the fluid. The value of Z is the average of values taken at two different temperatures. The attempted temperature compensation is not very accurate at low signal values.

The resulting uncertainty bands for strain gage drag disks are:

2σ error band below 10% FS .... 56% reading
2σ error band above 10% FS .... 19% reading

The following items need to be considered when applying the above error bands to THTF data:

1. Percentage error estimates for the drag disks were compared with the subcooled data immediately preceding blowdown for the tests from which the calibration data were obtained. Average error values of 9.2% of readings (1σ) above 10% FS and 30% of readings (1σ) below 10% FS tend to support the uncertainty bands derived from calibration runs.

2. The strain gage transducer elements are exposed to the temperature environment of the loop. Temperatures significantly outside of the temperature range used during calibration will degrade the accuracy of the instrument further, especially below 10% FS.

D.8 Transient Response and Transient Errors

It is generally understood that no instrument responds infinitely fast to changes in the physical parameters being measured. That is, if the environment were to change suddenly from 200 arbitrary units to 400 arbitrary units, an instrument would initially read some value near 200 units and would approach a reading of 400 units asymptotically. A good approximation for many instruments is first-order lag (see Fig. D.9) defined by

$$V_r = V_o + (1 - e^{-T/\tau})(V_f - V_o) .$$

That is, the value indicated by the instrument (V_r) is equal to the original value (V_o) plus the value of the step function ($V_f - V_o$) multiplied by an exponential delay factor, where T is the elapsed time and τ is the 63.2% instrument response time, and V_f is the final value of the step function. Instrument error as a function of time would be represented by the area between V_f and the instrument reading line.

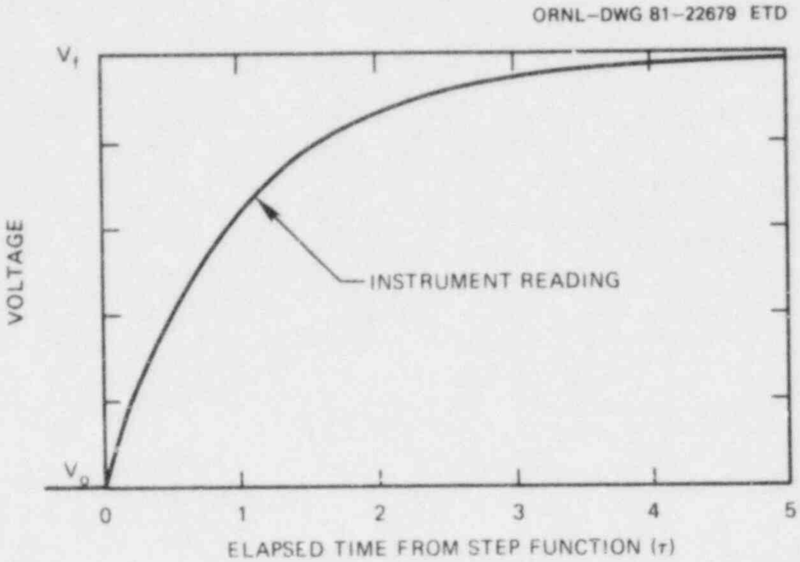

Fig. D.9. Instrument reading as a function of response time assuming first-order lag.

An additional problem in the THTF uncertainty analysis is introduced because the signal is sampled over discrete time intervals instead of continuously. It may be difficult to identify the exact starting point of a step function. If the step change in physical parameter occurs very near in time to the DAS sample (relative to the instrument response time), the instrument reading at that point will be in error by the total value of the change. If the DAS samples five or more response times after the step function, less than a one percent error (expressed as percent of the step function) will result.

Some arbitrariness is required, therefore, to provide a consistent definition of transient error. The method chosen was to assume that the step function occurred midway between two DAS sampling intervals (n and n + 1 in Fig. D.10). The error is measured at each sample point as the distance in engineering units between the modeled instrument reading and the assumed final value of the physical parameter V_f (vertical dashed lines in Fig. D.10). The uncertainty is expressed as the average of all the errors observed during an averaging interval (typically, 150 or 500 ms). The size of the step function and the length of the averaging interval were chosen with test conditions in mind.

As an example, let us consider the errors in the reading of a gamma densitometer (Sect. D.2) as a function of time. The response time on the ionization chamber is estimated at 16 ms. Assuming that the observed density decreases instantly from 750 kg/m (46.8 lb/ft) to 0 (a worst-case, blowdown situation), the errors observed at the DAS and the average error for a 100-ms averaging interval reported are shown in Table D.3.

The following items need to be considered when applying transient uncertainty values in the appendices to THTF data:

1. Although first-order lag modeling is appropriate for most instruments, it is at best a close approximation to the true instrument response.

ORNL-DWG 81-22680 ETD

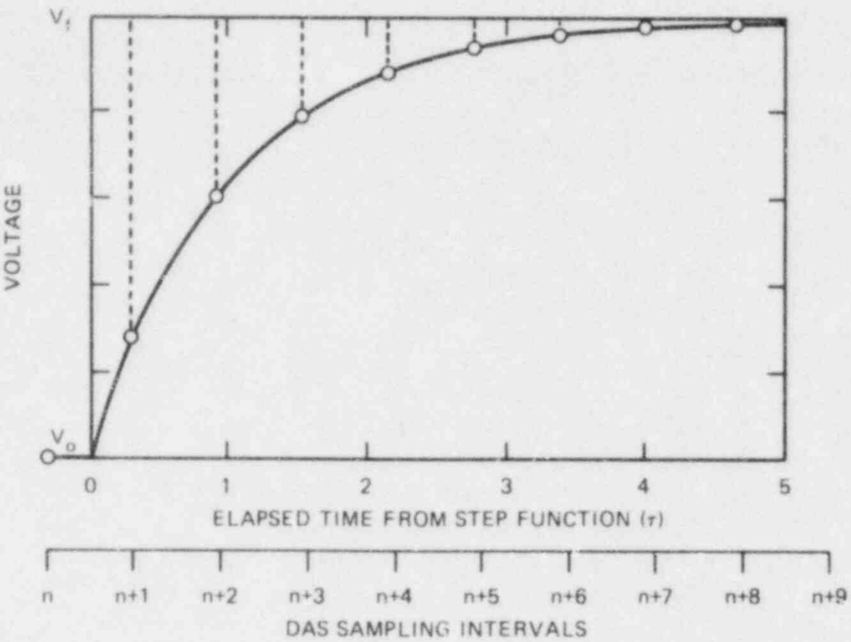

Fig. D.10. Instrument error as a function of DAS sampling assuming first-order lag.

Table D.3

DAS interval n + 1n = 0.01 s	Error (kg/m^3)	Error (lb/ft^3)
1	549	34.2
2	249	18.3
3	157	9.8
4	84	5.3
5	45	2.8
6	24	1.5
7	13	0.8
8	7	0.4
9	4	0.2
10	2	0.1
Average	118	7.4

2. The instrument response times are estimates. When these estimates are known from averages, the standard deviation is large, indicating wide variation from instrument-to-instrument. As a result, a particularly slow instrument of a given type might show errors a factor of 2 or more worse than the average would indicate.

3. The average uncertainty values noted in the tables are extremely sensitive to the averaging interval chosen. Average errors that appear

insignificant over a 500-ms averaging interval may well become significant over a 150-ms interval. A careful analysis of Table D.3 is illustrative in this light.

4. Step functions were chosen that were thought to be either representative or worst-case possibilities on a test-by-test basis. It is possible, however, that steps more severe than those chosen may have occurred.

D.9 General Comments

1. All of the above error bands were derived assuming that the specified instrument was in nominal working condition and had been recently calibrated using normal THTF calibration techniques. The error bands will not apply to defective instruments.

2. The error bands stated apply only to those items covered in the above discussion. Although every attempt has been made for the examination to be exhaustive and for the results to be conservatively stated, there is always the possibility that excessive instrument noise or out-of-spec components will cause actual readings to be outside of the given error limits (stated as 2σ).

3. The error bands given herein represent the experimenter's best judgment of the applicable uncertainties. Two points should be noted, however. First, the estimation of transient contributions to the uncertainty involves a number of assumptions and judgments. These have been documented in Sect. D.8, and the steady-state and transient contributions to the uncertainty have been listed separately in the tables to facilitate the reader who wishes to use his own estimates of the transient contribution to uncertainty if he chooses. Second, most of the data available on specific sources of instrument errors were obtained in single-phase flow. Thus, the experimenters had to rely primarily on engineering judgment to combine and extrapolate this data to two-phase flow. In most cases there is no experimental, two-phase flow data that can be used to verify the resulting uncertainty estimates.

D.10 Steady-State and Transient Instrument Uncertainties

Table D.4 provides a cross reference for instrument application numbers (IAN) and type codes. The first column provides the type code as an integer between 1 and 113, the second column lists the form of the IAN, and the "Remarks" column provides additional information to properly correlate type code to IAN for all instruments.

Tables D.5–D.6 provide a summary listing of steady-state and transient error bands by test. Table D.5 has values stated in SI units. Table D.6 is the English unit version of Table D.5. Nominal step function refers to a step size that is characteristic of transient phenomena that occur during the period when data are analyzed.

The first column in each table gives a brief instrument description. The second column provides the instrument type code. (Use Table D.4 to

Table D.4. Type Code — Instrument Application Number Table

Type Code	I.A.N	Remarks
		Special FRS Sheath Thermocouples [0.38 mm//0.015 inch]
1	TE-3nnal	nn = 01, 14, 17, 21, 34, 37, 38, 50, 54, or 60 a = A, E, or F 1 = 1, 2, 3, 4, 5, 6, 7, 8; or E, F, or G
		Regular FRS Sheath Thermocouples [0.51 mm//0.020 inch]
1	TE-3nnal	nn = 01-64 (except 19,22,36,46) and (excluding 01, 14, 17, 21, 34, 37, 38, 50, 54, 60 for tests 3.06.6B, 3.08.6C, 3.07.9, 3.09.10I-X and Mothball) a = A, B, or C 1 = A, B, C, D, E, F, G, H, U, or Y
		Special FRS Middle Thermocouples [0.38 mm//0.015 inch]
2	TE-3nnMl	nn = 01, 14, 17, 21, 34, 37, 38, 50, 54, or 60 M = M 1 = 1, 2, 3, 4, 5, 6, 7, 8; or E, F, or G
		Regular FRS Middle Thermocouples [0.51 mm//0.020 inch]
2	TE-3nnMl	nn = 01-64 (except 19, 22, 36, 46) and (excluding 01, 14, 17, 21, 34, 37, 38, 50, 54, 60 for tests 3.06.6B, 3.08.6C, 3.07.9, 3.09.10I-X and Mothball) M = M 1 = A, B, C, D, E, F, or G
		Subchannel Thermocouples
3	TE-12nn	nn = 01-81
		Shroud Wall Thermocouples
4	TE-18na	n = 1, 2, 3, 4, 5, 6, or 7 a = N, E, S, or W
		Miscellaneous and Process Thermocouples
5	TE-xxx	xxx = 5B, 408B, 520B, 521, 901, 920, 921, 922, 923, 924, 925, 926, 927, or 936
		Loop and Process Thermocouples
6	TE-xxx	xxx = 1, 2, 6, 24, 29, 40, 45, 57, 62, 67, 116, 150, 151, 152, 153, 172, 208, 212, 222, 228, 256, 266, 281, 282, 284
		Spacer Grid Thermocouples
7	TE-29na	n = 1, 2, 3, 4, 5, or 6 a = A, B, C, D, E, or F

Table D.4 (continued)

Type Code	I.A.N	Remarks
8	TE-18nal	Array Rod Thermocouples n = 8 or 9 a = A or B l = A, B, C, D, E, F, or G
9	TE-361-aJ	O-ring Area Thermocouples a = A, B, or C J = J
10	TE-nab	Shroud Box Thermocouples n = 0, 1, 2, 3, 4, 5, 6, 7, 8, or 9 a = A or B b = E or S
23	PE-xxx	Strain Gage Pressure Cells [20700 kPa//3000 psi] xxx = 15, 16, 26, 27, 42, 43, 44, 58, 63, 68, 76, 88, 106, 118, 156, 174, 201, 209, 224, 258, 268, 276, 281, 282, 283, 286, 425, 427, 454, 474
24	PE-32	Force Balance Pressure Cell [both ranges]
25	PE-102	Strain Gage Pressure Cell [1380 kPa//200 psi]
26	PDE-xxx	Strain Gage dP Cell [± 1380 kPa//± 200 psi] xxx = 35, 46, 167, 217 21 except for tests 3.09.10I-X and 3.10.10 60 except for test 3.05.5B
27	PDE-78	Strain Gage dP Cell [± 6900 kPa//1000 psi]
28	PDE-xxx	Strain Gage dP cell [± 345 kPa//± 50 psi] xxx = 7, 53, 65, 111, 203 21 only for tests 3.09.10I-X and 3.10.10 60 only for test 3.05.5B 200 except for 3.02.10C-H and Mothball 251 except for 3.02.10C-H and 3.09.10I-X
29	PE-nnn	Strain Gage Pressure Cell [2400 kPa//350 psi] nnn = 526 or 616
31	EIE-13nn	FRS Heater Rod Currents nn = 01-64 (excluding 19, 22, 36, 46)
32	EIE-xx	Generator Currents xx = 9, 10, 11, 12

Table D.4 (continued)

Type Code	I.A.N	Remarks
		Generator Voltage
33	EEE-xx	xx = 9, 10, 11, 12
34	EWE-77A	Primary Pump Power
		Momentum Flux Flow (Drag Disk) [9 cm//3.5 inch spool piece]
35	FMFE-xxxx	xxx = 22, 38, 170, 220
		206 except for 3.09.10I-X
		254, 264 only for 3.05.5B
36	SE-72	Primary Pump Speed
		Break Wire Detector
37	XE-430a	a = A or B
		Momentum Flux Flow (Drag Disk) [5 cm//2 inch spool piece]
40	FMFE-xxx	xxx = 14, 55, 61, 66, 114, 154, 155
		206 only for 3.09.10I-X
		254, 264 except for 3.04.5B
		Strain Gage dP Cell [± 25 kPa//± 100 inches water]
41	PDE-200	only for tests 3.02.10C-H
		Strain Gage dP Cell [± 125 kPa//± 500 inches water]
42	PDE-204	only for test 3.05.5B
	PDE-261	except for 3.08.6C, 3.07.9, 3.09.10I-X, and Mothball
		Strain Gage dP Cell [± 41 kPa//± 6 psi]
43	PDE-nnn	nnn = 199, 271
		204 except for 3.05.5B
		251 only for 2.02.10C-H
		261 only for 3.08.6C, 3.07.9, 3.09.10I-X, Mothball
		Experimental INEL Level Prone
50	LE-14nn	nn = 01 through 19
71	TE-28B	Linearized Resistance Thermometer Device
		Capacitive dP Cell
75	PDE-nnn	nnn = 180 through 188
		189 except on 3.09.10I-X and Mothball
		set at 0-6.2 kPa (0-30 inches) except for 3.05.5B
		set at 0-37.5 kPa (0-150 inches) only for 3.05.5B

Table D.4 (continued)

Type Code	I.A.N	Remarks
76	ZE-336U ZE-346L	Inbundle Gamma Densitometer Position Indicator except for 3.09.10I-X and Mothball
77	ZE-346L	Inbundle Gamma Densitometer Position Indicator only for 3.09.10I-X and Mothball
78	PDE-251	Capacitance dP Cell [25 kPa//100 inches] only for 3.09.10I-X
79	PDE-200	Capacitance dP Cell [50 kPa//200 inches] only for Mothball
80	PDE-189	Capacitance dP Cell [7.5 kPa//30 inches] only for 3.09.10I-X and Mothball
95	FE-nnn	Turbine Flowmeter—Heat Exchanger Secondary Flow nnn = 522, 620, 720
96	FE-550	Turbine Flowmeter—Heat Exchanger Secondary Flow
97	PDE-48	Force Balance dP Cell [166 kPa//24 psi]
98	PDE-30	Force Balance dp Cell [345 kPa//50 psi]
99	TDE-28	Differential Temperature
105	PDE-761 LE-100	Force Balance dP Cell
106	DE-xxx	Single Beam Gamma Densitometer xxx = 20, 36, 168, 218 Triple Beam Gamma Densitometer xxx = 204A, 204B, 204C, 252A, 252B, 252C, 262A, 262B, 262C
107	FE-xxx	Orifice Place/Force Balance Flowmeter xxx = 1A [0-5.0E-2 m^3/s or 0-800 gpm] 238 [0-1.0E-4 m^3/s or 0-1.6 gpm] only 3.09.10I-X Orifice Place/Capacitance Flowmeter xxx = 282 [0-2.5E-3 m^3/s or 0-39.3 gpm] 283 [0-3.3E-4 m^3/s or 0-5.2 gpm] 927 [0-1.4E-4 m^3/s or 0-2.1 gpm]

Table D.4 (continued)

Type Code	I.A.N	Remarks
		Orifice Plate/Force Balance Flowmeter
108	FE-18A	[4.4E-2 m³/s or 700 gpm] except for 3.01.10C-H, 3.09.10I-X and Mothball
	FE-18A	[1.7E-4 m³/s or 2.7 gpm] only for 3.01.10C-H, 3.09.10I-X and Mothball
	FE-238	except for 3.09.10I-X
		Instrument Spool Piece Turbine Flowmeter
109	FE-xxx	[3E-4 m³/s or 5 gpm] xxx = 250, 260 only for tests 3.01.10C-H, 3.09.10I-X, and Mothball
		[6E-4 m³/s or 10 gpm] xxx = 232, 280
		[1.4E-2 m³/s or 225 gpm] xxx = 3, 51, 59, 64, 110,
		[1.4E-2 m³/s or 225 gpm] xxx = 250, 260 except for 3.01.10C-H, 3.05.5B, 3.09.10I-X, and Mothball
		[1.4E-2 m³/s or 225 gpm] xxx = 202 only for tests 3.01.10C-H, 3.09.10I-X
		[6E-2 m³/s or 1000 gpm] xxx = 19,34,166,216,440,460
		[6E-2 m³/s or 1000 gpm] xxx = 250, 260 for 3.05.5B
		[6E-2 m³/s or 1000 gpm] xxx = 202 except for tests 3.01.10C-H, 3.09.10I-X
		Resistance Thermometer Device
110	TE-xxx	xxx = 4B, 101, 210A, 525, 557, 615, 627, 727
		Inbundle Gamma Densitometer
111	DE-xxx	xxx = 336U, 346L
		Orifice Plate/Force Balance Flowmeter
112	FE-238	same as type code 107 FE-238
113	LE-760	Force Balance dP Cell

Table D.5. Test 3.05.5B

THTF Instrument Error Bands						
Instrument Description	Type Code	Instrument Range	Steady State Error	Transient Error	Estimated Response Time	Assumed Value of Step Fn.
Rod Sheath Thermocouple 0.38 mm OD	1	273 K 1309 K	3.7K < 623 K 10.3 K	0.8 K[a]	7 ms	300 K
Rod Sheath Thermocouple 0.51 mm OD	1	273 K 1309 K	3.7K < 623 K 10.3 K	3.8 K[a]	12 ms	300 K
Rod Middle Thermocouple 0.38 mm OD	2	273 K 1309 K	3.7K < 623 K 10.3 K	0.8 K[a]	7 ms	300 K
Rod Middle Thermocouple 0.51 mm OD	2	273 K 1309 K	3.7K < 623 K 10.3 K	3.8 K[a]	12 ms	300 K
Bundle Subcnn Thermocouple 1.02 mm OD	3	273 K 1309 K	3.7K < 623 K 10.3 K	1.5 K	140 ms	5 K
Shroud Box Thermocouple 1.57 mm OD	4	273 K 1309 K	3.7K < 623 K 10.3 K	2.7 K	350 ms	5 K
System Thermocouple 3.2 mm OD	5	273 K 1309 K	3.7K < 623 K 10.3 K	3.8 K	870 ms	5 K
System (Nanmac) Thermocouple 6.4 mm OD	6	273 K 1309 K	3.7K < 623 K 10.3 K	0.1 K	18 ms	5 K
Spacer Grid Thermocouple 1.02 mm OD	7	273 K 1309 K	3.7K < 623 K 10.3 K	1.4 K	140 ms	5 K
Array Rod Thermocouple 1.02 mm OD	8	273 K 1309 K	3.7K < 623 K 10.3 K	1.4 K	140 ms	5 K

Table D.5 (continued)

THTF Instrument Error Bands

Instrument Description	Type Code	Instrument Range	Steady State Error	Transient Error	Estimated Response Time	Assumed Value of Step Fn.
Rod Sheath Thermocouple 0.51 mm OD	9	273 K 1309 K	3.7K < 623 K 10.3 K	3.8 K[a]	12 ms	300 K
Shroud Box Thermocouple 1.57 mm OD	10	273 K 1309 K	3.7K < 623 K 10.3 K	2.7 K	350 ms	5 K
Strain Gage Pressure Cell	23	20700 kPa	200 kPa	N.S.[j]	0.16 ms	550 kPa
Force Balance Pressure Cell	24	3400 kPa 17000 kPa	100 kPa	430 kPa	300 ms	550 kPa
Force Balance Pressure Cell	24	3400 kPa 27000 kPa	160 kPa	430 kPa	300 ms	550 kPa
Strain Gage Pressure Cell	25	1380 kPa	17 kPa	N.S.	0.32 ms	550 kPa
Strain Gage D.P. Cell	26	±1380 kPa	43 kPa	N.S.	0.32 ms	550 kPa
Strain Gage D.P. Cell	27	±6900 kPa	210 kPa	N.S.	0.32 ms	35 kPa
Strain Gage[g] D.P. Cell	28	±345 kPa	11 kPa	N.S.	0.32 ms	35 kPa
Strain Gage Pressure Cell	29	2400 kPa	24 kPa	N.S.	0.16 ms	550 kPa
Rod Heater Current	31	800 amp	0.85% Rdg	24 amp	50 ms	75 amp
Generator Current	32	1000 amp	0.85% Rdg	95 amp	50 ms	300 amp
Generator Voltage	33	300 volt	0.76% Rdg	32 volt	50 ms	100 volt

Table D.5 (continued)

THTF Instrument Error Bands						
Instrument Description	Type Code	Instrument Range	Steady State Error	Transient Error	Estimated Response Time	Assumed Value of Step Fn.
Primary Pump Power	34	750 kW	greater of 0.5 kW or 0.3% Rdg	6.3 kW	150 ms	10 kW
Strain Gage Drag Disk	35	±0.1E5 kg/ms² ±1.0E5 kg/ms²	56% Rdg 19% Rdg	790 kg/ms²	16 ms	7500 kg/ms
Primary Pump Speed	36	100 rpm 5400 rpm	20 rpm	13 rpm	150 ms	20 rpm
Breakwire Detector	37	5 volt	30 ms	N.A.	20 ms	N.A.
Strain Gage Drag Disk	40	±0.2E5 kg/ms² ±2.1E5 kg/ms²	56% Rdg 19% Rdg	790 kg/ms²	16 ms	7500 kg/ms²
Strain Gage D.P. Cell	41	±25 kPa	0.8 kPa	N.S.	0.32 ms	35 kPa
Strain Gage D.P. Cell	42	±125 kPa	4 kPa	N.S.	0.32 ms	35 kPa
Strain Gage D.P. Cell	43	±41 kPa	2 kPa	N.S.	0.32 ms	35 kPa
Level[i] Indicator	50	±10 volts	***	***	***	***
RTD	71	273 K 700 K	1.1 K 2.7 K	9.9 K	10 sec	10 K
Capacitive D.P. Cell	75	6.2 kPa	0.1 kPa	0.71 kPa	131 ms	1.2 kPa
Capacitive D.P. Cell	75	37.5 kPa	0.4 kPa	0.51 kPa	74 ms	1.2 kPa
Position Indicator	76	3.92 m	0.5% Rdg	N.A.	N.A.	N.A.
Position Indicator	77	3.33 m	0.5% Rdg	N.A.	N.A.	N.A.

Table D.5 (continued)

THTF Instrument Error Bands						
Instrument Description	Type Code	Instrument Range	Steady State Error	Transient Error	Estimated Response Time	Assumed Value of Step Fn.
Capacitive D.P. Cell	78	25 kPa	1.3 kPa	13.6 kPa	110 ms	25 kPa
Capacitive D.P. Cell	79	50 kPa	0.5 kPa	14.1 kPa	68 ms	35 kPa
Capacitive D.P. Cell	80	7.5 kPa	0.1 kPa	0.07 kPa	125 ms	1.2 kPa
Turbine[f] Flowmeter	95	0.9E-3 m^3/s 9.5E-3 m^3/s	4.1% Rdg	1.3E-4 m^3/s	11 ms 1.2 ms	6.3E-3 m^3/s
Turbine[f] Flowmeter	96	0.3E-3 m^3/s 3.2E-3 m^3/s	4.1% Rdg	1.3E-4 m^3/s	8 ms 1 ms	6.3E-3 m^3/s
Force Balance D.P. Cell	97	166 kPa	1 kPa	28 kPa	300 ms	35 kPa
Capacitive D.P. Cell	98	345 kPa	18 kPa	8.7 kPa	38 ms	35 kPa
Differential Temperature	99	228 K 283 K	3.8 K	9.9 K	10 sec	10 K
Liquid Level	105	3.81 m	0.023 m	0.16 m	300 ms	0.2 m
Liquid Level	105	1408 m	8.5 m	0.16 m	300 ms	0.2 m
Gamma Densitometer	106	1000 kg/m^3	104 kg/m^3	25 kg/m^3	16 ms	240 kg/m^3
Orifice[c] Flowmeter	107	1.0E-4 m^3/s	2.5E-6 m^3/s	7.9E-6 m^3/s	300 ms	1E-5 m^3/s
Orifice[c] Flowmeter	107	1.35E-4 m^3/s	3.4E-6 m^3/s	1.1E-5 m^3/s	300 ms	1.4E-5 m^3/s
Orifice[c] Flowmeter	107	3.32E-4 m^3/s	8.3E-6 m^3/s	2.6E-5 m^3/s	300 ms	3.3E-5 m^3/s

Table D.5 (continued)

THTF Instrument Error Bands						
Instrument Description	Type Code	Instrument Range	Steady State Error	Transient Error	Estimated Response Time	Assumed Value of Step Fn.
Orifice[c] Flowmeter	107	2.48E-3 m³/s	6.2E-5 m³/s	2.0E-4 m³/s	300 ms	2.5E-4 m³/s
Orifice[c] Flowmeter	107	5.0E-2 m³/s	1.3E-3 m³/s	3.9E-3 m³/s	300 ms	5E-3 m³/s
Orifice[d] Flowmeter	108	1.7E-4 m³/s	4.2E-6 m³/s	1.3E-5 m³/s	300 ms	1.7E-5 m³/s
Orifice[e] Flowmeter	108	4.4E-2 m³/s	1.1E-3 m³/s	3.5E-5 m³/s	300 ms	4.4E-3 m³/s
Turbine[f,h] Flowmeter	109	±0.3E-4 m³/s ±3.0E-4 m³/s	4.1% Rdg	3.1E-6 m³/s	8 ms 1 ms	1.5E-4 m³/s
Turbine[f,h,b] Flowmeter	109	±0.6E-4 m³/s ±6.1E-4 m³/s	2.5% Rdg	N.A.	8 ms 1 ms	N.A.
Turbine[f,h,l] Flowmeter	109	±1.3E-3 m³/s ±1.4E-2 m³/s	4.1% Rdg	1.3E-4 m³/s	13 ms 2 ms	5.3E-3 m³/s
Turbine[f,h,l] Flowmeter	109	±0.6E-2 m³/s ±6.1E-2 m³/s	4.1% Rdg	1.3E-4 m³/s	18 ms 2 ms	6.3E-3 m³/s
RTD	110	273 K 700 K	1.1 K 2.7 K	9.9 K	10 sec	10 K
Inbundle Gamma Densitometer	111	1000 kg/m³	104 kg/m³	25 kg/m³	16 ms	240 kg/m³
Orifice[c] Flowmeter	112	1.0E-4 m³/s	2.5E-6 m³/s	7.9E-6 m³/s	300 ms	1E-5 m³/s
Liquid Level	113	1.18 m	0.007 m	0.16 m	300 ms	0.20 m

Table D.5 (continued)

Documentation of Steady-State and Transient Error Bands

Steady-State Error Bands: Two-standard deviations compared to in-situ standard or twice the root-sum-square of uncertainties, whichever is applicable.

Transient Error Bands: Assuming first-order lag function, response times (TAU), and step function (Vf − Vo) indicated—the average error seen by the DAS assuming the step function occurred midway between DAS samples. The averaging interval is 500 ms for thermocouples and 150 ms for all other instruments.

Total Error: The total error due to steady state error and transient error is the sum of the steady state and transient error bands.

Footnotes:

a. Error bands apply to the environment as sensed at the surface of the thermocouple sheath. Larger errors may occur when data is modelled to provide temperatures at other points. Transient response is estimated by using the response time (25 ms or less) prior to swaging the sheath (0.71 mm swaged to 0.51 mm OD), then scaling using the rule: response time is inversely proportional to the outside diameter squared (OD**2 scaling). An additional 7% improvement in response time was allowed for packing of the boron nitride during swaging. The smaller thermocouples (0.51 mm swaged to 0.38 mm OD) were estimated from the values of the larger thermocouples by first scaling the 25 ms response time to the unswaged 0.51 mm diameter using OD**2 scaling, then applying OD**2 scaling and the 7% improvement for packing to the swaged 0.38 mm OD.

b. This instrument is fitted with Flow Technology electronics that time 10-blade passings. Averaging improves the steady-state error bands but degrades transient response.

c. Range applies specifically to instruments calibrated in subcooled liquid at a density of 1000 kg/m**3.

d. Range applies specifically to instruments calibrated in subcooled liquid at a density of 860 kg/m**3.

e. Range applies specifically to instruments calibrated in subcooled liquid at a density of 750 kg/m**3.

f. Error bands apply specifically to instruments calibrated in subcooled liquid. Extended range electronics provide readings out to 0.227 m^3/s for the 8.89E-2 meter diameter models; 0.028 m^3/s for the 5.08E-2 meter diameter models, but the error bands apply only to 150% of nominal maximum range.

g. Strain gage D.P. Cells used as pit cells are connected to different segments of the test section by long lines. These long lines induce resonant oscillations in the instrument that increase the steady-state errors bands to 35 kPa, and the transient error bands to 400 kPa.

h. The turbine flowmeters (type code 109) have a flow range such that:
-3.0E-4<Flow<-0.3E-4 .OR. 0.3E-4<Flow<3.0E-4,
-6.1E-4<Flow<-0.6E-4 .OR. 0.6E-4<Flow<6.1E-4,
-1.4E-3<Flow<-0.1E-3 .OR. 0.1E-3<Flow<1.4E-3,
-6.1E-2<Flow<-0.6E-2 .OR. 0.6E-2<Flow<6.1E-2,

i. The INEL level probe is an experimental device, and as such, does not have well documented error bands.

j. No significant error over a 500 ms averaging interval.

k. N.A. implies not applicable.

l. Flow Technology supplies calibration constants over the ranges 6.3E-4 to 1.9E-2 m^3/s and 5.0E-3 to 6.3E-2 m^3/s respectively. The uncertainty bands for these instruments should approach the quoted values for these ranges, but special care may be required. See the section on turbine flowmeters in the critical instruments section.

Table D.5 (continued)

Basis for Steady-State and Transient Error Bands by Type Code

Type Code	Steady State	Transient
1	Critical instrument	Manufacturer's spec, OD**2 scaling
2	Critical instrument	Manufacturer's spec, OD**2 scaling
3	Critical instrument	Work of Carroll and Sheppard
4	Critical instrument	Work of Carroll and Sheppard
5	Critical instrument	Work of Carroll and Sheppard
6	Critical instrument	Manufacturer's spec
7	Critical instrument	Work of Carroll and Sheppard
8	Critical instrument	Work of Carroll and Sheppard
9	Critical instrument	Manufacturer's spec, OD**2 scaling
10	Critical instrument	Work of Carroll and Sheppard
23	Critical instrument	Table B.2
24	Manufacturer's spec	Table B.2
25	Bench Cal. + DAS	Table B.2 (inferred)
26	Critical instrument	Table B.2
27	Critical instrument	Table B.2
28	Critical instrument	Table B.2
29	Critical instrument	Table B.2 (inferred)
31	Critical instrument	Table B.2 (inferred)
32	Inferred (type code 31)	Table B.2 (inferred)
33	Critical instrument	Table B.2 (inferred)
34	Manufacturer's spec	Manufacturer's spec
35	Critical instrument	Table B.2
36	Bench Cal. + DAS	Inferred (type code 34)
37	From test 3.03.6AR	From test 3.03.6AR
40	Critical instrument	Table B.2
43	Critical instrument	Table B.2 (inferred)
50	*******************	********************
71	Bench Cal. & specs	Table B.2
75	Critical instrument	Manufacturer's spec
76	Engineering judgement	N.A.
77	Engineering judgement	N.A.
78	Critical instrument	Inferred (type code 75)
79	Inferred (type code 75)	Inferred (type code 75)
80	Inferred (type code 75)	Inferred (type code 75)
95	Inferred (type code 109)	Work of N. Chen
96	Inferred (type code 109)	Work of N. Chen
97	Critical instrument	Table B.2
98	Critical instrument	Inferred (typed code 75)
99	Inferred (type code 71)	Inferred (type code 71)
105	Manufacturer's spec	Table B.2 (inferred)
106	Critical instrument	Work of R. Shipp (manufacturer's spec)
107	In-situ calibration	Table B.2 (inferred)
108	Inferred (type code 107)	Table B.2 (inferred)
109	Critical instrument	Work of N. Chen
110	Bench Cal. & specs	Table B.2
111	Inferred (type code 106)	Inferred (type code 109)
112	Inferred (type code 107)	Table B.2 (inferred)
113	Manufacturer's spec	Table B.2 (inferred)

Table D.6. Test 3.05.5B

THTF Instrument Error Bands						
Instrument Description	Type Code	Instrument Range	Steady State Error	Transient Error	Estimated Response Time	Assumed Value of Step Fn.
Rod Sheath Thermocouple 0.015 inch OD	1	32 F 1900 F	6.7F < 662 F 18.5 F	1.4 F[a]	7 ms	540 F
Rod Sheath Thermocouple 0.020 inch OD	1	32 F 1900 F	6.7F < 662 F 18.5 F	6.8 F[a]	12 ms	540 F
Rod Middle Thermocouple 0.015 inch OD	2	32 F 1900 F	6.7F < 662 F 18.5 F	1.4 F[a]	7 ms	540 F
Rod Middle Thermocouple 0.020 inch OD	2	32 F 1900 F	6.7F < 662 F 18.5 F	6.8 F[a]	12 ms	540 F
Bundle Subchn Thermocouple 0.040 inch OD	3	32 F 1900 F	6.7F < 662 F 18.5 F	2.7 F	140 ms	9 F
Shroud Box Thermocouple 0.062 inch OD	4	32 F 1900 F	6.7F < 662 F 18.5 F	4.9 F	350 ms	9 F
System Thermocouple 0.125 inch OD	5	32 F 1900 F	6.7F < 662 F 18.5 F	6.8 F	870 ms	9 F
System (Nanmac) Thermocouple 0.25 inch OD	6	32 F 1900 F	6.7F < 662 F 18.5 F	0.2 F	18 ms	9 F
Spacer Grid Thermocouple 0.040 inch OD	7	32 F 1900 F	6.7F < 662 F 18.5 F	2.5 F	140 ms	9 F
Array Rod Thermocouple 0.040 inch OD	8	32 F 1900 F	6.7F < 662 F 18.5 F	2.5 F	140 ms	9 F

Table D.6 (continued)

THTF Instrument Error Bands						
Instrument Description	Type Code	Instrument Range	Steady State Error	Transient Error	Estimated Response Time	Assumed Value of Step Fn.
Rod Sheath Thermocouple 0.020 inch OD	9	32 F 1900 F	6.7F < 662 F 18.5 F	6.8 F[a]	12 ms	540 F
Shroud Box Thermocouple 0.062 inch OD	10	32 F 1900 F	6.7F < 662 F 18.5 F	4.9 F	350 ms	9 F
Strain Gage Pressure Cell	23	3000 psi	29 psi	N.S.[j]	0.16 ms	80 psi
Force Balance Pressure Cell	24	500 psi 2500 psi	15 psi	62 psi	300 ms	80 psi
Force Balance Pressure Cell	24	500 psi 3900 psi	23 psi	62 psi	300 ms	80 psi
Strain Gage Pressure Cell	25	200 psi	2.5 psi	N.S.	0.32 ms	80 psi
Strain Gage D.P. Cell	26	+200 psi	6.2 psi	N.S.	0.32 ms	80 psi
Strain Gage D.P. Cell	27	+1000 psi	30 psi	N.S.	0.32 ms	5 psi
Strain Gage[g] D.P. Cell	28	+50 psi	1.6 psi	N.S.	0.32 ms	5 psi
Strain Gage Pressure Cell	29	350 psi	3.5 psi	N.S.	0.16 ms	80 psi
Rod Heater Current	31	800 amp	0.85% Rdg	24 amp	50 ms	75 amp
Generator Current	32	1000 amp	0.85% Rdg	95 amp	50 ms	300 amp
Generator Voltage	33	300 volt	0.76% Rdg	32 volt	50 ms	100 volt

Table D.6 (continued)

THTF Instrument Error Bands

Instrument Description	Type Code	Instrument Range	Steady State Error	Transient Error	Estimated Response Time	Assumed Value of Step Fn.
Primary Pump Power	34	750 kW	greater of 0.5 kW or 0.3% Rdg	6.3 kW	150 ms	10 kW
Strain Gage Drag Disk	35	+0.7E4 lb/fts^2 +7.0E4 lb/fts^2	56% Rdg 19% Rdg	530 lb/fts^2	16 ms	5000 lb/fts^2
Primary Pump Speed	36	100 rpm 5400 rpm	20 rpm	13 rpm	150 ms	20 rpm
Breakwire Detector	37	5 volt	30 ms	N.A.	20 ms	N.A.
Strain Gage Drag Disk	40	+1.4E4 lb/fts^2 +1.4E5 lb/fts^2	56% Rdg 19% Rdg	530 lb/fts^2	16 ms	5000 lb/fts^2
Strain Gage D.P. Cell	41	+100 inch	3.2 inch	N.S.	0.32 ms	141 inch
Strain Gage D.P. Cell	42	+500 inch	16 inch	N.S.	0.32 ms	141 inch
Strain Gage D.P. Cell	43	+6 psi	0.3 psi	N.S.	0.32 ms	5 psi
Level[i] Indicator	50	+10 volt	***	***	***	***
RTD	71	32 F 800 F	2.0 F 4.9 F	17.8 F	10 sec	18 F
Capacitive D.P. Cell	75	25 inch	0.4 inch	2.9 inch	131 ms	4.8 inch
Capacitive D.P. Cell	75	150 inch	1.6 inch	2.0 inch	74 ms	4.8 inch
Position Indicator	76	155 inch	0.5% Rdg	N.A.	N.A.	N.A.
Position Indicator	77	131 inch	0.5% Rdg	N.A.	N.A.	N.A.

Table D.6 (continued)

THTF Instrument Error Bands						
Instrument Description	Type Code	Instrument Range	Steady State Error	Transient Error	Estimated Response Time	Assumed Value of Step Fn.
Capacitive D.P. Cell	78	+100 inch	5.2 inch	55 inch	110 ms	100 inch
Capacitive D.P. Cell	79	200 inch	2.0 inch	57 inch	68 ms	140 inch
Capacitive D.P. Cell	80	30 inch	0.4 inch	0.3 inch	125 ms	4.8 inch
Turbine[f] Flowmeter	95	15 gpm 150 gpm	4.1% Rdg	2.0 gpm	11 ms 1.2 ms	100 gpm
Turbine[f] Flowmeter	96	5 gpm 50 gpm	4.1% Rdg	2.0 gpm	8 ms 1 ms	100 gpm
Force Balance D.P. Cell	97	24 psi	0.15 psi	4 psi	300 ms	5 psi
Capacitive D.P. Cell	98	50 psi	2.6 psi	1.3 psi	38 ms	5 psi
Differential Temperature	99	+50 F	6.8 F	17.8 F	10 sec	18 F
Liquid Level	105	150 inch	0.9 inch	6.2 inch	300 ms	7.9 inch
Liquid Level	105	5.5E4 inch	336 inch	6.2 inch	300 ms	7.9 inch
Gamma Densitometer	106	62.4 lb/ft^3	6.5 lb/ft^3	1.6 lb/ft^3	16 ms	15 lb/ft^3
Orifice[c] Flowmeter	107	1.6 gpm	4E-2 gpm	0.13 gpm	300 ms	0.16 gpm
Orifice[c] Flowmeter	107	2.1 gpm	0.054 gpm	0.17 gpm	300 ms	0.22 gpm
Orifice[c] Flowmeter	107	5.3 gpm	0.13 gpm	0.41 gpm	300 ms	0.52 gpm

Table D.6 (continued)

THTF Instrument Error Bands						
Instrument Description	Type Code	Instrument Range	Steady State Error	Transient Error	Estimated Response Time	Assumed Value of Step Fn.
Orifice[c] Flowmeter	107	39.3 gpm	9.8 gpm	3.2 gpm	300 ms	4.0 gpm
Orifice[c] Flowmeter	107	800 gpm	21 gpm	62 gpm	300 ms	80 gpm
Orifice[d] Flowmeter	108	2.7 gpm	0.067 gpm	0.21 gpm	300 ms	0.27 gpm
Orifice[e] Flowmeter	108	700 gpm	17.4 gpm	0.55 gpm	300 ms	70 gpm
Turbine[f,h] Flowmeter	109	+0.5 gpm +5.0 gpm	4.1% Rdg	0.05 gpm	8 ms 1 ms	2.4 gpm
Turbine[f,h,b] Flowmeter	109	+1.0 gpm +10 gpm	2.5% Rdg	N.A.	8 ms 1 ms	N.A.
Turbine[f,h,l] Flowmeter	109	+22 gpm +225 gpm	4.1% Rdg	2.1 gpm	13 ms 2 ms	100 gpm
Turbine[f,h,l] Flowmeter	109	+100 gpm +1000 gpm	4.1% Rdg	2.1 gpm	18 ms 2 ms	100 gpm
RTD	110	32 F 800 F	2.0 F 4.9 F	17.8 F	10 sec	18 F
In-bundle Gamma Densitometer	111	62.4 lb/ft^3	6.5 lb/ft^3	1.6 lb/ft^3	16 ms	15 lb/ft^3
Orifice[c] Flowmeter	112	1.6 gpm	0.04 gpm	0.13 gpm	300 ms	0.16 gpm
Liquid Level	113	46 inch	0.3 inch	6.2 inch	300 ms	7.9 inch

Table D.6 (continued)

Documentation of Steady-State and Transient Error Bands

Steady-State Error Bands: Two-standard deviations compared to in-situ standard or twice the root-sum-square of uncertainties, whichever is applicable.

Transient Error Bands: Assuming first-order lag function, response times (TAU), and step function (Vf − Vo) indicated—the average error seen by the DAS assuming the step function occurred midway between DAS samples. The averaging interval is 500 ms for thermocouples and 150 ms for all other instruments.

Total Error: The total error due to steady state error and transient error is the sum of the steady state and transient error bands.

Footnotes:

a. Error bands apply to the environment as sensed at the surface of the thermocouple sheath. Larger errors may occur when data is modelled to provide temperatures at other points. Transient response is estimated by using the response time (25 ms or less) prior to swaging the sheath (0.028 inch swaged to 0.020 inch OD), then scaling using the rule: response time is inversely proportional to the outside diameter squared (OD**2 scaling). An additional 7% improvement in response time was allowed for packing of the boron nitride during swaging. The smaller thermocouples (0.020 inch swaged to 0.015 inch) were estimated from the values of the larger thermocouples by first scaling the 25 ms response time to the unswaged 0.020 inch diameter using OD**2 scaling, then applying OD**2 scaling and the 7% improvement for packing to the swaged 0.015 inch OD.

b. This instrument is fitted with Flow Technology electronics that time 10-blade passings. Averaging improves the steady-state error bands but degrades transient response.

c. Range applies specifically to instruments calibrated in subcooled liquid at a density of 62.4 lb/ft**3.

d. Range applies specifically to instruments calibrated in subcooled liquid at a density of 53.7 lb/ft**3.

e. Range applies specifically to instruments calibrated in subcooled liquid at a density of 46.8 lb/ft**3.

f. Error bands apply specifically to instruments calibrated in subcooled liquid. Extended range electronics provide readings out to 3600 gpm for the 3.5 inch diameter models; 445 gpm for the two inch diameter models, but the error bands apply only to 150% of nominal maximum range.

g. Strain gage D.P. Cells used as pit cells are connected to different segments of the test section by long lines. These long lines induce resonant oscillations in the instrument that increase the steady-state errors bands to 5 psi, and the transient error bands to 60 psi in the interval immediately following blowdown.

h. The turbine flowmeters (type code 109) have a flow range such that:
-5.0<Flow<-0.5 .OR. 0.5<Flow<5.0,
-10.0<Flow<-1.0 .OR. 1.0<Flow<10.0,
-225<Flow<-22 .OR. 22<Flow<225,
-1000<Flow<-100 .OR. 100<Flow<1000.

i. The INEL level probe is an experimental device, and as such, does not have well documented error bands.

j. No significant error over the averaging interval.

k. N.A. implies not applicable.

l. Flow Technology supplies calibration constants over the ranges 10 to 300 gpm and 80 to 1000 gpm respectively. The uncertainty bands for these instruments should approach the quoted values for these ranges, but special care may be required. See the section on turbine flowmeters in the critical instruments section.

Table D.6 (continued)

Basis for Steady-State and Transient Error Bands by Type Code		
Type Code	Steady State	Transient
1	Critical instrument	Manufacturer's spec, OD**2 scaling
2	Critical instrument	Manufacturer's spec, OD**2 scaling
3	Critical instrument	Work of Carroll and Sheppard
4	Critical instrument	Work of Carroll and Sheppard
5	Critical instrument	Work of Carroll and Sheppard
6	Critical instrument	Manufacturer's spec
7	Critical instrument	Work of Carroll and Sheppard
8	Critical instrument	Work of Carroll and Sheppard
9	Critical instrument	Manufacturer's spec, OD**2 scaling
10	Critical instrument	Work of Carroll and Sheppard
23	Critical instrument	Table B.2
24	Manufacturer's spec	Table B.2
25	Bench Cal. + DAS	Table B.2 (inferred)
26	Critical instrument	Table B.2
27	Critical instrument	Table B.2
28	Critical instrument	Table B.2
29	Critical instrument	Table B.2 (inferred)
31	Critical instrument	Table B.2 (inferred)
32	Inferred (type code 31)	Table B.2 (inferred)
33	Critical instrument	Table B.2 (inferred)
34	Manufacturer's spec	Manufacturer's spec
35	Critical instrument	Table B.2
36	Bench Cal. + DAS	Inferred (type code 34)
37	From test 3.03.6AR	From test 3.03.6AR
40	Critical instrument	Table B.2
43	Critical instrument	Table B.2 (inferred)
50	*******************	********************
71	Bench Cal. & specs	Table B.2
75	Critical instrument	Manufacturer's spec
76	Engineering judgement	N.A.
77	Engineering judgement	N.A.
78	Critical instrument	Inferred (type code 75)
79	Inferred (type code 75)	Inferred (type code 75)
80	Inferred (type code 75)	Inferred (type code 75)
95	Inferred (type code 109)	Work of N. Chen
96	Inferred (type code 109)	Work of N. Chen
97	Critical instrument	Table B.2
98	Critical instrument	Inferred (typed code 75)
99	Inferred (type code 71)	Inferred (type code 71)
105	Manufacturer's spec	Table B.2 (inferred)
106	Critical instrument	Work of R. Shipp (manufacturer's spec)
107	In-situ calibration	Table B.2 (inferred)
108	Inferred (type code 107)	Table B.2 (inferred)
109	Critical instrument	Work of N. Chen
110	Bench Cal. & specs	Table B.2
111	Inferred (type code 106)	Inferred (type code 109)
112	Inferred (type code 107)	Table B.2 (inferred)
113	Manufacturer's spec	Table B.2 (inferred)

cross reference to IANs.) The third column provides the nominal instrument range. The fourth and fifth columns give the steady-state and transient error bands, respectively. The sixth and seventh columns provide the estimated response time and step function values used to estimate the transient uncertainty value.

The English version tables are intended for reference only. Exact correspondence of entries will be limited by significant figure rounding.

The values quoted for both steady-state and transient errors are estimates based on several assumptions. It is the responsibility of the data user to ascertain the appropriateness of these assumptions when using the included error bands for THTF data analysis.

References

1. K. A. Brownlee, *Statistical Theory and Methodology in Science and Engineering*, p. 80, John Wiley and Sons, Inc., New York, 1965.

2. J. B. Scarborough, *Numerical Mathematical Analysis*, 3rd Ed., p. 429, The John Hopkins Press, Baltimore, 1955.

3. K. A. Brownlee, *Statistical Theory and Methodology in Science and Engineering*, p. 340, John Wiley and Sons, Inc., New York, 1965.

4. Unpublished report, *Summary Two and Three Dimensional Analysis of Turbine Flowmeter Response in Two-Phase Flow*, MPR Associates, Inc. (October 11, 1977).

5. Internal memo from R. L. Anderson, I&C Division ORNL, to B. J. Veazie, *Error in BDHT Thermocouple*, June 18, 1980.

Appendix E

DENSITY OBTAINED FROM THREE-BEAM DENSITOMETER

An annular model[1] is used for obtaining composite density from the three-beam gamma densitometers installed on selected THTF spool pieces. The model solves for a uniform density for each region shown in Fig. B.24 using the density indicated by each of the three beams and the length of each beam within each region. The composite pipe density is then calculated as an area-weighted average of the three region densities. This results in an equation for the composite density of:

$$\bar{\rho} = 0.3784\rho_A + 0.5117\rho_B + 0.1099\rho_C ,$$

where $\bar{\rho}$ is the composite average pipe density and ρ_A, ρ_B, and ρ_C, are the measured beam densities respectively. The calculated composite density is shown graphically in Figs. E.1 and E.2, for the external downcomer upper spool piece and bundle outlet spool piece composite densities, respectively.

An uncertainty estimate for homogeneous flows may be obtained using a standard propagation-of-errors method and the uncertainty estimates for

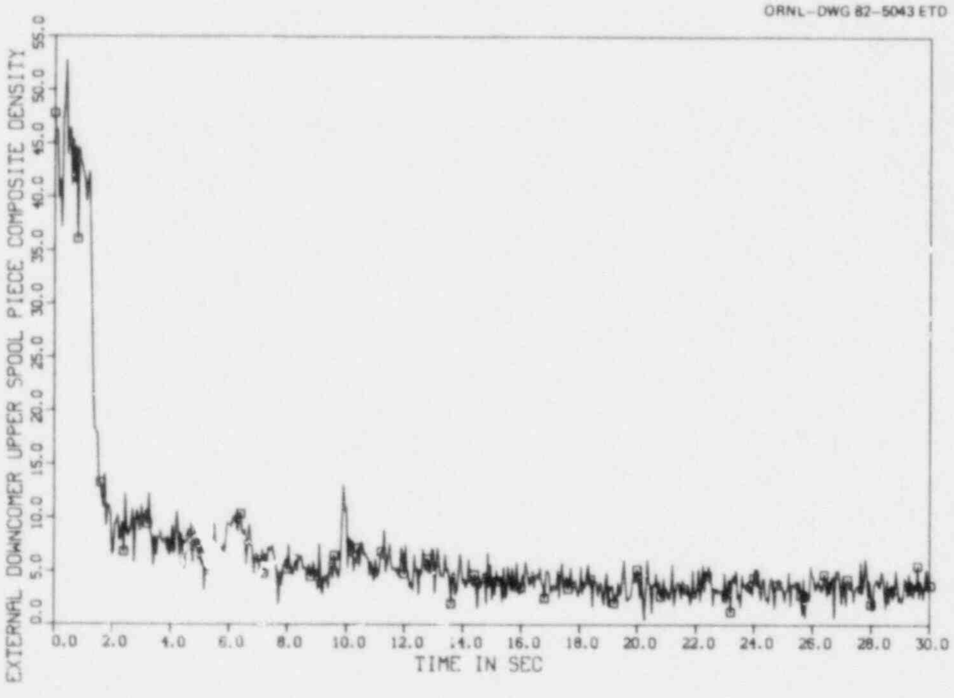

Fig. E.1. Test 3.05.5B double-ended cold-leg break simulation.

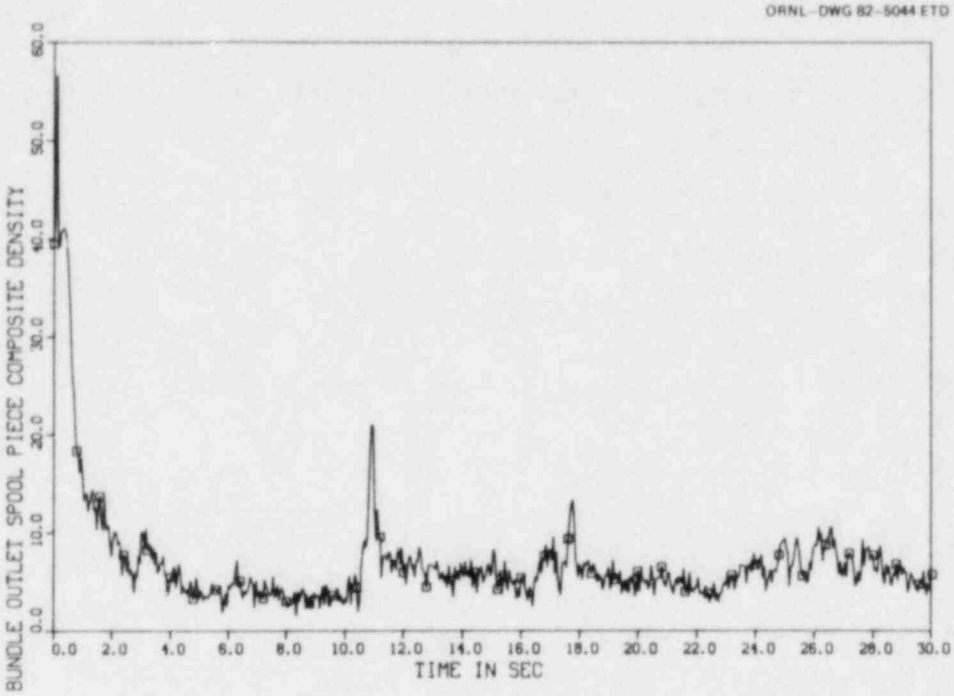

Fig. E.2. Test 3.05.5B double-ended cold-leg break simulation.

the individual beams. The standard deviation may be estimated as

$$\sigma = [(0.3784\sigma_A)^2 + (0.5117\sigma_B)^2 + (0.1099\sigma_C)^2]^{0.5} .$$

Substituting the reported 2σ single-beam values of 104 kg/m^3 (6.5 lb_m/ft^3) into the above equation gives a 2σ value of 67 kg/m^3 (4.2 lb_m/ft^3) for the composite three-beam densitometer measurements.

Reference

1. K. G. Turnage et al., *Advanced Two-Phase Instrumentation Program Quarterly Progress Report for April–June 1978*, ORNL/NUREG/TM-279 (January 1979).

NUREG/CR-2525, Vol. 6
ORNL/NUREG/TM-407/V6
Dist. Category R2

Internal Distribution

1-2. W. G. Craddick
3-7. D. K. Felde
8. S. S. Gould
9. H. W. Hoffman
10. A. L. Lotts
11-15. D. G. Morris
16-20. C. B. Mullins
21-23. L. J. Ott
24-28. J. J. Robinson
29. T. W. Robinson, Jr.
30. K. N. Schwinkendorf
31. A. G. Sutton
32. H. E. Trammell
33. ORNL Patent Office
34. Central Research Library
35. Document Reference Section
36-37. Laboratory Records Department
38. Laboratory Records, RC

External Distribution

39-43. Director, Division of Reactor Safety Research, Nuclear Regulatory Commission, Washington, DC 20555
44. Office of Assistant Manager for Energy Research and Development, Department of Energy, Oak Ridge Operations Office, Oak Ridge, TN 37830
45-46. Technical Information Center, Department of Energy, Oak Ridge, TN 37830
47-391. Given distribution as shown under category R2 (10-NTIS)

☆ U.S. GOVERNMENT PRINTING OFFICE: 1982-546-067/56